

DISS. ETH No. 27281

Assessing functional and structural visual outcomes in human acute optic neuritis and murine experimental optic neuritis

A thesis submitted to attain the degree of

DOCTOR OF SCIENCES of ETH ZURICH

(Dr. sc. ETH Zurich)

presented by

CARLA ANDREA WICKI

MSc ETH HST

born on 30.05.1992

citizen of Mauensee

accepted on the recommendation of

Prof. Dr. Nicole Wenderoth

Prof. Dr. Sven Schippling

Prof. Dr. Andreas Luft

2021

Acknowledgments

I would like to thank the members of my thesis committee:

I would like to thank Sven Schippling for giving me the opportunity to do my PhD in his research group, for all the helpful advices and discussions, as well as for sharing his knowledge with me. I also gratefully acknowledge the continuous support provided by Nicole Wenderoth and Andreas Luft throughout my PhD. In their role as co-supervisors, they provided constructive comments, valuable scientific advice and encouragement for the present work.

I would also like to thank the following people for their enormous support throughout my PhD:

I'm very grateful to the whole "MINDS team" for sharing their enthusiasm for the field of MS research with me, for all their crucial scientific advices, for the enjoyable working atmosphere and importantly for all the personal support provided by them throughout the past years. Special thanks to Praveena Manogaran, you not only taught and supported me a lot, but I had also fun working with you. Many thanks also to James Hanson for providing valuable scientific feedback on all the projects and for the plenty of interesting discussions we had during lunches. Thank you Tanja Simic, that I could always count on your professional and most importantly moral support. Thanks also to Christine Walker-Egger for much valuable advice in the early stages of my PhD. It was a pleasure to be a part of our team.

A special thanks for the positive working environment goes also to the entire "nims team", including Andreas Lutterotti, Roland Martin, Ilijas Jelcic, Veronika Kana, all the residents of the MS outpatient unit, and all of the other members of the Department of Neurology. In particular, I would like to thank Andreas Lutterotti, for taking over responsibility for the ACSON trial. Thank you also to Lukas Imbach, Christina Gerth-Kahlert, Fabienne Fierz and Konrad Weber who enabled a good cooperation for the ACSON trial.

I would also like to thank Christian Grimm for providing support, encouragement and resources particularly in the last year of my PhD.

Thanks also to the animal imaging center, including Mark Augath, Valerio Zerbi, Markus Rudin, and Aileen Schröter for providing support with the implementation of the mice MRI studies in their lab.

Finally, and definitely not least, I would like to thank my wonderful family, Gabriela, Bruno, Flavio, Anina & Timo Wicki, my boyfriend Flavio Eiholzer, and all my friends for all the invaluable support that you provide every single day.

Summary

Optic neuritis (ON) is an acute inflammatory, demyelinating event affecting the optic nerve, and a common manifestation in multiple sclerosis (MS). It can affect MS patients throughout their disease course, and 20 % of patients present with acute ON as their initial symptom. ON primarily affects the optic nerve in its myelinated portion, but also triggers neurodegeneration in the entire afferent visual pathway (AVP) through retrograde and anterograde (trans-synaptic) degeneration. Visual outcomes are diverse, including severe persistent visual impairment. High-dose corticosteroids are the current mainstay in the therapy of acute autoimmune ON. However, despite clear acceleration of functional visual recovery in the short-term, any mid- to long-term impact on visual outcomes remains unproven.

Apart from its high prevalence and clinical relevance, ON also offers a unique model to study neurodegeneration as well as the potential of neuroprotective and –regenerative therapies: a clinical episode of acute ON can be assigned in its occurrence to an approximate time window, and in its impact on tissue integrity to a discrete, anatomically isolated structure. The AVP is retinotopically organized, linking its structural integrity with clinical function. Almost the entire AVP can be probed using imaging tools of different modalities, including optical coherence tomography (OCT) and structural magnetic resonance imaging (MRI) techniques such as diffusion-tensor-imaging (DTI). Furthermore, the function of the AVP can be assessed by simple but sensitive measurements such as low-contrast visual acuity (LCVA). Therefore, ON provides an optimal paradigm to study the consequences of an MS-relapse on tissue integrity and function.

In the first section of this thesis, we reviewed the growing relevance of monitoring the thicknesses of different retinal layers using OCT to reveal AVP damage in MS. We summarized that the thicknesses of the macular ganglion cell and inner plexiform layer (GCIP) and the peripapillary retinal nerve fiber layer (pRNFL) are informative with regard to early detection of neuronal degeneration and long-term axonal damage, respectively, of the retinal ganglion cells (RGCs) in MS. A significant body of literature demonstrates that OCT-derived measures are not only associated with visual function, but also with other clinically relevant parameters such as grey matter atrophy or the Expanded Disability Status Scale (EDSS) score – a standard measure of overall disability in MS. Additionally, based on current research in the field, the review paper also highlights the possible role of the macular inner nuclear layer (INL) in detecting inflammatory disease activity and response to treatment in MS. Taking into account that ON is the main driver of neuro-axonal retinal damage in MS, we highlighted the further importance of the application of OCT in patients with ON.

Although a great number of cross-sectional OCT studies in ON have been published to date, longitudinal studies remain relatively rare but are indispensable in order to achieve better knowledge

Summary

of the temporal dynamics and magnitude of retinal neuro-axonal and functional visual damage following ON. Therefore, in a retrospective longitudinal study, we attempted to describe the changes in retinal structure and visual function over one year following clinically first-ever unilateral ON in both affected and unaffected eyes, using OCT as well as high-contrast visual acuity (HCVA) and LCVA testing. We found that the GCIP and pRNFL had substantial thinning in ON eyes, with early GCIP thinning (74.5 % of the total reduction occurring within the first month), and slightly later thinning of pRNFL (87.8 % within the first three months following ON). Furthermore, we found that the INL thickness was significantly increased in ON eyes (by month 1), but also, and more surprisingly, in the contralateral non-ON (NON) eyes (by month 12) following clinically unilateral ON, which is a novel finding. It is possible that subclinical involvement of the fellow eye resulted in this INL increase, indicating bilateral retinal pathology, although further research is needed to confirm this hypothesis. Additionally, we observed severely impaired visual acuity in ON eyes at onset of symptoms. Even though we detected functional improvement over time, particularly in HCVA, LCVA remained clinically impaired up to the final study time point. Overall, this data can have an impact on future therapeutic strategies by highlighting the particular importance of early treatment of ON.

Pathology of the optic nerve and retina has also been described in murine models of MS, including myelin oligodendrocyte glycoprotein (MOG) peptide-induced experimental autoimmune encephalomyelitis (EAE). Therefore, in a longitudinal EAE study, we aimed to further investigate the mechanisms involved in ON-induced pathology of the AVP using a multimodal imaging approach. Because the retina is void of myelin, an important contributor to chronic neuro-axonal damage following ON, namely demyelination, cannot be assessed using OCT. Therefore, we assessed the utility of DTI as a means to investigate AVP pathology following ON, allowing the assessment of the myelinated portion of the optic nerve and tract. Consistent with previous literature, we found a gradual decrease in fractional anisotropy values in the optic nerve and tract implying white matter tissue damage in EAE. In parallel, radial diffusivity (RD) significantly increased in EAE mice, likely reflecting ongoing demyelination. Hence, we concluded, that DTI is valuable in capturing demyelination of the optic nerve and tract in EAE. In order to avoid permanent neuro-axonal tissue loss and associated disability, the search for new strategies to either prevent demyelination or enhance remyelination is of increasing importance in the field of MS. Therefore, eligible outcome measures should be able to capture these target mechanisms, pointing out the valuable role of RD as a biomarker.

Currently, there are no satisfactory neuroprotective therapies or visual rehabilitation programs available for patients with ON. As visual function has been rated as one of the most important bodily functions by MS patients, the high prevalence of visual impairment in MS following episodes of ON remains a major unsolved problem in the disease management.

Summary

With the aim of finding new therapeutic options that specifically target long-term prevention of persistent visual disability, we performed an interdisciplinary literature review. We found a significant body of preclinical as well as clinical evidence showing that low-current electrical stimulation of the retina and optic nerve in optic neuropathies of different causes may have neuroprotective and -restorative effects on RGCs. Clinical research exploring the potential of this so-called repetitive transorbital alternating current stimulation (rtACS) in patients with autoimmune ON has not yet been performed. We discussed why we would expect a beneficial effect of rtACS on remyelination, on other repair-promoting mechanisms in RGCs, and also on visual outcomes in patients with a first-ever acute ON. Moreover, we presented an optimal study design to investigate the safety, tolerability and preliminary efficacy of rtACS in this specific patient cohort.

Zusammenfassung

Die Sehnervenentzündung (Optikusneuritis) ist eine akute entzündliche Demyelinisierung des Sehnervs und tritt häufig im Rahmen einer Multiplen Sklerose (MS) auf. Die MS ist eine entzündliche degenerative Autoimmunerkrankung des zentralen Nervensystems. Im Laufe der Krankheit zeigen rund 70 % aller MS-Patienten Symptome einer Optikusneuritis, bei 20 – 25 % der Patienten ist die Optikusneuritis sogar die Erstmanifestation der MS.

Die Optikusneuritis attackiert vor allem den myelinisierten Anteil des Sehnervs, die entzündliche Demyelinisierung führt jedoch oft zu einer sekundären Degeneration der retinalen Ganglienzellen und auch in posterior gelegenen Strukturen des visuellen Systems kann es zu degenerativen Veränderungen kommen. Patienten erholen sich unterschiedlich gut nach einer Optikusneuritis, wobei permanente Sehverluste nicht ausgeschlossen werden können. Zurzeit ist eine systemische Therapie mit Methylprednisolon die Standardbehandlung. Sie wirkt entzündungshemmend und beschleunigt dadurch die Erholung der Sehfunktion. Da die Therapie aber nicht direkt neuroprotektiv oder -regenerativ wirkt, wird der Grad der Rückbildung von Sehstörungen, die sogenannte Restsymptomatik, nicht signifikant durch die Therapie beeinflusst. Ausser der Therapie mit Methylprednisolon existiert keine andere zugelassene Behandlungsmöglichkeit.

Nebst der hohen Prävalenz und klinischen Relevanz bietet die Optikusneuritis ein einzigartiges Modell, um die Demyelinisierung und Degeneration von Neuronen und deren Axonen, sowie mögliche Therapieeffekte auf diese Prozesse hin zu untersuchen: Eine Optikusneuritis kann in ihrem Auftreten einem ungefähren Zeitfenster und in ihrer Auswirkung auf die Integrität des Gewebes einer anatomisch gut begrenzten Struktur, nämlich dem visuellen System, zugeordnet werden. Durch die retinotopie Organisation des visuellen Systems ist die strukturelle Integrität eng mit der klinischen Funktionsweise verknüpft. Mit geeigneten Methoden wie beispielweise der optischen Kohärenztomographie (optical coherence tomography, OCT) oder mit technisch fortgeschrittenen Verfahren der Magnetresonanztomographie wie der Diffusions-Tensor-Bildgebung (diffusion tensor imaging, DTI) kann nahezu das komplette visuelle System untersucht werden. Zudem kann die Funktionsweise mit leicht anwendbaren, diagnostischen Methoden, wie der Überprüfung des Niederkontrastsehens, beurteilt werden. Daher bietet die Optikusneuritis ein optimales Studienparadigma, um die Folgen eines MS-Schubes auf die Integrität und Funktion des betroffenen Gewebes zu untersuchen.

Im ersten Abschnitt dieser Doktorarbeit haben wir anhand der bestehenden Literatur die zunehmende Bedeutung der nichtinvasiven Messungen der Dicke der einzelnen Netzhautschichten mittels der optischen Kohärenztomographie zusammengefasst, um pathologische Veränderungen im visuellen System von MS-Patienten zu charakterisieren. Es scheint, dass insbesondere die Dicke

Zusammenfassung

der makulären Ganglienzell- und der inneren Plexiformen Schicht (ganglion cell and inner plexiform layer, GCIP), sowie der peripapillären Nervenfaserschicht (peripapillary retinal nerve fiber layer, pRNFL) aussagekräftig sind im Hinblick auf die Früherkennung von neuronalen, sowie langfristigen axonalen Schädigungen der retinalen Ganglienzellen. Parameter der optischen Kohärenztomographie widerspiegeln aber nicht nur die visuelle Funktion, sondern scheinen auch mit anderen klinisch relevanten Parametern wie beispielsweise der Hirnatrophie oder dem EDSS-Wert (Expanded Disability Status Scale), welcher den Schweregrad der Behinderung eines MS-Patienten angibt, zu korrelieren. Im von uns verfassten Review wird zudem auch die Rolle der makulären inneren Körnerschicht (inner nuclear layer, INL) von MS-Patienten hinsichtlich ihrer möglichen Assoziation mit der entzündlichen Krankheitsaktivität und dem Ansprechen auf Behandlungen besprochen.

Obwohl bereits eine grosse Anzahl von Querschnittsstudien veröffentlicht wurde, die die Bedeutung der optischen Kohärenztomographie bei Patienten mit einer Optikusneuritis untersucht haben, sind Längsschnittstudien noch relativ selten. Diese sind jedoch unabdingbar, um die zeitliche Abfolge und das Ausmass der neuro-axonalen Schädigung der Netzhaut, sowie der visuellen Funktion als Folge einer Optikusneuritis besser zu verstehen. Deshalb haben wir in einer retrospektiven Längsschnittstudie Daten von 41 Patienten mit einer erstmaligen akuten Optikusneuritis über ein Jahr analysiert. Veränderungen der Netzhautstruktur und der Sehfunktion des betroffenen wie auch des nicht-betroffenen Auges wurden mittels der optischen Kohärenztomographie sowie der Überprüfung des Hoch- und Niederkontrastsehens beschrieben. Es zeigte sich, dass die durchschnittliche GCIP-Dicke, in den betroffenen Augen über die Zeit signifikant abgenommen hat. Bereits einen Monat nach Beginn der Optikusneuritis wurde nahezu 75 % der während eines Jahres gemessenen GCIP-Abnahme erreicht. Auch bei der pRNFL wurde im Durchschnitt drei Monate nach Beginn der Optikusneuritis bereits 87,8 % der Dickenreduktion erreicht. Darüber hinaus stellten wir fest, dass die INL-Dicke der betroffenen Augen einen Monat nach Symptomstart signifikant erhöht war. Überraschenderweise war aber auch die INL-Dicke der kontralateralen, nicht-betroffenen Augen zwölf Monate nach Erstmanifestation signifikant erhöht, ein Befund der so noch nicht in der bestehenden Literatur zu finden ist. Es ist möglich, dass eine subklinische Beteiligung des nicht-betroffenen Auges zu diesem INL-Anstieg führte, was auf eine bilaterale Netzhautpathologie bei klinisch einseitiger Optikusneuritis hinweisen würde. Weitere Untersuchungen sind jedoch erforderlich, um diese Hypothese zu bestätigen. Zusätzlich beobachteten wir, dass die visuelle Funktion der betroffenen Augen zu Beginn der Optikusneuritis sehr stark beeinträchtigt war. Obwohl eine Verbesserung über die Zeit festzustellen war, insbesondere im Hochkontrastsehen, blieb das Niederkontrastsehen der betroffenen Augen bis zum Ende der Studie klinisch relevant beeinträchtigt. Unsere Daten haben auch eine wichtige Konsequenz für zukünftige Therapiestudien und Therapieanwendungen, indem sie die Wichtigkeit einer frühzeitigen Behandlung bei

Zusammenfassung

Optikusneuritiden hervorheben, um permanente neurodegenerative Veränderungen der Netzhaut zu verhindern.

Pathologische Veränderungen des Sehnervs und der Netzhaut wurden auch in einem Mausmodell für die MS, der sogenannten Experimentellen autoimmunen Enzephalomyelitis (EAE), beschrieben. In einer Längsschnittstudie haben wir die Mechanismen, die der Optikusneuritis-induzierten Pathologie zu Grunde liegen, mithilfe einer multimodalen Bildgebungsplattform in EAE-Mäusen weiter untersucht. Da die Netzhaut frei von Myelin ist, kann ein wichtiger Treiber für die Entwicklung von permanenten neuro-axonalen Schäden nach einer Optikusneuritis, nämlich die Demyelinisierung, mithilfe der optischen Kohärenztomographie nicht analysiert werden. Deshalb wurde untersucht, ob sich die Anwendung von nichtinvasiver Diffusions-Tensor-Bildgebung, welche die Untersuchung des myelinisierten Anteils des Sehnervs erlaubt, als nützlich erweist, um die Optikusneuritis-assoziierte Pathologie weiter zu erforschen. In Übereinstimmung mit bereits bestehender Literatur fanden wir eine allmähliche Abnahme der fraktionalen Anisotropie im Sehnerv und in der Sehbahn von EAE-Mäusen, was mit einer Abnahme der richtungsabhängigen Diffusion von Wassermolekülen gleichkommt und somit indirekt auf eine Schädigung der weissen Substanz hindeutet. Parallel dazu nahm die radiale Diffusivität, das heisst, die Diffusion senkrecht zu den Nervenfasern bei EAE-Mäusen über die Zeit signifikant zu und wies somit auf eine Demyelinisierung der Axone hin. Daraus haben wir geschlossen, dass die Diffusions-Tensor-Bildgebung zur Erfassung der EAE-induzierten Demyelinisierung im Sehnerv sowie der Sehbahn im Mausmodell von Nutzen ist. Um eine irreversible Schädigung des neuro-axonalen Gewebes und die damit verbundene neurologische Behinderung zu vermeiden, erweist sich die Suche nach neuen Therapiestrategien zur Verhinderung der Demyelinisierung oder zur Verbesserung der Remyelinisierung als zunehmend wichtig im Bereich der MS-Forschung. Entsprechend wichtig ist die Verfügbarkeit von Methoden, die genau jene Prozesse evaluieren können.

Gegenwärtig kann Patienten, die an einer Optikusneuritis erkrankt sind, keine zufriedenstellende Therapie, die neuroprotektive oder regenerative Wirkung hat und so auf die Erhaltung beziehungsweise Wiedererlangung der Sehfunktion abzielt, angeboten werden. Da die Sehfunktion von MS-Patienten als eine der wichtigsten Körperfunktionen eingestuft wurde, bleibt die hohe Prävalenz von anhaltenden visuellen Einschränkungen im Anschluss an eine Optikusneuritis damit ein ungelöstes Problem im Krankheitsmanagement. In der Hoffnung, die zukünftige Behandlung von Betroffenen zu verbessern, führten wir eine interdisziplinäre Literaturrecherche zur Suche nach neuen Therapieansätzen durch. Dabei sind wir auf eine beträchtliche Anzahl von präklinischen und klinischen Studien gestossen, die postulieren, dass eine nichtinvasive, leichte Wechselstromstimulation der Netzhaut und des Sehnervs bei Optikusneuropathien unterschiedlicher Ursachen eine neuroprotektive sowie regenerierende Wirkung auf die retinalen Ganglienzellen haben kann. Bis zum heutigen Zeitpunkt gibt es jedoch keine Studien, die das

Zusammenfassung

Potential dieser sogenannten repetitiven transorbitalen Wechselstromstimulationstherapie spezifisch bei Patienten mit einer Optikusneuritis untersucht haben. Basierend auf Erkenntnissen aus bereits bestehenden Studien diskutieren wir im letzten Abschnitt dieser Doktorarbeit die Gründe warum diese Therapie eine fördernde Wirkung auf die Remyelinisierung, sowie auf andere protektive und regenerative Mechanismen haben könnte und dadurch auch bei Patienten mit einer erstmaligen, akuten Optikusneuritis das Sehvermögen langfristig verbessern könnte. Zudem stellen wir ein Studiendesign vor, um die Sicherheit, Verträglichkeit und vorläufige Wirksamkeit dieser Therapie bei Patienten mit einer erstmaligen, akuten Optikusneuritis optimal zu untersuchen.

Table of contents

Table of contents

Acknowledgments	2
Summary.....	3
Zusammenfassung.....	6
List of figures.....	15
List of tables	16
List of abbreviations	17
1 General introduction.....	20
1.1 Preface.....	20
1.2 Multiple sclerosis.....	20
1.3 Optic neuritis	23
1.3.1 Multiple sclerosis associated optic neuritis	23
1.3.2 Inflammatory optic neuritis not associated with multiple sclerosis.....	24
1.3.3 Murine experimental autoimmune optic neuritis.....	24
1.4 The visual pathway	25
1.4.1 The afferent visual pathway.....	25
1.4.2 The human retina and optic nerve.....	26
1.4.3 The murine retina and optic nerve.....	27
1.4.4 Assessing the integrity of the visual system	28
1.5 Transcranial electrical stimulation.....	29
1.6 Objectives and Outline	32
1.6.1 Chapter 2	32
1.6.2 Chapter 3	33
1.6.3 Chapter 4	33
1.6.4 Chapter 5	33
1.6.5 Chapter 6	33
2 Optical coherence tomography as a means to characterize visual pathway involvement in multiple sclerosis.....	34
2.1 Preface.....	34
2.2 Abstract.....	34
2.3 Introduction	34
2.4 Optical coherence tomography.....	36
2.5 Characterising visual pathway involvement with OCT	38

Table of content

2.5.1	Optic neuritis	38
2.5.2	Microcystic macular oedema	42
2.5.3	Primary retinal pathology.....	43
2.5.4	Posterior visual pathway pathology	43
2.6	Clinical relevance of OCT findings in MS.....	44
2.7	Conclusion	47
2.8	Author Contributions.....	47
2.9	Affiliations.....	47
2.10	Financial support and sponsorship	48
2.11	Conflicts of interest.....	48
3	Bilateral retinal pathology following a first-ever clinical episode of autoimmune optic neuritis.....	49
3.1	Preface.....	49
3.2	Abstract.....	49
3.3	Introduction	49
3.4	Methods	50
3.4.1	Study design	50
3.4.2	Standard protocol approvals, registrations, and patient consents.....	50
3.4.3	Subject eligibility.....	50
3.4.4	Visual acuity.....	51
3.4.5	Optical coherence tomography.....	51
3.4.6	Statistics.....	51
3.5	Results	52
3.5.1	Patient demographics and clinical characteristics.....	52
3.5.2	Structural retinal damage following ON	52
3.5.3	Visual functional changes following ON.....	56
3.5.4	Association between macular damage and visual outcomes	57
3.6	Discussion.....	57
3.7	Author Contributions.....	61
3.8	Acknowledgments	62
3.9	Study funding	62
3.10	Affiliations.....	62
3.11	Disclosures	62
3.12	Supplemental Data.....	63
4	Longitudinal characterization of afferent visual pathway pathology in experimental optic neuritis using a multimodal imaging approach	65

Table of content

4.1	Preface.....	65
4.2	Introduction	65
4.3	Feasibility study.....	66
4.3.1	Methods	66
4.3.1.1	Animals.....	67
4.3.1.2	MRI assessment	67
4.3.2	Results.....	70
4.3.3	Discussion.....	71
4.4	Longitudinal reliability study.....	72
4.4.1	Methods	72
4.4.1.1	Animals.....	72
4.4.1.2	MRI assessment	72
4.4.1.3	Statistics	72
4.4.2	Results.....	73
4.4.3	Discussion.....	73
4.5	Longitudinal sensitivity study	75
4.5.1	Methods	75
4.5.1.1	Animals.....	75
4.5.1.2	MRI assessment	76
4.5.1.3	Statistics	76
4.5.2	Results.....	77
4.5.2.1	Clinical assessment	77
4.5.2.2	MRI assessment	77
4.5.3	Discussion.....	82
4.5.3.1	Diagnosis of EAE-induced ON using T2-weighted imaging	83
4.5.3.2	Assessment of EAE-induced optic nerve pathology using DTI	83
4.5.3.3	Assessment of EAE-induced optic tract pathology using DTI	86
4.5.3.4	Conclusion	87
4.5.3.5	Limitations and Outlook.....	88
4.6	Author Contributions.....	89
4.7	Acknowledgements	89
4.8	Study funding	89
5	Repetitive transorbital alternating current stimulation (rtACS) in human acute optic neuritis: Design of a pilot study to test safety, tolerability and preliminary efficacy (ACSON)	90
5.1	Preface.....	90
5.2	Abstract.....	90
5.3	Introduction	90

Table of content

5.3.1	Background.....	90
5.3.2	Preclinical evidence for beneficial effects of optic nerve stimulation	92
5.3.3	Clinical evidence for beneficial effects of optic nerve stimulation.....	94
5.3.4	Optic nerve stimulation in ON – explanation for choice of study population	96
5.3.5	Study significance, aims, hypotheses and outcomes.....	98
5.4	Methods	99
5.4.1	Study design	99
5.4.2	Standard protocol approvals, registrations, and patient consents.....	100
5.4.3	Randomization and masking	100
5.4.4	Participants / subject eligibility.....	101
5.4.5	Study outcomes	102
5.4.6	Safety and tolerability assessments	102
5.4.7	Visual acuity.....	102
5.4.8	Optical coherence tomography.....	103
5.4.9	Colour vision	103
5.4.10	Perimetry.....	103
5.4.11	Vision-related quality of life (vision-related QoL) questionnaire	103
5.4.12	Pattern-reversal visual evoked potential (PR-VEP)	103
5.4.13	Patient demographics and clinical characteristics.....	104
5.4.14	Assessments in Participants Who Prematurely Stop the Study	104
5.4.15	Repetitive transorbital alternating current stimulation	104
5.4.16	Standard-of-care corticosteroid treatment for ON	106
5.4.17	Concomitant interventions.....	106
5.4.18	Data management.....	106
5.4.19	Proposed statistical analyses	107
5.5	Author Contributions.....	110
5.6	Acknowledgement.....	110
5.7	Study funding	111
5.8	Supplemental Data.....	112
5.8.1	Supplemental tables.....	112
5.8.2	Inclusion criteria	115
5.8.3	Exclusion criteria.....	116

Table of content

5.8.4	Criteria for withdrawal/ discontinuation of participants	116
5.8.5	Safety outcomes	117
5.8.6	Primary efficacy outcomes	117
5.8.7	Secondary efficacy outcomes.....	117
5.8.8	Other Outcomes of Interest	117
6	General Conclusions and Outlook	118
6.1	OCT as a means to characterize visual pathway involvement in MS.....	118
6.2	Bilateral retinal pathology following a first-ever clinical episode of autoimmune ON	119
6.3	Longitudinal characterization of AVP pathology in experimental ON using a multimodal imaging approach	122
6.4	Repetitive transorbital alternating current stimulation in human acute ON: Design of a pilot study to test safety, tolerability and preliminary efficacy (ACSON)	125
6.5	Concluding remarks	127
	References.....	128
	Curriculum Vitae.....	146

List of figures

Figure 1-1. Illustration of typical stimulation waveforms delivered by tDCS and tACS.....	29
Figure 2-1. Segmented macula OCT B-scan of a healthy individual.. ..	36
Figure 2-2. Spectral-domain OCT scan protocols.	38
Figure 2-3. Typical OCT findings in MS patients with a previous ON: pRNFL thickness.	40
Figure 2-4. Typical OCT findings in MS patients with a previous ON: pRNFL trend report.....	40
Figure 2-5. Typical OCT findings in MS patients with a previous ON: GCL thinning.....	41
Figure 2-6. Typical OCT findings in MS patients with a previous ON: INL thickening.	42
Figure 2-7. Typical OCT findings in MS patients: microcystic macular oedema.	43
Figure 2-8. Typical OCT findings in MS patients without a previous ON: pRNFL thickness.....	44
Figure 3-1. Longitudinal retinal thickness in ON.....	54
Figure 3-2. Longitudinal visual acuity in ON.....	57
Figure 3-3. Structure-function correlation in ON.....	57
Figure 4-1. Sequence planning and slice selection for DTI and T2.	68
Figure 4-2. DTI analysis.....	69
Figure 4-3. FA maps obtained with the DTI protocol that was established in the feasibility study..	71
Figure 4-4. Longitudinal reliability of DTI measures.	74
Figure 4-5. Longitudinal body weight and EAE scores.....	77
Figure 4-6. Longitudinal T2-weighted scans.	78
Figure 4-7. Longitudinal FA and MD.	80
Figure 4-8. Longitudinal AD and RD.	81
Figure 4-9. Longitudinal FA maps.....	82
Figure 5-1. Schematic presentation of the study design and study procedures.....	100
Figure 5-2. Determination of individual stimulation parameters.....	105
Figure 5-3. Example of the therapy protocol at a single treatment day.....	106

List of tables

Table 3-1. Patient demographics and clinical characteristics at baseline examination.53

Table 3-2. Retinal thickness in NON eyes at baseline and in ON eyes over a 12-month period. ...55

Table 3-3. Retinal thickness in NON eyes over a 12 month period.....55

Table 3-4. Retinal thickness in NON eyes at baseline and in ON eyes in females.....63

Table 3-5. Retinal thickness in NON eyes at baseline and in ON eyes in males.63

Table 3-6. HCVA and LCVA in NON and ON eyes over a 12 month period.64

Table 4-1. DTI measurements in control and EAE mice in the optic nerve.78

Table 4-2. DTI measurements in control and EAE mice in the optic tract.79

Table 5-1. Clinical studies testing rtACS in optic neuropathies.....112

Table 5-2. Schedule of study visits and assessments for individual study participants.115

List of abbreviations

ACS: alternating current stimulation
ACSON trial: alternating current stimulation in optic neuritis trial
AD: axial diffusivity
ADEM: acute disseminated encephalomyelitis
AE: adverse event
AP: action potential
APC: antigen-presenting cell
APOSTEL: Advised Protocol for OCT Study Terminology and Elements
APP: amyloid precursor protein
AQP4: astrocytic water channel aquaporin-4
ART: automatic real-time tracking
AVP: afferent visual pathway
BBB: blood-brain barrier
BDNF: brain-derived neurotrophic factor
BM: Bruch's membrane
BRB: blood-retinal barrier
CCT: Cambridge Colour Test
CFA: complete Freund's adjuvant
CI: confidence interval
CIS: clinically isolated syndrome
CNS: central nervous system
CSF: cerebrospinal fluid
CTC: Clinical Trials Center
DA: detection ability
DMT: disease-modifying therapies
Dpi: days post immunization
DTI: diffusion tensor imaging
EAE: experimental autoimmune encephalomyelitis
eCRF: electronic case report forms
EDSS: Expanded Disability Status Scale
ELM: external limiting membrane
EPI: echo-planar imaging
ERG: electroretinography
ETDRS: Early Treatment of Diabetic Retinopathy Study
EV: eigenvalue
EVP: efferent visual pathway
FA: fractional anisotropy
fMRI: functional magnetic resonance imaging
GABA: γ -aminobutyric acid
GCIP: ganglion cell and inner plexiform layer
GCL: ganglion cell layer
GAF: green autofluorescence imaging
GFAP: glial fibrillary acidic protein
HCVA: high-contrast visual acuity
HLA: histocompatibility leukocyte antigen
HRA: Heidelberg Retina Angiograph
IBA1: allograft inflammatory factor 1
IGF-1: Insulin-like growth factor 1

List of abbreviations

ILM: inner limiting membrane
IL-1 β : interleukin 1 beta
IMD: investigational medical device
INL: inner nuclear layer
IPL: inner plexiform layer
IRL: inner retinal layer
ITT: intention to treat
LCVA: low-contrast visual acuity
LGN: lateral geniculate nucleus
Lme: linear mixed-effects model
LogMAR: logarithm of the minimum angle of resolution
LTD: long-term depression
LTP: long-term potentiation
MBP: myelin basic protein
MD: mean diffusivity
MME: microcystic macular oedema
MoA: mode of action
MOG: myelin oligodendrocyte glycoprotein
MRI: magnetic resonance imaging
MS: multiple sclerosis
MSD: mean standard deviation
M0: month 0, M1: month 1, M3: month 3, M6: month 6, M12: month 12
N: nasal
n: number of subjects
NEFM: neurofilament-M
NEI-VFQ-25: National Eye Institute Visual Function Questionnaire-25
NIBS: non-invasive brain stimulation
NMDA: N-methyl-D-aspartate
NMOSD: Neuromyelitis optica spectrum disorder
NON: non optic neuritis
OCT: optical coherence tomography
OD: oculus dexter/ right eye
ON eyes: refer to the optic neuritis eyes of the main study cohort
ON: optic neuritis
ONH: optic nerve head
ONL: outer nuclear layer
ONNT: optic neuritis treatment trial
OPC: oligodendrocyte progenitor cells
OPL: outer plexiform layer
OS: oculus sinister/ left eye
PLP: proteolipid protein
PMB: papillomacular bundle
PP: per protocol
PPMS: primary progressive diseases course
PR: photoreceptors
pRNFL: peripapillary retinal nerve fibre layer
QoL: quality of life
RD: radial diffusivity
RF: radiofrequency

List of abbreviations

RGC: retinal ganglion cell
RIS: radiologically isolated syndrome
RNFL: retinal nerve fibre layer
RNS: reactive nitrogen species
ROI: region-of-interest
ROS: reactive oxygen species
RRMS: relapsing-remitting MS
rtACS: repetitive transorbital alternating current stimulation
SAE: severe adverse event
SC: superior colliculus
SD: standard deviation
SD-OCT: Spectral-domain OCT
SPMS: secondary progressive disease course
SSL: Stroke severity level
STDP: spike-timing-dependent plasticity
T: temporal
TNF- α : tumour necrosis factor alpha
tACS: transcranial alternating current stimulation
TcES: transcorneal electrical stimulation
tDCS: transcranial direct current stimulation
tES: transcranial electrical stimulation
TMEM119: transmembrane protein 119
TMS: transcranial magnetic stimulation
tRNS: transcranial random noise stimulation
TTX: tetrodotoxin
USZ: University Hospital Zurich
VA: visual acuity
VEP: visual evoked potential
VF: visual field
VRT: visual restitution training
V1: primary visual cortex
WM: white matter
YFP: yellow fluorescent protein
 Δ GCIP, Δ INL, Δ pRNFL: the difference between the retinal layer thickness of an ON eye at each time point and the retinal layer thickness of the corresponding NON eye at baseline

1 General introduction

1.1 Preface

The text of this chapter is partially taken from C.A. Wicki's master thesis entitled "Temporal dynamics of structural and functional retinal damage in acute optic neuritis" (accepted in 2017 by ETH D-HEST. Supervised by S. Schippling and M. Schwab).

1.2 Multiple sclerosis

Multiple sclerosis (MS) is a chronic inflammatory, multifocal, demyelinating and neurodegenerative autoimmune disease of the central nervous system (CNS). MS is primarily thought to result from a breakdown of immune tolerance against components of the myelin sheath that surrounds the axons of CNS neurons (Steinman 2001).

With more than two million people affected worldwide, MS is among the most frequent causes of neurological disability in young adults with a typical age of 20 - 40 years at first manifestation (Kingwell et al. 2013). As in many other autoimmune disorders, there is a female preponderance in MS, with reported gender ratios ranging from 1.1 to 3 females : 1 male (Luessi, Siffrin, and Zipp 2012; Kingwell et al. 2013).

The aetiology of MS has not been completely understood, but an interplay between a complex polygenetic trait and environmental risk factors is likely involved. Genetic risk factors are mainly associated with the histocompatibility leukocyte antigen (HLA) gene complex, with the HLA-DR15 haplotype playing a major role in MS (Sospedra and Martin 2005, 2016). Infection with Epstein-Barr virus, a lack of vitamin D, obesity in early life and cigarette smoking are among the most important environmental risk factors (Ascherio and Munger 2007a, 2007b, 2016).

The immunopathogenesis in MS is a very complex multicellular process and is still not fully understood. From central tolerance escaped, activated autoreactive CD4⁺ and CD8⁺ T-cells from the periphery enter the CNS through the blood-brain barrier (BBB) (via the perivascular space) or the blood-cerebrospinal fluid (CSF) barrier (via the subarachnoid space) and target CNS myelin antigens like myelin basic protein (MBP), proteolipid protein (PLP) and myelin oligodendrocyte glycoprotein (MOG) (Lubetzki, Williams, and Stankoff 2005; Goverman 2009; Sospedra and Martin 2016). There, CNS-resident antigen-presenting cells (APCs) such as macrophages, dendritic cells and likely also microglial and astroglial cells, reactivate the locally infiltrated T-cells which, in response, secrete pro-inflammatory cytokines (e.g. tumour necrosis factor, IFN γ , IL-17). These soluble mediators (particularly chemokines and adhesion molecules) trigger the recruitment of other immune cells, including activated microglia, astrocytes, macrophages and dendritic cells, thereby amplifying

cytokine release even further (Roed et al. 2005; Goverman 2009; Lubetzki and Stankoff 2014). Furthermore, the activity of immunomodulatory regulatory T-cells appear to be suppressed in MS, particularly in the relapsing-remitting phase (Sospedra and Martin 2016). In recent years, it has become clear that B-cells are also involved in MS pathology. They act as APCs for autoreactive T-cells, secrete pro-inflammatory cytokines and produce pathogenic myelin-specific antibodies from differentiated plasma cells (Sospedra and Martin 2005; Lubetzki and Stankoff 2014). The exact role of B-cells is still not completely understood, but their importance is further supported by the beneficial effects of B-cell depleting antibody-therapies like Rituximab (trade name: MabThera®) and Ocrelizumab (trade name: Ocrevus®) (Martin et al. 2016). An interplay of all these cells and associated secretion products (cytokines, reactive oxygen (ROS) and nitrogen (RNS) species, proteolytic enzymes, etc.) create a hostile, pro-inflammatory environment and mediate the demyelination and local axonal damage, that eventually results in the initiation of apoptotic signalling cascades, secondary degeneration and related clinical disability in MS (Siffrin et al. 2010; Friese, Schattling, and Fugger 2014; Mahad, Trapp, and Lassmann 2015).

Alternatively, in a subset of MS patients, it has been proposed that the disease evolves directly within the CNS through neurodegenerative processes rather than immunopathological mechanisms starting in the periphery (Siffrin et al. 2010; Sospedra and Martin 2016; Brambilla 2019).

MS has a heterogeneous clinical presentation but is most often defined by an early, mainly inflammatory and a later, predominantly neurodegenerative, stage of disease (Steinman 2001). In the early stage of the disease, 85 % of patients suffer from relapsing-remitting MS (RRMS). Patients show different neurological deficits during relapsing phases, including optic neuritis (ON), limb weakness, ataxia and sensory disturbances (Steinman 2001). These characteristic attacks are followed by varying periods of remission. This first stage of the disease is thought to be mainly mediated by autoimmune reactions resulting in acute inflammation and demyelinating lesions in the brain and spinal cord (Steinman 2001). Due to the brain's compensatory mechanisms, some patients exhibit almost no clinical disability in episodes of remission, although nerve fibres start to decline irreversibly even in this early stage of the disease (Bjartmar, Wujek, and Trapp 2003; Luessi, Siffrin, and Zipp 2012; Mahad, Trapp, and Lassmann 2015). Hence, neurodegenerative processes already play an important role early in the disease course. Reasons for this are not yet fully understood, but the failure of efficient remyelination appears to play a significant role (Franklin and Ffrench-Constant 2008; Luessi, Siffrin, and Zipp 2012). Chronic demyelination is thought to be an important contributor to axonal degeneration (Bruce, Zhao, and Franklin 2010; You et al. 2020). However, grey matter structures are also affected, even during the earliest phases of the disease (Calabrese et al. 2015). Further, the retina, which contains unmyelinated axons, is strongly affected in many MS patients,

suggesting that there are several other important triggers besides the failure of efficient remyelination, which contribute to neurodegeneration in MS (Green et al. 2010).

Approximately 10 years after disease onset, the majority of patients develop gradually to a secondary progressive disease course (SPMS) highlighted by further axonal loss, chronic demyelinated lesions, gliosis and atrophy of the brain and spinal cord. This phase is mostly responsible for progressive chronic neurological disability in patients (Prineas et al. 2001; Ayache and Chalah 2016).

About 10 % of MS cases have a primary progressive disease course (PPMS) (Bogosian et al. 2016). PPMS patients are affected by a relatively slow, but non-remitting, worsening disease course that even characterizes disease onset (Lublin et al. 2014; Bogosian et al. 2016). Despite a lot of similarities between the three subtypes of MS, each of them have their own specific clinical challenges.

According to the latest revisions of the McDonald diagnostic criteria, the current diagnosis of MS is based on clinical and paraclinical findings, mainly including magnetic resonance imaging (MRI) of the CNS and laboratory testing such as inspecting for CSF-specific oligoclonal bands. This criteria is built up on two main principles: dissemination of clinical episodes or lesions in time, meaning that lesions have to be present at different time points and dissemination of lesions in space, implying that lesions have to occur in at least two independent loci within the CNS (Polman et al. 2011; Thompson et al. 2018).

A monophasic clinical episode resembling the characteristics of a typical MS attack, but not yet fulfilling the criteria of dissemination in time, is called clinically isolated syndrome (CIS). The absence of clinical symptoms but a coincidental MRI finding suggestive of MS is called radiologically isolated syndrome (RIS). These patients have a higher risk to eventually develop MS (Lublin et al. 2014; Thompson et al. 2018).

Most of the currently approved disease-modifying MS therapeutics primarily target the early inflammatory phase of the disease through immunomodulatory and immunosuppressive mechanisms (Luessi, Siffrin, and Zipp 2012). Since there is a lack of approved neuroprotective and repair promoting treatments, there is a need for optimized therapeutic approaches that specifically target these aspects and thereby prevent chronic progressive disability (Aktas, Albrecht, and Hartung 2016; Villoslada 2016; Lubetzki et al. 2020).

To summarize, MS is characterized by inflammation, demyelination and neurodegeneration (Luessi, Siffrin, and Zipp 2012). Neuro-axonal damage can occur even in early stages of the disease and is

the pathological substrate of persistent disability in MS (Luessi, Siffrin, and Zipp 2012). Therefore, further understanding of the biological mechanisms and temporal evolution underlying neuro-axonal damage in MS is essential to identifying potential neuroprotective targets and the right time point for therapeutic interventions in the future (Tallantyre et al. 2010).

1.3 Optic neuritis

1.3.1 Multiple sclerosis associated optic neuritis

ON is an acute inflammatory and demyelinating insult of the optic nerve, that is often associated with MS (Toosy, Mason, and Miller 2014). Due to its high prevalence, ON is considered as one of the core characteristics of the disease. Typical ON symptoms include acute onset of pain upon eye movement and unilateral impairment of vision, for example colour vision deficits, impaired contrast vision and visual field dysfunction. Because spontaneous partial recovery is possible within the first weeks of ON onset, MS-associated ON has traditionally been considered to be relatively benign. However, today we know that residual visual deficits, particularly in low-contrast visual acuity (LCVA), are common, and are associated with permanent secondary neuro-axonal damage of the optic nerve and retina (Hickman et al. 2002; Walter et al. 2012b; Sanchez-Dalmau et al. 2017). This leads to a characteristic thinning of the inner retinal layers, in particular the macular ganglion cell layer (GCL) and the peripapillary retinal nerve fibre layer (pRNFL), that can be detected by optical coherence tomography (OCT) (Calabresi and Elliot M. Frohman 2015; Peter A. Calabresi et al. 2015).

Since the 'Optic Neuritis Treatment Trial' (ONTT) in 1992, high-dose corticosteroids are currently the best available approved therapy to treat acute ON (Beck et al. 1992). Nonetheless, the 1-year follow-up of the ONTT found that corticosteroids did not impact long-term visual outcome and only accelerated short-term functional recovery (Beck and Cleary 1993). Any significant long-term benefits of corticosteroids to visual outcomes following MS-associated ON presently remains unproven (Beck and Gal 2008; Shams and Plant 2009; Bennett, Nickerson, et al. 2015; Petzold et al. 2020). In ON patients refractory to short-term benefits of corticosteroids, plasma exchange might help (Bennett, Nickerson, et al. 2015; Jenkins and Toosy 2017).

Once the acute phase has subsided, inflammation eventually partially resolves and a certain degree of remyelination results in partial visual recovery (Toosy, Mason, and Miller 2014). Cortical plasticity may also play a role in visual recovery post-ON (Miller et al. 2005a). However, as in other CNS injuries, axonal regeneration after damage is very limited in the visual system (London, Benhar, and Schwartz 2013). Around the injured axons a neurotoxic environment is produced by different factors, including chronic demyelination, oxidative stress, shortage of neurotrophic factors, excitotoxic levels of neurotransmitters and the presence of molecules that inhibit neurite outgrowth, such as Nogo A (London, Benhar, and Schwartz 2013). As a consequence, visual deficits often persist in varying

degrees, presumably representing persistent demyelination and irreversible axonal loss (Hickman et al. 2004; Sanchez-Dalmau et al. 2017).

1.3.2 Inflammatory optic neuritis not associated with multiple sclerosis

In addition to MS, there are several other possible causes for ON. Among the various differential diagnoses, astrocytic water channel aquaporin-4 (AQP4)-antibody and MOG-antibody associated ON are two of the most important, and both are proposed to be associated with the risk of permanent severe visual deficits (Toosy, Mason, and Miller 2014; Jelcic et al. 2019; Sotirchos et al. 2019). Neuromyelitis optica spectrum disorder (NMOSD) is a rare autoimmune inflammatory astrocytopathic CNS disease that presents with a higher prevalence of optic nerve pathology (in particular ON) and spinal cord involvement (transverse myelitis) than MS (Jarius et al. 2008; Bennett, de Seze, et al. 2015). About 80 % of NMOSD patients are positive for a highly specific serum autoantibody against AQP4, collectively also known as NMO-IgG, which has facilitated the differentiation of NMOSD from MS (Papadopoulos and Verkman 2012). MOG-antibody associated diseases have recently also gained more interest, as – in addition to forms of paediatric acute disseminated encephalomyelitis (ADEM) – they appear to be at risk of both severe repeated ON and myelitis. Although sharing remarkably similar clinical phenotypes, MOG-associated disease is pathologically distinct from NMOSD patients positive for anti-AQP4 antibodies, in that the target antigen is directed at CNS myelin, therefore representing an oligodendropathy rather than astrocytopathy (Hohlfeld et al. 2016; Havla et al. 2017). MOG is expressed on the myelin surface and antibodies against it have been identified in a variety of autoimmune CNS diseases, including paediatric ADEM, subgroups of NMOSD and MS (Hohlfeld et al. 2016). Although showing significant clinical and pathological differences compared to MS, visual impairment, primarily due to acute ON, appear to be very prominent in all these diseases (Manogaran et al. 2016). Stiebel-Kalish and colleagues demonstrated that the effect of high-dose steroids on visual outcome in AQP4-, and anti-MOG- associated ON is critically dependent on the timing of application, with earlier intervention being superior (Stiebel-Kalish et al. 2019). Similar evidence for MS-associated ON is not yet available.

1.3.3 Murine experimental autoimmune optic neuritis

Inflammatory demyelination and neuro-axonal degeneration has also been described in murine experimental autoimmune ON, particularly in the context of MOG peptide-induced experimental autoimmune encephalomyelitis (EAE), the most broadly used animal model of MS (Sun et al. 2007; Horstmann et al. 2013; Dietrich et al. 2019).

In order to actively induce EAE, animals are injected with peptides of myelin proteins emulsified with strong adjuvants such as complete Freund's adjuvant and along also receive injections with pertussis toxin, which is supposed to have modulatory effects on the BBB (Constantinescu et al. 2011; Bittner et al. 2014). As a consequence, peripheral myelin-specific T-cells are activated and migrate across

the BBB into the CNS. Local reactivation of T-cells by APCs amplifies the inflammatory response even further. These animals eventually develop demyelinating lesions, neuro-axonal damage and gliosis, resembling MS pathology (Constantinescu et al. 2011; Bittner et al. 2014).

In MOG-induced ON, longitudinal OCT measures of the thicknesses of the inner retinal layers, which serve as a marker of neuro-axonal damage, have been shown to mirror a slightly accelerated, otherwise comparable dynamics as observed in human ON (Manogaran et al. 2018). In a longitudinal study over a time period of 33 days, it became visible that next to persistent inflammatory mediated demyelination, glial pathology is likely an important contributor to early neuro-axonal damage of the retinal ganglion cells (RGCs) in MOG-induced ON (Manogaran et al. 2019).

1.4 The visual pathway

1.4.1 The afferent visual pathway

From the retina, visual information travels along the optic nerve to the optic chiasm, where axons from the temporal halves of each retina continue into the optic tract on the same side, while axons from the nasal halves cross in the optic chiasm to the optic tracts on the contralateral side. The visual information continues along the optic tracts reaching the lateral geniculate nucleus (LGN) of the thalamus. From the LGN visual information travels through the optic radiations to the primary visual cortex (V1) where it is further processed. A minority of LGN fibres terminate in the superior colliculus (SC) rather than in V1, and are responsible for pupillary functions (Kolappan et al. 2009).

The visual pathway can be divided into the anterior pathway, including pre-geniculate structures and into the posterior pathway, including post-geniculate structures. This terminology should not be mistaken with the categorization of the afferent and the efferent visual pathway. The afferent visual pathway (AVP) consists of the retina, optic nerves, optic chiasm, optic tracts, LGN, optic radiations and the V1. The AVP is primarily dedicated to the perception, transmission and processing of visual information. ON is the most common AVP related clinical manifestation in MS patients (Costello 2016). The AVP is retinotopically organized, meaning that the spatial organization of retinal neurons and thus also of the representation of the visual field is preserved throughout the visual system. Anatomical integrity is perfectly linked with the clinical function and thus damage can be precisely mapped along the visual pathway (Costello 2013).

The efferent visual pathway (EVP) coordinates eye and pupillary movements. It encompasses the pupils and the associated autonomic pathways, neural mechanisms of ocular motility and the cranial nerves involved in eyelid function (Costello 2016). EVP symptoms are less frequently observed, but are also common in MS patients, typically manifesting as ocular misalignment, diplopia and nystagmus (Costello 2016).

1.4.2 The human retina and optic nerve

The retina and optic nerve, embryonically developed from the floor of the diencephalon, are considered a part of the CNS (London, Benhar, and Schwartz 2013). Once light transverses into the eye, it is pinpointed on the retina. Before arriving at the photoreceptors in the outer retina, light must first pass through the RNFL, GCL, inner plexiform layer (IPL), inner nuclear layer (INL; including the amacrine, bipolar, and horizontal cells), and the outer plexiform layer (OPL). The photoreceptors, more precisely the cones and rods, span the outer retina, with the synaptic processes found in the OPL, the cell bodies in the outer nuclear layer (ONL) and the inner segments (filled with mitochondria) as well as the outer segments (containing the light-sensitive photopigments) in the photoreceptor layer (Prasad and Galetta 2011).

The photoreceptors convert the electromagnetic energy of the light into an electrochemical signal (Syc et al. 2012). The electrochemical signal is modified through a series of cellular connections and relayed to the RGCs, whose cell bodies and dendrites are located in the GCL and IPL, respectively, while their axons constitute the RNFL. The retina is devoid of myelin and is therefore an exceptional CNS structure. As such, the retina appears to be an ideal model for investigating neuro-axonal degeneration without the interference of inflammatory demyelination. The RGC axons serve as the final common output pathway of visual information from the retina to the brain (Devin D. MacKay et al. 2015).

The macula is located temporal to the optic nerve head (ONH) and encompasses the fovea in its centre. The fovea contains the highest density of cones across the retina and is responsible for central vision (Hirsch and Curcio 1989). On the other hand, rods are almost absent in the fovea, but are mainly localized in the rod-dominated parafovea and perifovea (Srinivasan et al. 2008). The axons of the foveal ganglion cells exit the eye via the temporal margin of the ONH, forming the papillomacular bundle (PMB) (Prasad and Galetta 2011). A lack of retinal photoreceptors in the region of the optic disc gives rise to the monocular blind spot.

Besides the aforementioned neuronal cells, the retina also possesses Müller cells, the most abundant glial cell in the retina (Newman and Reichenbach 1996). Müller cells span the entire retina, with their cell bodies located in the INL (Petzold et al. 2014). Müller cells express numerous voltage-gated channels and neurotransmitter receptors and modulate neuronal activity by regulating the extracellular concentration of potassium ions, glutamate and γ -aminobutyric acid (GABA) (Newman and Reichenbach 1996). Thus, Müller cells play an important role in retinal function.

The blood-retinal barrier (BRB) consists of the outer vascular (tight junctions between retinal capillary endothelial cells) and the inner epithelial (tight junctions between retinal pigment epithelial cells)

components. It regulates ion, protein, and water flux across the retina, thereby maintaining the specialized retinal environment (Cunha-Vaz, Bernardes, and Lobo 2011; Runkle and Antonetti 2011). The BRB is essential for maintaining the eye as an immune privileged site, and is therefore required for proper vision (Cunha-Vaz, Bernardes, and Lobo 2011).

To summarize, the retina itself includes five types of neurons: photoreceptor cells, bipolar cells, horizontal cells, amacrine cells and ganglion cells. The main information flow from photoreceptors to the optic nerve goes along a three-neuron chain – from photoreceptors to bipolar cells to ganglion cells (Kolappan et al. 2009).

When the approximately 1.2 million axons of the RGCs leave each eye at the ONH, they form the optic nerve or also known as the cranial nerve II. The optic nerve is divided into the prelaminar intraocular segment and the compartments posterior to the lamina cribrosa, namely the intraorbital, intracanalicular, and intracranial segment. The ONH is dominated by the presence of astrocytes, which take over similar functions to the Müller cells (Brooks, Komáromy, and Källberg 1999). When RGC axons pass the lamina cribrosa, they are myelinated by oligodendrocytes and encompassed by all three meningeal layers (i.e. the pia mater, subarachnoid space filled with CSF, arachnoid mater and dura mater) (Selhorst and Chen 2009; Prasad and Galetta 2011). Similar to the retina, tight junctions are also found between capillary endothelial cells of the optic nerve, forming a blood-optic nerve barrier, which, however, appears to be absent in the prelaminar region of the ONH (Hayreh 2011). The optic nerve partially decussates at the optic chiasm and from there forms the optic tract, projecting primarily to the LGN and partially also to the SC (Prasad and Galetta 2011). Considering that more than 50 % of the brain's pathways are dedicated to functional networks related to the visual system, it is not surprising that vision is of paramount importance for quality of life (Prasad and Galetta 2011).

1.4.3 The murine retina and optic nerve

The murine and human AVP share many common characteristics including a similar gross architecture and functional organization of the retina, as well as similar wiring from the retina to the V1 with the LGN being the relay station (Brooks, Komáromy, and Källberg 1999; Chalupa and Williams (Eds.) 2008; Veleri et al. 2015). Nonetheless, the AVP of mice presents with some differences. The human retina contains three subtypes of cones, namely the L- (long, 564 nm), M- (medium, 533 nm) and S- (short, 437 nm) wavelength cones that allow for trichromatic vision, while in the mouse, a nocturnal animal, the retina consists of only two cone subtypes, lacking the L-cones. Moreover, the mouse retina lacks of a cone-only region such as the fovea found in humans (Veleri et al. 2015). Nonetheless, similar to humans, the mouse retina has only one type of rods (Veleri et al. 2015). In the murine GCL, more than 50 % of the cells are 'displaced' amacrine cells, while in the human GCL, it varies between 3 % found in the foveal region and up to 80 % in the peripheral region

(May 2008). Comparative to humans, the intraocular part of the RGCs is also void of myelin in mice, and the retrobulbar part is myelinated by oligodendrocytes. However myelination starts more posterior and a collagen-like structure similar to the human lamina cribrosa does not exist (May and Lutjen-Drecoll 2002; May 2008). Another difference is that in mice, the majority of RGC axons decussate at the optic chiasm, while in humans only approximately 50 % cross to the contralateral side (Erskine and Herrera 2014). Finally in mice, only a subpopulation projects to the LGN, whilst the majority of RGCs axons project to the SC of the midbrain unlike in humans where the LGN is the main target (Chalupa and Williams (Eds.) 2008).

1.4.4 Assessing the integrity of the visual system

In MS, visual function can be assessed by the use of high-contrast (HCVA) and LCVA charts, colour vision tests, visual field tests and vision-related quality of life questionnaires (e.g. the National Eye Institute Visual Function Questionnaire-25 (NEI-VFQ-25)) (Petzold et al. 2014; Balcer et al. 2015).

Electrophysiological tests, such as visual evoked potential (VEP) examinations, quantify the cortical response to defined visual stimuli, and may serve as an indication of demyelination, or remyelination (Hanson et al. 2016). The conventional idea is that an increase in the VEP latency indicates demyelination, while the subsequent recovery of conduction velocity indicates remyelination along the visual pathway (Odom et al. 2016; Petzold 2017).

Neuro-axonal damage within the AVP can indirectly be monitored by OCT (retina) and MRI (optic nerves, optic tracts, optic radiations and primary visual cortices) (Petzold 2017). Different MRI techniques are available for the assessment of inflammatory disease activity and neuro-axonal degeneration beyond the retina. Conventional T2- and T1-weighted MRI images including measures of T2 lesion load, T1 black holes and T1 post-gadolinium active lesions, are important indices to monitor disease activity and progression in MS clinical practice, however, they are not specific to the AVP (McFarland et al. 2002; Polman et al. 2011; Miller et al. 2014). In comparison, more advanced MRI techniques such as diffusion tensor imaging (DTI), can be used to indirectly probe the microstructural integrity of the white matter tracts, by characterizing the diffusivity of water and also the degree of tissue anisotropy at specific locations along the AVP (Mori and Zhang 2006; Aung, Mar, and Benzinger 2013; Kuchling et al. 2017).

As such, almost the entire AVP can be probed by the use of safe non-invasive *in vivo* multimodal imaging tools, with most techniques being readily available for both humans and mice. Thus, the AVP may serve as a model to translationally investigate the complex processes of autoimmune inflammatory demyelination and neurodegeneration, the main contributor of clinical disability in MS (Luessi, Siffrin, and Zipp 2012).

1.5 Transcranial electrical stimulation

Transcranial magnetic stimulation (TMS) and transcranial electrical stimulation (tES) are the most often used non-invasive brain stimulation (NIBS) techniques to induce or modulate neural activity. In the case of TMS, a waveform generator passes current to a coil which is held over the subject's head, whereas in tES, current is sent to electrodes which are typically placed on the scalp. In the brain, an exogenous electric field is induced by the time-varying magnetic field of the coil (Faraday's law) or directly injected through the current conducted from the electrodes (Paulus, Peterchev, and Ridding 2013). Typically, but not always, TMS induces timed bursts of action potentials (APs) through suprathreshold stimulation, while tES does not directly induce APs when a neuron is silent, but rather modulates spontaneous neuronal activity through subthreshold stimulation (Paulus, Peterchev, and Ridding 2013; Reed and Cohen Kadosh 2018). In both techniques, neural membrane polarization shifting is thought to be the main biological mechanism involved (Peterchev et al. 2012).

This section is not intended to introduce all aspects of NIBS techniques in detail, but rather to give a broad overview focusing on alternating current stimulation (ACS) approaches. Existing tES techniques include the frequently used transcranial applied protocols such as transcranial direct current stimulation (tDCS), alternating current stimulation (tACS) and random noise stimulation (tRNS), but also the less often used repetitive transorbital alternating current stimulation (rtACS) and transcorneal electrical stimulation (TcES) protocols (Bikson et al. 2019).

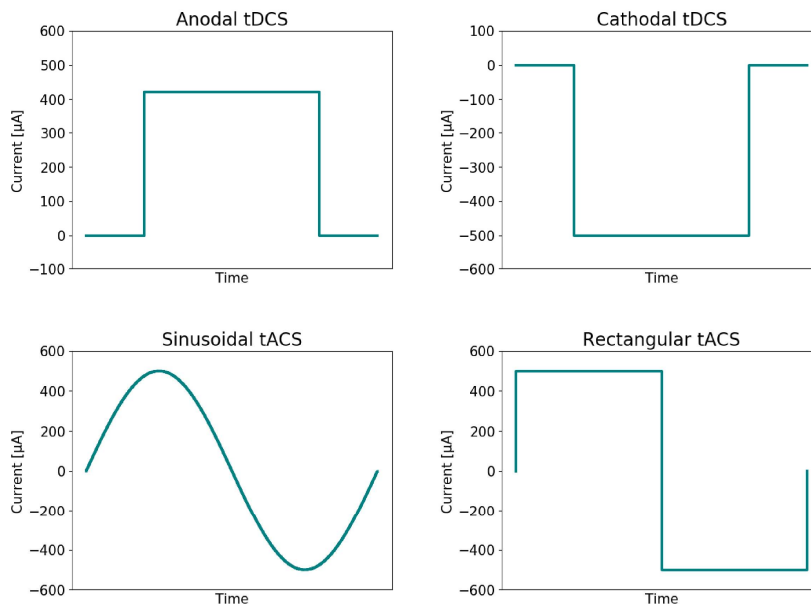


Figure 1-1 Illustration of typical stimulation waveforms delivered by transcranial direct current stimulation and alternating current stimulation.

In transcranial direct current stimulation (tDCS), low-intensity (anodal and cathodal) constant electric current is applied (first row). In alternating current stimulation (tACS), low-intensity alternating current, typically with a biphasic sinusoidal or sometimes rectangular waveform, is applied (second row).

Anodal tDCS will increase cortical excitability of the brain area below the electrode by depolarizing the resting membrane potential, thus pushing the neurons closer to their threshold potential, whereas cathodal tDCS will decrease cortical excitability by hyperpolarizing the transmembrane potentials, thus decreasing the spontaneous firing rate (Paulus 2011; Stagg and Nitsche 2011).

The application of an alternating current in tACS (in contrast to direct current in tDCS) fluctuates the membrane potential around its resting potential, typically in a sinusoidal wave (Antal and Paulus 2013; Reed and Cohen Kadosh 2018) (**Figure 1-1**). tACS intends to interact with the brain's ongoing natural cortical oscillatory activity and coherence, which may be altered in psychiatric disorders (Buzsaki and Watson 2012) but also diseases such as MS (Backner et al. 2020). Physiological brain rhythms or oscillations endogenously generated by fluctuations in local field potentials (induced by synchronous firing of neuronal populations) include a broad range of frequencies, some of them being linked to specific brain locations and behaviours (Battleday et al. 2014). These oscillations have been shown to play an important role in the communication within and across brain areas and thus the functioning of the brain as a whole (Buzsaki and Watson 2012; Battleday et al. 2014). For example, α -rhythms (8-12 Hz) are most prominent over the occipital or visual cortex during relaxed wakefulness with eyes closed and appear to play an important role in visual processing (Schürmann and Basar 2001; Kanai et al. 2008) and top-down control of cortical activation (Klimesch, Sauseng, and Hanslmayr 2007).

Similar to tACS, rtACS uses alternating current and so far has mainly been tested as a therapeutic intervention for patients with visual impairment linked to optic neuropathies such as glaucoma (Sabel, Thut, et al. 2020). However, unlike typical tACS, rtACS delivers the current via periorbital electrodes, directly stimulating the retina and optic nerve, and primarily targeting the visual pathway. Moreover, rtACS often uses an alternating current with varying frequencies (instead of a fixed frequency) and employs not only sinusoidal, but also rectangular waveforms (Fedorov et al. 2011). The word repetitive indicates multiple stimulation sessions; in clinical trials to date, protocols often consisted of 10 stimulation sessions (Fedorov et al. 2011; Gall et al. 2011; Sabel, Fedorov, et al. 2011; Schmidt et al. 2013; Gall et al. 2016). In comparison to transcranial applications, effects of transorbital stimulation techniques are less diffuse due to the high electrical conductivity of the vitreous (as opposed to the skull). Modelling studies have computed highest current densities in the anterior visual pathway, with lower densities at cortical areas (Gall et al. 2016; Haberbosch, Datta, et al. 2019). Stimulation effects of rtACS likely start with an activation of the retina, which in turn further propagates the stimulation effects via the optic nerve and tract to the posterior visual pathway, while tACS effects are more directly targeting cortical areas (Abd Hamid et al. 2015; Henrich-Noack, Sergeeva, and Sabel 2017). Nonetheless, there is some evidence that in occipital tACS, cortical effects result, at least partially, from retinofugal pathway stimulation (Haberbosch, Schmidt, et al.

2019). Importantly, computed current and charge densities of transorbital applications were within defined tES safety limits (Haberbosch, Datta, et al. 2019).

Comparable to rtACS, TcES applications deliver the current via special contact lens electrodes instead of periorbital skin-electrodes to stimulate the retina and optic nerve (Kurimoto et al. 2010; Schatz et al. 2011; Schatz et al. 2017).

There is evidence that the effects of tES on network activity (excitability, connectivity and amplitude, frequency and phase/ coherence of oscillations), for example, measured via electroencephalography, may influence related behaviours such as cognitive, motor, somatosensory and visual performance (Abd Hamid et al. 2015; Antal and Herrmann 2016). For example, increased α -power upon occipital tACS (Neuling, Rach, and Herrmann 2013; Helfrich et al. 2014) or rtACS (Fedorov et al. 2011; Sabel, Fedorov, et al. 2011; Bola et al. 2014; Gall et al. 2016) has been reported to be associated with improved visual perception. Assuming that stimulation intensity is chosen correctly and the stimulation or driving frequency is close enough to the brain's Eigenfrequency, a synchronization or phase-locking of the brain's endogenous oscillations with the extrinsically-applied oscillation may occur, a phenomenon called neuronal entrainment (Fröhlich 2015; Antal and Herrmann 2016; Woods et al. 2016). In simple terms, it is hypothesized that synchronization of neuronal networks is associated with increased power of entrained oscillations, while desynchronization is associated with decreased power (Reato et al. 2013). The effect of extrinsically applied stimulation on single neurons is small, but (with appropriate frequency and amplitude) enhanced within an active, coherent network of synaptically connected neurons, which may permit the modulation of the rate and timing of neuronal firing during stimulation (i.e. online). Nonetheless, in reality, neuronal network dynamics are more complex, and factors such as interactions between inhibitory and excitatory neurons and between network oscillations may contribute and are being more difficult to predict (Reato et al. 2013; Huang et al. 2017). Yet, particularly if entrainment is targeted, the consideration of the naturally occurring oscillations of the target network appears to be important for successful determination of stimulation parameters (Antal and Herrmann 2016).

If applied with appropriate parameters, tDCS (Stagg and Nitsche 2011), tACS (Zaehle, Rach, and Herrmann 2010; Neuling, Rach, and Herrmann 2013; Vossen, Gross, and Thut 2015) and rtACS (Sabel, Fedorov, et al. 2011; Gall et al. 2016) may even induce so-called offline effects, or aftereffects outlasting the stimulation period. These prolonged effects on cortical plasticity are proposed to be driven by synaptic plasticity via mechanisms similar (but not equal and limited) to Hebbian long-term potentiation (LTP) or long-term depression (LTD), or the more recent concept of spike-timing-dependent plasticity (STDP) (Zaehle, Rach, and Herrmann 2010; Vossen, Gross, and Thut 2015; Huang et al. 2017; Wischnewski et al. 2018; Sabel, Thut, et al. 2020). At the neuronal level, N-methyl-D-aspartate (NMDA) receptors and changes in the intracellular concentration of calcium,

GABA, glutamate and glutamine have been shown to play a role in the induction of these LTP-like or LTD-like effects (Stagg and Nitsche 2011; Reed and Cohen Kadosh 2018). Additionally, beneficial effects on the surrounding glial cells as well as on the vascular and immune systems have been described (Woods et al. 2016; Henrich-Noack, Sergeeva, and Sabel 2017). Nevertheless, to date too few mechanistic studies exist to completely understand the neural processes underlying the stimulation effects, and many open questions remain.

Since tES effects appear to be brain-state dependent, determination of stimulation parameters is crucial (Peterchev et al. 2012); in ACS approaches particularly the current frequency, phase, and amplitude, as well as the duration of the stimulation, should be carefully considered (Antal and Paulus 2013; Reed and Cohen Kadosh 2018). Moreover, parameters are often tailored in relation to individual measures, for example the brain's natural frequency of the target network or the individual's phosphene threshold intensity (Peterchev et al. 2012).

tRNS, a more recent tES technique, delivers an electrical current that randomly alternates its frequency and intensity within a certain range. Increased cortical excitability and other effects described upon tRNS may underlie a mechanism called stochastic resonance (Antal and Paulus 2013; Reed and Cohen Kadosh 2018).

A number of helpful publications have presented excellent overviews on the importance of dosing (Peterchev et al. 2012), the most important safety considerations (Fertonani, Ferrari, and Miniussi 2015; Bikson et al. 2016; Antal et al. 2017; Haberbosch, Datta, et al. 2019), and the use of appropriate nomenclature (Bikson et al. 2019) in NIBS techniques.

1.6 Objectives and Outline

The primary goal of this PhD project is to better understand the temporal evolution of the main pathological mechanisms, namely inflammation, demyelination and neuro-axonal degeneration in both, human acute ON as well as murine experimental autoimmune ON, using a multimodal imaging approach. A further objective is to present the study design of a clinical trial to optimally assess safety, tolerability and preliminary efficacy of rtACS in patients with an acute first-ever ON.

1.6.1 Chapter 2

In chapter 2, we review how in the last years, OCT has become an important tool to properly characterize visual pathway involvement in MS, making the use of OCT highly attractive for both MS clinical practice and MS research (Wicki, Hanson, and Schippling 2018). We discuss, how retinal OCT can assist in clinical MS management, specifically with regards to diagnosis, monitoring and prognosis with a focus on MS-associated ON. Furthermore, we summarize the most important and

current findings on OCT research, which suggest that OCT not only enables the quantification of retinal neuro-axonal damage, but also possibly reflects inflammatory disease activity in MS.

1.6.2 Chapter 3

In chapter 3, in order to further improve our understanding of the mechanisms of neurodegeneration following a first-ever clinical episode of acute ON, we investigate the temporal dynamics of structural retinal and functional visual alterations in ipsilateral and contralateral eyes of patients, using OCT and LCVA testing (Wicki et al. 2020). Based on our findings of the timing of macular ganglion cell and inner plexiform layer (GCIP) and pRNFL thinning, we discuss the optimal time window for future interventions, targeting the protection or regeneration of RGCs in ON.

1.6.3 Chapter 4

In chapter 4, we further characterize retinal, optic nerve and tract pathology in murine experimental autoimmune ON, by performing *in vivo* MRI and OCT followed by *ex-vivo* immunohistochemical analyses of the tissue. We aim to establish an optimized non-invasive imaging platform to quantitatively assess AVP pathology in EAE, so that future studies can more accurately evaluate the neuroprotective or -regenerative capacity of new therapeutic interventions in this preclinical setting. Since this was a shared PhD project with P. Manogaran, who was conducting the OCT and *ex-vivo* part, this thesis chapter is only focusing on the MRI part, which was conducted by C.A. Wicki.

1.6.4 Chapter 5

In chapter 5, we present the design of a prospective phase I/IIa pilot study, to optimally test the safety, tolerability and preliminary efficacy of low-current electrical stimulation of the retina and optic nerve in the (sub-) acute phase of ON, using rtACS. We discuss in detail, why we believe that rtACS has the potential to improve functional and structural visual outcomes in patients with a clinically first-ever ON and why there is enough circumstantial evidence to justify conducting such a study. In order to properly assess possible stimulation effects, we discuss the importance of the correct choice of methods to test functional (visual acuity, visual field, color vision and VEP), structural (OCT), patient-reported (NEI-VFQ-25) as well as safety (adverse event reporting) outcomes.

1.6.5 Chapter 6

In the final chapter we summarize the most important results obtained in the framework of this thesis and draw general conclusions about the possible significance of our findings in the field of MS. In addition we discuss possible implications as well as limitations of our findings and give a possible outlook on future research directions.

2 Optical coherence tomography as a means to characterize visual pathway involvement in multiple sclerosis

2.1 Preface

This chapter has been published as **Wicki C. A.**, Hanson J., Schippling S.,. Optical coherence tomography as a means to characterize visual pathway involvement in multiple sclerosis. *Current Opinion in Neurology*, **2018**. The chapter includes figures from the book chapter published as J.V. Hanson, **C.A. Wicki**, P. Manogaran, A. Petzold, S. Schippling. Chapter 11 OCT and Multiple Sclerosis. OCT and Imaging in Central Nervous System Diseases: The Eye as a Window to the Brain. *Springer Nature*, **2020**. C.A. Wicki made the figures for this book chapter.

2.2 Abstract

Purpose of review: Optical coherence tomography (OCT) is a non-invasive *in vivo* imaging tool that enables the quantification of the various retinal layer thicknesses. Given the frequent involvement of the visual pathway in multiple sclerosis (MS), OCT has become an important tool in clinical practice, research and clinical trials. In this review, the role of OCT as a means to investigate visual pathway damage in MS is discussed.

Recent findings: Evidence from recent OCT studies suggests that the peripapillary retinal nerve fibre layer (pRNFL) appears to be an ideal marker of axonal integrity, while the macular ganglion cell and inner plexiform layer (GCIP) thickness enables early detection of neuronal degeneration in MS. The thickness of the macular inner nuclear layer (INL) has been suggested as a biomarker for inflammatory disease activity and treatment response in MS. OCT parameters may also be used as an outcome measure in clinical trials evaluating the neuroprotective or regenerative potential of new treatments.

Summary: OCT provides insights into MS beyond the visual pathway. It is capable of quantifying the major pathological hallmarks of the disease, specifically inflammation and neuro-axonal degeneration. OCT therefore has the potential to become another mainstay in the monitoring of MS patients.

Keywords: Afferent visual pathway, low-contrast visual acuity, multiple sclerosis, optical coherence tomography, optic neuritis

2.3 Introduction

Multiple sclerosis (MS) is the most common chronic inflammatory demyelinating disorder of the central nervous system (CNS) and the main cause of non-traumatic neurological disability in young adults (Kingwell et al. 2013). Inflammation, demyelination and neurodegeneration are key pathological features of MS (Trapp and Nave 2008). Neuro-axonal damage occurs even in the earliest stages of the disease, as demonstrated in clinically isolated syndrome (CIS), and is

responsible for persistent neurological disability (Calabrese et al. 2007; Henry et al. 2008; Luessi, Siffrin, and Zipp 2012; Oberwahrenbrock et al. 2013). Despite a heterogeneous clinical presentation, impaired vision is a frequent symptom and among the most common early manifestations of the disease (Miller, Chard, and Ciccarelli 2012; Toosy, Mason, and Miller 2014), with 21 % of CIS patients presenting with optic neuritis (ON) (Miller, Chard, and Ciccarelli 2012). ON represents the most frequent involvement of the afferent visual pathway (AVP) in MS, causing neuro-axonal damage of the optic nerves and retina leading to chronic functional impairment (Costello 2016). A recent study showed that visual function is rated by MS patients as their most important bodily function, independently of disease duration or disability (Heesen et al. 2018). However, involvement of the optic nerve even in the absence of a clinical history of ON has frequently been found in MS (Ikuta and Zimmerman 1976; Oberwahrenbrock et al. 2012; Abalo-Lojo et al. 2017). The AVP has been proposed as an ideal model to study both neurodegeneration and repair in MS, due to its retinotopic organization throughout (ensuring that anatomical structure is linked to corresponding visual function) and anatomical discreteness (Costello 2013). Optical coherence tomography (OCT) permits the assessment and quantification of the retinal layers by generating a high-resolution cross-sectional view of the retina (**Figure 2-1**) (Frohman et al. 2008). The use of OCT in both research and clinical practice, plays an important role in monitoring the integrity of the retinal architecture, and also in gaining a better understanding of the process of neuronal degeneration following ON.

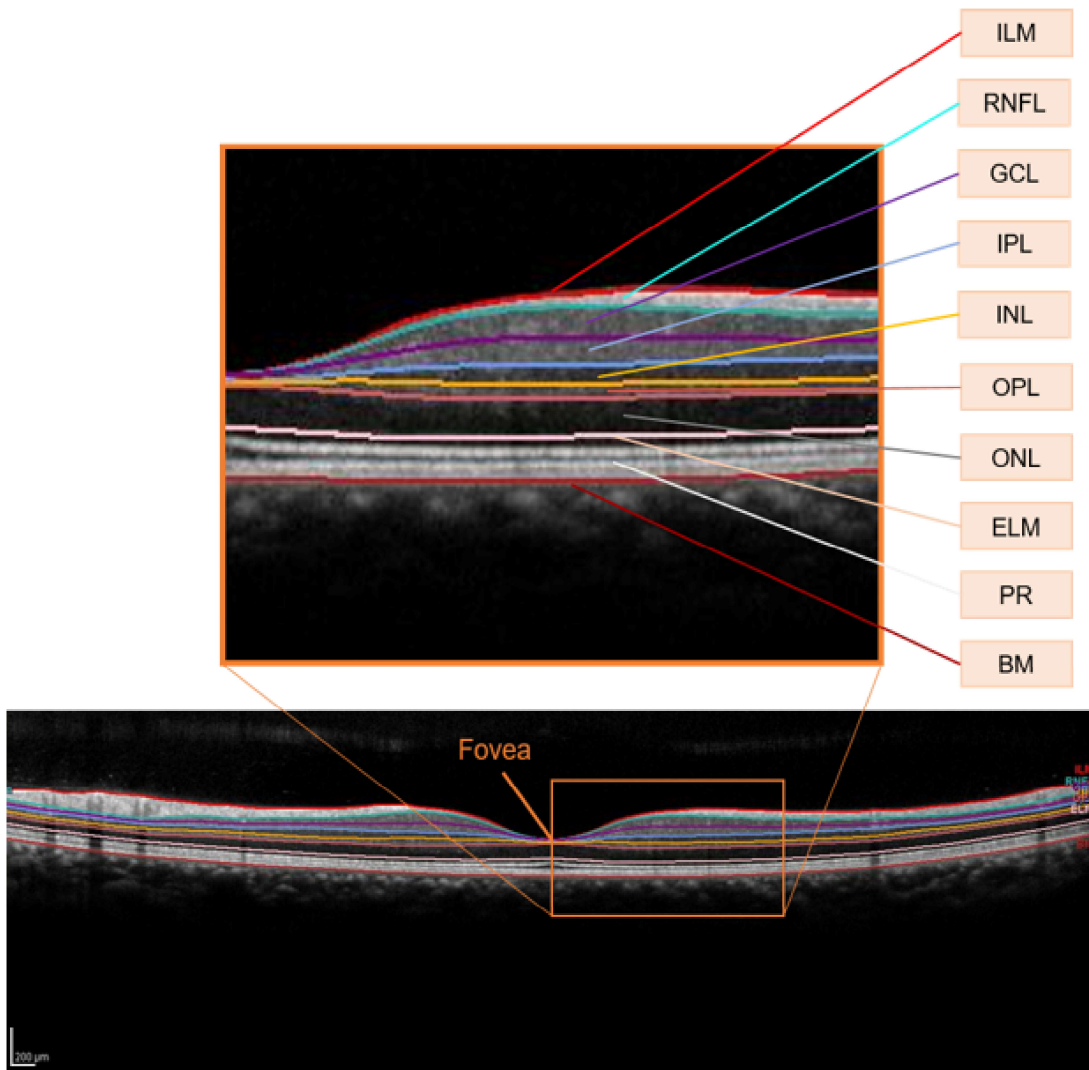


Figure 2-1 Segmented macula OCT B-scan of a healthy individual, showing the delineation of the retinal layers.

The different retinal layers are shown: ILM: inner limiting membrane; RNFL: retinal nerve fibre layer; GCL: ganglion cell layer; IPL: inner plexiform layer; INL: inner nuclear layer; OPL: outer plexiform layer; ONL: outer nuclear layer; ELM: external limiting membrane; PRL: photoreceptor layers; BM: Bruch's membrane. Note that GCL and IPL are typically aggregated to form the ganglion cell and inner plexiform layer (GCIP), and other layers may also be aggregated, depending on the segmentation software used and/or aims of individual studies. Figure by Carla Wicki taken from Hanson, Wicki et al. 2020.

2.4 Optical coherence tomography

OCT generates tomographic, two-dimensional *in vivo* images of the retina using low-coherent, near-infrared light. It is rapid, non-invasive, well-tolerated, cost-effective, and reproducible (Frohman et al. 2008; Kim et al. 2009). Contemporary spectral-domain OCT (SD-OCT) technology allows the visualization of the neural retina with an axial resolution in the range of 3-6μm (Potsaid et al. 2008; Schippling. 2015). Two of the most common scan protocols are the optic nerve head (ONH) and macular volume scans (**Figure 2-2**). The ONH scan (also described as the peripapillary ring scan) generates circular two-dimensional B-scans centred on the optic disc. This protocol facilitates

measurement of the thickness of the peripapillary retinal nerve fibre layer (pRNFL) around the ONH (Schuman et al. 1996; Savini et al. 2005). Scan quality control should be performed, for example according to the OSCAR-IB consensus criteria (Tewarie et al. 2012; Schippling et al. 2015). As the pRNFL contains unmyelinated axons of the retinal ganglion cells (RGCs), a thickness reduction most likely reflects axonal thinning or loss rather than loss of myelin, rendering the pRNFL an ideal marker of axonal damage (Costello et al. 2006; Petzold et al. 2017). The macular volume scan consists of two-dimensional B-scans centred over the fovea from which a three-dimensional image of the central retina is extrapolated. For post-processing the macula is divided into sectors according to the ETDRS (Early Treatment of Diabetic Retinopathy Study) grid ('Photocoagulation for diabetic macular edema. Early Treatment Diabetic Retinopathy Study report number 1. Early Treatment Diabetic Retinopathy Study research group' 1985). Current SD-OCT devices typically ship with proprietary software, which delineates the borders of the retinal layers (a process known as 'automated segmentation') and calculates the thicknesses and volumes of the individual retinal layers. Manual verification and, if necessary, correction of the automated segmentation is recommended in order to ensure accuracy (Oberwahrenbrock et al. 2018). As the boundary between the macular ganglion cell layer (GCL) and inner plexiform layer (IPL) is difficult to accurately distinguish, the two layers are often combined for analysis as the macular ganglion cell layer + inner plexiform layer (GCIP). pRNFL, total macular volume, and, more recently, GCIP and the inner nuclear layer (INL) appear to be the most widely studied retinal layers in MS research. Reductions in GCIP thickness are assumed to reflect primarily thinning of the GCL and, thus, atrophy of the cell bodies of the RGCs; GCIP thickness is therefore used as a biomarker for neurodegeneration within the retina (Syc et al. 2012; Petzold et al. 2017). The INL consists of the amacrine, bipolar and horizontal cells as well as the cell bodies of the Müller cells, the most abundant glial cell of the retina (Petzold et al. 2014). In recent years, researchers have proposed the INL as a biomarker for inflammation in MS (Knier et al. 2016; Petzold et al. 2017). Together, the peripapillary ring scan and the macular volume scan permit a comprehensive overview of the retina and retinal pathology (Forooghian et al. 2008). In recent years, crucial efforts were made to provide standardized acquisition protocols, guidance for quality control and recommendations for reporting, resulting in a substantial improvement of research (Tewarie et al. 2012; Schippling et al. 2015; Cruz-Herranz et al. 2016).

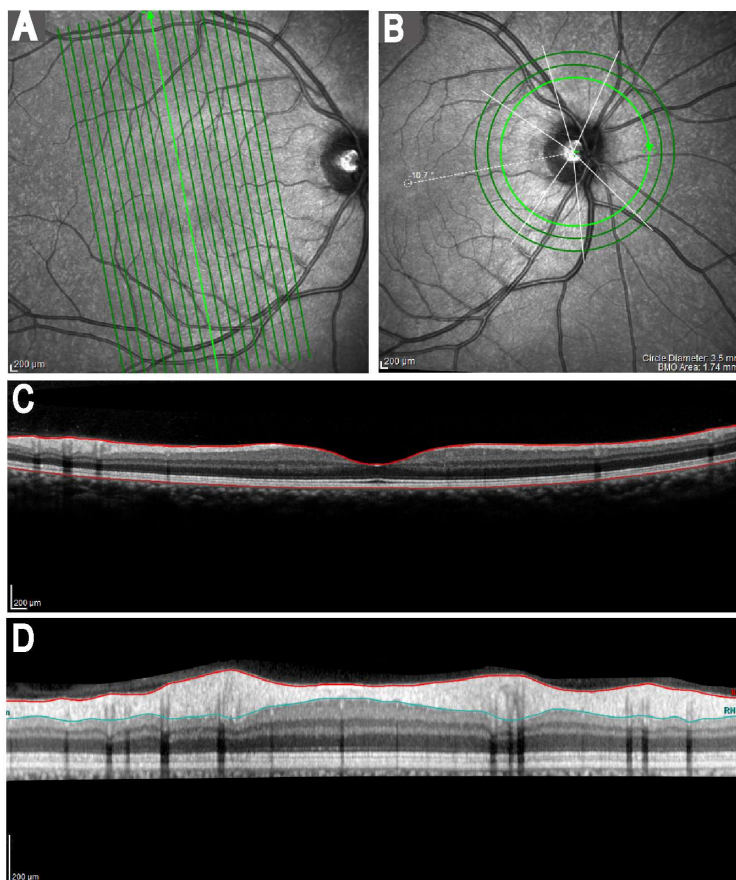


Figure 2-2 Spectral-domain OCT scan protocols.

Retinal infrared fundus images of the macular volume scan (A) and optic nerve head scan (B), followed by the respective B-scans, with the automated segmentation of the total macular thickness (upper border: inner limiting membrane, lower border: Bruch's membrane) (C) and peripapillary retinal nerve fibre layer (upper border: inner limiting membrane (red line), lower border: blue line)) (D).

2.5 Characterising visual pathway involvement with OCT

Pathological OCT findings may be due to various underlying aetiologies. The following section summarizes the most important pathological OCT findings associated with MS.

2.5.1 Optic neuritis

Acute ON is an inflammatory, demyelinating event affecting the optic nerve, and is frequently associated with MS (Toosy, Mason, and Miller 2014). 20 – 25 % of all MS patients manifest with acute ON as their clinical index event, while up to 70 % of patients are affected at some point during their disease course (Miller et al. 2005a; Toosy, Mason, and Miller 2014). Acute onset of unilateral retrobulbar pain upon eye movement, reduced vision, colour desaturation and visual field defects are typical symptoms suggestive of ON (Hickman et al. 2002). Symptoms worsen over days or weeks, followed by partial recovery over a period of months. A recent study suggests that patients are frequently left with persistent visual impairment, in particular affecting low-contrast visual acuity (LCVA), colour vision, and visual quality of life (National Eye Institute Visual Function Questionnaire-25 (NEI-VFQ-25)) (Sanchez-Dalmau et al. 2017). The pathophysiology of acute optic nerve lesions

resembles that of MS brain lesions, where inflammatory demyelination is predominantly mediated by autoreactive T-cells, with involvement from B-cells, microglia, and antibodies (Roed et al. 2005). In approximately one third of ON patients acute inflammation is also present in the retina around the ONH, as evidenced by an initial increase in pRNFL thickness, most likely reflecting inflammatory oedema (Kupersmith et al. 2011) (**Figure 2-3**). Resolution of this oedema over time may mask concurrent pRNFL thinning. The current mechanistic understanding is that alongside inflammatory demyelination, the optic nerve suffers from axonal damage. This results in retrograde degeneration from the retrobulbar optic nerve towards the ganglion cell bodies of the retina (Shindler et al. 2008). Using OCT, retrograde degeneration can be visualized in a reduction of pRNFL (**Figure 2-3, Figure 2-4**) and GCIP thickness (**Figure 2-5**) (Costello et al. 2006; Syc et al. 2012). Two important prospective longitudinal studies found a progressive decline of pRNFL thickness over 12 months following ON, with most of the reduction occurring within the first three months post-onset (Costello et al. 2015; Gabilondo et al. 2015). Similar results were found for the macular GCIP thickness (Gabilondo et al. 2015). Importantly, as opposed to pRNFL, measures of macular GCIP are usually uncontaminated by inflammatory oedema and degeneration of retinal neurons is detectable as early as one month after ON onset (Gabilondo et al. 2015). The rate of atrophy becomes lower with longer disease duration, suggestive of a plateau effect (Balk et al. 2016). ON also appears to affect outer retinal layers, namely the INL, outer plexiform layer (OPL), outer nuclear layer (ONL) and photoreceptor complex (PR), suggesting trans-synaptic alterations (Al-Louzi et al. 2016). These outer retinal layers exhibit thickening rather than thinning, which may indicate outer retinal inflammation (Al-Louzi et al. 2016) (**Figure 2-6**).

Although ON is frequently associated with MS, there are many other possible aetiologies of ON. Among the various differential diagnoses, neuromyelitis optica spectrum disorder (NMOSD) and myelin oligodendrocyte glycoprotein (MOG)-antibody associated ON are of particular importance (Jenkins and Toosy 2017). Signs suggestive of atypical non MS-related ON include painless or very painful onset, simultaneous bilateral involvement, severe or complete visual loss with poor recovery, or haemorrhages and exudates detectable on fundoscopy (Jenkins and Toosy 2017).

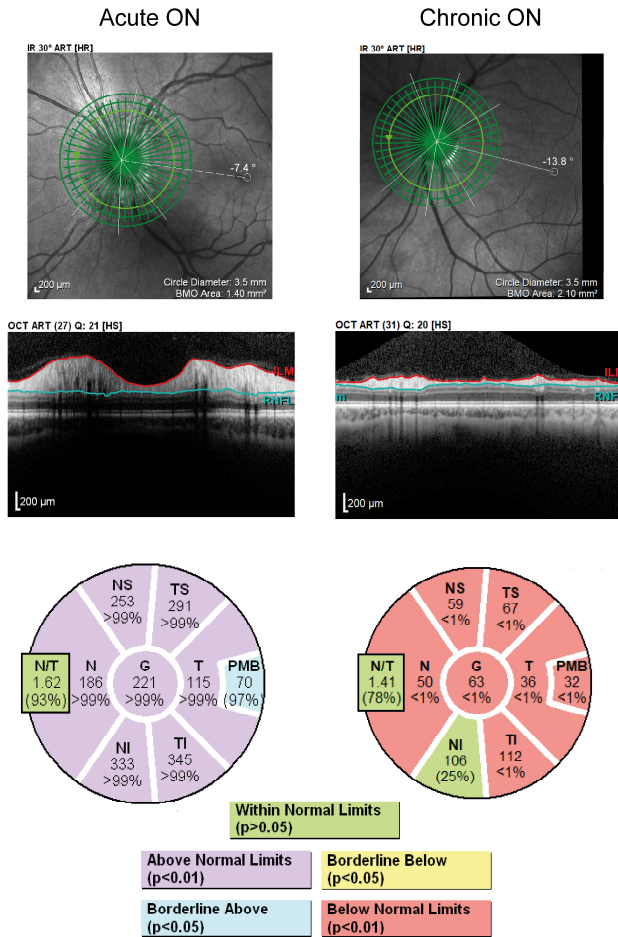


Figure 2-3 Typical OCT findings in MS patients with a previous ON: pRNFL thickness.

OCT scans of the peripapillary retinal nerve fibre layer (pRNFL) in a multiple sclerosis (MS) patient with acute optic neuritis (ON) (left), and in a patient one year after ON (right). The patient with acute ON has inflammatory oedema around the optic nerve head, which is reflected in pRNFL thickness measurements significantly thicker than normal values, whereas the patient with chronic ON shows significant atrophy of the pRNFL, with thickness values reduced compared to normal values. Abbreviations: G: global, I: inferior, N: nasal, T: temporal. Figure by Carla Wicki taken from Hanson, Wicki et al. 2020.

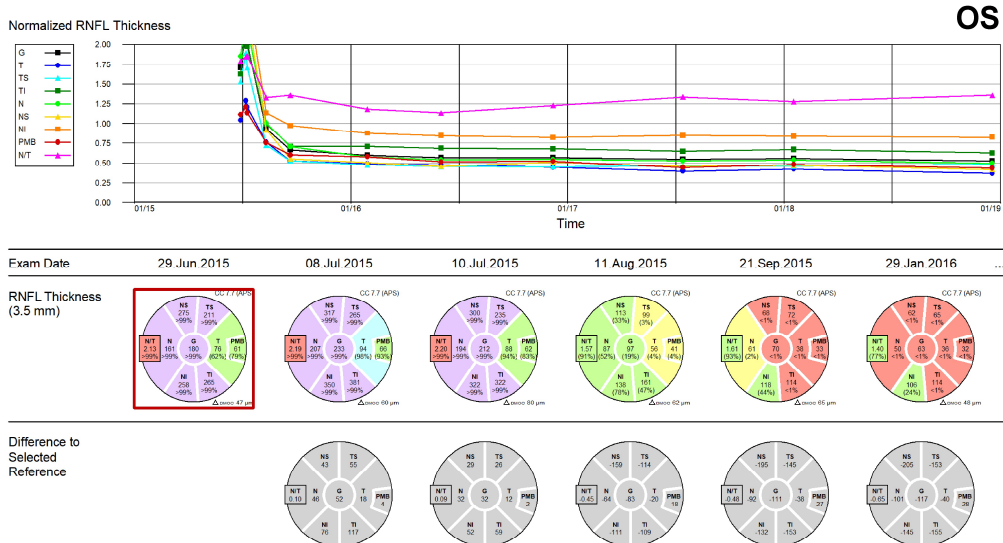


Figure 2-4 Typical OCT findings in MS patients with a previous ON: pRNFL thickness trend report.

The peripapillary retinal nerve fibre layer (pRNFL) thickness change in the left eye of a 28-years old multiple sclerosis (MS) patient with a first-ever unilateral optic neuritis (ON) over one year. Optic disc swelling with a corresponding thickening of the pRNFL (compared to normative data) is followed by a thickness decrease over time.

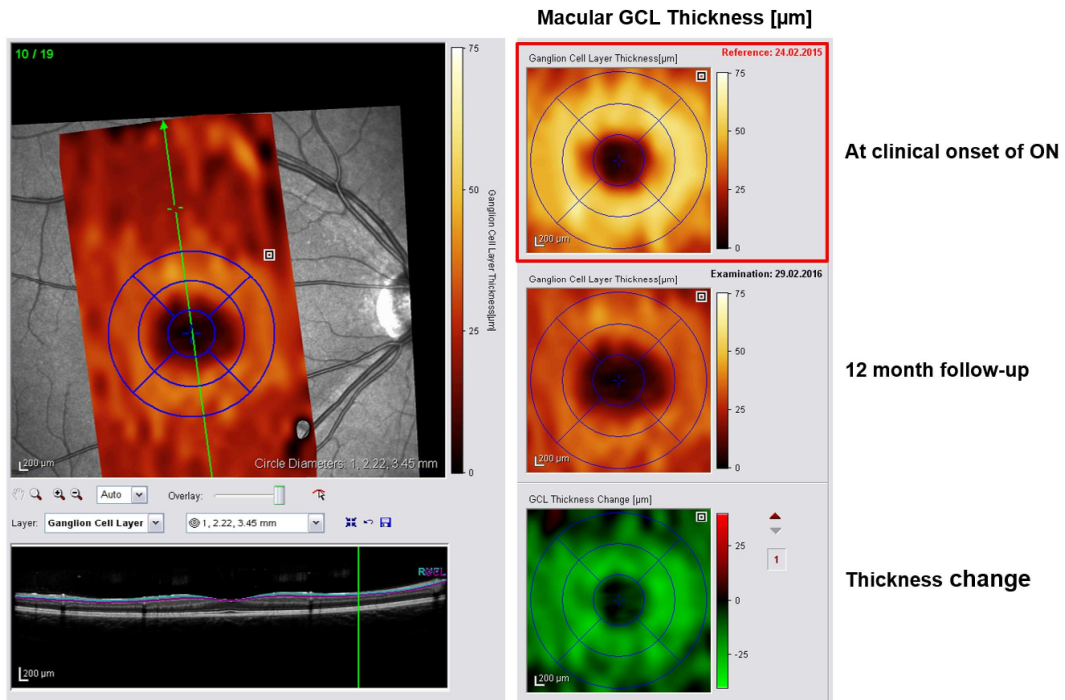


Figure 2-5 Typical OCT findings in MS patients with a previous ON: GCL thinning.

Optical coherence tomography (OCT)-derived macular ganglion cell layer (GCL) thickness (μm) for the right eye of a multiple sclerosis (MS) patient. **(Left)** For post-processing the macula is divided into sectors according to the ETDRS grid. **(Right)** Shown is a typical case of macular GCL atrophy following an episode of optic neuritis (ON): Baseline macular GCL thickness is in a normal range at clinical presentation of ON, displayed on the thickness map by the yellowish colour, but shows an apparent decrease in its thickness at the 12 month follow-up examination, illustrated by the dark reddish colour. The bottom image shows the change of GCL thickness between the two examination time points. Figure by Carla Wicki taken from Wicki et al. 2018.

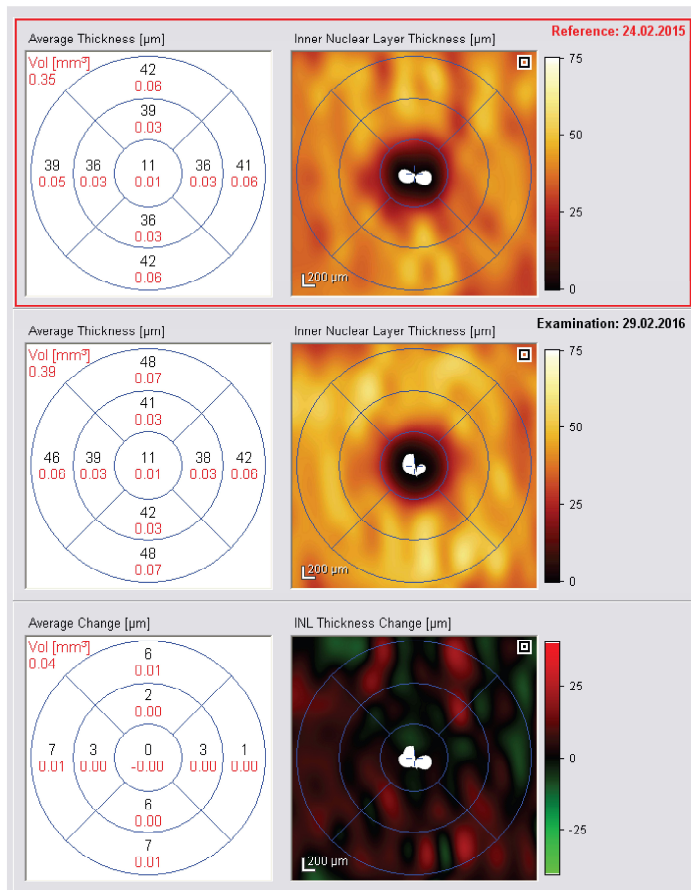


Figure 2-6 Typical OCT findings in MS patients with a previous ON: INL thickening.

OCT thickness maps of the inner nuclear layer (INL) of a multiple sclerosis (MS) patient with optic neuritis (ON), showing OCT data acquired in the acute phase of ON (top) and one year later (middle). INL is slightly thicker at follow-up, reflected in the small positive thickness change values when the two examinations are compared (bottom). Figure by Carla Wicki taken from Hanson, Wicki et al. 2020.

2.5.2 Microcystic macular oedema

Microcystic macular oedema (MME) can be observed in around 5 % of patients with MS and present as discrete, cyst-like spaces restricted to the INL (Gelfand et al. 2012; Saidha et al. 2012) (**Figure 2-7**). Various aetiologies have been proposed, including a disruption of the blood-retinal barrier (Saidha et al. 2012). The prevalence of MME is higher in eyes with, but can also be found in eyes without, a history of ON (Gelfand et al. 2012).



Figure 2-7 Typical OCT findings in MS patients: microcystic macular oedema.

OCT B-scan of the left eye of a patient with multiple sclerosis (MS) and microcystic macular oedema (MME). The B-scan shows cystoid lesions confined to the inner nuclear layer (INL), pathognomonic for MME. Figure by Carla Wicki taken from Hanson, Wicki et al. 2020.

2.5.3 Primary retinal pathology

Saidha and colleagues described a subset of MS patients with a novel OCT-defined phenotype characterised by normal pRNFL thickness but reduced macular thickness (with disproportionate thinning of the INL and ONL) when compared with other MS patients and healthy controls, unattributable to retrograde degeneration, and interpreted as evidencing primary retinal pathology (Saidha, Syc, Ibrahim, et al. 2011). Using electroretinography (ERG) and OCT, we recently showed evidence of bipolar cell and photoreceptor dysfunction (located in the INL and ONL, respectively) in the absence of corresponding structural changes and independent of ON (Hanson et al. 2018). The ERG findings are corroborated by You and colleagues in a cohort without previous ON (You et al. 2018). Together, these findings support the idea of primary retinal abnormalities in MS patients.

2.5.4 Posterior visual pathway pathology

In MS patients without prior ON, pRNFL thinning is associated with atrophy of the optic radiations and primary visual cortex as assessed by magnetic resonance imaging (MRI) (**Figure 2-8**). Authors have interpreted that lesions in the posterior visual pathway may result in a thinning of the pRNFL by trans-synaptic (via the lateral geniculate nucleus of the thalamus) retrograde axonal degeneration, however this needs to be verified by more mechanistic studies (Pfueller et al. 2011; Gabilondo et al. 2014; Klistorner et al. 2014). In eyes without prior ON, it has been proposed that posterior visual

pathway pathology accounts for as much as 35 – 40 % of pRNFL thinning (Bermel and Villoslada 2014; Klistorner et al. 2014). Conversely, optic nerve pathology may also result in trans-synaptic anterograde degeneration, affecting parts of the posterior visual pathway, as indicated by more severe visual cortex atrophy in MS patients with a previous history of ON (Petzold et al. 2010; Gabilondo et al. 2014).

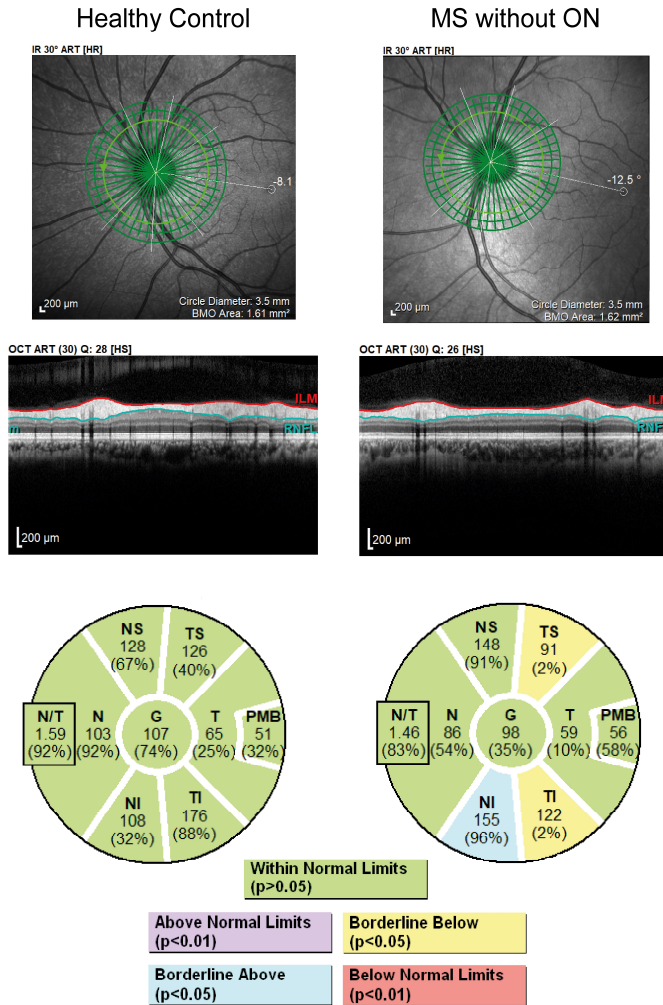


Figure 2-8 Typical OCT findings in MS patients without a previous ON: pRNFL thickness.

Peripapillary retinal nerve fibre layer (pRNFL) analysis from the left eyes of a healthy individual and a multiple sclerosis (MS) patient without previous optic neuritis (ON), obtained from a Spectralis OCT device (Heidelberg Engineering, Heidelberg, Germany). The global averaged (G) thickness is reduced in the patient with MS, as are the thicknesses of the majority of the individual sectors; in the case of the temporal superior (TS) and temporal inferior (TI) sectors, thickness is below the 95th percentile of age-matched normal values and so is classified as borderline below average (and colour-coded yellow) by the proprietary software. The borderline above average thickness in the nasal inferior (NI) sector in the MS patient is an artefact caused by a retinal blood vessel. Figure by Carla Wicki taken from Hanson, Wicki et al. 2020.

2.6 Clinical relevance of OCT findings in MS

In order to validate the utility of OCT as a clinical and research tool in MS, the functional relevance and implications of the structural retinal changes discussed above is of critical importance. There is a significant body of evidence showing that OCT outcomes are associated with both visual and

overall disability, disease activity, and, increasingly, response to treatment in MS (Walter et al. 2012a; Knier et al. 2016; Martinez-Lapiscina et al. 2016).

Firstly, measures of visual performance including visual acuity, colour vision, and perimetry have been shown to correlate with the thicknesses of the pRNFL and even more strongly with the thickness of the macular GCIP (Frohman et al. 2009; Saidha, Syc, Durbin, et al. 2011; Walter et al. 2012a; Lampert et al. 2015; Ortiz-Perez et al. 2016). In particular, low-contrast visual acuity (LCVA) has been shown to strongly correlate with OCT outcomes, and is probably the most sensitive measure to capture visual dysfunction following ON (Balcer et al. 2017). The importance of LCVA monitoring becomes obvious when considering the higher prevalence of residual low-contrast as opposed to high-contrast visual functional impairment following ON (Balcer et al. 2017). Moreover, a study with ON patients demonstrated that the GCIP and pRNFL thickness changes within the first month following ON onset could predict visual recovery, measured by LCVA and colour vision, at month six (Sanchez-Dalmau et al. 2017). Visual recovery after ON tends to be better in females than males and may also be associated with serum vitamin D levels (Costello et al. 2015; Burton et al. 2017).

A significant relationship between OCT parameters and electrophysiological tests such as the visual evoked potential (VEP) and ERG has been observed in MS (Sriram et al. 2014). VEP and ERG examinations are performed in order to quantify the cortical (VEP) and retinal (ERG) response to precisely defined visual stimuli (Hanson et al. 2016).

The Expanded Disability Status Scale (EDSS), widely used to assess MS-related disability, is weighted towards motor impairment and problems with gait, while visual functional deficits are highly underrepresented (Kurtzke 1983). Despite this, studies of MS patients without previous ON have found that a pRNFL thickness value below a certain threshold (varying by OCT device), measured at any given time point in the disease, was predictive of a more severe disability progression (as measured by EDSS) relative to those patients with greater pRNFL thickness (Martinez-Lapiscina et al. 2016). Further, a strong relationship between cognitive impairment and atrophy of the pRNFL and macular GCIP has been found (Coric et al. 2017). Additionally, a reduction in QOL is associated with a reduction in the thickness of the pRNFL (Garcia-Martin et al. 2013).

Likewise, the presence of MME has been associated with disease severity in MS patients (Gelfand et al. 2012; Saidha et al. 2012). It has been suggested that an increase in INL thickness, with or without visible MME, may be reflective of inflammatory disease activity in MS (Saidha et al. 2012). Patients with relapsing-remitting MS, who had relapses or new gadolinium-enhancing lesions during a three year follow-up period, had higher baseline INL thicknesses compared with patients who did

not have relapses (Saidha et al. 2012). Knier and colleagues recently reported that INL thickness was greater in untreated MS patients than healthy control subjects, and that patients responding to immune therapies show a normalization of INL thickness, indicating a reduction in inflammatory disease activity (Knier et al. 2016). As a result, the INL has gained significant interest as a possible biomarker for treatment response (Knier et al. 2016). Subsequent findings from the same centre show an association between INL volume and prospective MRI activity (T2 lesion load and number of gadolinium-enhancing lesions) (Knier et al. 2017), providing further evidence for the emerging importance of the INL in MS.

In addition, several studies have shown that injury in the AVP reflects global CNS damage in MS that can be quantified using MRI (Gordon-Lipkin et al. 2007; Abalo-Lojo et al. 2014; Saidha et al. 2015). Currently, MRI is the mainstay of diagnosis and monitoring of MS and the most accepted surrogate marker of disease progression. pRNFL thinning has been shown to be associated with whole-brain atrophy (Gordon-Lipkin et al. 2007; Abalo-Lojo et al. 2014). Furthermore, Saidha and colleagues have found that GCIP atrophy reflects grey matter atrophy over time, an important measure of disease progression (Fisher et al. 2008; Saidha et al. 2015; Schipling 2017). However, MRI is expensive and time-consuming. As a sensitive, accurate, rapid and cost-effective tool, OCT provides an excellent complement to MRI for monitoring CNS integrity in patients with MS.

Consequent to the remarkable development of OCT technology over recent years, particularly with regard to retinal layer segmentation, OCT may be helpful in the characterization of pathologically distinct MS phenotypes. For example, patients exhibiting primary retinal pathology have been proposed to have an aggressive form of MS, characterized by more rapid disability progression (Saidha, Syc, Ibrahim, et al. 2011), as have patients with MME (Gelfand et al. 2012). Consideration of disease phenotype, stage, activity, and progression of individual patients is important for optimal disease management and OCT will increasingly play a vital role in the assessment and management of these patients.

Inner retinal layer (RNFL; GCIP) changes are already detectable in CIS patients not yet diagnosed with MS but presenting with a first clinical event suggestive of MS (Oberwahrenbrock et al. 2013). Hence, OCT may potentially aid the early detection of at-risk patients and facilitate early diagnosis of MS. As irreversible axonal and neuronal injury can occur even in the earliest stages of MS, early detection and treatment is a high priority (Villoslada and Martinez-Lapiscina 2017).

Moreover, differential diagnosis is of great importance; for instance, the prognosis and treatment of ON depends strongly on the underlying cause (Toosy, Mason, and Miller 2014). ON associated with AQP4-seropositivity has been associated with a more severe clinical outcome, as have some (but

not all) cases of MOG-seropositive ON (Jarius et al. 2016). Early diagnosis and appropriate treatment are paramount to avoid severe functional sequelae, including blindness, which further emphasises the utility of OCT in patients with acute ON (Manogaran et al. 2016; Pache et al. 2016; Havla et al. 2017).

During recent years, OCT measures have been proven as appropriate outcome measures in MS clinical trials, often in combination with LCVA and other clinical measures (Sormani and Pardini 2017). In particular, ON has been proposed as a unique clinical model to study the potential of neuro-protective and neuro-regenerative therapies. The thickness of the pRNFL may serve as a robust long-term axonal outcome measure, whilst the thickness of the macular GCIP is considered an early measure of neuronal integrity (Aktas, Albrecht, and Hartung 2016; Petzold 2017; Petzold et al. 2017). Results from recent longitudinal OCT studies focusing on the timing of neuro-axonal loss in MS may have important implications for future clinical trial planning, in particular with regards to the timing of treatment intervention. As atrophy is most pronounced at early stages of the disease course, early or even hyperacute intervention may be the most promising strategy to prevent irreversible neuro-axonal degeneration (Balk et al. 2016; Petzold 2017).

2.7 Conclusion

OCT has been validated as a reliable tool for quantifying the major pathological hallmarks of MS disease: inflammation, axonal loss and neuronal degeneration (Petzold et al. 2014; Toosy, Mason, and Miller 2014; Balcer et al. 2015; Petzold et al. 2017). OCT has the potential to become a mainstay in the monitoring of MS patients as it may provide important complementary information to MRI, thereby assisting in the clinical decision-making process. OCT may also be used as an outcome measure in clinical trials of new compounds with neuro-protective and -regenerative potential.

2.8 Author Contributions

C.A. Wicki did the primary literature review, wrote the original draft of the review, and made all the figures. **J.V.M. Hanson** and **S. Schippling** provided substantial revisions and editing of the review.

2.9 Affiliations

From the Department of Health Sciences and Technology, ETH Zurich (C.A.W.); Neuroimmunology and Multiple Sclerosis Research, Department of Neurology, University Hospital Zurich and University of Zurich (C.A.W., J.V.M.H., S.S.); and Department of Ophthalmology, University Hospital Zurich and University of Zurich (J.V.M.H.).

2.10 Financial support and sponsorship

CAW has received a travel grant from Teva. JVMH and SvS are supported by the Clinical Research Priority Program of the University of Zurich and the Swiss MS Society. JVMH has previously received travel support and speaker fees from Biogen.

2.11 Conflicts of interest

None.

3 Bilateral retinal pathology following a first-ever clinical episode of autoimmune optic neuritis

3.1 Preface

This chapter has been published as **Wicki C.A.**, Manogaran P, Hanson J.V.M, Simic T, Schippling S. Bilateral retinal pathology following a first-ever clinical episode of autoimmune optic neuritis, *Neurology Neuroimmunology & Neuroinflammation*, **2020**. The chapter includes material from C.A. Wicki's master thesis entitled "Temporal dynamics of structural and functional retinal damage in acute optic neuritis" (accepted in 2017 by ETH D-HEST. Supervised by S. Schippling and M. Schwab).

3.2 Abstract

Objective: This longitudinal study aimed to assess changes in retinal structure and visual function following a first-ever episode of acute optic neuritis (ON).

Methods: Clinical and optical coherence tomography (OCT) data obtained over a period of 12 months was retrospectively analysed in 41 patients with a first-ever clinical episode of acute ON. OCT scans, as well as high- and low-contrast visual acuity (HCVA/ LCVA) were acquired at baseline and 1, 3, 6 and 12 months thereafter. Macular ganglion cell and inner plexiform layer (GCIP), peripapillary retinal nerve fibre layer (pRNFL), and macular inner nuclear layer (INL) thicknesses were assessed by OCT. Linear mixed-effects models were used to analyse OCT variables of ipsilateral ON and contralateral non-ON (NON) eyes over time.

Results: The mean change of GCIP thickness in ON eyes was significant at all follow-up timepoints, with nearly 75 % of the total reduction having occurred by month 1. In ON eyes, thinner GCIP thickness at month 1 correlated with lower LCVA at month 3. Mean pRNFL thickness in ON eyes differed significantly from NON eyes at all post-baseline timepoints. INL thickness was significantly increased in ON eyes (month 1) but also in contralateral NON eyes (month 12).

Conclusions: Retinal structural damage develops rapidly following acute ON and is associated with subsequent functional visual deficits. Our results also suggest bilateral retinal pathology following unilateral ON, possibly caused by subclinical involvement of the contralateral NON eyes. Moreover, our data may assist in clinical trial planning in studies targeting tissue damage in acute ON.

3.3 Introduction

Optic neuritis (ON) is an acute inflammation of the optic nerve and a frequent clinical manifestation of multiple sclerosis (MS) (Miller et al. 2005b; Luessi, Siffrin, and Zipp 2012; Toosy, Mason, and Miller 2014). Within the retina, ON-associated neuro-axonal damage manifests as peripapillary retinal nerve fibre layer (pRNFL) and macular ganglion cell layer thinning, which can be detected *in vivo* using optical coherence tomography (OCT) (Costello et al. 2006; Frohman et al. 2008; Green et al. 2010; Syc et al. 2012). Studies have found that pRNFL and the combined macular ganglion

cell and inner plexiform layer (GCIP) thickness strongly correlated with functional visual outcomes in ON (Walter et al. 2012a; Balcer et al. 2017). A multi-centre study recently found that pRNFL thickness below a certain threshold was predictive of a more disabling disease course (Martinez-Lapiscina et al. 2016).

In addition to the inner retina, changes to the outer retina (e.g. inner nuclear layer; INL), have been observed after ON (Al-Louzi et al. 2016; Petzold et al. 2017; Hanson et al. 2018).

Interestingly, previous studies have found that the clinically unaffected contralateral eye may display some degree of dysfunction following unilateral ON (Klistorner et al. 2009; Raz et al. 2013; Schnurman et al. 2014). Structural data to date, is only available for the outer retina over six months after ON (Gabilondo et al. 2015), or for the inner retina over 12 months (Costello et al. 2015).

Although a number of cross-sectional OCT studies in ON have been published (Walter et al. 2012a; Balk et al. 2014), longitudinal studies are still scarce (Costello et al. 2015; Gabilondo et al. 2015; Petzold et al. 2017).

The primary goal of this study was to describe the temporal dynamics and magnitude of retinal structural and functional visual damage in patients with a first-ever ON in the affected and unaffected eyes. Further objectives included investigating the association between early macular damage and visual outcomes and exploratory analysis of gender-specific differences during ON.

3.4 Methods

3.4.1 Study design

41 patients with a first-ever acute ON were identified retrospectively by chart review and their clinical and OCT data were analysed longitudinally over a period of 12 months following the episode. Patient data was acquired at baseline (defined as symptom onset \pm 28 days max. after onset of ON) and, relative to baseline, at 1 (24-38 days), 3 (79-107 days), 6 (158-214 days), and 12 (310-434 days) months thereafter between 2014 and 2017.

3.4.2 Standard protocol approvals, registrations, and patient consents

The study was approved by the Ethics Committee of the Canton of Zurich, Switzerland (reference KEK-ZH-Nr.2013-0001) and all subjects signed a general informed consent form.

3.4.3 Subject eligibility

Subjects with a first-ever episode of ON, including idiopathic ON and ON in the context of MS (diagnosed according to the 2010 revised McDonald criteria (Polman et al. 2011)), were included in the study. ON was diagnosed by experienced clinicians from the Departments of Neurology and Ophthalmology at the University Hospital Zurich, Switzerland. Patients were included if OCT and visual acuity assessments were performed at baseline and at least one more of the pre-defined timepoints. Exclusion criteria included: previous clinical history of ON in either eye, retinal pathology (visible upon ophthalmological or OCT examination) or any other ocular or systemic disease which

could affect vision or retinal structure (e.g. diabetes mellitus, uncontrolled hypertension), refractive error ≥ 6.0 dioptres, and history of eye surgery.

3.4.4 Visual acuity

High-contrast visual acuity (HCVA) and LCVA were recorded at each visit with habitual refractive correction. HCVA was tested using Early Treatment Diabetic Retinopathy (ETDRS)-style charts (100 % contrast) and LCVA was tested with Sloan letter charts (2.5 % contrast). For both, the number of correctly identified letters was recorded and specified with the logarithm of the minimum angle of resolution (LogMAR) scale (Ferris et al. 1982).

3.4.5 Optical coherence tomography

OCT was performed using a single Heidelberg Spectralis® OCT device (Software version 1.9.10.0, Heidelberg Engineering, Heidelberg, Germany) by three experienced OCT operators. The device is equipped with a TruTrack® eye tracking program. OCTs were performed without pupillary dilation in a darkened room. Scans were acquired at baseline and 1, 3, 6, and 12 months after ON. The macular volume protocol was performed in high-resolution mode and involved 19 consecutive vertical B-scans (25 Automatic Real-time Tracking [ART], 1536 A-scans per B scan, 240 μ m between B-scans) crossing the macula using an integrated macular volume protocol ("PPoleV"). The pRNFL thickness protocol involved a high resolution peripapillary ring scan (12° and 3.5mm diameter, 30 ART) centred over the optic nerve head (ONH). For post-processing, retinal layer segmentation was performed automatically using the built-in Heidelberg Retina Angiograph (HRA)/ Spectralis Viewer Module (v.6.3.4.0). The mean thickness of the macular ganglion cell layer, inner plexiform layer and INL was calculated by centring the 1.00mm, 2.22mm, 3.45mm ETDRS grid on the fovea and averaging the thickness of all quadrants. GCIP thickness was the summation of the ganglion cell layer and inner plexiform layer. The software calculated the mean pRNFL thickness, 360° around the ONH. All ONH scans fulfilled the OSCAR-IB quality consensus criteria (Schippling et al. 2015). All scans were reviewed by a single author (CAW) and, when necessary, segmentation boundaries manually corrected. OCT data have been reported in line with the Advised Protocol for OCT Study Terminology and Elements (APOSTEL) recommendations (Cruz-Herranz et al. 2016).

3.4.6 Statistics

Statistical analyses were performed using R version 3.3.1 (R Core Team, 2016; <http://www.r-project.org>). To assess if time between symptom onset and baseline examination may influence the OCT analysis, an unpaired, two-sample t-test was used to compare the mean baseline GCIP thickness of the ON eyes between early (≤ 7 days) and late (> 7 days) presenting patients. All retinal layers derived from OCT measurements were analysed independently of each other. For each layer, a linear mixed-effects model was used to assess the differences between ipsilateral ON eyes and contralateral non-optic neuritis (NON) eyes over time. The response variable of the model was either the Δ GCIP, Δ pRNFL or Δ INL (the difference between the retinal layer thickness of an ON eye at each timepoint and the retinal layer thickness of the corresponding NON eye at baseline). All

comparisons were made to the baseline of the NON eyes assuming that the baseline of the NON eyes is non-pathological and therefore suitable as an intra-individual control. This approach is further supported by previous studies suggesting that analysis of inter-eye thickness differences is more accurate in detecting retinal ganglion cell (RGC) damage than absolute thicknesses (Brandt et al. 2018), and that within-subject comparisons are more sensitive than comparisons to a healthy control group (Kupersmith et al. 2011; Kupersmith, Anderson, and Kardon 2013). All models included timepoints, age, gender, disease duration, steroid treatment (yes/ no) and disease modifying therapy (DMT) (yes/ no) as fixed effects and a random effect accounted for intra-individual comparisons; furthermore the model is known to efficiently handle missing values (Ibrahim and Molenberghs 2009). The residuals of the model were tested for normality with the Shapiro-Wilk test and by inspection of the residuals and Q-Q plots. The relationship between GCIP thickness and LCVA in ON eyes was assessed by Spearman's rank correlations. All p-values were Bonferroni corrected for multiple comparisons. p-values ≤ 0.05 were considered statistically significant.

3.5 Results

3.5.1 Patient demographics and clinical characteristics

Patient demographics and clinical characteristics obtained at baseline clinical evaluation are detailed in **Table 3-1**. In total, 41 patients (28 females and 13 males; mean age: 32.4 years) were included in the study. 30 patients (73.2 %) had an ON in the context of MS, while 11 cases (26.8 %) were diagnosed with idiopathic ON. In cases with bilateral ON (n=2), the more severely affected eye at baseline was classified as the ON eye. From the less severely affected eye, only baseline results were analysed and used to calculate inter-eye differences over time, while the follow-up data were excluded. The mean time from clinical onset of ON to baseline examination was 10 days. The average GCIP thickness in ON eyes was not significantly different (p=0.13) between patients presenting early or late for baseline examination. One patient had a clinical ON event during follow-up, affecting the contralateral eye at month 12; the data for this eye at month 12 was excluded from analysis.

3.5.2 Structural retinal damage following ON

GCIP thickness in NON eyes remained stable, whereas GCIP thickness in ON eyes decreased over time. The mean Δ GCIP differed significantly in ON eyes at all timepoints (p<0.0001) post-ON (**Figure 3-1, Table 3-2**). ON eyes had a mean GCIP reduction over the 12 month follow-up period of 14.1 μ m (SD: 3.2 μ m), with 74.5 % of the change occurring within the first month, and 100 % within three months following ON (**Figure 3-1, Table 3-2**). Except for timepoints, none of the covariates (age, gender, disease duration, steroid treatment and DMT) appeared to have a significant effect on the response variables (Δ GCIP, Δ pRNFL, or Δ INL), but were nevertheless included in the statistical model, as pre-planned. In comparison, the mean longitudinal GCIP thickness in NON eyes showed an absolute reduction of 1.1 μ m (SD: 2.2 μ m) over the same period (**Table 3-3**).

Table 3-1 Patient demographics and clinical characteristics at baseline examination.

	Total	Female	Male
Number of patients	41	28	13
Mean age (SD) [years]	32.4 (9.4)	32.0 (10.8)	33.3 (5.4)
Mean disease duration (SD) [days]			
Median [days]	184 (730)	207 (873)	134 (234)
Minimum [days]	2	2	2
Maximum [days]	4611	4611	804
Cause of ON			
Idiopathic ON	11	8	3
CIS	7	6	1
RRMS	22	14	8
PPMS	1	0	1
ON presentation			
Unilateral	39	27	12
Bilateral	2	1	1
Mean time from clinical onset of ON to baseline scan (SD) [days]	10 (7)	11 (8)	8 (4)
Patients treated with corticosteroids	37	25	12
Patients treated with DMT	17	11	6
Ethnicity			
European	38	27	11
South Asian	1	0	1
West African	1	0	1
North American	1	1	0

CIS: clinical isolated syndrome, DMT: disease modifying therapies, ON: optic neuritis, PPMS: primary progressive multiple sclerosis, RRMS: relapsing remitting multiple sclerosis, SD: standard deviation.

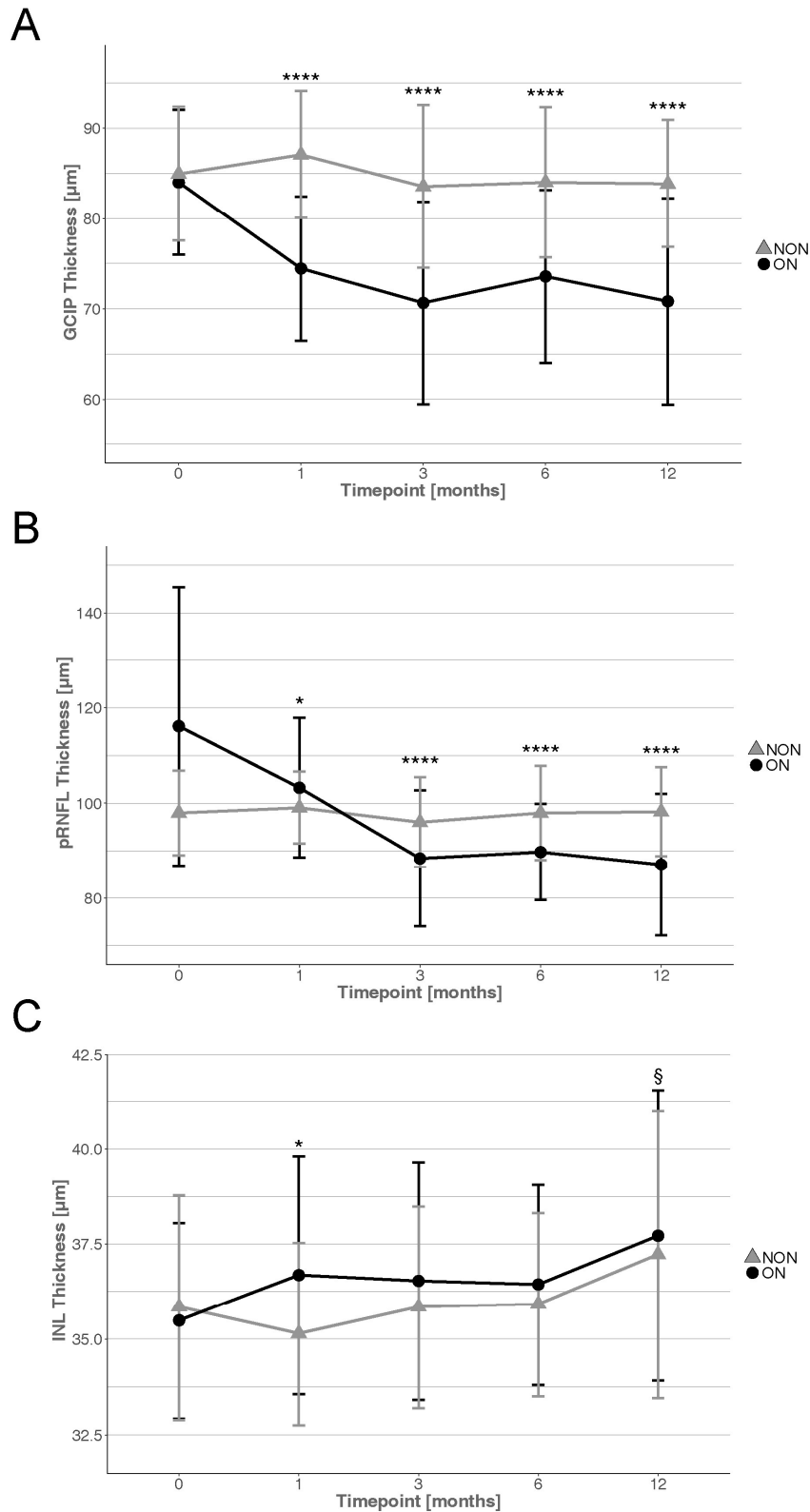


Figure 3-1 Longitudinal retinal thickness in optic neuritis.

(A) Reduction in mean macular ganglion cell and inner plexiform layer (GCIP) thickness in optic neuritis (ON) eyes at baseline and in the subsequent 12 months compared to baseline mean GCIP thickness in non-optic neuritis (NON) eyes. (**** $p < 0.0001$). (B) Mean peripapillary retinal nerve fibre layer (pRNFL) thickness in NON and ON eyes at baseline and in the subsequent 12 months. (* $p < 0.05$, **** $p < 0.0001$). (C) Inter-eye difference between macular inner nuclear layer (INL) thickness in ON eyes and baseline contralateral INL thickness (* $p < 0.05$). Intra-eye difference in macular INL thickness in NON eyes over time (§ $p < 0.05$). Error bars represent standard deviations.

Table 3-2 Retinal thickness in NON eyes at baseline and in ON eyes over a 12-month period.

	NON	ON				
macular GCIP	M0	M0	M1	M3	M6	M12
mean (SD) [μm]	85.0 (7.4)	84.0 (8.0)	74.5 (8.0)	70.7 (11.2)	73.6 (9.6)	70.8 (11.4)
absolute change (SD) [μm]	NA	-0.9 (1.8)	-10.5 (2.1)	-14.3 (2.5)	-11.4 (2.4)	-14.1 (3.2)
number of eyes	40	36	21	25	22	15
pRNFL	M0	M0	M1	M3	M6	M12
mean (SD) [μm]	98.0 (8.9)	116.2 (29.3)	103.2 (14.7)	88.4 (14.3)	89.7 (10.2)	87.1 (14.9)
absolute change (SD) [μm]	NA	18.2 (4.8)	5.3 (3.4)	-9.6 (3.2)	-8.2 (2.6)	-10.9 (4.1)
number of eyes	41	41	22	25	22	15
macular INL	M0	M0	M1	M3	M6	M12
mean (SD) [μm]	35.8 (2.9)	35.5 (2.6)	36.7 (3.1)	36.5 (3.1)	36.4 (2.6)	37.7 (3.8)
absolute change (SD) [μm]	NA	-0.4 (0.6)	0.8 (0.8)	0.7 (0.8)	0.6 (0.7)	1.9 (1.1)
number of eyes	40	36	21	25	22	15

GCIP: ganglion cell and inner plexiform layer, INL: inner nuclear layer, M0: month 0, M1: month 1, M3: month 3, M6: month 6, M12: month 12, NA: not applicable, NON: non-optic neuritis eye, ON: optic neuritis, pRNFL: peripapillary retinal nerve fibre layer, SD: standard deviation.

Table 3-3 Retinal thickness in NON eyes over a 12 month period.

macular GCIP	M0	M1	M3	M6	M12
mean (SD) [μm]	85.0 (7.4)	87.1 (7.0)	83.6 (9.0)	84.0 (8.3)	83.9 (7.0)
absolute change (SD) [μm]	NA	2.1 (1.9)	-1.4 (2.1)	-0.9 (2.1)	-1.1 (2.2)
number of scans	40	21	24	21	15
pRNFL	M0	M1	M3	M6	M12
mean (SD) [μm]	98.0 (8.9)	99.0 (7.6)	96.0 (9.5)	98.0 (9.9)	98.2 (9.4)
absolute change (SD) [μm]	NA	1.1 (2.1)	-2.0 (2.4)	0.0 (2.5)	0.2 (2.8)
number of scans	41	21	24	21	15
macular INL	M0	M1	M3	M6	M12
mean (SD) [μm]	35.8 (2.9)	35.1 (2.4)	36.0 (2.6)	35.9 (2.4)	37.2 (3.8)
absolute change (SD) [μm]	NA	-0.7 (0.7)	-0.2 (0.7)	0.1 (0.7)	1.4 (1.1)
number of scans	40	21	24	21	15

GCIP: ganglion cell and inner plexiform layer, INL: inner nuclear layer, M0: month 0, M1: month 1, M3: month 3, M6: month 6, M12: month 12, NA: not applicable, NON: non-optic neuritis eye, pRNFL: peripapillary retinal nerve fibre layer, SD: standard deviation.

Although we observed numerical differences between males and females in terms of GCIP reduction after 12 months (males: $-19.8\mu\text{m}$, SD: $4.9\mu\text{m}$ vs. females: $-10.3\mu\text{m}$, SD: $4.1\mu\text{m}$), these differences did not reach statistical significance (**Table 3-4, Table 3-5**).

Mean baseline pRNFL thickness in ON eyes was $116.2\mu\text{m}$ (SD: $29.3\mu\text{m}$) and had an average thickness difference of $+18.2\mu\text{m}$ (SD: $4.8\mu\text{m}$) compared to contralateral NON eyes (**Table 3-2, Figure 3-1**). The mean ΔpRNFL was significantly different at months 1 ($p<0.05$), 3 ($p<0.0001$), 6

($p < 0.0001$) and 12 ($p < 0.0001$) post-ON. Although most of the total pRNFL reduction (87.8 %) occurred within the first 3 months post-ON, thickness continued to slowly decline up until month 12 (**Table 3-2**). In NON eyes, mean pRNFL thickness values between 96.0 μm and 99.0 μm were reported over the 12 month period (**Table 3-3**). At baseline, females had a mean pRNFL thickness of 113.9 μm (SD: 31.3 μm) in ON eyes and a difference of +15.79 μm (SD: 6.1 μm) compared to their respective NON eyes, while the ON eyes in males had a mean pRNFL thickness of 121.0 μm (SD: 24.9 μm) and a difference of +23.4 μm (SD: 7.4 μm) compared to the respective NON eyes. By month 6, females and males had almost identical mean pRNFL thicknesses. Subsequent to month 6, pRNFL thickness stabilised until month 12 in females, whilst males experienced a further decline (**Table 3-4, Table 3-5**).

The baseline mean INL thickness was similar in NON and ON eyes (**Table 3-2, Figure 1**). However, a significant inter-eye difference between month 1 macular INL thickness in ON eyes and baseline contralateral INL thickness ($p < 0.05$) was found (**Figure 3-1**).

The INL thickness in ON eyes showed more pronounced changes over time in males than in females. At month 1 following ON, mean INL thickness was similar in males and females. In female ON eyes, mean INL thickness remained nearly unchanged up to month 12, whereas in male ON eyes mean INL thickness increased by 3.0 μm (SD: 1.6 μm) at month 12 (**Table 3-4, Table 3-5**).

In NON eyes, almost no change in mean INL thickness was observed at months 1, 3 and 6, but there was a significant increase at month 12 (+1.4 μm , SD: 1.1 μm , $p < 0.05$) compared to baseline (**Table 3-3**). Although small in magnitude, this increase nevertheless represents a change of +3.9 % by month 12 when compared to the baseline examination.

3.5.3 Visual functional changes following ON

Visual acuity of ON eyes was lowest at the acute phase of ON and was worse compared to that of NON eyes (**Figure 2, Table 3-6**). Subsequently, visual acuity recovered partially; while HCVA improved rapidly in ON eyes and was comparable to measurements in the NON eyes already at month 3, LCVA never reached the level of NON eyes during the entire observation period (**Figure 3-2**). Namely, ON eyes displayed a mean LCVA inter-eye difference of 0.23 LogMAR, corresponding to 11-12 letters at month 12.

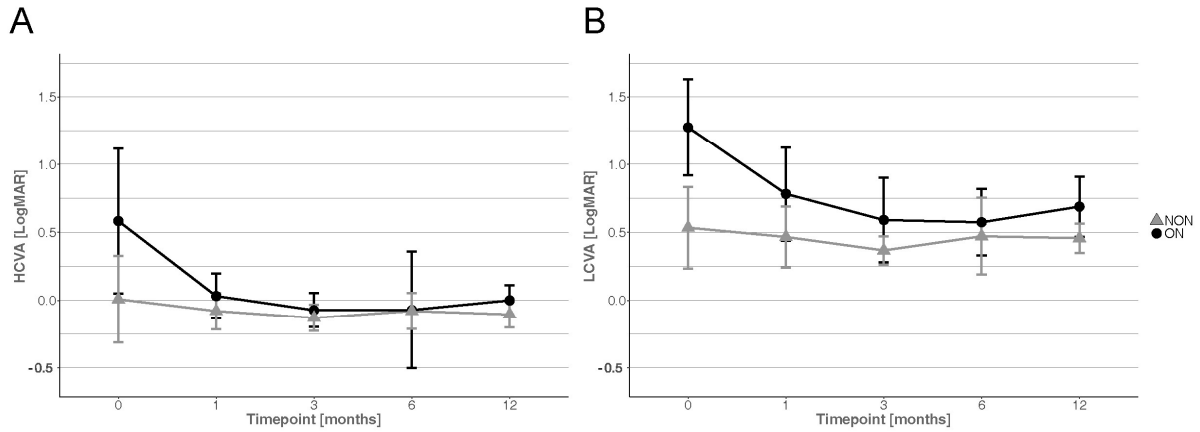


Figure 3-2 Longitudinal visual acuity in optic neuritis.

Best-corrected mean high-contrast visual acuity (HCVA) (A) and low-contrast visual acuity (LCVA) (B) measures in optic neuritis (ON) eyes and non-optic neuritis (NON) eyes over a 12 month period. Error bars represent standard deviations.

3.5.4 Association between macular damage and visual outcomes

Thinner GCIP thickness at month 1 was correlated with lower LCVA at month 3 ($\rho = -0.63$, $p = 0.01$) in ON eyes (**Figure 3-3**). No statistically significant relationship was found between GCIP thickness and LCVA at month 6 or 12. Furthermore, no associations were observed between GCIP thickness at month 1 and HCVA at any timepoint.

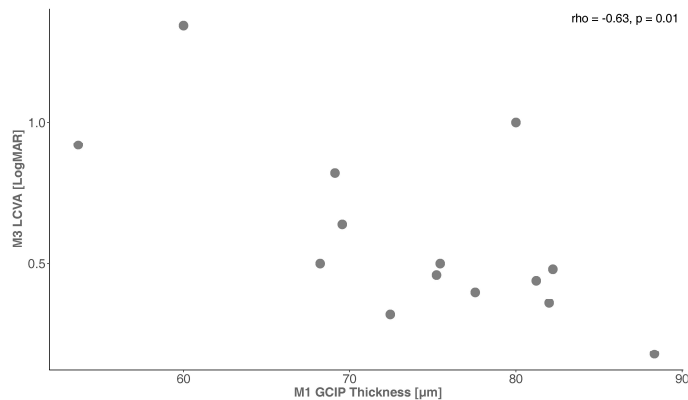


Figure 3-3 Structure-function correlation in optic neuritis.

In optic neuritis eyes, the mean macular ganglion cell and inner plexiform layer (GCIP) thickness at month 1 (M1) was negatively correlated with low-contrast visual acuity (LCVA) at month 3 (M3) ($\rho = -0.63$, $p = 0.01$). The relationship was assessed by Spearman's rank correlation.

3.6 Discussion

We found that an episode of acute ON can result in extensive neuro-axonal retinal damage of the ipsilateral eye, confirming previous longitudinal reports (Costello et al. 2015; Gabilondo et al. 2015).

Significant GCIP thinning was already detectable at 1 month after ON, and also at all subsequent timepoints.

The status of the retina distal to GCIP beyond 6 months post-ON has previously not been documented. We measured a small, but significant increase in INL thickness in the clinically (seemingly) unaffected NON eyes at month 12, suggestive of bilateral retinal pathology in clinically unilateral ON.

Similarly, a significant inter-eye difference between month 1 INL thickness in ON eyes and baseline contralateral INL thickness was observed. Although the detected changes are numerically small, the INL thickness increase in the ON eyes recorded was similar in magnitude to previous findings, including a large meta-analysis (Petzold et al. 2017). All of these previously reported changes to INL thickness, including the current findings, are below the axial resolution of the OCT device used in this study ($\sim 5\mu\text{m}$), however several studies have recorded that the detection limit for retinal layer thickness changes is approximately $1\mu\text{m}$ (Oberwahrenbrock et al. 2015; Knier et al. 2016). Thus, it is likely that the observed INL thickening is meaningful. Nevertheless, it may be prudent to be cautious when interpreting such findings at the individual-patient level. Recently, it has been suggested that the INL shows promise as a possible marker of MS inflammatory disease activity and response to treatment, with INL thickening being associated with more active or breakthrough disease (Green et al. 2010; Gelfand et al. 2012; Saidha et al. 2012; Knier et al. 2016). Therefore INL thickening in ON eyes may be due to mechanisms related to inflammation within or impacting the INL (Green et al. 2010; Gelfand et al. 2012; Knier et al. 2016). Increased INL thickness has also been associated with the presence of microcystic macular oedema (MMO), particularly in patients with a history of MS-related ON or neuromyelitis optica spectrum disorders (NMOSD) (Saidha et al. 2012; Gelfand et al. 2013). In our cohort, signs of MMO were only observed in one patient, in whom only pRNFL data was analysed. Moreover, none of the 11 idiopathic ON cases could be confirmed as NMOSD (Wingerchuk et al. 2015) (eight were seronegative for aquaporin-4 antibodies (AQP4-IgG), while the other three were untested). Neither MMO nor NMOSD appears to explain the mean INL increase we detected.

The change in INL thickness in the NON eyes may indicate subclinical involvement of the fellow eyes in our ON patients. Whilst this structural finding is novel in the literature, we may draw parallels with two results from functional studies and data from a clinical trial in ON. Schnurman showed abnormalities of the ONH component of the multifocal electroretinogram in ON eyes but also, to a lesser extent, in the NON eyes of the same patients (Schnurman et al. 2014). In a substudy of a recent clinical trial assessing the monoclonal anti-LINGO-1 antibody Opicinumab in acute ON, fellow eyes of placebo-treated, but not Opicinumab-treated, patients showed progressive multifocal visual evoked potential (VEP) amplitude loss over 8 months (Klistorner, Chai, et al. 2018). Similarly, Raz

and colleagues found changes to the latency of late peaks of the VEP of NON eyes which were not attributable to demyelination; the authors attributed these changes to an adaptive mechanism in order to maximise preservation of stereopsis in their unilateral ON patients (Raz et al. 2013). We are unable to reach firm conclusions as to the aetiology of our INL thickness changes but, we suggest subclinical inflammation of the fellow eye as a potential candidate. Alternatively, given the proposed role of the INL as a marker for global inflammatory disease activity in MS, the increased INL thickness in NON eyes at month 12 may be indicative of ongoing or future disease activity independent of ON. However, the fact that Balk and colleagues did not observe a significant annualized change in INL volume in MS eyes without a recent history of ON (Balk et al. 2019); may argue against this hypothesis.

By month 12, the magnitude of macular GCIP thinning was -16.6 % in ON eyes relative to the baseline of contralateral NON eyes. An important finding of our study, is the extremely rapid evolution of macular GCIP atrophy in affected eyes, with nearly 75 % of the entire reduction observed over 12 months occurring within the first month of presentation, and 100 % occurring by month three. Gabilondo and colleagues described comparable temporal dynamics of GCIP atrophy subsequent to ON, reporting 57.2 % of the total reduction in thickness occurring within the first 2 months and 73.4 % within the first 3 months (Gabilondo et al. 2015). Our results have important implications for future interventions and clinical trial design: as the magnitude of change is most pronounced early in the course of ON, very early, if not prophylactic intervention, may be the best strategy to prevent tissue damage in acute ON. Moreover, sample size calculations for future clinical trials may be based on the data presented here. Notably, NON eyes had some level of RGC degeneration above thresholds of physiological aging (Balk et al. 2016), consistent with a recent report on longitudinal retinal changes in NON eyes among MS patients and again suggesting subclinical involvement of the contralateral eye in ON (Gabilondo et al. 2015).

pRNFL thickness of ON eyes was increased at baseline examination, most likely indicative of inflammatory oedema. At month 1, peripapillary thickening was still evident but had reduced substantially. Subsequently, pRNFL reduced in thickness, reaching most of its total reduction (87.8 %) by month 3 and showing a moderately sustained decline until month 12, in line with previous studies (Henderson et al. 2010; Costello et al. 2015).

To ensure that our data regarding the temporal course of GCIP, pRNFL and INL thickness changes are not artefactual (due to assessing different subjects at different timepoints), we performed a sub-analysis of patients who had both baseline and month 12 examinations. The results of this sub-analysis confirmed GCIP and pRNFL thinning, as well as INL thickening, one year after ON (data not shown).

Treatment with corticosteroids (mean time between onset of ON and administration: 10 days) was included as a dichotomous variable in the statistical model and was found to have no significant influence on the OCT measures assessed. In NMOSD, the effect of steroids on visual outcomes appears to depend critically on the timing of application, with an optimal effect being achieved with administration ≤ 4 days after onset (Stiebel-Kalish et al. 2019). Yet, in MS-associated ON, both timing and overall impact of steroid treatment has not been shown conclusively. Future studies may consider including temporal information on steroid treatment as a continuous variable in the statistical models.

A profound reduction in HCVA as well as LCVA was observed in ON eyes at baseline. Whilst HCVA recovered rapidly in the majority of patients, with the mean reaching the level of the unaffected eye at month 6, LCVA remained impaired for the entire study period, with a clinically relevant (Balcer et al. 2017) inter-eye difference of 11-12 letters.

We also addressed a putative link between early changes to macular architecture after ON and subsequent visual functional loss. LCVA at month 3 tended to be worse in ON eyes with GCIP thinning at month 1. The lack of a significant association between early GCIP thickness and LCVA at months 6 or 12 may be due to diminished statistical power with smaller sample sizes at these timepoints. No correlation was found between early GCIP thickness and HCVA at any timepoint during follow-up, which is unsurprising given the functional improvement in HCVA up to the level of the contralateral eye at month 6. Together, these results illustrate the importance of LCVA monitoring to properly identify functional visual recovery in MS-associated ON.

An exploratory objective of the study was to analyse gender-specific differences in the outcome of acute ON episodes. Female preponderance is well-known in MS. However, previous studies have reported that once the disease manifests, men are more severely affected than women, characterized by a more rapid disease progression and worsening of clinical outcomes (Koch et al. 2010). To date, few studies have looked into potential influences of gender effects on visual outcomes in ON (Costello et al. 2012; Costello et al. 2015). Those studies which have analysed the effects of gender on recovery after ON have suggested poorer outcomes in males (Costello et al. 2012; Costello et al. 2015). Whilst our raw data was consistent with these previous findings (men demonstrated greater structural changes in GCIP, pRNFL and INL thickness compared to females), our analyses did not reveal statistically significant effects of gender. This may be due to the low number of males included in our study (n=13). As previous work did not state explicitly whether results were corrected for multiple testing (Costello et al. 2012; Costello et al. 2015), it remains

possible that our negative findings regarding gender also reflect differences in statistical analysis methods.

Our study has a number of limitations. As a consequence of its retrospective nature, data were not available for all patients at each follow-up timepoint, resulting in a smaller sample size at follow-ups compared to baseline and also in a slightly different cohort at each timepoint. In addition, the study lacked a dedicated healthy control group. Although all comparisons were made to the baseline of the NON eyes based on the assumption that the baseline of the NON eyes is non-pathological, it cannot be completely ruled out that NON eyes previously experienced retinal pathology following subclinical ON. The latter also holds true for the ON eyes.

The characterization of temporal dynamics underlying neuro-axonal damage in ON and factors associated with a poor functional outcome is important for optimizing timing, patient selection, and mechanisms to target in future interventions. Thus, future prospective studies in ON including the contralateral eyes are needed to confirm the findings reported here in larger cohorts. Such studies may also add clinical relapse rate or radiological disease activity as outcomes, to better assess the clinical significance of the OCT findings reported and to further improve our understanding of the basic mechanisms underlying tissue damage in ON. Such results may pave the way for targeted interventions with the aim of reducing functional visual sequelae.

Overall, our results indicate that macular structural damage develops rapidly in acute ON patients in affected eyes and correlates with functional visual outcomes. LCVA recovery is incomplete following an episode of acute ON. We also provide preliminary evidence for structural pathology involving the contralateral, clinically unaffected eyes which may be explained by subclinical involvement of the fellow eye in ON. Our results further strengthen the importance of early intervention when planning for clinical trials targeting tissue protection in acute ON.

3.7 Author Contributions

C.A. Wicki was involved in conceptualization of the study, wrote the original draft of this manuscript, including the making of the figures and tables. C.A. Wicki partially conducted the OCT examinations and did the OCT post-processing as well as data analysis and interpretation. **P. Manogaran** and **J.V.M. Hanson** were involved in conceptualization of the study, partially conducted the OCT examinations and critically revised the manuscript. **T. Simic** was critically involved in the coordination of study visits and reviewed the manuscript. **S. Schipling** was involved in the design of the study, obtaining funding for the study, and providing critical revisions for the manuscript.

3.8 Acknowledgments

We would like to thank all our subjects who participated in this study. We also thank Sebastian C. Lukas and Elisabeth D. Olbert for assisting in the collection of data. This work has been previously presented at European Committee for Treatment and Research in Multiple Sclerosis and awarded a Poster Prize (ECTRIMS 2017, Paris, FR).

3.9 Study funding

This study was supported by the Swiss National Science Foundation (320030_175770). None of the funding sources had any role in designing the study, in collection, analysis, or interpretation of data, or in writing the article.

3.10 Affiliations

From the Department of Health Sciences and Technology, ETH Zurich (C.A.W.); Neuroimmunology and Multiple Sclerosis Research, Department of Neurology, University Hospital Zurich and University of Zurich (C.A.W., P.M., T.S., J.V.M.H., S.S.); Department of Information Technology and Electrical Engineering, ETH Zurich (P.M.); and Department of Ophthalmology, University Hospital Zurich and University of Zurich (J.V.M.H.).

3.11 Disclosures

CAW has received travel grants from Teva and Merck Sereno. PM has received travel grants from Merck Sereno and Sanofi Genzyme. TS reports no disclosures. JVMH is supported by the Clinical Research Priority Program of the University of Zurich. SvS is supported by the Swiss National Science Foundation (320030_175770), the Myelin Repair Foundation, the Clinical Research Priority Program of the University of Zurich and the Swiss MS Society, has received research grants from Novartis and Sanofi Genzyme, and consultancy and speaking fees from Biogen, Merck Sereno, Novartis, Roche, Sanofi Genzyme, and Teva. Full disclosure form information provided by the authors is available with the full text of this article at Neurology.org/NN.

3.12 Supplemental Data

Table 3-4 Retinal thickness in NON eyes at baseline and in ON eyes over a 12 month period in females.

	NON	ON				
macular GCIP	M0	M0	M1	M3	M6	M12
mean (SD) [μm]	84.4 (6.9)	83.8 (7.7)	74.4 (8.9)	71.7 (11.6)	75.0 (9.2)	74.2 (11.1)
absolute change (SD) [μm]	NA	-0.7 (2.0)	-10.1 (2.6)	-12.7 (3.0)	-9.4 (2.5)	-10.3 (4.1)
number of eyes	28	26	16	19	18	8
pRNFL	M0	M0	M1	M3	M6	M12
mean (SD) [μm]	98.1 (8.6)	113.9 (31.3)	102.9 (14.4)	89.3 (15.1)	89.7 (10.1)	88.8 (15.0)
absolute change (SD) [μm]	NA	15.8 (6.1)	4.8 (4.0)	-8.8 (3.8)	-8.4 (2.9)	-9.4 (5.6)
number of eyes	28	28	16	19	18	8
macular INL	M0	M0	M1	M3	M6	M12
mean (SD) [μm]	35.1 (2.4)	35.0 (2.5)	36.8 (3.4)	36.1 (3.1)	36.1 (2.7)	35.5 (2.6)
absolute change (SD) [μm]	NA	-0.1 (0.7)	1.8 (1.0)	1.0 (0.8)	1.0 (0.8)	0.5 (1.0)
number of eyes	28	26	16	19	18	8

GCIP: ganglion cell and inner plexiform layer, INL: inner nuclear layer, M0: month 0, M1: month 1, M3: month 3, M6: month 6, M12: month 12, NON: non-optic neuritis eye, ON: optic neuritis, pRNFL: peripapillary retinal nerve fibre layer, SD: standard deviation.

Table 3-5 Retinal thickness in NON eyes at baseline and in ON eyes over a 12 month period in males.

	NON	ON				
macular GCIP	M0	M0	M1	M3	M6	M12
mean (SD) [μm]	86.1 (8.7)	84.7 (9.3)	74.82 (4.5)	67.3 (10.2)	67.1 (9.7)	66.4 (11.1)
absolute change (SD) [μm]	NA	-1.4 (3.9)	-11.3 (3.2)	-18.8 (4.8)	-19.1 (5.4)	-19.8 (4.9)
number of eyes	12	10	5	6	4	7
pRNFL	M0	M0	M1	M3	M6	M12
mean (SD) [μm]	97.6 (9.9)	121.0 (24.9)	104.0 (16.7)	85.5 (12.4)	89.8 (12.2)	85.1 (15.7)
absolute change (SD) [μm]	NA	23.4 (7.4)	6.4 (7.4)	-12.1 (5.8)	-7.9 (6.7)	-12.5 (6.6)
number of eyes	13	13	6	6	4	7
macular INL	M0	M0	M1	M3	M6	M12
mean (SD) [μm]	37.6 (3.5)	36.8 (2.3)	36.1 (1.5)	37.9 (2.9)	38.0 (1.9)	40.6 (3.2)
absolute change (SD) [μm]	NA	-0.8 (1.2)	-1.5 (1.2)	0.3 (1.5)	0.4 (1.4)	3.0 (1.6)
number of eyes	12	10	5	6	4	7

GCIP: ganglion cell and inner plexiform layer, INL: inner nuclear layer, M0: month 0, M1: month 1, M3: month 3, M6: month 6, M12: month 12, NON: non-optic neuritis eye, ON: optic neuritis, pRNFL: peripapillary retinal nerve fibre layer, SD: standard deviation.

Table 3-6 HCVA and LCVA in NON and ON eyes over a 12 month period.

HCVA	M0	M1	M3	M6	M12
NON: mean (SD) [LogMAR]	0.01 (0.32)	-0.08 (0.13)	-0.13 (0.1)	-0.08 (0.13)	-0.1 (0.1)
ON: mean (SD) [LogMAR]	0.58 (0.53)	0.03 (0.17)	-0.07 (0.13)	-0.07 (0.43)	0.0 (0.11)
LCVA	M0	M1	M3	M6	M12
NON: mean (SD) [LogMAR]	0.53 (0.3)	0.47 (0.22)	0.37 (0.1)	0.47 (0.28)	0.46 (0.11)
ON: mean (SD) [LogMAR]	1.27 (0.36)	0.78 (0.34)	0.59 (0.31)	0.57 (0.24)	0.69 (0.02)

HCVA: high-contrast visual acuity, LCVA: low-contrast visual acuity, M0: month 0, M1: month 1, M3: month 3, M6: month 6, M12: month 12, NON: non-optic neuritis eye, ON: optic neuritis eye, SD: standard deviation.

4 Longitudinal characterization of afferent visual pathway pathology in experimental optic neuritis using a multimodal imaging approach

4.1 Preface

This study was a shared PhD project of C.A. Wicki and P. Manogaran. C.A. Wicki conducted the diffusion tensor imaging (DTI) and T2 weighted imaging acquisition and analysis. P. Manogaran conducted the optical coherence tomography (OCT), green autofluorescence imaging (GAF), visual evoked potential (VEP), electroretinography (ERG) and *ex-vivo* data collection and analysis. This thesis chapter is only focusing on the magnetic resonance imaging (MRI) part and not including the data obtained by P. Manogaran. We will make every endeavour to publish a scientific manuscript combining all the measures at a later date.

4.2 Introduction

Early gliosis and inflammatory demyelination of the optic nerve accompanied by neuro-axonal degeneration of the visual pathway is observed in myelin oligodendrocyte glycoprotein (MOG) peptide-induced experimental autoimmune encephalomyelitis (EAE), often referred as experimental autoimmune optic neuritis (ON) (Brown and Sawchenko 2007; Horstmann et al. 2013).

In recent years, our lab has started to establish a multimodal non-invasive imaging platform to quantitatively assess afferent visual pathway (AVP) involvement in this animal model of multiple sclerosis (MS), using OCT, MRI and *ex-vivo* analysis (Manogaran et al. 2018; Manogaran et al. 2019). DTI is an advanced MRI technique that can be used to indirectly probe the structural integrity of the optic nerve and tract fibres, while OCT allows for monitoring of retinal structures. *Ex-vivo* analyses add valuable morphological substrate to the *in-vivo* obtained imaging data.

DTI provides information about the magnitude and preferred direction of diffusing water protons (Kollias 2009; Aung, Mar, and Benzinger 2013). The application of magnetic field gradients in at least 6 non-collinear directions can be used to estimate diffusion within a voxel in a 3D ellipsoid (3x3 matrix) termed the diffusion tensor (Kollias 2009). The ellipsoid orientation is characterized by three principal tensor axes (eigenvectors) and its shape by three eigenvalues (EVs) (Kollias 2009). The ellipsoid eccentricity defines fractional anisotropy (FA), which is a scalar value that describes the degree of tissue anisotropy within a voxel with values between 0 (diffusion is isotropic) and 1 (diffusion occurs only along one axis) (Aung, Mar, and Benzinger 2013). The average of all EVs or mean diffusivity (MD) is a measure of the total diffusion magnitude within a voxel. Thus, FA and MD are believed to indirectly represent microstructural white matter (WM) tract integrity, whereby a decrease in FA or an increase in MD indicates impaired integrity due to either axonal injury, demyelination or a combination of both (Mori and Zhang 2006; Aung, Mar, and Benzinger 2013).

These two measures are not specific, and cannot distinguish between the two pathological mechanisms though. However, since water diffusion is restricted by CNS structures, the EVs can also be used to describe directional diffusivity with longitudinal changes being more specific to the underlying disease processes. For instance, radial diffusivity (RD; average of the shorter EVs: 2nd and 3rd EV) represents water movement perpendicular to axonal fibre tracts, while axial diffusivity (AD; longest or 1st EV) measures diffusivity parallel to fibre tracts (Aung, Mar, and Benzinger 2013). In a healthy intact axon, we would expect high AD because less obstacles hinder the movement along the axon fibres and low RD, since the axonal membrane and the surrounding myelin sheaths restrict water movement across the fibres. In MS, an increase in RD is consistently believed to correlate with demyelination, while altered AD is less understood, but has been linked to axonal damage, with previous studies observing decreased AD in acute lesions and increased AD in chronic MS lesions (Aung, Mar, and Benzinger 2013; Kuchling et al. 2017; Mahajan and Ontaneda 2017).

The objective of our study was to further improve the multimodal imaging platform, in order to increase accuracy in investigating the longitudinal mechanisms of demyelination and neurodegeneration in the visual system of individual EAE mice. Moreover, we aimed to establish an imaging platform that is optimized for future preclinical testing of neuroprotective or neuroregenerative candidates.

The following chapter is subdivided into a feasibility, reliability and sensitivity study to probe and validate our modified MRI set-up for non-invasive, *in-vivo* longitudinal assessment of the pre- and post-chiasmal visual pathway in EAE.

4.3 Feasibility study

Since we experienced difficulties with intubation in previous studies in EAE, a free-breathing setup was established in order to refine the MRI procedure for the animals and therefore to better incorporate the 3Rs (refine, reduce, replace), the guiding principles for the use of animals in science (Kilkenny et al. 2010; Smith et al. 2018). In addition, the MRI protocol from an earlier study (Manogaran et al. 2018) was slightly adjusted to optimize the quality of the images.

4.3.1 Methods

The description of the methods section is partially taken from chapter 4.2.1 of P. Manogaran's doctoral thesis (DISS. ETH No. 26744) entitled "The afferent visual pathway as a model for assessing neurodegeneration in experimental autoimmune encephalomyelitis – a translational optical coherence tomography approach" (accepted in 2020) and is similar to previously published methods (Manogaran et al. 2018; Manogaran et al. 2019).

4.3.1.1 Animals

The study was performed in conformity with the Swiss Animal Welfare Law (License No.: 174/18). A total of three healthy female wild-type C57BL/6JRj (Janvier, Le Genest-St Isle, France) mice (13 – 15 weeks old) were examined over 4 time points (at baseline, week 1, week 2 and week 8) to test the feasibility of using a new mouthpiece that allows the mice to breath freely during the MRI acquisition. Mice had access to food and water *ad libitum* and were housed in a light-dark cycle of 12:12 hours. To reduce artificial light related damage to the eyes, all cages were kept on the bottom rack and provided with red houses in the cage.

4.3.1.2 MRI assessment

Anaesthesia for the MRI examination was induced with 3.5 % isoflurane, supplied in a mixture of pure oxygen and air (500 O₂: °800 air/CA). Directly after induction of anaesthesia mice were transferred to the 7T animal MRI scanner (Biospec 70/16, Bruker, Germany) equipped with a cryogenic quadrature transceiver surface coil (Bruker BioSpin AG, Fällanden, Switzerland).

Prior to MRI examination, all mice received 100 µl of a balanced electrolyte solution (Lactated Ringer's Solution by B Braun Medical) subcutaneously in order to minimize dehydration. Moreover, an eye gel (Lacrinorm; Carbomerum 980) was applied to the eyes to retain eye moisture during examination.

Anaesthesia was maintained with 1.7 – 2.3 % isoflurane, supplied in a mixture of 1 : 2 pure oxygen and air (200°O₂ : °400 air/CA), while the animals were spontaneously breathing. The animals were positioned onto an animal cradle made from Plexiglass with a built-in heating system (circulating warm water bath). Since DTI is sensitive to motion, atraumatic ear and bite bars were used to optimize positioning and fixation of the mouse head. The head was positioned straight and centred, so that the optic nerves were pointing approximately along the axis of the magnet, allowing for the optic nerve and tract to be imaged in the coronal plane. Diffusion properties of water are affected by temperature changes, therefore body temperature was monitored using a rectal thermometer and maintained at 37.0°±1°C (Fotemp, Optocon, Dresden, Germany). Concurrently, respiratory rate was continuously monitored using a breathing sensor (ADInstruments, LabChart v8.0.5.04.07.2014) and maintained at 80 ± 10 breaths per minute. After completion of the MRI examination, another eye ointment (Lacrinorm; Carbomerum 980 or Bepanthen with 5 % Dexpanthenol) was applied to both eyes to protect the eyes from irritation.

For optimal performance, coil tuning and matching was performed on the first mouse of each scanning day. After acquiring the initial positioning sequences (localizer and more detailed tri-pilot scan), an adjustment sequence (AdjRefG) was conducted to optimally calibrate the radiofrequency (RF) pulse power over the optic nerve and tract.

In order to detect T2 signal hyperintensity regions around the optic nerves indicative of inflammation, a T2-weighted multi-slice Fast Spin-Echo (TurboRARE) sequence with the following parameters was acquired: TE 33 ms, TR 2500 ms, 14 axial slices with a slice thickness of 0.5 mm, slice gap 0.1 mm, Resolution $75 \mu\text{m}^2$ (matrix size 200×200 mm, FOV 15×15 mm), number of averages = 2 (acquisition time: 02:05 min). In addition, to optimize magnetic field homogeneity and to avoid image distortion, localized shimming over the optic nerve and tract was performed.

Multi-shell ($B_0 = 1000 \text{ s/mm}^2$; $B_1 = 2000 \text{ s/mm}^2$) DTI was performed using an echo-planar imaging (EPI) sequence with the following parameters to assess the structural integrity of the optic nerve and tract: TE 25.8 ms, TR 2500 ms, number of averages = 1, 64 diffusion directions, number of exp. per direction = 2, maximum B-value 2535.23 s/mm^2 , Resolution $78 \mu\text{m}^2$ (matrix size 192×192 mm, FOV 15×15 mm), echo spacing 0.96 ms, 14 axial slices with a slice thickness of 0.5 mm, and slice gap 0.1 mm (acquisition time: 44:40 min). The slice geometry and orientation, as well as the shim volume were always copied over from the T2 to the DTI sequence to ensure similar grid positioning for the two scans. To ensure consistent slice positioning, the last slice was always placed over the indent of the border of the olfactory bulb, using the sagittal view (**Figure 4-1**). Slice 10 and 11 were used for the optic nerve measures (DTI and T2), while slice 6 was used for the optic tract readouts (DTI only). In addition, for the DTI sequence, a saturation pulse was placed below the region-of-interest (ROI).

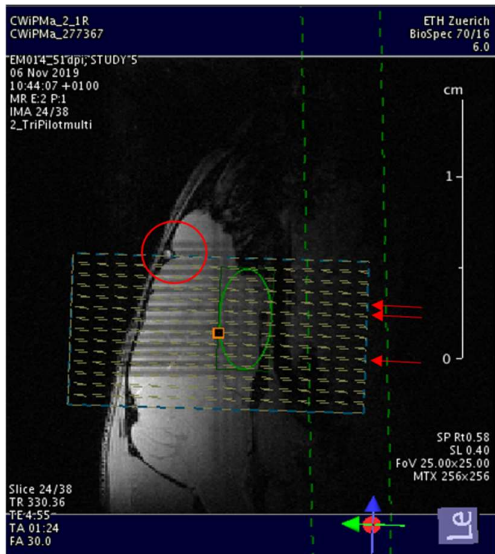


Figure 4-1 Sequence planning and slice selection for diffusion tensor imaging and T2.

To ensure consistent slice positioning, the last slice was always positioned over the indent of the border of the olfactory bulb, using the sagittal view (indicated by the red circle). Slice 10 and 11 were used for the optic nerve measures (diffusion tensor imaging, DTI and T2), while slice 6 was used for the optic tract readouts (DTI only) (indicated by the red arrows). The shimming ellipsoid (in green) was placed such that it covered the optic nerve and tract throughout the applicable slices and ensured homogenization of the magnetic field in the region-of-interest (ROI). Additionally, for the DTI sequence only, a saturation pulse was placed below the ROI.

The DTI images were re-constructed using Paravision 6.0 and analysed using Paravision 5.1 (Bruker, BioSpin GmbH). For quantitative analysis, FA (supposed to reflect the strength of diffusion directionality or the degree of tissue anisotropy), MD (supposed to reflect the total diffusion within a voxel), AD (supposed to represent diffusivity parallel to fibres), and RD (supposed to represent diffusivity perpendicular to fibres) values were obtained from the optic nerves and tracts, using a manually segmented ROI based analysis: a circle, respectively an ellipsoid was drawn within the optic nerve and tract (**Figure 4-2**). The DTI metrics were calculated from the eigenvalues (λ_1 , λ_2 and λ_3) and based on the following equations:

$$FA = \sqrt{\frac{1}{2} \frac{\sqrt{(\lambda_1 - \lambda_2)^2 + (\lambda_2 - \lambda_3)^2 + (\lambda_3 - \lambda_1)^2}}{\sqrt{\lambda_1^2 + \lambda_2^2 + \lambda_3^2}}}$$

$$MD = \frac{\lambda_1 + \lambda_2 + \lambda_3}{3}$$

$$RD = \frac{\lambda_2 + \lambda_3}{2}$$

$$AD = \lambda_1$$

In order to minimize partial volume effects and to be conservative in the measurements, the outer rim of the optic nerve and tract was excluded for the ROI analysis. The quality of all scans has been checked by visually inspecting the FA maps for artifacts and for poor illumination.

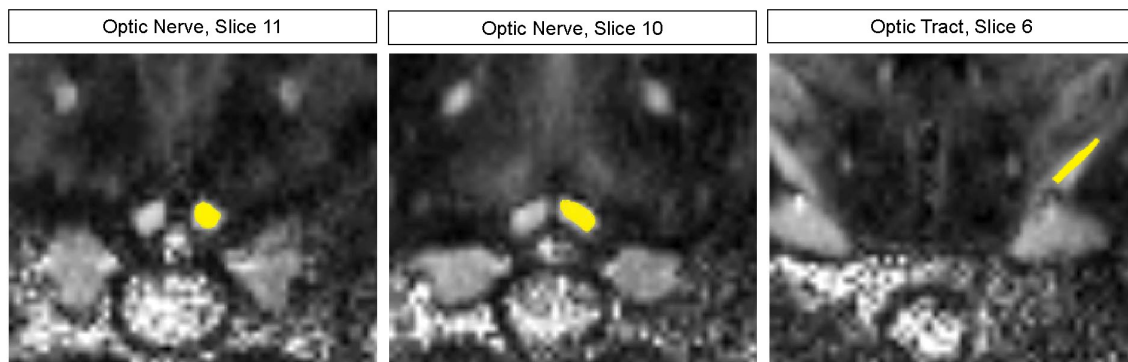


Figure 4-2 Diffusion tensor imaging analysis.

A grey-scale map of the fractional anisotropy values from the optic nerve and tract displays anisotropic areas brighter than isotropic areas. Manually segmented region-of-interests are shown in yellow.

4.3.2 Results

The new MRI setup allowed for the anesthetization of the mice without performing the challenging procedure of endotracheal intubation. Although the mice had no mechanical breathing support during the approximately one hour long MRI examination, they showed no problems in maintaining spontaneous respiration. Also, no anaesthesia-related complications were observed post-examination.

With regards to the MRI protocol, a few adjustments were made to the protocol that was previously established by our group (Manogaran et al. 2018), to further optimize image quality. The Tri-pilot positioning scan included more slices in order to facilitate accurate grid positioning for the following DTI and T2 scans. Furthermore, the slice thickness of the adjustment sequence, to optimally adjust the power of the RF pulse to the optic nerve and tract, had been increased from 2 mm to 7 mm. While maintaining sufficient focus on the ROI, this also allowed coverage of the rest of the brain, so that tractography of the entire visual pathway could be a possible approach in the future. Additionally, we introduced a multi-shell DTI protocol with two b-values instead of one to further facilitate future tractography studies. DTI quality improved when we obtained 64 diffusion directions with 2 experiments per direction instead of 60 diffusion directions with 1 experiment per direction. Moreover, we slightly modified the geometry for both the DTI and the T2 sequence: we increased the number of axial slices from 8 to 14 and reduced the slice gap from 0.25 mm to 0.1 mm (the slice thickness was kept at 0.5 mm). Otherwise, the protocol is similar to the one published in 2018 (Manogaran et al. 2018).

Initially, we had difficulties with respiratory motion artifacts and image quality was variable between animals. Therefore, in order to achieve a more stable breathing rate in the range of 80 ± 10 breaths per minute, the isoflurane levels have been continuously adjusted, based on the livestream of the breathing rate sensor. Moreover, head immobilization was optimized by the correct use of non-traumatic teeth and ear bars. Regarding the fixation of the animal inside the magnet, we observed that the image quality of animals with the head positioned closer to the cryogenic coil, was consistently superior. As a consequence, we modified the set-up by placing a small foam-roll under the chin and front legs of the mice to position the animal closer to the coil. After incorporating these adjustments, the obtained images were of high quality and the optic nerve (Slice 10 and 11) and tract (Slice 6) were easily identifiable on the FA maps of the appertaining slices (**Figure 4-3**).

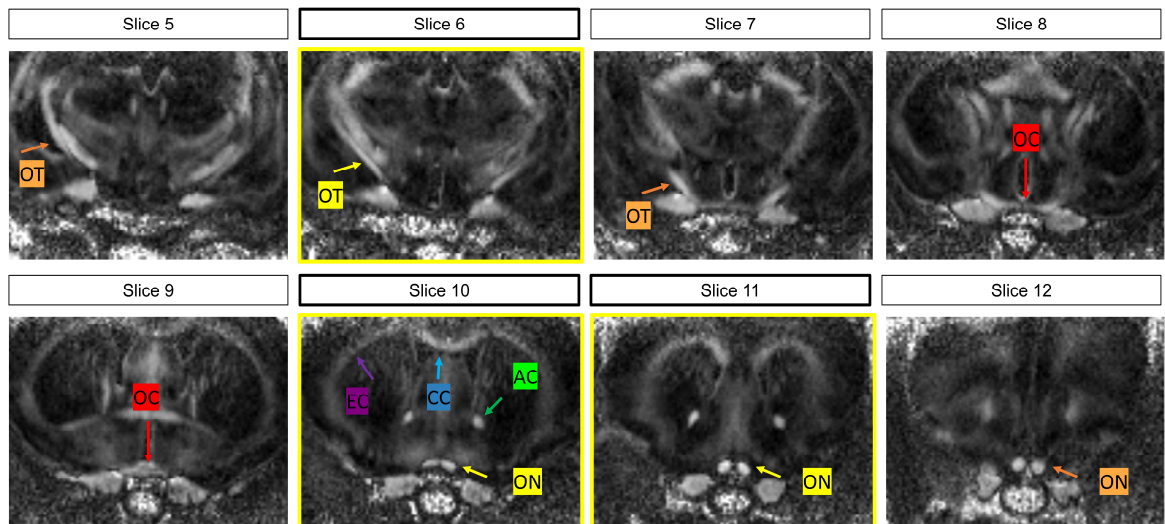


Figure 4-3 Fractional anisotropy maps of slice 5–12 obtained with the diffusion tensor imaging protocol that was established in the feasibility study.

The diffusion tensor imaging (DTI) analysis includes the regions highlighted by yellow arrows (slice 10 and 11 for optic nerve measures and slice 6 for optic tract measures). The other arrows indicate other white matter tracts that are nicely visible on the fractional anisotropy maps, but have not been analysed in this study. AC: anterior commissure, CC: corpus callosum, EC: external capsule, OC: optic chiasm, ON: optic nerve, and OT: optic tract.

4.3.3 Discussion

Tracheal intubation of mice is a complicated procedure and requires a considerable amount of staff training. If not performed routinely, intubation is stressful for the mice and may cause damage to the pharynx, larynx, trachea or esophagus and can even result in death (Watanabe et al. 2009). With the use of a free-breathing setup, anesthesia-related complications during or after MRI examination have been eliminated. Nevertheless, for some MRI studies that require long acquisition times, intubation and mechanical ventilation are indispensable (Tremoleda, Macholl, and Sosabowski 2018).

The importance of measures to reduce experiment-related stress is highlighted by the observation that EAE presentation may be influenced by the hypothalamic-pituitary-adrenal axis – the main response system to stress (Heesen et al. 2007).

Good image quality critically depends on proper animal immobilization. Moreover, the head of the animal needs to be positioned as high, straight and centered as possible inside the magnet. Overall, the feasibility study provided support for the further use of the new free-breathing setup to continue our MRI studies in EAE mice. However, prior to drawing firm conclusions, data on longitudinal reliability is required.

4.4 Longitudinal reliability study

Because the mice were intubated for imaging in our previous studies, we continued with a within-subject longitudinal reliability study to evaluate if DTI would still provide consistent measurements, when using the new free-breathing setup.

For this study, the wild-type C57BL/6JRj mouse line was supplemented by a Thy1-YFP-16 transgenic mice line, expressing yellow fluorescent protein (YFP) in retinal ganglion cells (RGCs). In these mice, it is possible to image RGCs in vivo longitudinally, by exciting and quantifying the YFP-positive cells with a 515 nm green autofluorescence (GAF) laser, that is integrated in a modified Heidelberg Spectralis OCT device. An additional aim of the longitudinal reliability study was therefore to assess, if the change in the mouse type influences the MRI measures.

4.4.1 Methods

4.4.1.1 Animals

The description of the animal section is partially taken from chapter 4.2.1 of P. Manogaran's doctoral thesis (DISS. ETH No. 26744) entitled "The afferent visual pathway as a model for assessing neurodegeneration in experimental autoimmune encephalomyelitis – a translational optical coherence tomography approach" (accepted in 2020) and is similar to previously published methods (Manogaran et al. 2018; Manogaran et al. 2019).

The study was performed in conformity with the Swiss Animal Welfare Law (License No.: 174/18). Three healthy 14 – 16 weeks old wild-type C57BL/6JRj (Janvier, Le Genest-St Isle, France) mice (2 males 1 female) and three healthy 14 – 16 weeks old C57BL/6J-Tg 16Jrs/J (Thy1-YFP-16) mice (1 male and 2 females) were longitudinally assessed at baseline, as well as 12, 16, 28 and 51 days thereafter. Breeding pairs homozygous for Thy1-YFP-16 were purchased from Jackson Laboratory (ME, USA) and maintained in a breeding colony at the Laboratory Animal Services Centre (LASC) at the University of Zurich (Breeding License: 101 LASC:102321). Mice had access to food and water *ad libitum* and were housed in a light-dark cycle of 12:12 hours. To reduce artificial light related damage to the eyes, all cages were kept on the bottom rack and provided with red houses in the cage.

4.4.1.2 MRI assessment

MRI examinations were performed identically to the methods described in the feasibility study (chapter 4.3.1.2).

4.4.1.3 Statistics

Statistical analyses were performed using R version 3.6.1 (R Core Team, 2019; <http://www.r-project.org>). A linear-mixed effects model (function lmer in library lme4) was employed to analyse if there was a difference in optic nerve FA within-subjects between time points, and if there was a

difference in values between wild-type and transgenic mice. The model accounted for intra-subject, inter-eye dependencies, since we obtained measurements from two eyes per mouse, with time points and group as covariate. A similar analysis was conducted for the optic tract but using an averaged FA value of the left and right tract, since fibres partially cross at the chiasm. To ensure that the model is suitable for the data, the residuals were tested for normality by inspection of the residuals plot (function plot in default core R library) and Q-Q plot (function qqnorm in default core R library). If the Type II Wald chisquare test (function Anova in library car) indicated that the covariates appear to have a significant influence on the response variable, the least squares mean test (function lsmeans in library lsmeans) was used to investigate differences between specific comparisons for these models. All p-values were corrected for multiple testing using Bonferroni correction (function p.adjusted in default core R library). Statistical significance was considered for p-values ≤ 0.05 . The measures of day 16 were excluded from statistical analysis, since we had technical issues on this scanning day (problems with coil tuning and matching).

4.4.2 Results

There were no statistically relevant within-subject age-related changes in FA measurements over the four time points (optic nerve: $p=0.79$, optic tract: $p=0.083$). There was also no statistically significant difference in FA measurements between Thy1-YFP-16 mice and wild-type C57BL/6JRj mice in both the optic nerve and tract (optic nerve: $p=0.72$, optic tract: $p=0.95$) (**Figure 4-4**). Additionally, when comparing the current FA measures to healthy mice from a previously published study (Manogaran et al. 2018), the values were reproducible and comparable.

No statistical analysis was performed on the diffusion values, but visualization of the data indicated that the diffusion values remained stable over time (**Figure 4-4**). The absolute diffusion values are slightly different from previously published values (Manogaran et al. 2018), which is not surprising when considering that the images were reconstructed on a slightly different b-value because of adjustments to the MRI protocol.

4.4.3 Discussion

Successful establishment of a free-breathing setup will refine the experiment procedures for both, the animals and researchers. Especially in longitudinal studies with fragile EAE mice, intubation is a high risk for the animals. Reducing the number of anesthesia-related complications will indirectly also reduce the total number of animals needed, since a lower drop-out rate can be expected.

Overall, MRI outcomes were neither showing any relevant within-subject fluctuations at the different time points, nor between different groups (wildtype versus transgenic). We conclude that the optic nerve and tract MRI measures obtained with the new protocol and free-breathing device setup are reliable for the longitudinal assessment of healthy Thy1-YFP-16 mice. Whether this is also true under pathological conditions such as in EAE mice remains to be investigated.

In the feasibility and longitudinal reliability study, we eliminated the risk associated with intubation, and experiment procedures have been refined accordingly. The setup is now ready to be used for the longitudinal sensitivity study in EAE mice.

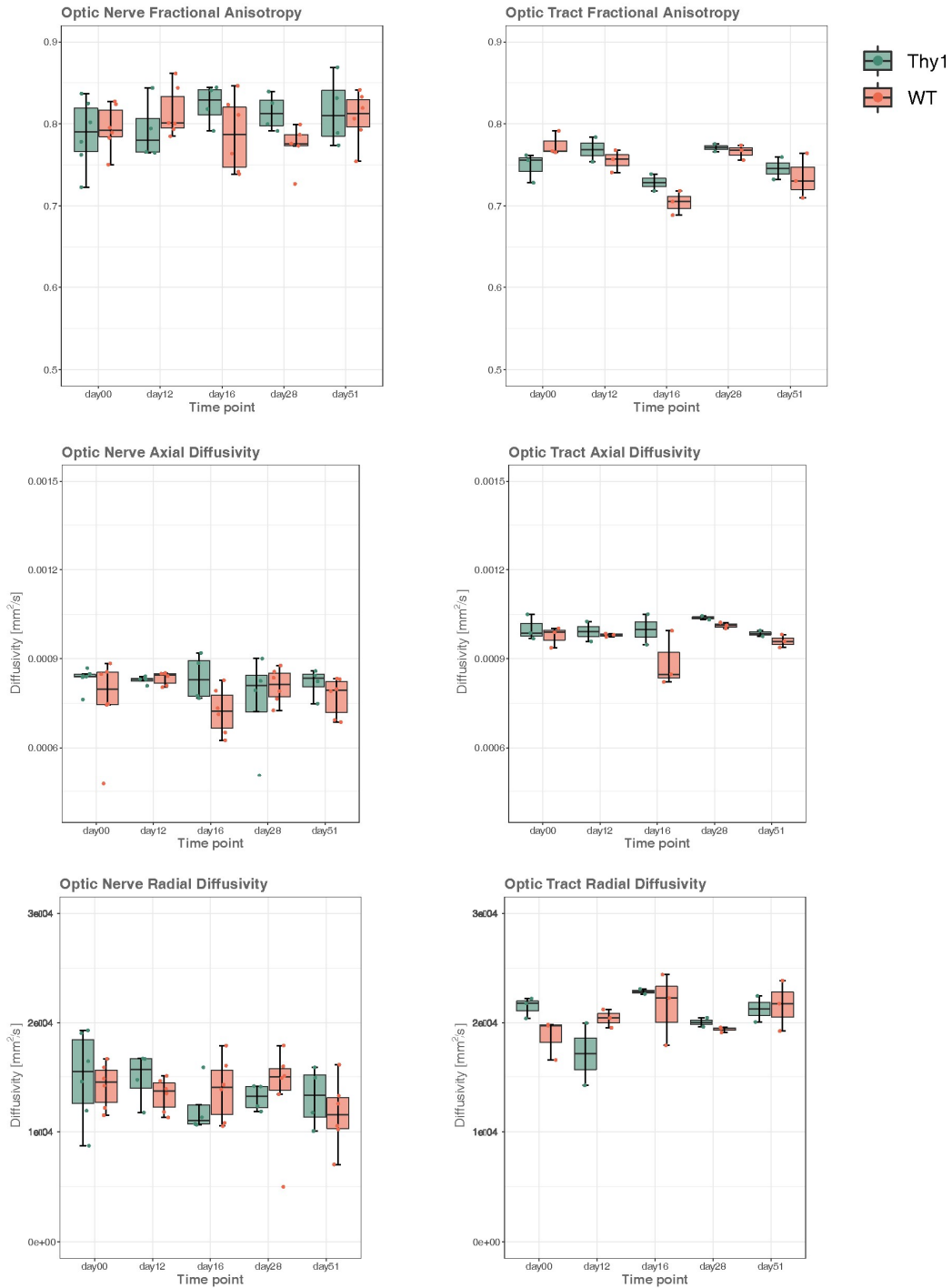


Figure 4-4 Longitudinal reliability of diffusion tensor imaging measures.

Boxplots of the fractional anisotropy (FA), axial diffusivity and radial diffusivity over time in Thy1-YFP-16 transgenic (green) and wild-type (WT) (orange) mice in the optic nerves (left) and optic tracts (right). FA is a scalar value between 0 (diffusion is isotropic) and 1 (diffusion occurs only along one axis). Please note, that the measures of day 16 were excluded from statistical analysis because of technical issues on this scanning day.

4.5 Longitudinal sensitivity study

Finally, we performed a longitudinal sensitivity study to assess the sensitivity of non-invasive structural MRI, OCT and GAF imaging, complemented with functional VEP and ERG assessments and *ex-vivo* analysis to distinguish between control and EAE mice and to characterize EAE-induced pathology in the retina, optic nerve and tract over time.

Although several studies have already been performed to investigate the pathological processes involved in experimental ON (Brown and Sawchenko 2007; Horstmann et al. 2013), many open questions remain. For example, it is not completely understood, to what extent inflammation, demyelination, and RGC loss impacts the DTI observed changes in microstructural integrity of the optic nerve and tract in EAE. Furthermore, the association between structural DTI or OCT measures and functional outcomes such as the VEP latency or the ERG amplitude need to be further investigated in EAE. Moreover, it is still unclear if neuro-axonal damage of the RGCs is solely a secondary process of inflammatory demyelination or if primary pathology independent of demyelination also plays an important role. To what extent glial pathology is involved in RGC damage in EAE, how MOG-specific it is and if it might instead be a response to complete Freund's adjuvant (CFA), also merits further investigation. In this study, we have tried to address some of these unresolved issues.

This thesis chapter is not intended to report all study findings, but rather to focus on the MRI part. In this study, we hypothesized that the T2-signal increases around the optic nerve as a secondary measure of inflammation. Further, we hypothesized that FA and AD progressively decrease, while, in parallel, MD and RD continuously increase in the optic nerve and tract during the first month of EAE.

4.5.1 Methods

4.5.1.1 Animals

The description of the animal section is partially taken from chapter 4.2.1 of P. Manogaran's doctoral thesis (DISS. ETH No. 26744) entitled "The afferent visual pathway as a model for assessing neurodegeneration in experimental autoimmune encephalomyelitis – a translational optical coherence tomography approach" (accepted in 2020) and is similar to previously published methods (Manogaran et al. 2018; Manogaran et al. 2019).

The study was performed in conformity with the Swiss Animal Welfare Law (License No.: 174/18). For the sensitivity study, a total of thirteen female 16 – 18 weeks old C57BL/6J-Tg 16Jrs/J (Thy1-YFP-16) (Jackson Laboratory, USA) mice were included. Two of the thirteen mice had to be excluded early from the study, because of visible abnormalities on their baseline (prior to EAE induction) retinal fundus images. EAE was induced in eight mice by immunization with an emulsion of MOG₃₅₋₅₅ (Hooke Laboratories, Lawrence, MA, USA) in CFA, injected subcutaneously into both flanks

(0.2 mg/mouse), followed by intraperitoneal administration of pertussis toxin in phosphate-buffered saline (PBS) on day 0 of immunization and again on day 1 (4 µg/ml/mouse/day)). Three control mice were immunized with a CFA-only emulsion (no MOG peptide; Hooke Laboratories, Lawrence, MA, USA) injected subcutaneously in both flanks (0.2 mg/mouse), followed by intraperitoneal administration of pertussis toxin in PBS on day 0 and day 1 (4 µg/ml/mouse/day). Animals were weighed and scored daily after showing the first signs of symptoms, as assessed by the EAE disability score (0 = no detectable signs of EAE, 0.5 = distal limp tail, 1 = complete limp tail, 1.5 = limp tail and hind limb weakness, 2.0 = unilateral partial hind limb paralysis, 2.5 = bilateral partial hind limb paralysis, 3.0 = complete bilateral hind limb paralysis, 3.5 = complete bilateral hind limb paralysis and partial forelimb paralysis, 4.0 = moribund, 5.0 = death). MRI examinations were performed at baseline (3 and 4 days prior to immunization), 15/16 days post immunization (dpi) (peak of EAE symptoms), and 28/29 dpi (partial recovery of EAE symptoms). These time points were based on a previous study (Manogaran et al. 2018). Mice had access to food and water *ad libitum*. Additionally, to ensure nutrition following EAE induction, food and water (i.e. HydroGel, Clear H2O, Westbrook ME, USA) were placed on the cage floor as soon as mice exhibited an EAE score of 1.5 or greater. Moreover, to improve the wellbeing of the animals, particularly to prevent severe body weight loss that can be observed in EAE, high-energy food gels (i.e. DietGel Boost, Clear H2O, Westbrook ME, USA) were provided in the cages 3 days prior to EAE induction. The mice were housed in a light-dark cycle of 12:12 hours. To reduce artificial light related damage to the eyes, all cages were kept on the bottom rack and provided with red houses in the cage.

4.5.1.2 MRI assessment

MRI examinations were performed identically to the methods described in the feasibility study (chapter 4.3.1.2). DTI data of slice 11 of one of the EAE mice at peak had to be excluded due to low quality. Therefore, for this mouse and time point, the DTI measures of the optic nerve were only based on one slice instead of the average of slice 10 and 11.

4.5.1.3 Statistics

Statistical analyses were performed using R version 3.6.1 (R Core Team, 2019; <http://www.r-project.org>). A linear-mixed effects model (function `lmer` in library `lme4`) was employed to analyse if there was a difference in MRI readouts within-subjects between time points, and if there was a difference in values between control and EAE mice. The model accounted for intra-subject, inter-eye dependencies, since we obtained measurements from two eyes per mouse. For optic nerve FA, AD and RD, the model included time points and group as covariates, while the model for MD also included eyes as covariate (which appeared to have a significant effect within the model). A similar analysis was conducted for the optic tract but using an averaged FA value of the left and right tract, because fibres partially cross at the chiasm. Therefore, all optic tract models only included time points and group as covariates. To ensure that the model is suitable for the data, the residuals were tested for normality by inspection of the residuals plot (function `plot` in default core R library) and Q-

Q plot (function qqnorm in default core R library). If the Type II Wald chisquare test (function Anova in library car) indicated that the covariates appear to have a significant influence on the response variable, the least squares mean test (function lsmeans in library lsmeans) was used to investigate differences between specific comparisons for these models. All p-values were corrected for multiple testing using Bonferroni correction (included in the lsmeans function in library lsmeans). Statistical significance was considered for p-values ≤ 0.05 .

4.5.2 Results

4.5.2.1 Clinical assessment

EAE onset started around 14 dpi and was characterized by tail and hind limb weakness. Peak of disease or an EAE score of 3 (complete bilateral hind limb paralysis) was observed from 16 dpi till 19 dpi, followed by partial recovery of symptoms back to a median EAE score of 2 (unilateral partial hind limb paralysis) by 29 and 30 dpi. The maximum body weight loss was reached around 20 dpi and stabilized thereafter (**Figure 4-5**). All mice were able to complete MRI examinations at all time points without serious anaesthesia-related complications.

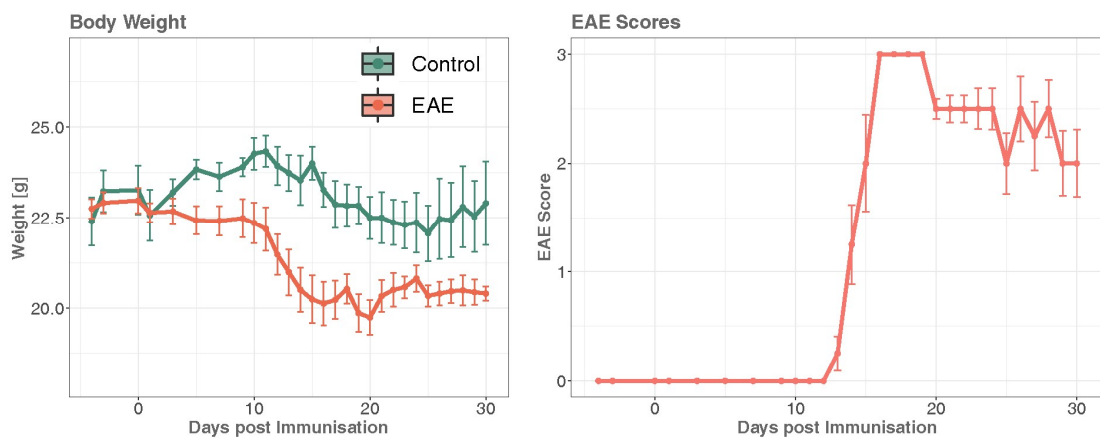


Figure 4-5 Longitudinal body weight and experimental autoimmune encephalomyelitis scores.

(**Left**) Body weight (mean \pm SD) over time in control complete Freund's adjuvant-only immunized mice (green) and experimental autoimmune encephalomyelitis (EAE) (orange) mice. (**Right**) EAE scores (median \pm SE) in EAE mice over time.

4.5.2.2 MRI assessment

In order to assess ON associated inflammation and oedema, the T2 images were qualitatively assessed for high signal intensity regions around the optic nerve. At peak, a visible increase in T2 signal hyperintensities around the optic nerves compared to the baseline of the individuals was observed in 7 out of 8 EAE mice on at least one of the two adjacent optic nerve slices. For one EAE mouse no increase was observed at any time point. In general, the increase in hyperintensities was less prominent at recovery compared to peak. In the control group, no clear increase in T2 signal was seen at any time point (**Figure 4-6**).

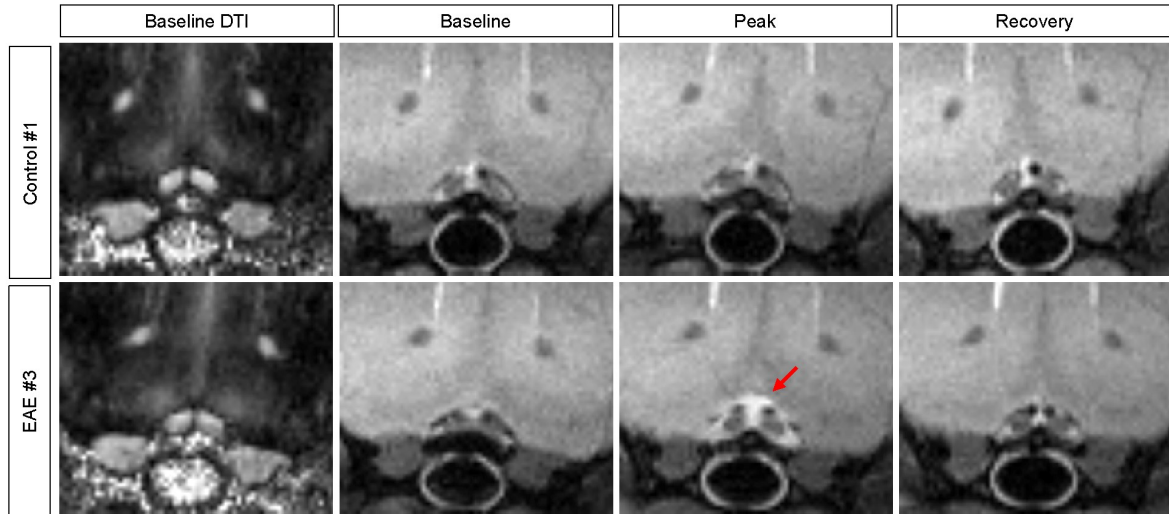


Figure 4-6 Longitudinal T2-weighted scans.

Longitudinal T2-weighted images in a complete Freund's adjuvant-only immunized control mouse (top row) and an experimental autoimmune encephalomyelitis (EAE) mouse (bottom row). The red arrow indicates the observed T2 signal increase around the optic nerves indicative of inflammation. For both mice, the spatially co-registered baseline fractional anisotropy map is also shown (left).

At baseline, DTI results were similar in EAE and control mice for both the optic nerve (**Table 4-1**) and the optic tract (**Table 4-2**). The baseline results also resembled the values obtained in the longitudinal reliability study, indicating good reliability of the MRI readouts.

Table 4-1 DTI measurements in control and EAE mice in the optic nerve. The median as well as the minimum and maximum value of FA, MD, AD and RD in the optic nerve are presented for control CFA-only immunized and EAE mice at baseline (prior to immunization or -4/-3 dpi), peak of symptoms (15/16 dpi), and partial recovery of symptoms (28/29 dpi).

Group	TP	#	FA	MD [mm ² /s]	AD [mm ² /s]	RD [mm ² /s]
control (n=3)	dpi-4/-3	6	0.796 (0.767-0.837)	0.00039 (0.00037-0.00042)	0.00086 (0.00083-0.00093)	0.00016 (0.00012-0.00017)
	dpi15/16	6	0.786 (0.735-0.838)	0.00039 (0.00036-0.00042)	0.00085 (0.00083-0.00088)	0.00016 (0.00012-0.00019)
	dpi28/29	6	0.841 (0.776-0.857)	0.00037 (0.00037-0.0004)	0.00088 (0.00083-0.00094)	0.00012 (0.00011-0.00016)
EAE (n=8)	dpi-4/-3	16	0.804 (0.719-0.853)	0.00037 (0.00031-0.00043)	0.00085 (0.00073-0.00093)	0.00014 (0.0001-0.00019)
	dpi15/16	16	0.698 (0.552-0.806)	0.00042 (0.00032-0.00045)	0.00086 (0.00062-0.00093)	0.00021 (0.00014-0.00026)
	dpi28/29	16	0.663 (0.525-0.848)	0.00044 (0.00035-0.00047)	0.00081 (0.00071-0.00088)	0.00024 (0.00011-0.00029)

AD: axial diffusivity, CFA: complete Freund's adjuvant, dpi: days post immunization, EAE: experimental autoimmune encephalomyelitis, FA: fractional anisotropy, MD: mean diffusivity, n: number of animals, RD: radial diffusivity, TP: time point, #: number of observations

Table 4-2 DTI measurements in control and EAE mice in the optic tract. The median as well as the minimum and maximum value of FA, MD, AD and RD in the optic tract are presented for control CFA-only immunized and EAE mice at baseline (prior to immunization or -4/-3 dpi), peak of symptoms (15/16 dpi), and partial recovery of symptoms (28/29 dpi).

Group	TP	#	FA	MD [mm ² /s]	AD [mm ² /s]	RD [mm ² /s]
control (n=3)	dpi-4/-3	3	0.766 (0.75-0.788)	0.00048 (0.00047-0.00049)	0.001 (0.00103-0.00104)	0.0002 (0.00019-0.00022)
	dpi15/16	3	0.757 (0.757-0.766)	0.0005 (0.00049-0.0005)	0.0011 (0.00105-0.00109)	0.00021 (0.000213-0.000214)
	dpi28/29	3	0.786 (0.754-0.787)	0.00047 (0.00047-0.00049)	0.001 (0.00099-0.00107)	0.0002 (0.00019-0.0002)
EAE (n=8)	dpi-4/-3	8	0.763 (0.718-0.802)	0.00048 (0.00046-0.0005)	0.001 (0.00097-0.0012)	0.0002 (0.00017-0.00023)
	dpi15/16	8	0.702 (0.655-.0784)	0.00047 (0.00042-0.00051)	0.00095 (0.0008-0.001)	0.00024 (0.00019-0.00027)
	dpi28/29	8	0.668 (0.555-0.745)	0.00048 (0.000427-0.0005)	0.0009 (0.0008-0.001)	0.00027 (0.00018-0.00031)

AD: axial diffusivity, CFA: complete Freund's adjuvant, dpi: days post immunization, EAE: experimental autoimmune encephalomyelitis, FA: fractional anisotropy, MD: mean diffusivity, n: number of animals, RD: radial diffusivity, TP: time point, #: number of observations

While in the control group MRI measures remained stable over time, the values changed longitudinally in the EAE group. Compared to baseline (median: 0.804, min: 0.719, max: 0.853), optic nerve FA values were already significantly decreased at 15/16 dpi ($p \leq 0.0001$, median: 0.698, min: 0.552, max: 0.806) and continued to decrease further till 28/29 dpi ($p \leq 0.0001$, median: 0.663, min: 0.525, max: 0.848) in EAE. Significantly different FA values between EAE and controls were found at 28/29 dpi ($p \leq 0.01$). Similarly, MD values of the optic nerve were significantly increased at peak ($p \leq 0.01$) and partial recovery ($p \leq 0.001$) of EAE compared to baseline. Optic nerve MD values did not reach a statistically relevant group difference at any time point (**Figure 4-7**). Regarding changes in directional diffusivity within the EAE group, optic nerve RD values were significantly increased at both follow-up time points compared to baseline ($p \leq 0.0001$), while optic nerve AD values remained unchanged throughout the observation period (**Figure 4-8**). Moreover, at the final time point, RD was significantly different between control and EAE mice in the optic nerve ($p \leq 0.01$).

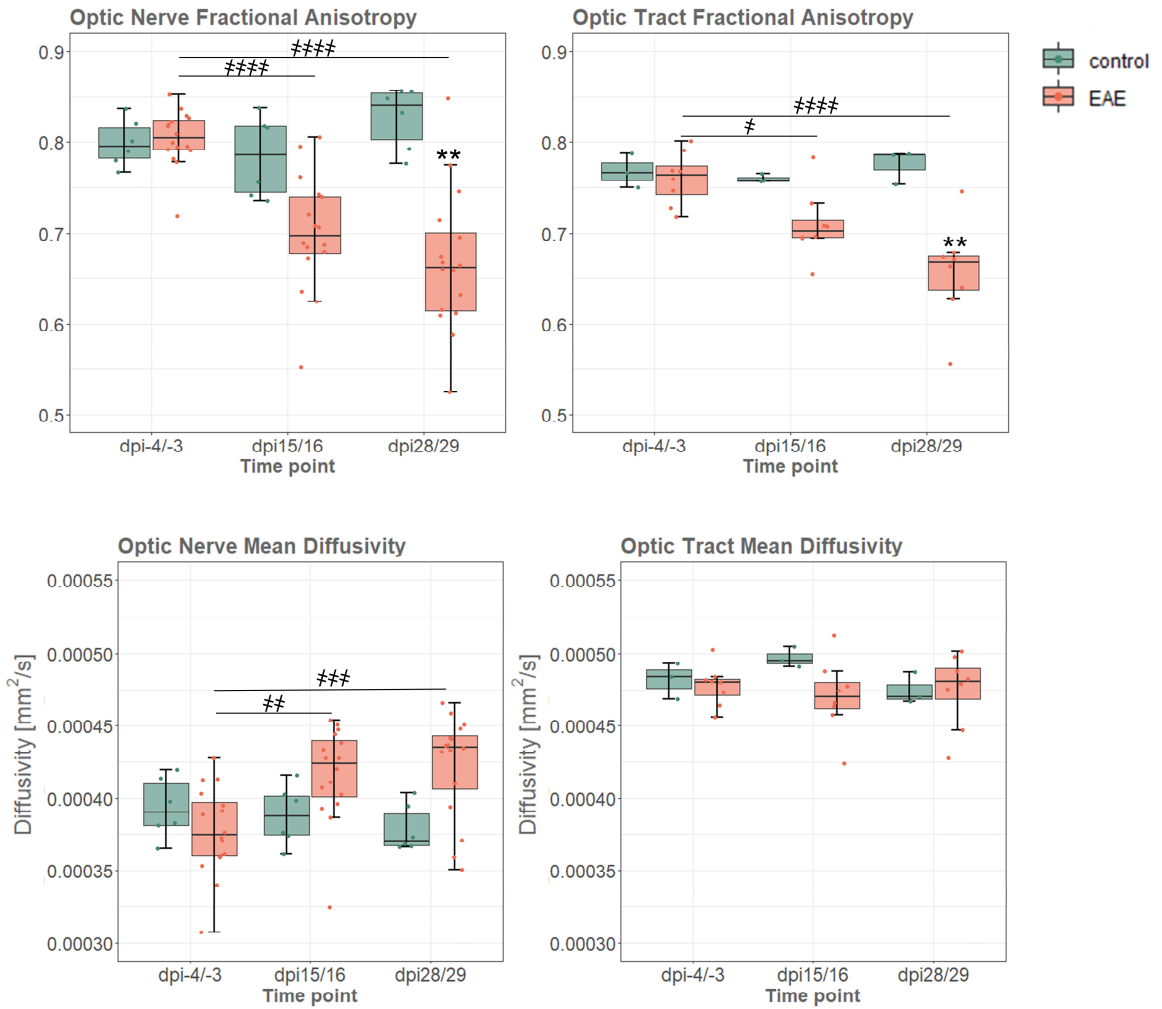


Figure 4-7 Longitudinal fractional anisotropy and mean diffusivity.

Boxplots of fractional anisotropy (FA) and mean diffusivity (MD) over time in control complete Freund's adjuvant-only immunized (green) and experimental autoimmune encephalomyelitis (EAE) (orange) mice in the optic nerves (left) and optic tracts (right). Bonferroni corrected p-values between control and EAE (inter-group): ** $p \leq 0.01$. Bonferroni corrected p-values between baseline and follow-up in EAE (intra-group): # $p \leq 0.05$, ## $p \leq 0.01$, ### $p \leq 0.001$, #### $p \leq 0.0001$. dpi: days post immunization.

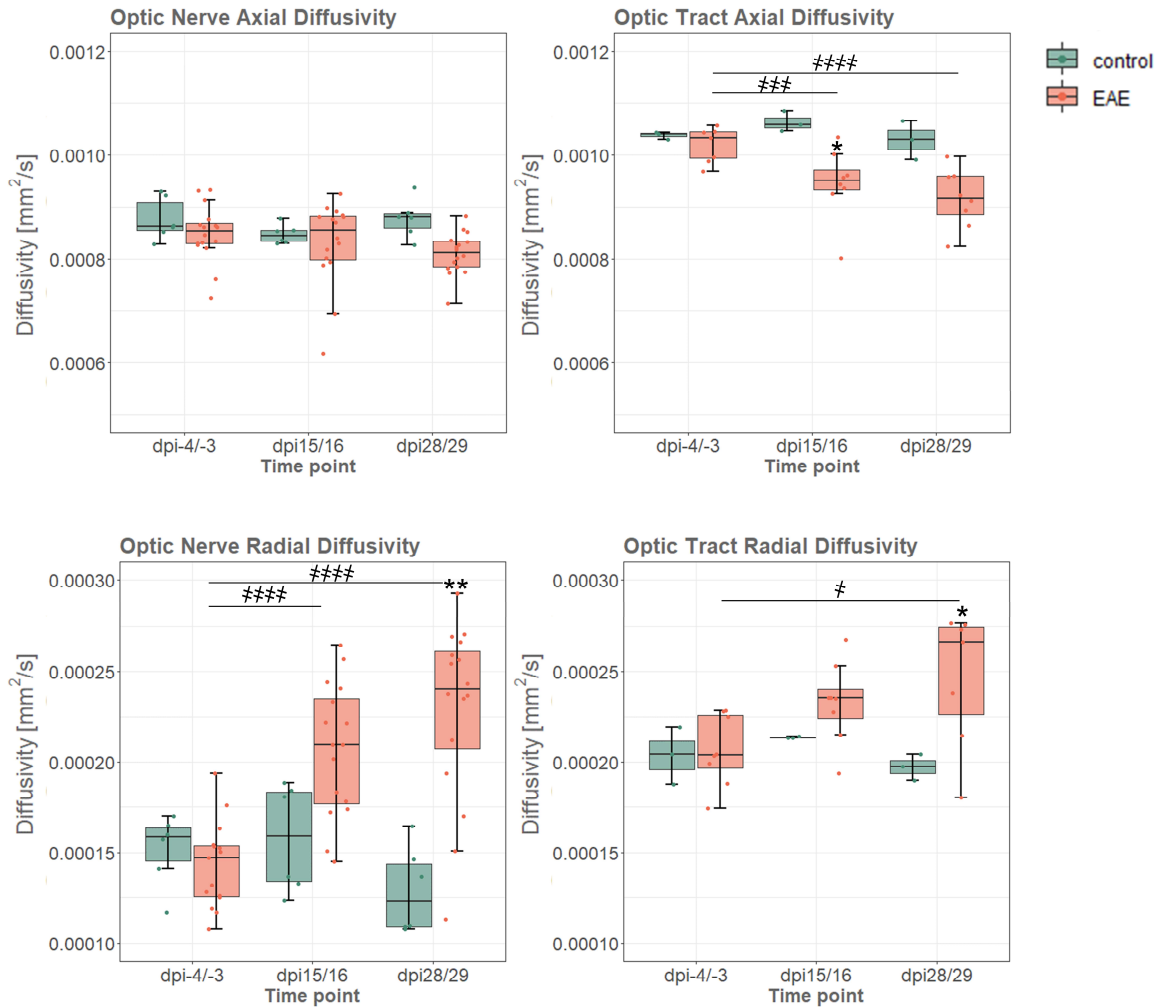


Figure 4-8 Longitudinal axial diffusivity and radial diffusivity.

Boxplots of axial diffusivity (AD) and radial diffusivity (RD) over time in control complete Freund's adjuvant-only immunized mice (green) and experimental autoimmune encephalomyelitis (EAE) (orange) mice in the optic nerves (left) and optic tracts (right). Bonferroni corrected p-values between control and EAE (inter-group): * $p \leq 0.05$, ** $p \leq 0.01$. Bonferroni corrected p-values between baseline and follow-up in EAE (intra-group): # $p \leq 0.05$, ### $p \leq 0.01$, #### $p \leq 0.001$. dpi: days post immunization.

Correspondingly, optic tract FA values in EAE were significantly lower at peak ($p > 0.05$, median: 0.702, min: 0.655, max: 0.784) and at partial recovery ($p \leq 0.0001$, median: 0.668, min: 0.555, max: 0.745) compared to their baseline (median: 0.763, min: 0.718, max: 0.802). In addition, optic tract FA was significantly lower in the EAE group at 28/29 dpi ($p \leq 0.01$) compared to controls at the same time point. The decrease in anisotropy is apparent on the FA maps, where optic nerves and tracts are darker with longer EAE disease duration (**Figure 4-9**). MD values were not significantly different at any time point in the optic tract within or between groups (**Figure 4-7**). Also in the optic tract, EAE led to a progressive increase in RD, but only reached statistical significance at the final time point (> 0.05) when compared to values obtained from prior to MOG-immunization. At 28/29 dpi, optic tract RD in the EAE group was also significantly greater as compared to the control group ($p \leq 0.05$). As

opposed to results from the optic nerve, immunization with MOG led to a continuous decrease of AD values in the optic tract within EAE, reaching statistical relevance at 15/16 dpi ($p \leq 0.001$) and at 28/29 dpi ($p \leq 0.0001$) compared to baseline (**Figure 4-8**). A group difference in optic tract AD was observed at 15/16 dpi ($p \leq 0.05$).

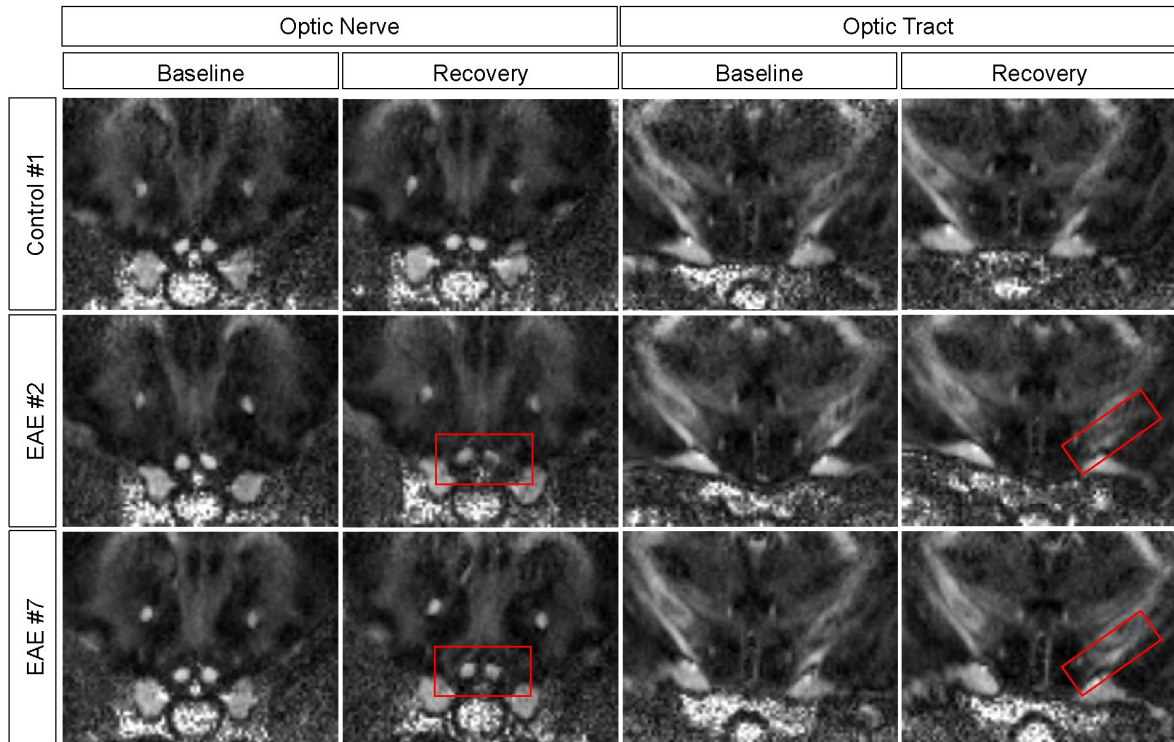


Figure 4-9 Longitudinal fractional anisotropy maps.

The decrease in anisotropy over time is illustrated by darker optic nerves and tracts on the fractional anisotropy (FA) map at partial recovery compared to baseline in experimental autoimmune encephalomyelitis (EAE) (indicated by red rectangles).

4.5.3 Discussion

In this study, the sensitivity of our refined MRI protocol to longitudinally assess the optic nerve and tract for signs of EAE-induced demyelination and axonal damage has been probed.

EAE disease presentation was milder than previously observed: the start of the development of EAE symptoms was slightly delayed and the partial recovery of symptoms was more pronounced compared to former studies (Manogaran et al. 2018; Manogaran et al. 2019). We had no issues with MRI related dropouts and all mice recovered well from the one hour long free-breathing anaesthesia at all time points. Also, no relevant motion artifacts have been observed and the quality of the images remained high throughout the study period. We concluded therefore that the new free-breathing setup and optimized MRI protocol is suitable to monitor EAE mice longitudinally.

4.5.3.1 Diagnosis of EAE-induced ON using T2-weighted imaging

In previous studies, our lab has observed that almost 90–100 % of MOG-induced EAE mice develop bilateral ON by 11 dpi (Manogaran et al. 2018; Manogaran et al. 2019). The observed T2 hyperintensities around the optic nerve confirmed what has been observed in a former study (Manogaran et al. 2018) and indicated the possible presence of inflammatory activity in the optic nerve of EAE mice. However, in order to verify the manifestation of ON, *ex-vivo* results, particularly the immunofluorescence analysis of T-cells (i.e. CD3), microglia (i.e. allograft inflammatory factor 1, IBA1 and transmembrane protein 119, TMEM119) and astrocytes (i.e. glial fibrillary acidic protein, GFAP), is needed.

4.5.3.2 Assessment of EAE-induced optic nerve pathology using DTI

In line with our expectations, optic nerve FA values within the EAE group were significantly reduced at 15/16 dpi and 28/29 dpi compared to baseline; simultaneously MD and RD values were significantly increased. At the final time point, optic nerve FA and RD were also significantly different between control and EAE mice.

The decrease in FA and increase in MD suggested a decline in tissue anisotropy or more isotropic diffusion, respectively an increase in overall diffusivity, thus indicated impaired structural integrity of the optic nerve fibres in EAE. This is in agreement with *ex-vivo* findings from our previous study, which have demonstrated that typical signs of concurrent inflammatory demyelination (extensive infiltration of T-cells in combination with decreased myelin basic protein, MBP) and axonal degeneration (decreased neurofilament-M, NEFM) were observed as early as 11 dpi in the optic nerve (Manogaran et al. 2019). More precisely, microglia activity and astrogliosis were already observed at 7 dpi and at 9 dpi which further exacerbated until 33 dpi (Manogaran et al. 2019). Similarly, amyloid precursor protein (APP) progressively increased from 9 dpi onwards and indicated impaired axonal transport (Manogaran et al. 2019). At 33 dpi severe pathology was also confirmed by histological assessments, which showed that many axons in the optic nerve were completely degenerated and remaining fibres were mainly unmyelinated and shrunken (Manogaran et al. 2019).

DTI has been used numerously to characterize changes in WM integrity in various animal models of CNS disorders (Xu et al. 2008; Winklewski et al. 2018). An increase in RD, arising from a repeal of the restrictive effects of myelin on the movement of water across axons, appears to be highly sensitive for myelin injury in different animal models such as retinal ischemia (Song et al. 2003; Sun, Liang, Le, et al. 2006; Sun et al. 2017) and cuprizone-induced demyelination (Song et al. 2005; Sun, Liang, Trinkaus, et al. 2006). Also in EAE, elevated RD values in the optic nerve and tract have been proposed to sensitively reflect demyelination (Sun et al. 2007; Nishioka et al. 2017; Manogaran et al. 2018; Nishioka et al. 2018). Likewise, RD appears to be elevated in areas prone to demyelination in human brains, such as it is the case for the optic nerve following an episode of ON (Trip et al. 2006; Kolbe et al. 2009; Naismith, Xu, Tutlam, Trinkaus, et al. 2010; Li et al. 2011; van der Walt et

al. 2013), but also in other regions of the MS brain (Naismith, Xu, Tutlam, Scully, et al. 2010; Rocca et al. 2016; Pawlitzki et al. 2020). Most of these clinical studies consistently reported the RD elevation to be accompanied by an increase in MD and a decrease in FA. The progressive increase in RD observed here is therefore highly suggestive for ongoing demyelination in EAE. Nonetheless, supportive evidence from immunofluorescence analysis (particularly a decrease in MBP) and electrophysiological findings (particularly an increase in VEP latency (Heidari et al. 2019)) is pending.

The results appear to be less clear with regards on the association between changes in AD and acute axonal damage. In this study, we found a minor decrease in optic nerve AD at the final time point in EAE, though this change was not significant. For acute axonal injuries that are presenting in the absence of co-inflammation, such as those induced by animal models of retinal ischemia (Song et al. 2003; Sun, Liang, Le, et al. 2006; Sun et al. 2017) or cuprizone-induced demyelination (Song et al. 2005; Sun, Liang, Trinkaus, et al. 2006), locally reduced AD values have been consistently reported. Elevated restriction for water diffusion along the fibres has been hypothesized to be caused by increased tissue barriers in form of cellular debris created by acute fragmentation of axons (Aung, Mar, and Benzinger 2013). The situation is more complex in EAE, where demyelination and axonal damage is not only presenting concurrently, but is also accompanied by massive inflammation (and associated oedema, nerve swelling and cellular infiltration), which is a potential confounder for DTI measures (Aung, Mar, and Benzinger 2013). Accordingly, the relation between axonal degeneration and AD is less consistent in EAE, with some studies reporting a decline in optic nerve AD (Sun et al. 2007; Manogaran et al. 2018; Nishioka et al. 2018), while others found no consistent changes (Nishioka et al. 2017). Also in human MS, discrepant findings on AD abnormalities have been reported. In early active MS lesions, AD has previously been found to be decreased (Naismith et al. 2009; van der Walt et al. 2013) or unchanged (Naismith, Xu, Tutlam, Scully, et al. 2010; Li et al. 2011). Conversely, a study that performed DTI in early clinically isolated syndrome (CIS) patients (within two months from clinical onset), observed a distributed pattern of decreased FA and increased diffusivities, including increased AD (Rocca et al. 2016). Similarly, different findings have been reported in chronic MS lesions, whereby AD has been found to be increased (Kolbe et al. 2009; Naismith, Xu, Tutlam, Trinkaus, et al. 2010; Klistorner, Wang, et al. 2018; Pawlitzki et al. 2020) or unchanged (Trip et al. 2006). Possible explanations for increased diffusion along (and also across) the fibres include the destruction of tissue barriers in chronically damaged or even completely lost axons, or even the replacement by glial tissue or cerebrospinal fluid (Aung, Mar, and Benzinger 2013; Ontaneda et al. 2017).

Based on previous *ex-vivo* studies which have shown that the murine optic nerve in MOG-induced EAE is highly susceptible to early demyelination and axonal damage (Horstmann et al. 2013; Manogaran et al. 2019), we assume that in the study presented here, DTI-derived AD failed to capture the latter. *Ex-vivo* analysis, particularly a decrease in NEFM and an increase in APP, as well

as OCT-detected thinning of the inner retinal layer (IRL; consisting of the unmyelinated portion of the axons, as well as cell bodies and dendrites of the RGCs) are remaining to confirm this hypothesis. Moreover, a reduction in the VEP amplitude would further support the presence of axonal damage in the visual pathway (Diem, Tschirne, and Bähr 2003; Barton et al. 2019).

Inflammation and gliosis has previously been suggested to have confounding effects on DTI measures (Aung, Mar, and Benzinger 2013; Chiang et al. 2014; Mahajan and Ontaneda 2017). Because inflammation plays a significant role in EAE pathology, we propose that a confounding effect on AD is one out of several possible explanation for the lack of a significant AD decrease in the optic nerve. In EAE, infiltration of T-cells into the optic nerve and the presence of inflammatory oedema has previously been found to be most extensive at 11 dpi, with diminished but still evident presence at later time point (at 33 dpi). In comparison, microglia activity and astrocytosis also started early but further aggravated over time (Manogaran et al. 2019). Nonetheless, in a former EAE study, significant optic nerve AD decrease at 28 dpi was found along with *ex-vivo* evidence of microglial activity and astrocytosis at 29 dpi (Manogaran et al. 2018). Thus, an AD difference was observed regardless of the inflammatory response, speaking against our hypothesis.

Another possibility for the lack of a significant AD decrease in the optic nerve could be the slightly later EAE onset and less severe EAE progression as compared to previous studies that may have resulted in milder axonal involvement (Manogaran et al. 2018; Manogaran et al. 2019). Perhaps, assessments at a later time point would have revealed decreased AD values in the optic nerve.

As the inflammatory response in this particular cohort of EAE mice was maybe slightly delayed in time, its most severe phase may lay temporally closer to the MRI examinations than in previous studies. Thus inflammation could have led to a more confounding effect on AD than previously, speaking in favour of the beforementioned hypothesis. However, if so, a confounding effect on RD and the other DTI measures neither can be ruled out.

It is well known that the EAE presentation is influenced by many factors, including the antigen used to induce EAE, but also the species, gender and age of the animals (Burrows et al. 2019). As such, these are other possible factors that may led to discrepant optic nerve AD results compared to previous studies. However, similar to our approach, previous studies were also performed in MOG-induced female EAE mice. The main difference was the inclusion of younger mice (Sun et al. 2007; Nishioka et al. 2018), which would not explain a more severe phenotype (Burrows et al. 2019).

Because of the limited sample size in this study, it is also possible that the study was underpowered to detect significant AD changes. In studies, where AD was significantly reduced in EAE, its

percentage change has been shown to be smaller than the percentage change observed in RD (Sun et al. 2007; Nishioka et al. 2018), making it maybe more susceptible to problems associated with small sample sizes.

In our view, an interplay of all these factors is most realistic to explain our finding. However, since complementary analysis of *ex-vivo*, OCT and VEP data is still pending, these hypotheses on the interpretation of the MRI results are in the end all speculations and not firm conclusions.

4.5.3.3 Assessment of EAE-induced optic tract pathology using DTI

Regarding the temporal evolution of optic tract FA and RD, similar trends to the optic nerve were observed, though with a slightly less pronounced change. Interestingly, the dynamics of AD and MD were different in the optic tract as compared to the nerve. Compared to baseline, optic tract FA and AD values were significantly reduced at both follow-up time points within the EAE group. Also RD was significantly increased at the final time point in EAE, while MD was not significantly different at any time point in the optic tract. A significant group difference was observed at the final time point for optic tract FA and RD, while AD was significantly different between groups at 15/16 dpi, but not at the later time point. Equally to the optic nerve, progressively reduced FA implied affected tissue integrity, while elevated RD suggested demyelination to be present in the optic tract in EAE. We believe that the temporally unchanged MD values in the optic tract are not indicating intact structure, but rather that the concomitant effect of increased RD and decreased AD likely cancelled each other, resulting in pseudo-normal MD values. According to previous literature, the decrease in AD observed here suggests acute axonal damage in the optic tract in EAE (Sun et al. 2007; Manogaran et al. 2018; Nishioka et al. 2018). Previous research on immunohistochemical analysis of murine tissue obtained 3 months after EAE-induction revealed significant involvement of the optic nerve and tract, with the former showing a greater percentage loss of phosphorylated neurofilament-positive and MBP-positive axons (Sun et al. 2007). Moreover a significant increase of microglia was only found in the optic nerve but not in the tract (Sun et al. 2007). Therefore, it appears contradictory, that significant AD changes were not observed in the optic nerve, which is thought to be a primary site of injury in EAE (Shindler et al. 2008; Horstmann et al. 2013; Hanson et al. 2020), but rather in the optic tract, that was likely injured through secondary anterograde degeneration. According to one of our possible hypothesis however, the sensitivity of AD to detect axonal damage is maybe diminished in the presence of severe inflammation. This could explain the discrepancies between the AD measures of the optic nerve and tract, with the latter possibly being less biased by co-existing inflammation. Another explanation could be primary pathology of the optic tract itself or retrograde trans-synaptic degeneration from more posterior parts of the visual pathway such as the optic radiation, which has also been found to be consistently affected in EAE (Brown and Sawchenko 2007). Following a focal MS lesion, anterograde and retrograde degeneration is also thought to be a major contributor for extending neuro-axonal damage along the human visual system (Gabilondo

et al. 2014; Tur et al. 2016). In summary, in the here presented study, detection of acute axonal damage by DTI likely failed in the optic nerve, but was possibly successful in the optic tract. These results need to be interpreted with caution though. First, further investigations are required to determine the underlying causes for these observations. Regrettably, our current *ex-vivo* procedure does not allow extraction of optic tract tissue and therefore further investigation of optic tract pathology by *ex-vivo* analysis is not possible.

No significant DTI changes in the optic nerve and tract have been observed in the CFA-only immunized control group, implying that the here observed effects on microstructural WM integrity in EAE were MOG-specific rather than a response to CFA.

4.5.3.4 Conclusion

As predicted, we found a progressive decrease of FA in the optic nerve and tract in EAE that indicated harmed WM microstructure. Despite a decrease in tissue anisotropy, MD was only found to be significantly increased in the optic nerve, but not in the tract. It is very probable, that MD is misleading in situations where changes in RD and AD show opposite trends, as it was the case in the optic tract. MD should therefore be interpreted with caution.

In contrast to our initial hypothesis, AD was not significantly reduced in the optic nerve in EAE, although some previous studies proposed AD to be reduced during acute axonal damage, which is typically the case in experimental ON. A good biomarker should not only have a high sensitivity for the underlying pathogenic process (in this case axonal damage for AD or demyelination for RD), but should also be relatively unaffected by comorbidities, for instance by co-inflammation, the time point of assessment (e.g. during acute, subacute, or chronic disease stage), etcetera. We speculate that in our study this was likely better fulfilled by RD and FA than by AD and MD. We therefore suggest, that more research is needed to further evaluate the usefulness of AD to robustly detect acute axonal damage in EAE and MS. In this context, we would like to make a short excursion, and highlight the usefulness of the OCT-derived IRL thickness to sensitively detect ON-induced neuro-axonal damage of the RGCs: longitudinal OCT measures over a time frame of at least 1 month following EAE induction, or in patients subsequent to symptom onset, have previously been proved to be highly sensitive to retinal atrophy following EAE- as well as MS-associated ON (Hanson et al. 2020). Yet, the OCT-analysis of the current study is still pending.

On the contrary, the literature regarding the association between RD and myelin pathology in MS and EAE is more unanimous. In harmony with previous research, we found a progressive increase in RD in the optic nerve and optic tract, which likely indicated EAE-induced demyelination. RD has also been proven to be clinically relevant: RD in MS gadolinium-enhanced lesions was predictive for lesion progression within one year, with an initial 40 % elevation of RD being associated with a 5-

fold higher risks for a lesions to be converted into a chronic black hole associated with severe tissue damage by 12 months of follow-up (Naismith, Xu, Tutlam, Scully, et al. 2010). In patients with a previous history of ON (lesion age of at least 6 months), increased optic nerve RD was strongly associated with more severe visual acuity impairment, retinal nerve fibre layer (RNFL) thinning, and VEP latency prolongation (Naismith, Xu, Tutlam, Trinkaus, et al. 2010). Moreover, a recent study observed faster thinning of the temporal RNFL following MS-associated ON in optic nerves with more severe permanent demyelination (determined by inter-eye asymmetry of the VEP latency), suggesting that chronic demyelination is indeed contributing to progressive loss of RGC axons (You et al. 2020). In order to avoid permanent neuro-axonal tissue loss and associated disability, the search for new strategies to either prevent demyelination or enhance remyelination is of increasing importance in the field of MS (Villoslada and Martinez-Lapiscina 2019; Lubetzki et al. 2020). Accordingly, eligible methods to properly investigate how drugs operate and interfere with these processes are needed. We suggest that a combined longitudinal assessment of the RD in spatially well-confined structures such as the optic nerve and tract, the VEP latency, and the OCT-derived IRL thickness may be a promising approach for future translational trials targeting remyelination and tissue protection in MS. Such a combined approach could in addition help in the stratification of patients into primarily demyelinating, degenerating or repairing/ remyelinating disease subgroups. Characterization of patients into pathogenetically distinct phenotypes would not only allow to better anticipate individual disease progression, but would also assist in making optimal treatment decision.

4.5.3.5 Limitations and Outlook

We acknowledge some limitations in our study. Because of COVID-19-measures at LASC our breeding colony temporarily had to be stopped and we could only start into the experiment with a total of thirteen mice instead of fifteen as planned originally. Even worse, two mice had to be excluded early from the study because of retinal abnormalities independent of EAE. In the end, the EAE group included eight (instead of ten) and the CFA-only control group three (instead of five) mice. The limited sample size, particularly in the control group, is likely the reason for a lack of significant between-group differences of optic nerve and tract FA and RD at the middle time point. Although no relevant between-group difference for the aforementioned parameters were found at the middle time point, the between-group differences were significant at the final time point. Additionally, a significant within-group change of optic nerve and tract FA and optic nerve RD at the middle and the final time, and optic tract RD at the final time point compared to baseline were observed, while there were no significant longitudinal within-group differences in the control group for any DTI indices. Future studies should investigate the potential of DTI to characterize disease pathology also at more chronic disease stages in EAE, when acute inflammation is subsided and myelin degradation and neuro-axonal damage is more severe. This would also allow to further study a potentially confounding effect of infiltrating inflammatory cells on DTI readouts, particularly AD. Finally, the main limitation is the currently pending analysis of the OCT, GAF, VEP, ERG and ex-

vivo data, which at this juncture hindered drawing any firm conclusions on the MRI findings observed here. In case the GAF results look promising, RGC cell death could be examined longitudinally within the same mouse. In combination with RD, GAF imaging would allow to more accurately monitor longitudinal neuro-axonal damage and demyelination in EAE *in vivo*. We will make every endeavour to publish a scientific manuscript combining all the measures at a later date.

4.6 Author Contributions

C.A. Wicki was involved in the study design, experimental implementation, and the methodology development for the MRI free-breathing setup. C.A. Wicki conducted DTI and T2 weighted imaging acquisition and data analysis and wrote the original draft of this chapter. **P. Manogaran** conducted the OCT, GAF, VEP, ERG and *ex-vivo* data collection and analysis for this study (not included in this thesis) and was also involved in the experimental implementation and design. P. Manogaran provided significant critical revision for this chapter. **V. Zerbi** provided supervision and was involved in methodology development for the MRI assessment. **M. Samardzija** provided supervision and was involved in methodology development for *ex-vivo* assessments. **C. Grimm** provided resources and supervision for the project. **S. Schippling** was involved in the conceptualization of the study, obtaining funding for the study, providing resources and supervision.

4.7 Acknowledgements

The authors would like to thank **V. Todorova** for her help in methodology development of the VEP and ERG. They also thank **A.N. Schad** for helping with the manual correction of the OCT segmentation and for assisting with *ex-vivo* post-hoc analysis. They also thank **C. Walker-Egger** for teaching C.A. Wicki the basics of mice MRI studies and providing the previously established MRI protocol. They also thank **M. Augath** for his technical support with MRI imaging and processing. The authors would also like to thank **M. Rudin**, **D. Razansky** and **A. Schröter** for providing resources and assistance with implementing the EAE studies at the animal imaging centre of ETH Zurich.

4.8 Study funding

This study was funded by the Swiss National Science Foundation (320030_175770).

5 Repetitive transorbital alternating current stimulation (rtACS) in human acute optic neuritis: Design of a pilot study to test safety, tolerability and preliminary efficacy (ACSON)

5.1 Preface

This chapter includes some text from the registration of the research project on ClinicalTrials.gov [NCT03862313](https://clinicaltrials.gov/ct2/show/study/NCT03862313). The original draft for the trial registration was written by C.A. Wicki and critically revised by S. Schippling.

5.2 Abstract

Background: Optic neuritis (ON) is an important manifestation and major source of persistent visual disability in multiple sclerosis (MS). Currently, no satisfactory therapies exist to prevent or reverse visual impairment in these patients.

Objective: Presentation of the design of a investigator-initiated, prospective, randomized, patient-blinded, sham-controlled, phase I/IIa pilot study that aims to assess the safety and preliminary efficacy of effects of repetitive transorbital alternating current stimulation (rtACS) in patients with a clinically first-ever, unilateral acute ON.

Methods: Patients will be recruited and randomly assigned to 10-days of active- or sham-rtACS treatment (12-15 patient per group). Safety of active- compared to sham-rtACS (given in addition to methylprednisolone) will be assessed by the occurrence of adverse events. Preliminary efficacy will be assessed by low-contrast visual acuity (LCVA) testing and optical coherence tomography (OCT)-derived thickness of the macular ganglion cell and inner plexiform layer (GCIP).

Status: We are currently recruiting patients for this study.

Conclusions: We believe that there is enough circumstantial evidence to justify testing this intervention in acute ON. Developing neuroprotective or -regenerative therapies that specifically target long-term prevention of persistent disability is a clear unmet medical need in MS. Demonstrating safety and satisfying tolerability together with neuroprotective and -regenerative efficacy of a novel, non-pharmacological treatment approach in ON would be a major breakthrough.

Trial Registration: ClinicalTrials.gov [NCT03862313](https://clinicaltrials.gov/ct2/show/study/NCT03862313) and kofam [SNCTP000003201](https://kofam.org/entry/SNCTP000003201).

5.3 Introduction

5.3.1 Background

Degeneration of central nervous system (CNS) neurons and axons is thought to be irreversible and the primary cause of neurological disability in MS (Bjartmar, Wujek, and Trapp 2003). Therefore, vision loss following damage to the retinal ganglion cells (RGCs), the third-order neurons of the visual pathway, has historically also been considered irreversible. In recent years, however, a paradigm shift has taken place (Sabel and Kasten 2000; Gall et al. 2011; Sabel, Fedorov, et al.

2011). Several studies in patients with glaucoma or other optic neuropathies of different origin have demonstrated that visual recovery appears possible even many years after clinical manifestation and well beyond the spontaneous recovery phase (Gall et al. 2011; Sabel, Fedorov, et al. 2011; Sabel, Henrich-Noack, et al. 2011; Gall et al. 2016). These authors argued that damage to the retina and optic nerve in optic neuropathies is rarely complete but rather partial, and that some RGC neurons survive. Nonetheless, some of the surviving RGCs may be partially damaged and functionally silenced or disturbed. According to their "residual vision activation theory", these authors hypothesized that reactivation and reorganization of these residual silenced cells is possible. They have claimed that recovery of visual function is dependent on stimulation, which could take the form of either active behavioural training or exogenous electric brain stimulation (Prilloff et al. 2010; Sabel, Henrich-Noack, et al. 2011; Sabel, Flammer, and Merabet 2018; Sabel, Thut, et al. 2020).

Active behavioural visual restitution training (VRT) usually includes a computer-based cumulative repetition of visual tasks, carried out daily for several months (Sabel and Kasten 2000; Sabel, Henrich-Noack, et al. 2011). The training aims at strengthening of residual visual structures by repetitively activating them and thus inducing mechanisms similar to long-term potentiation (LTP) (Sabel, Henrich-Noack, et al. 2011). Numerous studies have proposed that vision restoration is possible by behavioural VRT in patients with visual impairment due to damage to the anterior or posterior visual pathway (Kasten et al. 1998; Hyvärinen, Raninen, and Näsänen 2002; Sabel, Kenkel, and Kasten 2004; Sabel and Trauzettel-Klosinski 2005; Sahraie et al. 2006; Bouwmeester, Heutink, and Lucas 2007; Vanni et al. 2010; Dundon et al. 2015). However, these trainings are difficult to implement in a standardized manner and are very time-consuming for the patients. Thus, it is still challenging to draw firm conclusions regarding the clinical benefits of VRT.

The potential of improving visual function by electrical stimulation has been known of for more than 250 years: in 1755, Charles LeRoy produced perception of lights (phosphenes) in a blind man by passing an electrical charge through his eye (Sekirnjak et al. 2008). A phosphene is a phenomenon characterized by the experience of seeing light without light actually entering the eye. Phosphenes can be directly induced by electrical stimulation of the retina or the optic nerve, implying that the stimulation causes firing of RGCs. Ever since then, the concept of producing visual sensations through electrical stimulation of the visual system has been further explored and developed. Non-invasive, low-current electrical optic nerve stimulation (ONS) approaches are among the latest and arguably most promising attempts (Antal et al. 2017).

Here, we review previous research on electrical ONS in experimental and human optic neuropathies and argue for a potential role of this therapy in the treatment of acute optic neuritis (ON) episodes. Moreover, we present an optimal study design to assess safety, tolerability and preliminary efficacy of repetitive transorbital alternating current stimulation (rtACS) as a treatment to improve visual

functional as well as structural retinal outcomes in patients with a first-ever episode of autoimmune acute ON.

5.3.2 Preclinical evidence for beneficial effects of optic nerve stimulation

Preclinical studies in rodent models of optic neuropathies, mainly induced through experimental transection or crush of the optic nerve, have proposed that ONS can protect and may even enhance neuronal functioning and thus restoration of vision. Seven days after optic nerve transection, Morimoto and colleagues have reported an increased number of surviving retinal ganglion cells (RGCs) in rats receiving transcorneal electrical stimulation (TcES) as opposed to sham-treated rats (Morimoto et al. 2005). TcES is a methodology applied to electrically stimulate the optic nerve via corneal lens electrodes. Later studies complemented this finding, by reporting continuous enhancement of RGC survival up to one month after optic nerve crush (Henrich-Noack, Lazik, et al. 2013) and an increased number of regenerating RGC axons after TcES in rats with optic nerve crush (Tagami et al. 2009). Upregulation of neurotrophic factors such as brain-derived neurotrophic factor (BDNF) (Sato, Fujikado, Lee, et al. 2008), improved chorioretinal blood circulation (Morimoto et al. 2014; Fu et al. 2015), upregulation of Insulin-like growth factor 1 (IGF-1) expressed in retinal Müller glial cells (Morimoto et al. 2005; Sato, Fujikado, Morimoto, et al. 2008; Tagami et al. 2009), inhibition of pro-inflammatory cytokines such as interleukin 1 beta (IL-1 β) or tumour necrosis factor alpha (TNF- α) (Zhou et al. 2012), morphological alteration (Henrich-Noack, Voigt, et al. 2013), and a reduced activation of microglia (Yin et al. 2016), have been associated with ONS; all of these mechanisms are potentially important for the survival-promoting effects of ONS on the injured RGCs. At this point, it is worth mentioning, that a study in rats with myelin oligodendrocyte glycoprotein-induced experimental autoimmune encephalomyelitis, an important animal model of MS, showed that the temporal evolution and mechanisms of RGC death in experimental ON are comparable to the one observed in experimental transection of the optic nerve (Hobom et al. 2004).

Very few studies have investigated how ONS effects the functionality of the rodent visual system after optic nerve transection or crush. For example, short-term increase in the VEP amplitude of rats treated with TcES immediately after optic nerve crush has been reported (Miyake et al. 2007). Conversely, in other studies no effects on recovery of brightness discrimination (Henrich-Noack, Lazik, et al. 2013) or VEP measures (Henrich-Noack et al. 2017) were found in rats following TcES, despite enhanced RGC survival. It has been suggested that dendritic stripping and resulting input isolation in rats treated with ONS immediately after the optic nerve crush (in a hyperacute stage) may have partially protected the neurons from excitotoxic cell death, but simultaneously also impeded functional recovery (Henrich-Noack et al. 2017). Despite this, in a rat model of retinitis pigmentosa, whole-eye electrical stimulation improved electroretinography and optokinetic tracking outcomes (Hanif et al. 2016) and in healthy rats, TcES changed the EEG pattern (Sergeeva et al. 2012).

The determination of optimal stimulation parameters and time of intervention for RGCs have proven to be difficult. Intensity- and frequency-dependence have been observed and a range of parameters appear to be effective (Morimoto et al. 2002; Okazaki, Morimoto, and Sawai 2008; Xie et al. 2019). Symmetrical pulse waves instead of asymmetrical and repeated stimulation instead of a single application have been identified as more protective for axotomized RGCs (Morimoto et al. 2010). How these results can be transferred to clinics remains unclear at the present time.

Enhanced remyelination has been proposed as another possible mode of action (MoA) of ONS. In the CNS, myelination of axons is performed by mature oligodendrocytes, while in the PNS Schwann cells are responsible. Next to trophic and metabolic support for neurons, myelination enables fast saltatory action potential (AP) propagation (Franklin and French-Constant 2008; Bruce, Zhao, and Franklin 2010). The effect of physiologically occurring electrical neuronal activity (through the neurons endogenous capacity to fire APs) on CNS and PNS wiring and myelination during development has been examined in numerous studies – particularly also in the optic nerve. Experimental blockage of RGC activity has been shown to disturb postnatal development of the topographically organized retinotectal projections in several vertebrates (Fawcett and O'Leary 1985). Suppression of electrical activity of the RGCs was achieved through intraocular injection of different neurotoxins such as, for example, tetrodotoxin (TTX), which blocks voltage-gated sodium channels and consequently the firing of neurons. Likewise, the elimination of electrical activity of RGC axons, induced by unilateral sectioning of rat optic nerves, dramatically decreased the number of mitotic oligodendrocyte progenitor cells (OPCs) in the optic nerves (Barres and Raff 1993). In 1996, using a similar approach as described above, by either blocking or stimulating the firing potential of neighbouring neurons with intravitreal injections of neurotoxins, Demerens and colleagues also assessed the role of electrical activity on the postnatal myelination of optic nerve fibres in mice (Demerens et al. 1996). They reported a dramatic decrease in the number of myelinating oligodendrocytes and confirmed a decline in the number of myelinated RGC axons upon experimental downregulation of electrical activity of RGCs. Since the time of these studies, the idea of activity-dependent myelination has been addressed in several types of neurons (Stankoff et al. 2016). In dorsal root ganglia neurons, axon-glial adenosine (Stevens et al. 2002) and glutamate signalling (Wake et al. 2015) have been identified as important molecular mechanisms being involved in the activity-dependent promotion of myelination. These signalling molecules are likely involved in the induction of cell differentiation of OPCs into myelinating oligodendrocytes. Another study described similar findings in the mature murine premotor cortex, where neuronal electrical activity also appears to influence myelination through mechanisms that facilitate OPC differentiation (Gibson et al. 2014). Importantly, this study also linked enhanced myelination with improved motor function. Subsequent studies assessed whether experimental enhancement of neuronal activity may also influence the remyelination process of mature neuronal fibres in pathological conditions. In the case of successful remyelination, OPCs would likely start to proliferate in response to myelin

destruction, migrate to the site of injury, and differentiate into mature oligodendrocytes that then finally recreate a myelin sheath around the naked parts of the affected axon (Bruce, Zhao, and Franklin 2010). In addition, oligodendrocytes that survived may also contribute in the remyelination process (Villoslada and Martinez-Lapiscina 2019). Because of its complexity, the regulation of the remyelination process is not yet fully understood, but several growth factors, as well as activity-dependent interactions between astrocytes, microglia, and neurons seem to be involved (Bruce, Zhao, and Franklin 2010). In focally demyelinated rat peripheral nerves, electrical stimulation resulted in a more rapid clearance of myelin debris and return of Schwann cells into a myelinating state, which in turn improved remyelination (Zhang et al. 2013; McLean et al. 2014). Similarly, in a more recent study, electrical stimulation of cortical motor neurons promoted oligodendrocyte development and remyelination in the injured rat spinal cord and consequently enhanced functional recovery of fine movement in these rats' hind-paws (Li and Li 2017). In adult rats with a toxin-induced focal demyelinating lesion in the caudal cerebellar peduncle, suppression of electrical activity (and thus also of associated glutamate release) reduced the normally observed remyelination in this model significantly (Gautier et al. 2015). However, it remains unclear how this described phenomenon of activity-driven myelin plasticity influences neuronal function. Enhanced (re-)myelination may optimise the speed and timing of neurotransmission, two important factors involved in the orchestration of oscillatory activity and hence also in the functioning of neuronal circuits of the brain (Fields 2015). To sum up, there are hints that neuronal activity is not only capable of influencing myelination during development, but may also enhance oligodendrocyte differentiation, survival, and myelination capacity in both the healthy and damaged adult nervous system (de Faria et al. 2019).

5.3.3 Clinical evidence for beneficial effects of optic nerve stimulation

Within the last 10 years, various clinical trials have been performed in order to investigate the role of ONS in the treatment of human optic neuropathies such as glaucoma, anterior ischemic optic neuropathy (AION), and other optic neuropathies (Fedorov et al. 2010; Gall et al. 2010; Fedorov et al. 2011; Gall et al. 2011; Sabel, Fedorov, et al. 2011; Schmidt et al. 2013; Bola et al. 2014; Gall et al. 2014; Gall et al. 2015; Gall et al. 2016). These studies found beneficial effects of rtACS for vision restoration (Fedorov et al. 2010; Gall et al. 2010; Fedorov et al. 2011; Gall et al. 2011; Sabel, Fedorov, et al. 2011; Schmidt et al. 2013; Bola et al. 2014; Gall et al. 2014; Gall et al. 2015; Gall et al. 2016). rtACS is a methodology applied to electrically stimulate the retina and optic nerve in a non-invasive manner using periorbital electrodes that deliver weak alternating current. The stimulation was mostly applied in the α - and β -frequency range with an intensity just above the individuals' phosphene perception threshold.

In addition to the mechanisms observed in preclinical studies and described above, clinical studies using alternating current stimulation (ACS) approaches have proposed the following MoA: rtACS modulates brain activity in a way that neuronal entrainment of endogenous oscillations and synchronous activation of remaining RGCs increases the power and coherence of entrained

oscillations during stimulation. According to this hypothesis, neuronal entrainment is only possible if the brain's intrinsic frequency is close enough to the stimulation frequency (Fröhlich 2015; Antal and Herrmann 2016; Woods et al. 2016). Because α -oscillations are intrinsically prominent in the visual cortex, particularly during eyes-closed or in-the-dark resting condition (Schürmann and Basar 2001; Kanai et al. 2008), many studies targeting the visual system have therefore used frequencies in the α -range. In the best case, these online effects would induce strengthening of synaptic transmission through long-term potentiation (LTP)-like mechanisms, resulting in increased offline synchronization within and between visual networks and associated enhancement of visual perception after stimulation (Sabel, Thut, et al. 2020).

In line with this hypothesis, rtACS (Sabel, Fedorov, et al. 2011; Schmidt et al. 2013; Bola et al. 2014; Gall et al. 2016) and occipital transcranial alternating current stimulation (tACS) (Zaehle, Rach, and Herrmann 2010; Neuling, Rach, and Herrmann 2013; Helfrich et al. 2014; Vossen, Gross, and Thut 2015; Kasten, Dowsett, and Herrmann 2016) applying frequencies in the α -range have been shown to increase endogenous α -power over the occipito-parietal regions, that in some studies lasted beyond the stimulation period. Importantly, these α -power-increases have been associated with enhanced visual perception following both occipital tACS in healthy controls (Neuling, Rach, and Herrmann 2013; Helfrich et al. 2014) or rtACS in visually impaired patients (Fedorov et al. 2011; Sabel, Fedorov, et al. 2011; Bola et al. 2014; Gall et al. 2016). Additionally, re-organization of disturbed functional connectivity networks across the brain has been observed. For example a resynchronization of fronto-occipital α -band coherence has been described after 10 days of rtACS that positively correlated with improved visual detection ability and faster reaction times in the intact visual field (Bola et al. 2014).

Alternatively to neuronal entrainment, a post-inhibitory neural rebound phenomenon has been proposed to underly retinofugal ACS-induced occipital α -power enhancement (Haberbosch, Schmidt, et al. 2019). These authors reasoned that the reported α -enhancement upon tACS does not always coincide with a frequency-lock, which may be evidence against entrainment (Vossen, Gross, and Thut 2015; Haberbosch, Schmidt, et al. 2019).

Another study assessing TcES in healthy human subjects proposed increased chorioretinal perfusion to contribute to the beneficial effects on vision (Kurimoto et al. 2010). Similar findings have been recorded in animal models (Morimoto et al. 2014; Fu et al. 2015). The possible influence of the vascular system, as well as psychosocial factors, on vision restoration following ACS has also been discussed in two recent publications from Sabel and colleagues (Sabel, Flammer, and Merabet 2018; Sabel, Wang, et al. 2020).

Since 2014, a proprietary rtACS approach for patients with visual impairment caused by optic neuropathies has been commercially available (NextWave® 1.1 system; Neuromodtronic GmbH, previously named EBS Technologies GMBH, Germany) (Antal et al. 2017). The Neuromodtronic system is a class IIa investigational medical device (IMD) that uses non-invasive, low-dose, electrical current and so far has mainly been applied in patients with visual field loss due to stroke, AION, traumatic injuries, or glaucoma (Neuromodtronic GmbH, previously named EBS technologies GMBH, Germany) (Fedorov et al. 2010; Gall et al. 2010; Fedorov et al. 2011; Gall et al. 2011; Sabel, Fedorov, et al. 2011; Schmidt et al. 2013; Gall et al. 2014; Gall et al. 2016). In the supplementary data, **Table 5-1** summarizes the clinical studies that have used the NextWave® 1.1 system or its precursor to assess the potential of rtACS.

The established treatment consists of ten sessions, which take place on ten consecutive working days (Antal et al. 2017). Safety and efficacy of the system has been assessed in several clinical trials (Fedorov et al. 2010; Gall et al. 2010; Fedorov et al. 2011; Gall et al. 2011; Sabel, Fedorov, et al. 2011; Schmidt et al. 2013; Gall et al. 2014; Gall et al. 2016). Studies have found a significant improvement of visual functional outcomes such as visual fields, visual acuity, and subjectively perceived vision-related QoL among patients treated with active-rtACS as compared to sham-stimulation (Fedorov et al. 2010; Gall et al. 2010; Fedorov et al. 2011; Gall et al. 2011; Sabel, Fedorov, et al. 2011; Schmidt et al. 2013; Gall et al. 2014; Gall et al. 2016). Since commercial introduction of the system in 2014, no therapy-related severe adverse events (SAEs) have been reported (Antal et al. 2017; Sabel, Thut, et al. 2020). The most commonly reported AEs included skin irritation such as tingling, itching, and burning below the stimulation electrodes. Less often, drowsiness, fatigue, headache, and sleep disturbances have been described (Antal et al. 2017; Sabel, Thut, et al. 2020). So far, rtACS is considered to be a safe strategy to be applied in patients with vision impairment caused by optic neuropathies of different origins.

In summary, evidence from preclinical studies in experimental models of optic neuropathies, as well as clinical studies in human optic neuropathies, suggests that ONS may have neuroprotective and -regenerative potential on RGCs and other CNS structures involved in vision through remyelination-dependent, but also independent, mechanisms as detailed above. Clinical evidence supporting a possible role of rtACS as an interventional approach in patients with autoimmune ON, however, is not yet available.

5.3.4 Optic nerve stimulation in ON – explanation for choice of study population

ON patients frequently suffer from persistent functional visual impairment provoked by neurodegeneration of the optic nerve and retina secondary to inflammatory demyelination (Sanchez-Dalmau et al. 2017). An MS relapse or a clinically isolated syndrome (CIS) are frequent causes of

ON, and the pathophysiology of ON lesions is similar to other inflammatory demyelinating MS lesions (Roed et al. 2005; Toosy, Mason, and Miller 2014).

In MS, the autoreactive attacks against antigens in the myelin sheath are predominantly mediated by peripheral autoreactive T-cells infiltrating the CNS, but B-cells, associated antibodies, microglia, astrocytes, and activated monocyte-derived cells are also involved (Lubetzki, Williams, and Stankoff 2005; Goverman 2009; Sospedra and Martin 2016). In addition to mechanical pressure caused by initial oedematous ballooning of the fibres, several pathological mechanisms are initiated around the injured nerve. Release of reactive oxygen (ROS) and nitrogen (RNS) species and pro-inflammatory cytokines from activated microglia and other inflammatory cells results in mitochondrial injury and associated cell stress and energy deficiency (Fischer et al. 2012; Fischer et al. 2013; Friese, Schattling, and Fugger 2014; Lassmann and van Horssen 2016). The presence of signals inhibiting neurite outgrowth (e.g. myelin protein Nogo-A) and diminished levels of neurotrophic factors further produce a neurotoxic environment around the affected neurons (Lubetzki, Williams, and Stankoff 2005; London, Benhar, and Schwartz 2013; Pernet and Schwab 2014).

Concurrently, demyelination results in a local conduction block of varying degree and consequential disturbance of AP propagation (Lubetzki and Stankoff 2014). Ion channel alterations (for example, sodium channel redistributions) along the naked axons, disturbed axonal ATP production, and a lack of trophic support from myelin increase the neurons energy deficiency even more, making them extremely susceptible to degeneration (Miller et al. 2005a; Siffrin et al. 2010). Degeneration of chronically demyelinated axons is a major contributor to tissue damage and related clinical disability in MS (Franklin and Ffrench-Constant 2008; Bruce, Zhao, and Franklin 2010; Franklin et al. 2012; Mahad, Trapp, and Lassmann 2015; You et al. 2019; You et al. 2020). Interestingly, some demyelinating lesions remyelinate spontaneously and clinical symptoms partially recover (vision in case of ON), while others, particularly in later disease-stages, stay permanently demyelinated (Bruce, Zhao, and Franklin 2010). Failure of differentiation of OPCs into myelinating oligodendrocytes has been suggested as one of the main obstacles for successful remyelination attempts in MS (Kuhlmann et al. 2008; Zawadzka et al. 2010). Several studies have shown that remyelination in MS has the highest chance to be efficient in the acute and subacute phase of an inflammatory demyelinating event (Kuhlmann et al. 2008; Klistorner et al. 2010; Stangel et al. 2017). Its success depends also on many other factors, for example the endogenous electrical activity level of neurons, the presence of beneficial cytokines, positive (e.g. BDNF, NRG1, OLIG1) and negative (e.g. LINGO1) regulators, paracrine factors (e.g. phagocytosis of myelin debris), as well as the clinical characteristics of the patient (such as age, sex and disease stage) (Lubetzki, Williams, and Stankoff 2005; Stangel et al. 2017).

In acute ON, the hostile milieu that provokes the cells to undergo cell death could be counteracted through effects of external ONS. Counteractive effects might include improved remyelination as well as upregulation of trophic factors important for neuronal survival. As such, research on new strategies to enhance remyelination is of increasing relevance in the field of MS (Lubetzki et al. 2020).

In addition to focal processes such as resolution of inflammation and partial remyelination, more widespread neuroplastic network alterations appear to play a role in functional recovery in ON (Miller et al. 2005a; Toosy et al. 2005). Several functional magnetic resonance imaging (fMRI) studies in early CIS patients observed decreased functional connectivity within the visual networks in patients both with and without previous ON compared to healthy controls (Wu et al. 2015; Backner et al. 2020). In later stages, an increase in connectivity closer to that of a healthy brain was only reported in patients with previous ON, but not in non-ON patients (Gallo et al. 2012; Backner et al. 2018; Backner et al. 2020). These observed cortical and subcortical network changes may be a mechanism to compensate for ON-related damage and optimize visual function, indicating ongoing neuroplasticity that could potentially be targeted and promoted by electrical stimulation.

Additionally, we recently demonstrated that patients with a first-ever episode of acute ON are well suited to assess whether interventions have an effect on tissue damage and related visual outcomes if applied within a critical time window after the onset of symptoms (Wicki et al. 2020) (or chapter 3 of this thesis). Over a 12 month investigation time, we observed severe thinning of the inner retinal layers containing the RGCs and sustained impairment of LCVA in these patients. We proposed that the success of an intervention within this specific patient cohort could be quantified by longitudinal OCT and LCVA measures (Wicki, Hanson, and Schippling 2018; Wicki et al. 2020) (or chapter 2 and 3 of this thesis). Finally, we concluded that there is a large unmet medical need for new therapeutic approaches that aim not just to prevent or reduce inflammation, but rather promote neuroprotection and repair in ON. To the best of our knowledge, no data that specifically addresses the effects of rACS in acute human autoimmune ON have been reported to date.

5.3.5 Study significance, aims, hypotheses and outcomes

Other than the treatment with corticosteroids, which is to date not known to have a significant long-term effect on visual outcomes in MS-associated ON (Beck and Cleary 1993; Beck and Gal 2008; Shams and Plant 2009; Bennett, Nickerson, et al. 2015; Petzold et al. 2020), no treatment options are currently available. Therefore, research on new therapeutic approaches is needed.

The goal of this pilot study is the generation of safety and preliminary efficacy data on the effects of rACS on functional visual as well as structural outcomes in a first-ever episode of acute ON.

Based on the existing data of clinical studies applying rtACS in optic neuropathies such as glaucoma or AION and of pre-clinical animal studies, we hypothesize that rtACS is a safe intervention in ON and that the probability of detrimental effects is therefore presumably low. Safety and tolerability will be addressed by a structured interview obtained at the visits and the documentation of any clinical insults during the study period.

We further hypothesize that the application of rtACS in acute ON has the potential to improve visual outcomes in patients through neuroprotective effects and enhancement of neurorestoration within the visual system. Over recent years, LCVA has emerged as a leading candidate to properly quantify visual function in MS (Balcer et al. 2015). Thus, LCVA at 4 (and 16) weeks (post-treatment) in ON eyes provides an ideal primary functional outcome measure for this study. As a well validated marker of early RGC damage in MS, the thickness of the macular GCIP will be used to assess the effect of rtACS to the retinal structure (Wicki, Hanson, and Schippling 2018). More precisely, the main structural outcome measure will be the mean (\pm SD) change in macular GCIP thickness of the affected ON eyes at 4 (and 16) weeks (post-treatment) in comparison to baseline of the unaffected contralateral non-optic neuritis (NON) eye (pre-treatment). The selection of these outcome measures complies with current recommendations of experts in the field (Petzold et al. 2020).

A further, exploratory, goal will be to gain a better understanding of the mechanisms and effects of rtACS on the damaged visual system. Therefore, a number of secondary outcome measures will be included in this study. Secondary functional measures will include additional ophthalmological measures (high-contrast visual acuity (HCVA), results of colour vision, visual field and VEP testing, and patient-reported vision-related quality of life (QoL) scores). VEP examinations will be performed primarily to investigate the effect of rtACS on demyelination (as measured by P100 latency). Secondary structural outcomes include the OCT-derived pRNFL thickness (proposed as a marker for the integrity of the RGC axons) and the macular INL thickness (proposed as a marker for inflammatory disease activity in MS) (Knier et al. 2016; Petzold et al. 2017).

5.4 Methods

5.4.1 Study design

Alternating Current Stimulation in Optic Neuritis (ACSON) is an investigator-initiated, prospective, randomized, patient-blinded, sham-controlled, phase I/IIa monocentric pilot study, performed by the the Neuroimmunology and MS Section of the Department of Neurology in cooperation with the Department of Ophthalmology, University Hospital Zurich (USZ). A total of 24-30 patients (12-15 per group) will undergo 10-days of active- or sham- rtACS treatment. In addition, all patients, regardless of the treatment arm, will receive standard-of-care corticosteroid treatment. Therefore no study participant will have a disadvantage compared to patients undergoing the standard clinical procedure. The stimulation session start as soon as possible, not before initiation of corticosteroid

treatment, but at the latest within 3 weeks of symptom onset. We recently published a longitudinal study that underlined the importance of early intervention in this specific study cohort (Wicki et al. 2020). Study assessments will be performed before initiation of treatment (pre-treatment/ baseline), after completion of treatment (post-treatment/ between 5-15 days after the last stimulation) and after a 3-month treatment-free interval (follow-up/ \pm 2 weeks), as visualized in **Figure 5-1**. A more detailed schedule of the study visits and assessments for the individual study participants can be found in the supplementary data in **Table 5-2**.

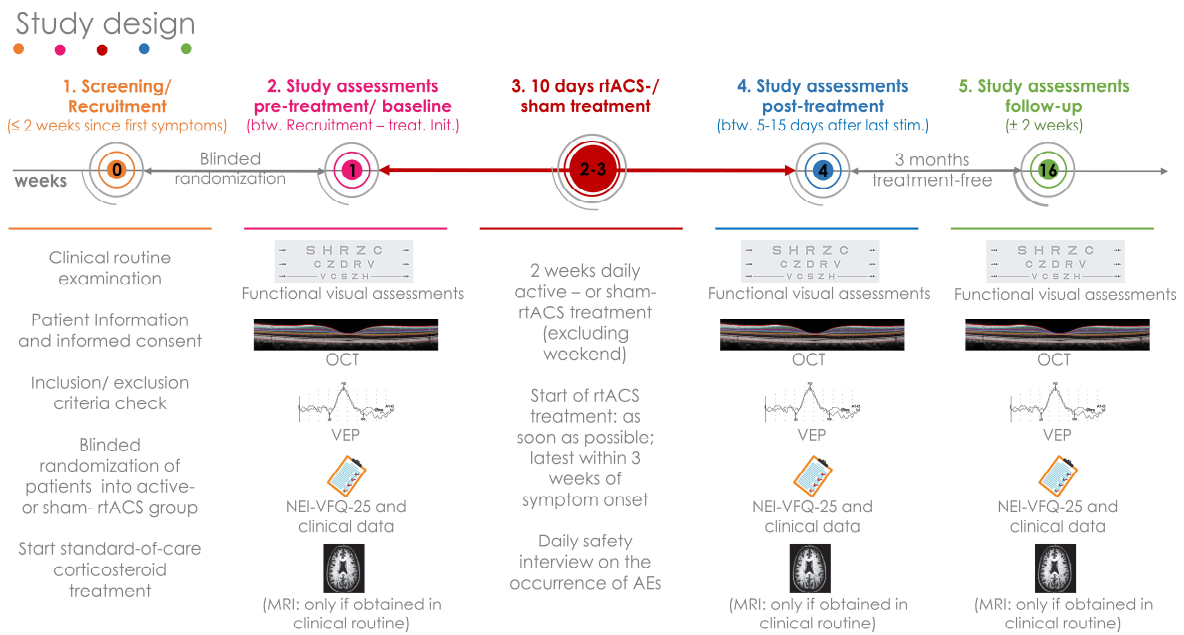


Figure 5-1 Schematic presentation of the study design and study procedure for an individual participant.

5.4.2 Standard protocol approvals, registrations, and patient consents

This category A clinical trial with an IMD is approved by the Ethics Committee of the Canton of Zurich, Switzerland (reference KEK-ZH-Nr. 2018-02353). Investigations are conducted in compliance with the investigation plan, the current version of the Declaration of Helsinki, the guidelines of the International Conference On Harmonisation of Good Clinical Practice (EN ISO 14155) as well as all national legal and regulatory requirements. All participants have to provide written informed consent before entering the study. The study is registered at the international trial registry ClinicalTrials.gov as [NCT03862313](https://clinicaltrials.gov/ct2/show/study/NCT03862313) and in the Swiss National Clinical Trials Portal *kofam* [SNCTP000003201](https://kofam.ch/SNCTP000003201).

5.4.3 Randomization and masking

Allocation to the treatment arms is performed using stratified block randomization. Gender is used as a stratification variable to achieve a comparable gender ratio in the two groups in order to account for female preponderance and possible sex-differences in MS. Based on epidemiological studies, we anticipated that approximately two-thirds of the patients will be females (Kingwell et al. 2013).

Simple manual randomization is performed to assign patients either to the active- or the sham-rtACS treatment group. With a recruitment goal of 24-30 patients, respectively 29-36 when including an anticipated drop-out rate of up to 20 %, a person prepared envelopes labelled with a randomization number X1-X24 for females and Y1-Y12 for males. The envelopes have been randomly filled in blocks of four with either “ACTIVE” or “SHAM” and afterwards sealed. The first eligible female participant passing the screening procedure was assigned to randomization number X1, the second to X2, and so on. Similarly, the first male participant passing the screening procedure was assigned to randomization number Y1, etcetera. After assignment to an intervention, only patients are blinded, but not investigators. The way of how the sham-stimulation works renders it impossible to blind the person who is performing the stimulation. The randomization results are recorded in a randomization log and in the corresponding electronic case report forms (eCRFs). Patients who withdraw from the study or have to be excluded, will be replaced, so the total number of 24-30 patients will be reached.

5.4.4 Participants / subject eligibility

After patient consenting, that is performed by the investigators, patient eligibility is assessed by experienced study physicians from the Department of Neurology and Ophthalmology at the University Hospital Zurich, Switzerland. Only patients that meet all of the inclusion criteria and none of the exclusion criteria participate in this study. **Most important inclusion criteria** include typical signs and symptoms suggestive of a first-ever episode of unilateral acute autoimmune, inflammatory, demyelinating ON, including idiopathic ON and ON suggestive of MS (typical CIS, or with an established diagnosis of relapsing-remitting MS (RRMS) according to latest panel criteria (Thompson et al. 2018)) and no better explanation, HCVA of ≤ 0.63 decimals (or LogMAR value of ≥ 0.2) on the affected eye (assessed using a Snellen chart), presentation in clinics within 14 days of ON symptom onset, standard-of-care corticosteroid treatment for ON, age (18-50 years), good knowledge of German (patient information and consent must be understood), contraception for females. **Most important exclusion criteria** include a previous clinical history of ON in either eye, obvious retinal pathology other than that associated with ON, recent history of eye surgery, severe nystagmus, known anti-aquaporin-4 (AQP4)- or myelin oligodendrocyte glycoprotein (MOG)-antibody seropositivity, known or suspected non-compliance, drug or alcohol abuse, participation in another study with an investigational drug/ device within the 30 days prior and during the present study and contraindications for rtACS, including implanted electronic devices, metallic artefacts in the head (excluding dentition), epilepsy, brain cancer, pregnancy, breastfeeding, increased intraocular pressure without appropriate treatment, arterial hypertension without appropriate treatment, acute retinal haemorrhage, skin irritations at intended positions of electrodes, cognitive deficits. **Abortion criteria** include the wish of the patient to withdraw from the study, safety concerns, fulfilling of any of the exclusion criteria, missing more than 2 treatment sessions and missing the baseline or both of the post-treatment study assessment visits. More details on the study population can be found in the **supplemental data**.

5.4.5 Study outcomes

Safety and tolerability will be evaluated in terms of the overall incidence and severity of AEs and SAEs compared between both treatment arms.

Preliminary efficacy outcome measures will be divided into functional and structural measures, with both being considered as equally important. Therefore the study will have two primary outcome measures. Outcome measures will be compared between the two treatment arms.

For functional outcome measures, in order to perform between treatment arm comparisons, the mean absolute cross-sectional values in ON eyes at 4 weeks (post-treatment) and 16 weeks (follow-up) will be compared between treatment arms. The primary functional outcome measure will be LCVA [LogMAR] at 4 (post-treatment) and 16 weeks (follow-up) in ON eyes.

For structural and electrophysiological outcome measures, the magnitude of change in ON eyes at 4 weeks (post-treatment) and 16 weeks (follow-up) compared to baseline of the unaffected contralateral NON eyes will be calculated (within treatment arms) and then compared between treatment arms. The reasoning for this approach of data analysis is described in one of our recent publications (paragraph 'Statistics'; or here chapter 3 of the thesis) (Wicki et al. 2020). The primary structural outcome measure will be the mean (\pm SD) change in macular GCIP thickness [μ m] of the affected ON eye at 4 (post-treatment) and 16 weeks (follow-up) in comparison to baseline of the unaffected contralateral NON eye (pre-treatment).

A complete overview on the safety outcomes and the preliminary secondary efficiency outcomes is available as **supplemental data**.

5.4.6 Safety and tolerability assessments

To address safety and tolerability, a structured interview on the occurrence of any AE is obtained daily during the treatment phase and monthly thereafter for up to 3 months. As recommended by safety, ethical, legal regulatory and application guidelines for low-intensity transcranial electric stimulation (Antal et al. 2017), the interview specifically queries for known AEs (such as itching, burning or fatigue) but also for unknown AEs by explicitly asking about “other AEs/ sensations”, so that AEs not yet reported can be detected.

In addition worsening of symptoms associated with ON (e.g. aggravation of LCVA loss, pain upon eye movements, etc.) and relapses are documented and analysed. Side effects associated with methylprednisolone (such as hot flushes, facial flushing, mood changes or hyperglycaemia) are also documented and distinguished from side effects associated with the rtACS treatment. Safety data is collected at the Department of Neurology and Ophthalmology.

5.4.7 Visual acuity

LCVA and HCVA testing is performed identically to the methods described in Chapter 3 and is performed at the Department of Neurology.

5.4.8 Optical coherence tomography

OCT is performed identically to the methods described in Chapter 3 and is performed at the Department of Neurology.

5.4.9 Colour vision

The Cambridge Colour Test (CCT) (Cambridge Research Systems Ltd, Rochester, UK) is used to examine subjects for colour vision deficiencies, by measuring chromatic discrimination along the protan, deutan and tritan color confusion axes. The CCT is a computerized test which generates Landolt "C" shaped targets differing in chromaticity from the background (Moura et al. 2008). The target is presented randomly in one of four orientations and the subject's task is to define the orientation of the "C" by pressing one of four corresponding keys. The test lasts approximately four minutes per eye. The chromatic discrimination thresholds along all three colour confusion axes is quantified with values up to 1100, with 1100 being the worst. As abnormal tritanopic (blue-yellow) discrimination performance is much more likely to be acquired (e.g. through ON) rather than congenital (which is not the case for abnormal protonomic or deuteranopic colour vision), only the tritan data will be analysed. Colour vision testing is performed at the Department of Ophthalmology.

5.4.10 Perimetry

Static visual field testing is performed using the dG2 protocol of the Octopus 900 perimeter (Haag-Streit, Switzerland) (Kaczorowski et al. 2015). Subjects must fixate a central point whilst lights of varying intensity are presented at different locations within the central visual field; the subject must press a button each time that they see a light. The examination takes 6-8 minutes per eye to complete. The mean standard deviation (MSD) of sensitivity thresholds from age-matched normal values (in dB) will be analysed. Perimetry is performed at the Department of Ophthalmology.

5.4.11 Vision-related quality of life (vision-related QoL) questionnaire

Visual QoL is assessed using the German version of the National Eye Institute Visual Function Questionnaire-25 (NEI-VFQ-25), a validated, reliable questionnaire to capture self-reported visual dysfunction (Balcer et al. 2000; Raphael et al. 2006). The questionnaire contains the following 12 sub-scales: general health, general vision, ocular pain, near activities, distance activities, vision-specific social functioning, vision-specific mental health, vision-specific role difficulties, vision-specific dependency, driving, colour vision and peripheral vision. The mean VFQ-25 composite score (calculated as an unweighted average of responses to all items except for the general health sub-scale) and selected sub-scale scores will be analysed. Questionnaires are filled by the patients at the Department of Neurology.

5.4.12 Pattern-reversal visual evoked potential (PR-VEP)

For the VEP examinations, a pattern-reversal VEP protocol is used in order to obtain the latency (time from pattern-reversal to the major positive peak of the VEP (P100 peak time) [ms]). To ensure high quality measures, the examinations are recorded according to guidelines issued by the

International Society for Clinical Electrophysiology of Vision (ISCEV) (Odom et al. 2016). A black and white checkerboard stimulus array is used to record the VEP. The VEP is recorded by a single recording channel with an adhesive midline occipital active electrode. During the examination, the patient must concentrate on a central fixation cross whilst the checkerboard stimulus array reverses in contrast polarity. No eye drops are required. VEP examinations are performed at the Department of Neurology.

5.4.13 Patient demographics and clinical characteristics

Medical, clinical history and relevant demographic data of patients is collected during clinical routine (stored in the Klinikinformationssysteme (KISIM) of USZ) and by filling out the in- and exclusion criteria questionnaire. Data is collected at the Department of Neurology and Ophthalmology.

5.4.14 Assessments in Participants Who Prematurely Stop the Study

All safety data, including data obtained from withdrawn participants is collected and analysed. If a patient withdraws early or has to be excluded from the study, he/ she has to be followed for assessments of safety as stipulated in the protocol and as indicated in the patient timeline (**Table 5-2**). In contrast, efficacy data is not further obtained after prematurely withdrawal from the study.

5.4.15 Repetitive transorbital alternating current stimulation

For the **active-rtACS treatment arm**, a CE-certificated proprietary class IIa IMD is used to deliver transorbital symmetrical rectangular current pulses in bursts (EYETRONIC NextWave® 1.1.0 system; Neuromodtronic GmbH, previously named EBS technologies GMBH, Germany). The stimulation is applied daily on 10 consecutive days (without weekends), each session lasting about 70-90 minutes (including preparation; stimulation itself 20-40 min). The system consists of special stimulation goggles, a supervisor unit to control the stimulation process, and an electroencephalography (EEG) cap. The EEG cap contains eight occipital electrodes (sintered Ag/AgCl; dimensions: 1.5 mm diameter) and is connected to a ground electrode (based on a conductive thread made of PA with silver coating) incorporated in a special wristband (dimensions: 20 mm width around the wrist; unstretched length of wristband approx. 16cm). The goggles are covered by a single-patient-use foam cushion to improve wearing comfort and contain four electrode adaptors (soldered components made of stainless steel and Ag/AgCl) that keeps the four superficial conductive felt electrodes (dimensions: 6.7 mm diameter) that allow direct skin contact, in place. A special neck band contains a return electrode (based on a conductive thread made of PA with silver coating; dimensions: 43 mm x 43 mm), that is centered on the back of the neck. The stimulation parameters are patient-individualized and determined daily before the start of each session. Patients are instructed to keep their eyes closed for the determination of the stimulation parameters. First, electrical impedance is measured at 5 Hz, 10 Hz, 15 Hz, and 20 Hz stimulation for all four periorbital electrodes and if possible kept below 15 k Ω (at least below 30 k Ω) for all the following steps. Then, individual α -frequency (calculated from the four most occipital electrodes) is determined by resting-state eyes-closed EEG recordings performed for 2 minutes. Next, separately for each electrode

channel, the phosphene current threshold and flicker fusion frequency are determined as described in **Figure 5-2**.

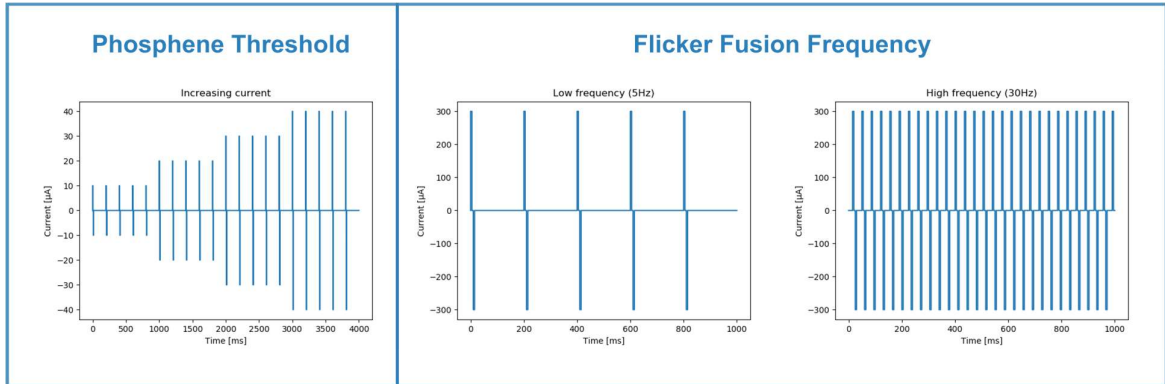


Figure 5-2 Determination of individual stimulation parameters with eyes closed.

(**Left**) With an initial current amplitude of $10\mu\text{A}$ and a consistent frequency of 5 Hz, the current threshold is determined by increasing the current amplitude by $10\mu\text{A}$ per second to an amplitude at which the patient first perceives phosphenes or a maximum current of $1200\mu\text{A}$. (**Right**) The flicker fusion frequency is determined by increasing the frequency by 1Hz per second (starting with 5Hz) until the patient perceives flicker fusion or to a maximum of 49Hz using the previously determined current strength.

The sessions consist of around 6-8 stimulation series per day; the workflow is described in **Figure 5-3**. During the actual stimulation, current strength is set at approximately 125 % of the individuals phosphene threshold recorded during 5Hz stimulation and stimulation frequencies vary between the individual's EEG α -frequency and his/ her flicker fusion frequency. Patients are instructed to keep their eyes open during the actual therapy. The stimulation is performed by trained operators in a darkened room at the Clinical Research Ward of the USZ Clinical Trials Center.

For the sham-rtACS treatment arm, in order to minimise potential placebo effects, the exact same IMD, setup, time schedule, etc. is used as for the active-rtACS group in order to generate the impression that active stimulation has also been applied in sham-patients. However, during the actual therapy patients do not receive current. Nonetheless, independent of the treatment arm, determination of phosphene threshold and flicker fusion frequency is conducted in all patients. Thus, sham-treated patients also experience phosphene perception. All patients, independent of the treatment arm, are informed that phosphenes may but not necessarily must occur during the subsequent actual stimulation. Importantly, the stimulation itself is noiseless during all stimulation steps, including the determination of the stimulation parameters.

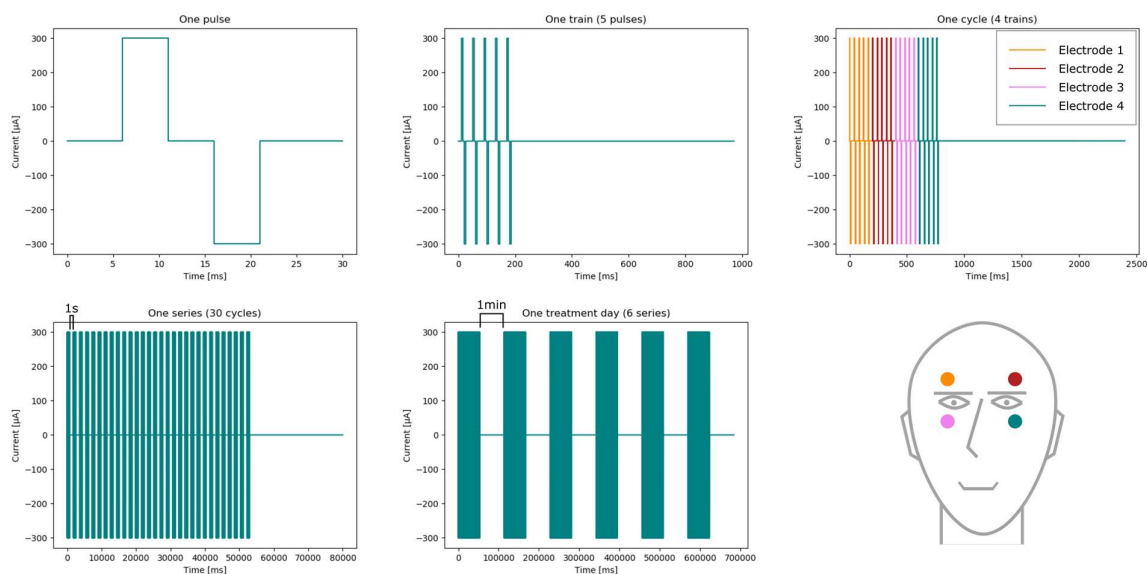


Figure 5-3 Example of the therapy protocol with eyes open at a single treatment day.

During the therapy, biphasic, symmetrical rectangular current pulses with a strength set at approximately 125 % of the individuals phosphene threshold (here 300 μA) are delivered by all four electrodes, with only one being active at any time. When each electrode delivered a train of pulses, a cycle is over and the stimulation is paused for 1 second. The repetition frequency varies between cycles, in a range of the individual's EEG α -frequency and his/ her flicker fusion frequency (for simplicity, the frequency is here fixed at 25Hz). Depending on the day, a single train consists of 2-9 pulses. A single treatment day consists of approximately 6 to 8 series, with about 30 to 40 cycles per series. Between series, there is a stimulation break of 1 minute.

5.4.16 Standard-of-care corticosteroid treatment for ON

In addition, all patients, regardless of the treatment arm, receive standard-of-care corticosteroid treatment at the recommended dose of 3 (-5) days of 1g methylprednisolone intravenously according to published guidelines (www.dgn.org) or at the discretion of the treating neurologist (e.g. some patients may received an additional course of steroids). Start of corticosteroid treatment is always before the first stimulation day.

5.4.17 Concomitant interventions

Patients are allowed to continue on their prior medication, but advised to keep the dosages at the same level whenever possible. This applies also to standard disease-modifying therapies (DMT) given for MS. Newly diagnosed MS patients are allowed to initiate standard MS therapy, but whenever possible according to their individual risk profile (clinical, MRI lesions), initiation starts after the first post-treatment study assessments (which is approximately 4-6 weeks after first symptoms). If a treatment is indicated according to treatment recommendations, the treatment is started, also if it is before the first post-treatment study assessment.

5.4.18 Data management

For data handling, in cooperation with the data management team of the Clinical Trials Center (CTC) Zurich, electronic case report forms (eCRFs) have been established, using a secure GCP-conform database program (REDCap®). Moreover, monitoring visits performed by an external monitor have been conducted during the course of the study for quality assurance.

5.4.19 Proposed statistical analyses

Statistical hypotheses

For simplicity and to formalize the statistical hypotheses, the following notions will be used:

- $LCVA_{w4}$: LCVA [LogMAR] of the ON eye (treated with either active- or sham- rtACS) at week 4 (post-treatment)
- $\Delta GCIP_{w4}$: The mean absolute difference between the GCIP thickness [μm] of the ON eye (treated with either active- or sham- rtACS) at week 4 (post-treatment) and the GCIP thickness [μm] of the corresponding NON eye at baseline (pre-treatment).
- $LCVA_{\text{active}, w4} - LCVA_{\text{sham}, w4}$: LCVA difference [LogMAR] at week 4 (post-treatment) between the active- and sham-rtACS group.
- $\Delta GCIP_{\text{active}, w4} - \Delta GCIP_{\text{sham}, w4}$: Difference in GCIP thickness difference [μm] at week 4 (post-treatment) between the active- and sham-rtACS group.

Hypotheses for primary functional endpoint:

Null hypothesis H_0 : $LCVA_{\text{active}, w4} - LCVA_{\text{sham}, w4} = 0$,

Alternative hypothesis H_1 : $LCVA_{\text{active}, w4} - LCVA_{\text{sham}, w4} \neq 0$

Hypotheses for primary structural endpoint:

Null hypothesis H_0 : $\Delta GCIP_{\text{active}, w4} - \Delta GCIP_{\text{sham}, w4} = 0$,

Alternative hypothesis H_1 : $\Delta GCIP_{\text{active}, w4} - \Delta GCIP_{\text{sham}, w4} \neq 0$

In addition to the 4-week time point (post-treatment), all hypotheses will be tested in a similar way at week 16 (follow-up). Week 16 data will be used for primary analysis, while week 4 data will be used for supportive analysis. Week 16 allows to assess mid-term rather than only short-term (week 4) efficacy, respectively to check if treatment effects sustain between end of treatment (week 4) and end of study (week 16)).

Datasets to be analysed/ analysis populations

The efficacy analyses will include all patients who completed the study (patients who missed no more than two stimulation session and performed the primary outcome assessments at least at baseline and at one of the two post-treatment time points), but not patients who withdrew or had to be excluded early from the study and therefore missed both of the post-treatment study assessment time points (per protocol (PP) population).

The safety analyses will include all randomized participants who received at least one dose of study treatment (intention to treat (ITT) population).

Primary analyses

Statistical analyses will be performed using R, a free software environment for statistical computing and graphics (R Development Core Team 2016; <http://www.r-project.org>). Treatment effects on the main functional outcome measure will be expressed as the mean LCVA [LogMAR] of the affected ON eye at week 4 (post-treatment) and 16 (follow-up) in the rtACS versus the sham-treated group ($LCVA_{active, w4} - LCVA_{sham, w4}$ and $LCVA_{active, w16} - LCVA_{sham, w16}$). Treatment effects on the main structural outcome measure will be expressed as the mean absolute difference of the macular GCIP thickness [μm] of the affected ON eye at weeks 4 (post-treatment) and 16 (follow-up) compared to baseline of the contralateral unaffected NON eye (pre-treatment) in the rtACS versus the sham-treated group ($\Delta GCIP_{active, w4} - \Delta GCIP_{sham, w4}$ and $\Delta GCIP_{active, w16} - \Delta GCIP_{sham, w16}$).

Descriptive statistics: We will begin by plotting the data (using boxplots and/ or scatterplots) to get a better understanding of how the data looks. The distribution of the data will be assessed to determine if the data should be assessed using parametric or non-parametric tests. This will be done using a Q-Q probability plot of the data, the Shapiro-Wilk test and by assessing kurtosis and skew. The central tendency (mean for parametric, median for non-parametric) and spread/ variability (standard deviation for parametric, and interquartile ranges for non-parametric) of data will be assessed for the two primary outcome measures (LCVA and GCIP thickness). GCIP thickness is a continuous scaled measure while LCVA is a discrete ordinal variable.

Hypothesis testing: For each primary outcome measure (LCVA and GCIP thickness) a linear mixed-effects model (lme) will be used to perform between-group comparisons (95 % CI performed at the 5 % significance level). The response variable of the lme model will either be the $LCVA_{w4}$ or the $\Delta GCIP_{w4}$. All models will include treatment (active- or sham-rtACS), gender, age, and time from onset of disease as fixed effects and a random nested effect will account for intra-individual inter-eye dependencies.

Linear mixed effects model in R: The package lme4 will be used.

$LCVA_{model} \leftarrow \text{lmer} (LCVA_{w4} \sim \text{Treatment}_{sham \text{ or } active} + \text{factor} (\text{Gender}) + \text{Age} + \text{Time from onset of disease} + (1 | \text{Subject_ID/eye}), \text{data} = \text{dt});$

$GCIP_{model} \leftarrow \text{lmer} (\Delta GCIP_{w4} \sim \text{Treatment}_{sham \text{ or } active} + \text{factor} (\text{Gender}) + \text{Age} + \text{Time from onset of disease} + (1 | \text{Subject_ID/eye}), \text{data} = \text{dt})$

Model diagnostics: To assess if the model fits the data appropriately, the residuals of the model will be tested for normality with the Shapiro-Wilk normality test and Q-Q plots. To check for constant variance the Tukey-Anscombe plot (residuals vs. fitted) will be examined. If model assumptions are not being met as expected, we will transform the dependent variable (e.g. by Log-transformation) to see if the model predicts the data better. In case this does not work, we will try to find another model which is fitting our data.

Correlations: The relationship between structural (GCIP thickness changes) and functional outcomes (LCVA) in ON eyes will be assessed by Spearman's rank correlations. We use Spearman's rank rather than Pearson's because we will treat LCVA as non-parametric since it is a discrete ordinal variable.

p-values on primary endpoints will be corrected for multiple comparisons. p-values ≤ 0.05 will be considered statistically significant.

Secondary analyses

Preliminary treatment effects on secondary functional outcome measures such as HCVA and colour vision will be expressed using the mean value of the affected ON eye at week 4 (respectively week 16), while structural measures such as the pRNFL and INL thicknesses will be expressed as mean absolute difference in thickness of the affected ON eyes at weeks 4 (respectively week 16) compared to baseline of the contralateral NON eyes (similar to primary analysis). For VEP analyses, recovery of affected optic nerve conduction velocity versus the unaffected NON eye at baseline will be compared between groups at week 16.

Descriptive statistics will be done in a similar way as for the primary analyses.

For the parametric analysis, between-group comparisons will be performed using a two-samples, two-tailed, unpaired t-test (95 % CI performed at the 5 % significance level). For the non-parametric analysis, variables will be compared using the Mann-Whitney test for either ordinal or continuous variables or Fisher test for categorical variables.

Due to the exploratory nature of this study and due to the fact that the secondary outcome measures are mainly examined for learning purposes and to gain a better understanding of the mechanisms of action of rtACS, multiple testing correction on p-values will not necessarily be performed on them. Anything that is not corrected for multiple comparisons is considered exploratory and statistically significant p-values merits further investigation but not a conclusive result.

Safety analysis

Cohort demographics, clinical characteristics and safety data will be summarized with descriptive statistics. For between-group comparisons, the number of AEs will be analysed using either a chi-squared test or for a contingency table with only a few entries (number of AEs) in some field, the Fisher's exact test.

Handling of missing data and drop-outs

Since drop-outs will be replaced the primary efficacy analysis will include only patients that successfully performed the pre-treatment and at least one of the post-treatment study assessments.

5.5 Author Contributions

C.A. Wicki was involved in the study design and wrote the original draft of the research grant that we received from Swiss MS Society for this project in 2018. In the role as coordinating co-investigator, C.A. Wicki wrote the original draft for the ethics application for this clinical Trial with IMD Category A that was approved by the Ethics Committee of the Canton of Zurich in February 2019. C.A. Wicki wrote the original draft of all study documents and prepared the Trial Master File and Investigator Site File. C.A. Wicki prepared study-specific working instructions for the entire study team. C.A. Wicki established a study-specific data management system for this study using REDCap. C.A. Wicki registered the study on ClinicalTrials.gov [NCT03862313](https://clinicaltrials.gov/ct2/show/study/NCT03862313) and kofam [SNCTP000003201](https://kofam.ch/STUDY/SNCTP000003201). C.A. Wicki organized the site initiation visit and was responsible for study-specific staff training. C.A. Wicki wrote the original draft of this thesis chapter. In their role as co-investigators, **R. Martin, I. Jelcic, L. Imbach**, provided support and enabled a good cooperation with the Department of Neurology of the USZ. In their role as co-investigators, **J.V.M. Hanson, C. Gerth-Kahlert, F. Fierz and K. Weber** provided support and enabled a good cooperation with the Department of Ophthalmology of the USZ. **J.V.M. Hanson** also provided critical revision on this thesis chapter. In the role as study coordinator, **T. Simic** provided support with coordinating functions. **A. Lutterotti** took over the role as sponsor- and principal investigator in February 2020 and provided resources and supervision. In the role as initial sponsor- and principal investigator (from February 2019 to January 2020), and thereafter as co-investigator, **S. Schippling** was involved in the design of the study, performed substantial critical revisions on the research grant, ethics application, registration forms and all other study documents, obtained funding for the study, and provided resources and supervision.

5.6 Acknowledgement

The authors would like to thank several people. **P. Manogaran** and the **Statistical Consulting Group of ETH Zürich** provided support with planning of the statistical analyses. **C. Walker-Egger** provided support with drafting the ethics application and establishing the data management system. The Research Ward group of the CTC Zurich, in particular **N. Leu-Möckli, F. Tay, D. Verner-**

Ruckstuhl and M. Spitaleri provided infrastructure for study implementation. The Regulatory Affairs group of the CTC Zurich, in particular **R. Schur R and S. Tresch** provided support with drafting the ethics application. The Data Management group of the CTC Zurich, in particular **D. Smolinski, C. Hyde and S. Weber** provided support with establishing the data management system. The senior physicians, **T. Weiss** and **F. Wolpert**, as well as the assistant physicians, **E. Binaghi, A. Di Giacomo, F. Capecchi, L. Disse, D. Lekaditi, C. Heuer, M. Hänsel, I. Reichen, N. Lohaus and R. Amon** of the Department of Neurology of the USZ provided help with patient screening. **P. Plattner** implemented study monitoring. **S. Brandt and S. Schmidt** from Charité Berlin and **C. Lubetzki and C. Louapre** from Institut du Cerveau et de la Moelle Epiniere, Pitie Salpetriere Hospital, Paris for scientific advice. The Neuromodtronic GmbH, in particular **K. Schweitzer and J. Rygus** provided the IMD used in this study and training for the correct use of the stimulation device. The Augenzentrum Eckert, Neu Ulm, in particular **C. Pletz and K Pisari** for demonstrating how to use the IMD.

5.7 Study funding

This study is partially funded by a Research Grant from the Swiss MS Society that has been acknowledged to the project in September 2018.

5.8 Supplemental Data

5.8.1 Supplemental tables

Table 5-1 Clinical studies testing rtACS as a therapy to improve visual outcomes in optic neuropathies using the NextWave® 1.1 system or its precursor (Neuromodtronic GmbH, previously named EBS technologies GMBH, Germany).

Reference/ Title	Study Design/ Study Population	Stimulation Protocol	Safety	Outcome Results	measures/
Gall et al., 2010 (Gall et al. 2010): Repetitive transorbital alternating current stimulation in optic neuropathy	<ul style="list-style-type: none"> ▪ Case report ▪ n=1 ▪ Optic nerve atrophy: accidental eyeball perforation with a screw driver while working as a motor mechanic 	<ul style="list-style-type: none"> ▪ EBS Technology ▪ Bursts of 10–15 pulse trains per channel applied with a single pulse duration of 8.7 ± 0.8 ms, Frequencies from 10-30 Hz ▪ Waveform: combination of square and sinusoidal pulses ▪ Eyes during stimulation: closed ▪ Sham: None. 	<ul style="list-style-type: none"> ▪ During or after rtACS: Except slight superficial skin irritations no side-effects ▪ No SAE. 	<ul style="list-style-type: none"> ▪ Perimetry (static, kinetic), campimetry, visual acuity (VA) ▪ Increase of detection ability (DA) and significant improvements of the visual field (VF) in static and kinetic perimetry (mean perimetric threshold). ▪ No difference of uncorrected VA before vs. after rtACS. 	
Fedorov et al. 2010 (Fedorov et al. 2010): Non-invasive alternating current stimulation induces recovery from stroke	<ul style="list-style-type: none"> ▪ Randomized, drug-controlled, single-blind ▪ 3 study arms: "Group drug" (n=30; control/ drug only), "Group optic nerve stimulation (ONS)" (n=32; only ONS), "Group drug/ ONS" (n=36; both drug and ONS) ▪ Ischemic stroke (21.4 months earlier) 	<ul style="list-style-type: none"> ▪ EBS Technology ▪ Waveform: square pulses ▪ Eyes: possibly closed, since electrodes were located on the eyelids ▪ Sham: None. 	<ul style="list-style-type: none"> ▪ Did not report AEs. ▪ No SAE. 	<ul style="list-style-type: none"> ▪ Stroke severity level (SSL) assessed by NIH-NINDS stroke scale before and after ONS treatment and at a 1-month follow-up ▪ After ONS, SSLs of groups ONS and drug/ONS significantly improved by 22.5% and 25.1% over baseline ▪ No change in control group (drug only) ▪ SSL improvements mainly due to recovery of motor, sensory and speech functions. ▪ After 1-month follow-up additional improvements for both group ONS and drug/ONS 	
Sabel et al., 2011 (Sabel, Fedorov, et al. 2011): Non-invasive alternating current stimulation	<ul style="list-style-type: none"> ▪ Randomized, sham-controlled double blind ▪ Two arms: active (n=12) vs. sham (n=10) stimulation ▪ Partial optic nerve lesions; visual field loss caused by damage to the optic nerve ▪ Lesion age > 6 months 	<ul style="list-style-type: none"> ▪ EBS Technology ▪ Sham: A clicking sound was presented and the same electrode montage set-up was used as for the active-stimulation. However, 	<ul style="list-style-type: none"> ▪ Minor side effects during treatment: <ul style="list-style-type: none"> ▪ Cutaneous sensations under the electrodes (n=5) ▪ Temporary sleeping difficulties (n=4) ▪ Spontaneous phosphenes independent of stimulation 	<ul style="list-style-type: none"> ▪ DA in defective VF assessed by high resolution perimetry ▪ Active but not sham-stimulation led to significant improvement of a VF detection deficit by 69%, and also significantly improved temporal processing of visual stimuli, detection performance in static perimetry, and VA 	

Chapter 5: ACSON – alternating current stimulation in optic neuritis

<p>improves vision in optic neuropathy</p>		<p>no current was applied.</p> <ul style="list-style-type: none"> ▪ Waveform: not reported ▪ Eyes: closed 	<p>(n=1)</p> <ul style="list-style-type: none"> ▪ No SAE. 	<ul style="list-style-type: none"> ▪ Improvements were associated with increased α-power at occipital sites
<p>Gall et al., 2011 (Gall et al. 2011): Noninvasive transorbital alternating current stimulation improves subjective visual functioning and vision-related quality of life in optic neuropathy</p>	<ul style="list-style-type: none"> ▪ Randomized, sham controlled, double blind ▪ Two arms: active (n=24) vs. sham-stimulation (n=18) ▪ VF impairments after optic nerve damage (mean lesion age: 5.5 years) ▪ Nonarteritic AION (n=8), arteritic AION (n=8), postinflammatory (n=4), posttraumatic (n=5), optic atrophy in the course of glaucomatous optic neuropathy (n=4), compressive optic neuropathy due to meningioma (n=3) or pituitary tumor (n=1), chronic papilledema after pseudotumor cerebri (n=1), haemorrhagic stroke (n=2), idiopathic optic atrophy (n=6) 	<ul style="list-style-type: none"> ▪ EBS Technology ▪ Waveform: sinusoidal vs square pulses ▪ Eyes closed ▪ Sham: A clicking sound was presented and the same electrode montage set-up was used as for the active-stimulation. However, no current was applied. But also performed phosphene threshold determination daily. 	<ul style="list-style-type: none"> ▪ Did not report AEs ▪ No SAE. 	<ul style="list-style-type: none"> ▪ Light detection ability (DA) in defensive VF assessed by high resolution perimetry ▪ Significant increase in DA, significant increase in patient-reported outcome measures (visual QoL)
<p>Fedorov et al., 2011 (Fedorov et al. 2011): Restoration of vision after optic nerve lesions with noninvasive transorbital alternating current stimulation: a clinical observational study</p>	<ul style="list-style-type: none"> ▪ Observational, open label (single arm with active stimulation only) ▪ n=446; lesion ages were 6.8 ± 6.5 years; all received active stimulation ▪ All patients had visual loss caused by damage of the optic nerve caused by either traumatic brain injury (TBI, n=209), inflammation (n=134), brain tumour (n=40), or vascular lesions (n=63). 	<ul style="list-style-type: none"> ▪ EBS Technology ▪ Waveform: sinusoidal vs square pulses ▪ Eyes: closed ▪ Trains of 2 to 9 pulses, pulse train frequency 5 to 20 Hz ▪ Sham: None. 	<ul style="list-style-type: none"> ▪ No SAEs after the therapy and during follow-up. ▪ During stimulation: 10% of patients minor pain or local warmth under the electrode ▪ Immediately after the session some vision blurring effects for 1-2 minutes. ▪ More rarely (<5%) weak headache, drowsiness, or poor sleep. ▪ Occasionally blood pressure fluctuations and general fatigue. 	<ul style="list-style-type: none"> ▪ VF by kinetic perimetry and VA ▪ tACS improved VF size in the right and left eye by 7.1% and 9.3% ($p < 0.001$), respectively. VF enlargements were present in 40.4% of right and 49.5% of left eyes. ▪ VA significantly increased in both eyes (right=0.02, left=0.015; $p < 0.001$). ▪ Visual improvements were associated with increased α-power in forehead areas
<p>Schmidt et al., 2013 (Schmidt et al. 2013): Progressive enhancement of α activity and</p>	<ul style="list-style-type: none"> ▪ Prospective, randomized, sham-controlled, single blind ▪ Two arms: active (n=18) vs. sham-stimulation (n=6) ▪ Minimal lesion age: 6 months ▪ Congenital optic neuropathy (n=7), 	<ul style="list-style-type: none"> ▪ EBS Technology ▪ Waveform: sinusoidal ▪ Eyes: closed ▪ Sham: The same electrode montage set-up was used as 	<ul style="list-style-type: none"> ▪ None of the subjects reported subjectively relevant AEs after ONS. ▪ 3 subjects reported a light frontal headache. ▪ No SAE. 	<ul style="list-style-type: none"> ▪ DA in defective VF assessed by high resolution perimetry ▪ Significant improvement in perimetric measures like detection accuracy (DA) ▪ α-power over bilateral occipital electrodes was significantly larger (but no direct

Chapter 5: ACSON – alternating current stimulation in optic neuritis

<p>visual function in patients with optic neuropathy: A two-week repeated session alternating current stimulation study</p>	<p>compressive neuropathy (n=4), AION (n=3), optic neuropathy after stroke (n=2), glaucomatous optic neuropathy (n=1), optic neuropathy due to pseudotumor cerebri (n=1), inflammatory optic neuropathy (n=2), idiopathic optic neuropathy (n=4).</p>	<p>for the active-stimulation. However, no current was applied.</p>		<p>association between α-power increase and VF improvement was found).</p>
<p>Gall et al., 2014 (Gall et al. 2014): Non-invasive alternating current stimulation to improve visual impairment after postchiasmatic lesions</p>	<ul style="list-style-type: none"> ▪ Prospective, randomized, controlled, blinded clinical trial ▪ Two arms: active (n=15) vs. sham-stimulation (n=14) ▪ Postchiasmatic lesions caused by unilateral stroke ▪ Lesion age > 6 months ▪ Only an abstract in Clinical Neurophysiology 125 Suppl 1: S36, 2014; Clinical-Trials.gov Identifier: NCT01418820. 	<ul style="list-style-type: none"> ▪ EBS Technology ▪ The amplitude of each current pulse was below 1000 μA ▪ Waveform: not reported. ▪ Eyes condition: not reported ▪ Sham: Same electrode montage set-up, minimal sham-stimulation with single bursts at a frequency of 5Hz 	<ul style="list-style-type: none"> ▪ Did not report AEs. ▪ No SAE. 	<ul style="list-style-type: none"> ▪ A progressive improvement of perimetric thresholds within areas of residual vision was reported only in the active-group. ▪ Central 5° VF was improved and defect depths in 30°-threshold perimetry was significantly reduced only in active-group. ▪ Vision-related QoL was increase only in active-group ▪ Health-related quality of life (Short Form Health Survey SF-12) did not change significantly in either group. ▪ Absolutely impaired areas of the VF defect did not change in either group.
<p>Gall et al., 2016 (Gall et al. 2016): Alternating Current Stimulation for Vision Restoration after Optic Nerve Damage: A Randomized Clinical Trial</p>	<ul style="list-style-type: none"> ▪ Multicentre, prospective, randomized, double-blind, sham-controlled trial ▪ Active (n=45 vs. sham (n=37) stimulation ▪ VF loss caused by glaucoma (n = 33), AION (n = 32), post-acute inflammation (n = 12), optic nerve compression (n = 5, of which 4 were tumour-induced and 1 intracranial haemorrhage), Leber's hereditary optic neuropathy (n = 3), congenital or unknown aetiology of optic atrophy (n = 5). 	<ul style="list-style-type: none"> ▪ EBS Technology ▪ Current strength: 125% of phosphene threshold ▪ Frequencies: between 8–25 Hz ▪ Waveform: square pulses ▪ Eyes: closed ▪ Sham: minimal sham-stimulation with single bursts at a frequency of 5Hz 	<ul style="list-style-type: none"> ▪ During stimulation: mild headache (n=2), cutaneous sensations (n=20), back pain and stiff neck (n=1) ▪ After stimulation: Temporary dizziness (n=1), transient vertigo (n=2), persistent vertigo for 0.5 hrs (n=1), mild headaches immediately after stimulation (n=6) ▪ No meaningful changes in autonomic activity ▪ 1 SAE, but unrelated to rtACS. 	<ul style="list-style-type: none"> ▪ VF mapping was conducted using high-resolution, super-threshold visual detection test (HRP) ▪ Significantly greater mean improvement in the VF for at least 2 months ▪ Improvement of near-threshold visual fields in the central 5° ▪ Significantly increased thresholds in static perimetry ▪ Improvements were associated with significantly increased occipital α-power and synchronization of functional connectivities between occipital and frontal regions. ▪ No significant change in VA

Table 5-2 Schedule of study visits and assessments for individual study participants.

Once enrolled in the study, the expected study duration for a single participant will be approximately 16 weeks (4 months).

Tests and Assessments	Screening/ Recruitment	pre-treatment/ baseline assessment	10 days rACS-/ sham treatment										post-treatment assessment	3 months treatment-free		follow-up assessment	
	week 0 (≤ 2 weeks since first symptoms)	week 1 (btw. recruit. and treat. init.)	week 2 - 3										week 4 (btw. 5-15 days after last treat.)	week 5 - 15		week 16 (± 2 weeks)	
			1	2	3	4	5	6	7	8	9	10		week 8	week 12		
Clinical routine examination	x																(x)
Patient Information & Informed consent	x																
Medical history & demographics	x																
Inclusion/ exclusion criteria check	x																
Randomization	x																
Start corticosteroid (standard-of-care) treatment	x																
LCVA, HCVA		x															x
Colour vision		x															x
Perimetry		x															x
OCT		x															x
VEP		x															x
NEI-VFQ-25 Questionnaire		x															x
Treatment			x	x	x	x	x	x	x	x	x	x	x				
Safety questionnaire (AE monitoring)		x	x	x	x	x	x	x	x	x	x	x	x	x*	x*~	x*~	x*
(MRI: only if obtained in clinical routine)		(x)												(x)			(x)
Approx. Duration	2 h	2-2.5 h	Each 1.5-2 h										2-2.5 h	15 min	15 min	2-2.5 h	

Symbols: The x* indicates that these assessments are meant for all patients, including the withdrawn participants (Efforts should be made to encourage the withdrawn participants to do the safety follow-ups as stipulated in the protocol). The x*~ indicates that these assessments (safety interview) can be done by phone if desired by the patient. The (x) indicates that these assessments are only done if they are part of the clinical routine examination.

5.8.2 Inclusion criteria

Participants fulfilling all of the following inclusion criteria are eligible for the study:

- Informed Consent as documented by signature (Appendix Informed Consent Form)
- Participants are capable of giving informed consent
- Participant who have a good knowledge of German (patient information and consent must be understood)
- Patients, presenting with typical signs and symptoms suggestive of a first-ever episode of unilateral acute autoimmune, inflammatory, demyelinating ON, including idiopathic ON and ON suggestive of MS (typical CIS, or with an established diagnosis of relapsing-remitting MS (RRMS) according to latest panel criteria (Thompson et al. 2018) and no better explanation)
- Patients with HCVA of ≤ 0.63 (decimal system) corresponding to a LogMAR value of ≥ 0.2 on

the affected eye (assessed using a Snellen chart)

- Patients presenting in clinics within 14 days of symptom onset
- In principle 18-50 year old female and male patients may be recruited. However, since the randomization of patients will be controlled for gender and participants will be enrolled one at a time on a continuous basis, the gender might become relevant late in the study (e.g. if the female block has already been fully recruited and only males might still be enrolled).
- Patients are receiving standard-of-care treatment for ON (cortisone therapy)

5.8.3 Exclusion criteria

The presence of any one of the following exclusion criteria will lead to exclusion of the participant:

- Patient without legal capacity who is unable to understand the nature, significance and consequences of the trial
- Women who are pregnant or have the intention to become pregnant during the course of the study (For women who can get pregnant, pregnancy will be omitted using a pregnancy test when checking for inclusion and exclusion criteria. Patients will be informed that they must use contraception during the study)
- Patients with a previous clinical history of ON in either eye
- Patients with obvious retinal pathology other than that associated with ON
- Patients who are unable to perform the study assessments (e.g. OCT examination) because of a severe nystagmus (repetitive, uncontrolled eye movements causing unsteady fixation)
- Patients with a recent eye surgery
- Patients with known anti-aquaporin-4 (AQP4)- or myelin oligodendrocyte glycoprotein (MOG)-antibody seropositivity
- Patients with contraindications to the class of device under study (for rtACS): implanted electronic devices, metallic artefacts in the head (excluding dentition), epilepsy, brain cancer, pregnancy, breastfeeding, increased intraocular pressure without appropriate treatment, arterial hypertension without appropriate treatment, acute retinal haemorrhage, skin irritations at intended positions of electrodes, cognitive deficits (unable to provide written informed consent or follow the instructions)
- Known or suspected non-compliance, drug or alcohol abuse
- Inability to follow the procedures of the study, e.g. due to language problems, psychological disorders, dementia, etc. of the participant
- Participation in another study with investigational drug/device within the 30 days preceding and during the present study
- Previous enrolment into the current study
- Enrolment of the investigator, his/her family members, employees and other dependent persons

5.8.4 Criteria for withdrawal/ discontinuation of participants

The following reasons may lead to an early withdrawal/ exclusion of participants from the study:

- Patient wishes to withdraw from the study
- Failure of the participant to attend the treatment sessions (>2 missed appointment)
- Failure of the participant to attend the pre-treatment (baseline) or both of the post-treatment (5-15 days after last treatment session and 16 weeks follow-up) study assessment visits (At the minimum the data for the primary outcome measures must be available; if only data of the secondary outcome measures are missing, this is not a reason to exclude the participants early from the study.)

- Participant meets exclusion criteria
- Safety reasons: If for any reasons participant's safety has to be questioned. (Treatment with rtACS must be discontinued if the subject develops any medical condition or AEs that do not permit further application, as determined by the therapist applying the treatment (trained study team member), the treating neurologist or the sponsor investigator (or his designee).)

5.8.5 Safety outcomes

- The total number of Adverse Events (AEs) during the 10 days of treatment
- The total number of AEs during the 3 months treatment-free follow-up period
- The minimum, maximum and mean number of AEs per patient
- The number of patients who had at least one AE
- The number of patients who stopped treatment due to AEs

5.8.6 Primary efficacy outcomes

- The primary functional outcome measure will be LCVA [LogMAR] at 4 (post-treatment) and 16 weeks (follow-up) in ON eyes.
- The primary structural outcome measure will be the mean (\pm SD) change in macular GCIP thickness [μ m] of the affected ON eye at 4 (post-treatment) and 16 weeks (follow-up) in comparison to baseline of the unaffected contralateral NON eye (pre-treatment).

5.8.7 Secondary efficacy outcomes

Secondary functional outcome measures will include:

- High-contrast visual acuity (HCVA) [LogMAR], colour vision [tritan] and visual field testing [dB] at 4 (post-treatment) and 16 weeks (follow-up) in ON eyes.
- Recovery of pattern-reversal visual evoked potential (PR-VEP) conduction velocity of the affected optic nerve [ms] compared to the intra-individual baseline of the unaffected optic nerve at 16 weeks (follow-up).
- Patient-reported vision-related Quality of life (QoL) assessed by the National Eye Institute Visual Function Questionnaire-25 (NEI-VFQ-25) at 4 (post-treatment) and 16 weeks (follow-up).

Secondary structural outcome measures will include:

- The mean (\pm SD) change in peripapillary retinal nerve fibre layer (pRNFL) thickness [μ m] of the affected ON eye at 4 (post-treatment) and 16 weeks (follow-up) in comparison to baseline of the contralateral NON eye.
- The mean (\pm SD) change in macular inner nuclear layer (INL) thickness [μ m] of the affected ON eye at 4 (post-treatment) and 16 weeks (follow-up) in comparison to baseline of the contralateral NON eye.

5.8.8 Other Outcomes of Interest

- Patient demographics (relevant personal data) and clinical characteristics (medical history).

6 General Conclusions and Outlook

Multiple sclerosis (MS) is the most frequent non-traumatic central nervous system (CNS) disorder in young adults worldwide (Kingwell et al. 2013). As a consequence of progressively accumulating neuro-axonal damage in patients, neurological disability may impact severely on an individual's life, and, when combined with the financial costs of treatment, the socioeconomic effects of MS are enormous (Luessi, Siffrin, and Zipp 2012; Dobson and Giovannoni 2019).

Optic neuritis (ON) is an important core manifestation of MS affecting up to 70 % of patients during the course of their disease (Toosy, Mason, and Miller 2014). Through neurodegeneration from the primary site of inflammatory demyelination in the optic nerve towards the retina and also along the posterior afferent visual pathway (AVP) towards the primary visual cortex, ON is the major source of persistent visual disability in MS (Miller et al. 2005b; Gabilondo et al. 2014; Toosy, Mason, and Miller 2014). In contrast to the traditional perception of ON as relatively benign, visual recovery is often incomplete and many patients are left with persistent functional impairment, in particular affecting low-contrast visual acuity (LCVA) and colour vision, both of which are relevant to vision-related quality of life (QoL) and daily functioning (Walter et al. 2012b; Findling et al. 2015; Sanchez-Dalmau et al. 2017).

Apart from its high prevalence and clinical relevance, ON also offers a unique model to study neurodegeneration as well as the potential of neuroprotective and –regenerative therapies, as the clinical onset of ON can usually be defined with a high degree of temporal precision, and its impact is confined to a discrete and well-defined anatomical region (Aktas, Albrecht, and Hartung 2016; Petzold 2017). The AVP is retinotopically organized, linking its structural integrity strongly with clinical function (Costello 2013; Martinez-Lapiscina et al. 2014). Nearly the entire AVP can be probed using imaging tools of different modalities, including optical coherence tomography (OCT) and diffusion-tensor-imaging (DTI). Furthermore, the function of the AVP can be assessed by simple but sensitive measurements such as LCVA (Balcer et al. 2017). Therefore, ON provides an optimal paradigm to study the consequences of an MS-relapse on tissue integrity and function.

6.1 OCT as a means to characterize visual pathway involvement in MS

Over the last years, optical coherence tomography (OCT) as a tool to non-invasively quantify the different retinal layer thicknesses, has proven a helpful method to properly characterize AVP involvement in MS (Wicki, Hanson, and Schippling 2018). In particular, the thicknesses of the macular ganglion cell and inner plexiform layer (GCIP) and the peripapillary retinal nerve fibre layer (pRNFL) are informative with regard to early detection of neuronal degeneration and long-term axonal damage of the retinal ganglion cells (RGCs) respectively. A systematic meta-analysis showed that the macular GCIP and pRNFL are significantly thinned in MS patients with a previous history of

ON, but also to a lesser extent in those MS patients without a former ON (Petzold et al. 2017). Furthermore, a conclusive, although numerically small, thickening of the macular inner nuclear layer (INL) was observed in eyes with a previous ON and was proposed to reflect inflammatory disease activity in MS (Petzold et al. 2017). There is also a significant body of literature demonstrating that OCT-derived measures are associated with other clinically relevant parameters such as grey matter atrophy (Saidha et al. 2015) or the Expanded Disability Status Scale (EDSS), a standard measure for overall disability in MS (Martinez-Lapiscina et al. 2016).

6.2 Bilateral retinal pathology following a first-ever clinical episode of autoimmune ON

To date, a great number of cross-sectional OCT studies in ON have been published. Results from longitudinal studies or studies using latest spectral-domain OCT technology, however, are relatively rare. Therefore, to achieve a better knowledge of the temporal dynamics and magnitude of retinal neuro-axonal and functional visual damage in ON, we performed a longitudinal study at the Department of Neurology at the University Hospital Zurich (USZ), Switzerland (Wicki et al. 2020).

In this monocentric retrospective study on 41 patients, we analysed the changes in retinal structure and visual function over 12 months following a first-ever episode of acute ON. OCT and visual acuity assessments were performed at baseline, and 1, 3, 6, and 12 months following clinical onset of ON, with comparisons of ipsilateral ON to the baseline of contralateral non-ON (NON) eyes performed over time (Wicki et al. 2020).

In terms of structure, we found that the retina of the affected ipsilateral ON eye displayed signs of early neuro-axonal damage, as revealed by a significant reduction of the macular GCIP thickness already at 1-month, and of the pRNFL thickness at 3-months following ON onset, corroborating previous research (Costello et al. 2015; Gabilondo et al. 2015). In fact, we observed that, on average 75 % of the total reduction in macular GCIP thickness recorded over one year was already present at 1 month, and 100 % at 3 months, following ON; this finding highlights the particular importance of fast treatment in ON. The pRNFL showed the characteristic pattern of an initial thickening in the first month following acute ON, which is believed to be associated with inflammatory oedema. Thereafter, a second phase of sustained thinning indicative of secondary degeneration of RGC axons was followed, which is in agreement with previous observations (Henderson et al. 2010; Costello et al. 2015).

A strength of this study was the very short time from clinical onset of ON to baseline examination, which was on average 10 days (as compared to other studies, with an average time of 18 days (Costello et al. 2015) or 12 days (Gabilondo et al. 2015)). Nonetheless, in regards to phase 2 and phase 3 trials employing the ON paradigm, it is important to even more accurately determine by what day within the first month the majority of change respectively neuro-axonal damage has occurred.

Therefore, future studies should focus in even more detail on the chronology of retinal degeneration during the very early phase of ON.

A limitation of OCT is that structural results do not allow direct conclusions to be drawn regarding the precise nature of retinal layer changes, due to a lack of pathological specificity. However, the assumption that inner retinal layer atrophy is caused by neuro-axonal damage is strongly supported by post-mortem analysis of retinal tissue from MS patients (Green et al. 2010). We may also draw parallels with results from two longitudinal animal studies, in which our group combined OCT assessments with *ex-vivo* analysis of the retina and optic nerve in mice with experimental autoimmune encephalomyelitis (EAE)-induced experimental ON (Manogaran et al. 2018; Manogaran et al. 2019). The so-called inner retinal layer (IRL), which is a combined thickness measure of the RNFL, GCL and IPL around the optic nerve head (ONH), was measured over a period of one month following EAE induction. Overall, the pattern of IRL changes occurred over a shorter timescale, but qualitatively very much resembled what we observed for the pRNFL (Manogaran et al. 2018; Manogaran et al. 2019). Electron microscopy revealed that the increase in IRL thickness co-occurred with the presence of inflammatory extra-cellular and intra-axonal oedema in the optic nerve. Histological evidence from later time points also confirmed that retrograde neuro-axonal degeneration from the optic nerve towards the retina correlated with OCT-detected IRL thinning (Manogaran et al. 2019). This further strengthens the assumption that OCT measures give valuable insights into the disease mechanisms involved in ON.

In addition to documenting the extremely rapid evolution of inner retinal atrophy in clinically affected eyes, a significant increase in the INL thickness of ON eyes was found at 1 month following ON (Wicki et al. 2020). Based on previous work providing evidence that the macular INL may be a biomarker for inflammatory disease activity in MS (Petzold et al. 2017), we suggest a possible linkage to inflammatory mechanisms within or affecting the INL.

In MS, bilateral simultaneous ON is very rare, with unilateral presentation being more typical (Burman, Raininko, and Fagius 2011). Interestingly, our longitudinal assessment of retinal damage during ON pathogenesis suggested subclinical involvement of the fellow eyes in ON, particularly affecting the INL: At 12 months after symptom onset, a delayed, but significant increase of the INL thickness was measured in the contralateral NON eyes of patients with clinically unilateral ON. Whilst a slight increase in INL thickness in eyes with a previous ON has been reported previously (Petzold et al. 2017; Hanson et al. 2018), INL changes in the contralateral NON eyes have not previously been described. When considered together with recently published data describing functional abnormalities in the fellow eyes of patients with unilateral ON (e.g. abnormalities of the VEP (Raz et al. 2013) or the ONH component of the multifocal ERG (Schnurman et al. 2014)), as well as clinical trial data suggesting effects of Opicinumab (a monoclonal anti-LINGO-1 antibody) treatment on the

multifocal VEP of the contralateral NON eye (Klistorner, Chai, et al. 2018)), we believe that our INL finding is of particular interest. However, it remains unclear whether these changes, which were first observed 12 months after the onset of ON and were not apparently present at previous time points, were truly sequelae of ON, or rather indicative of ongoing or future inflammatory MS-related disease activity. On that note, Knier and colleagues have studied a MS patient cohort without previous ON and recorded that the INL not only normalises in thickness in response to successful MS treatment, but also correlates with future MRI findings, making the INL more likely a biomarker of global disease activity in MS (Knier et al. 2016; Knier et al. 2017). The fact that we assessed a young cohort with likely active inflammatory disease- as evidenced by an ON relapse- reinforces this possibility. Therefore, it would have been helpful to directly compare this cohort to an age-matched cohort of MS patients without a recent history of ON. Since we did not have data from such a cohort available to us, we instead referred to findings from a recently published study with an observation period of 3 years from Balk and collaborators (Balk et al. 2019). In their study, no significant annualized change in INL volume in MS eyes without a recent history of ON was found, which is in line with the meta-analysis from Petzold and colleagues (Petzold et al. 2017). Instead, they found a significant increase in INL volume only in eyes affected by an ON event during the study period, and concluded that it may reflect inflammation of the adjacent optic nerve. Despite this, they still found an association of INL volume with previous clinical non-ON relapses in these patients, suggesting some relation with global MS disease activity (Balk et al. 2019). In summary, the results of Balk et al. indicate that MS disease activity independent of ON may not necessarily be the cause of our observed increase in INL thickness in contralateral NON-eyes. This may support our original interpretation of our results, i.e. that this INL increase was related to inflammation in the optic nerve, indicating subclinical involvement of the contralateral optic nerve in clinically unilateral ON. The idea of occult involvement of the fellow eyes is further strengthened by the observation that the GCIP thinning in the NON eyes was numerically greater than previously reported thresholds of physiological aging (Balk et al. 2016). Nonetheless, we are unable to draw firm conclusions on the underlying mechanisms of INL thickening and the possible bilateral retinal pathology following a first-ever clinically unilateral ON. The question of whether dynamic changes occur in retinal thicknesses of the contralateral eye following ON is important with regard to both the clinical interpretation of OCT assessments, as well as the design of OCT research studies and should therefore be explored further in clinical studies. Unfortunately, the animal model that is most commonly used to study ON is likely to be of only limited use in addressing this issue: almost all mice with myelin oligodendrocyte glycoprotein (MOG)-peptide induced EAE develop bilateral ON (Manogaran et al. 2018; Manogaran et al. 2019), making it impossible to study the effects of unilateral ON on the contralateral eye. Regardless, considering the small magnitude of the INL changes being observed, the clinical applicability of these changes at the individual level also remains unclear.

In terms of visual function, patients showed severely impaired visual acuity in ON eyes at disease onset (Wicki et al. 2020). Even though an improvement in high-contrast visual acuity (HCVA) over time was recorded, low-contrast visual acuity (LCVA) remained clinically relevantly impaired up to the final study time point or month 12. A summary of the important role of LCVA testing in adequately assessing visual function in MS is also given by Balcer and colleagues (Balcer et al. 2017). Of note, 37 out of the 41 patients followed up in this study received standard therapy with corticosteroids, meaning that this therapy was not capable of preventing persistent structural, as well as functional, AVP damage in these patients. This emphasizes that efficient treatment for acute ON and prevention of ensuing neurodegenerative changes undoubtedly remains an unmet medical need in MS.

In conclusion, this study effectively replicated the findings of previous studies describing changes in the ipsilateral inner and outer retinal layers following acute ON, supporting the hypothesis that the thicknesses of the macular GCIP and pRNFL are sensitive to injuries of the cell bodies, dendrites and axons of the RGCs. We reported a previously undescribed increase in INL thickness at 12 months post-ON in the contralateral eye. We hypothesise, that subclinical involvement of the fellow eye caused this increase, though further research is needed to confirm this hypothesis. Moreover, patients suffered a sustained and clinically relevant impairment of LCVA on the affected eyes. In consideration of future clinical trial planning, we recommend the use of the macular GCIP to detect early neuronal damage, while the thickness of the pRNFL provides a good marker for long-term axonal damage following first-ever ON. Our data also reinforce the particular importance of fast, maybe even prophylactic treatment in ON.

6.3 Longitudinal characterization of AVP pathology in experimental ON using a multimodal imaging approach

Because the high prevalence of visual dysfunction following ON is alarming, a better understanding of the exact mechanisms involved in the induction of neuro-axonal injury is needed. Here, animal models provide vital opportunities to further study the consequences of ON on tissue integrity and function. As described above, the typical characteristics of ON in humans, namely inflammatory demyelination and gliosis accompanied by neuro-axonal degeneration in the optic nerve and retina, have also been described in murine models of MS, including MOG-induced EAE (Sun et al. 2007; Horstmann et al. 2013; Dietrich et al. 2019).

Thus, in a longitudinal EAE study, we aimed to further investigate the mechanisms involved in ON-induced pathology of the AVP in more detail, using *in vivo* magnetic resonance imaging (MRI) and OCT followed by *ex-vivo* immunohistochemical analyses of the tissue (chapter 4 of this thesis). The methodology used were largely based on two previous publications by our group (Manogaran et al. 2018; Manogaran et al. 2019), but extended with the goal of further improving this non-invasive

imaging platform in order to more effectively capture AVP pathology in EAE, and to optimize the setting for future preclinical testing of neuroprotective or -regenerative candidates.

Because the retina is void of myelin, demyelination, an important contributor to chronic neuro-axonal damage following ON, cannot be assessed with OCT (Bruce, Zhao, and Franklin 2010; You et al. 2020). Therefore, in this thesis, we have assessed the utility of diffusion tensor imaging (DTI) as a means to investigate AVP pathology following ON, allowing the assessment of the myelinated portion of the optic nerve and tract. The MRI examination included a DTI and T2-weighted sequence to obtain measurements of axial diffusivity (AD), radial diffusivity (RD), and fractional anisotropy (FA) in the optic nerves and tracts, as well as regions of high T2 signal intensities around the optic nerves.

First, we confirmed feasibility and longitudinal reliability of a newly-established free-breathing (instead of tracheal intubation) MRI setup to locally assess microstructural white matter (WM) tract integrity in the optic nerve and tract in healthy mice. Following this, we performed a longitudinal study to investigate the sensitivity of the MRI measures to distinguish between control and EAE mice, and to characterize EAE-induced pathology in the pre- and post-chiasmal AVP over time. For this purpose, a total of eight EAE mice and three control mice underwent MRI examinations at baseline (3 and 4 days prior to immunization), 15/16 days post immunization (dpi) (at the peak of EAE symptoms), and 28/29 dpi (following partial recovery of EAE symptoms).

In EAE, T2 signal hyperintensities around the optic nerve were visible at 15/16 dpi and indicated the presence of inflammation in EAE. In agreement with previous literature, we found progressively decreased FA values in the optic nerves and tracts in EAE, reflecting a loss of directional diffusivity and thus indirectly implying impaired WM integrity due to axonal damage, myelin injury, or a combination of both (Mori and Zhang 2006; Aung, Mar, and Benzinger 2013). Using *ex-vivo* analysis at different time points post-immunisation, we previously showed that pathological processes in the optic nerve start early in EAE (Manogaran et al. 2019). These previously published immunohistochemical results of the optic nerve showed that microglia activity was already increased at 7 dpi (increased allograft inflammatory factor 1, IBA1 staining), followed by increased astrocytosis (increased glial fibrillary acidic protein, GFAP staining) and the first signs of impaired axonal transport (increased amyloid precursor protein, APP staining) at 9 dpi, and finally evidence of the first signs of inflammatory demyelination (extensive infiltration of CD3 positive T-cells and decreased myelin basic protein, MBP) and axonal injury (decreased neurofilament-M, NEFM) at 11 dpi. Together, these processes had cumulative effects that, in combination, led to severe optic nerve pathology by 33 dpi (Manogaran et al. 2019). Therefore, it is not surprising that FA was already significantly reduced at 15/16 dpi in the optic nerve and tract.

Results from DTI in this study showed that radial diffusivity (RD; water diffusivity perpendicular to axonal fiber tracts) significantly increased in the optic nerve of EAE mice already at 15/16 dpi and in the optic tract at 28/29 dpi. According to previous *ex-vivo* and DTI findings in EAE mice (Sun et al. 2007; Nishioka et al. 2017; Manogaran et al. 2018; Nishioka et al. 2018) and in human ON (Trip et al. 2006; Kolbe et al. 2009; Naismith, Xu, Tutlam, Trinkaus, et al. 2010; Li et al. 2011; van der Walt et al. 2013), this increase in RD most likely reflected ongoing demyelination. It is known that demyelination provokes a secondary phase of neuro-axonal damage and related clinical disability in MS (Franklin and Ffrench-Constant 2008; Bruce, Zhao, and Franklin 2010; Franklin et al. 2012; Mahad, Trapp, and Lassmann 2015; You et al. 2019; You et al. 2020). Therapies that either prevent demyelination or improve remyelination would be of great value in order to avoid progressive functional disability in MS patients (Villoslada and Martinez-Lapiscina 2019; Lubetzki et al. 2020). Therefore, outcome measures should be able to capture these target mechanisms, emphasizing the valuable role of RD as a biomarker to non-invasively and *in-vivo* capture demyelination.

The significance of altered AD is less well understood, but has been linked to axonal damage, with decreased AD found in acute MS lesions, and increased AD in chronic lesions (Aung, Mar, and Benzinger 2013; Kuchling et al. 2017; Mahajan and Ontaneda 2017). Contrary to the findings of earlier EAE studies (Sun et al. 2007; Manogaran et al. 2018; Nishioka et al. 2018), we did not observe a statistically significant difference in optic nerve AD in EAE mice. Since inflammation and gliosis has previously been suggested to have confounding effects on DTI measures (Aung, Mar, and Benzinger 2013; Chiang et al. 2014; Mahajan and Ontaneda 2017), we speculated that in our study, DTI may have been confounded by co-existing inflammation, which plays a significant role in EAE pathology (Manogaran et al. 2019). Other possible factors that may have resulted in no significant optic nerve AD changes include a lower inflammatory response and thus milder EAE presentation than previously observed, or insufficient statistical power because of a limited sample size.

Complementary analysis of *ex-vivo* and retinal OCT data for this study is still pending, thus it is not yet possible to draw firm conclusions regarding these reported MRI results. With this caveat, we conclude on the basis of the evidence currently available to us that DTI is primarily valuable in capturing demyelination of the optic nerve and tract in EAE, while in the present study, AD may have failed in detecting acute axonal damage. We propose that OCT-derived measures of the IRL may be more sensitive to EAE-induced neuro-axonal damage of the RGCs (Manogaran et al. 2018; Manogaran et al. 2019), although further research is needed to confirm this hypothesis. As such, the importance of a combined multimodal imaging approach including both DTI and OCT is emphasized.

In summary, we have shown that RD appears to be a sensitive biomarker for demyelination in experimental ON. Therefore, DTI may be helpful to evaluate if therapeutic interventions preserve WM-integrity in MS. Taking into account the fact that clinical studies are often extremely expensive

and time-consuming, in addition to being demanding for patients, it is important to first estimate the chance of success. In view of some of the latest clinical (Aktas, Albrecht, and Hartung 2016; Petzold 2017) and preclinical (Dietrich et al. 2019) studies, the growing relevance of ON as a clinical trial paradigm for evaluating new therapeutics with regards to neuroprotection and -repair is emphasized. We have also identified a candidate we would deem eligible to test within our preclinical multimodal imaging platform: hydroxytyrosol, an olive fruit extract which is a potent naturally-occurring antioxidant (Fu and Hu 2016). By preventing radical-mediated damage, hydroxytyrosol is thought to have neuroprotective potential (Fu and Hu 2016). We expected this study to shed further light on the potential neuroprotective capacity of hydroxytyrosol and its possible impact on the clinical management of acute ON, as well as MS in general. Because of its good safety profile, we would suggest investigation of not only therapeutic, but also prophylactic, application in EAE (Soni et al. 2006).

6.4 Repetitive transorbital alternating current stimulation in human acute ON: Design of a pilot study to test safety, tolerability and preliminary efficacy (ACSON)

Visual function has been rated by MS patients as the most important bodily function (even above motor and cognitive abilities), irrespective of disease duration (Heesen et al. 2018). Thus, the high prevalence of visual impairment in MS following episodes of (repeated) ON remains a major unsolved problem in the management of the disease.

While the development of immunomodulatory treatments has been very successful over the last two decades, there is still a lack of approved therapies that specifically promote neuroprotection and -repair (Luessi, Siffrin, and Zipp 2012; Aktas, Albrecht, and Hartung 2016; Villoslada 2016; Lubetzki et al. 2020). Corticosteroids are the standard treatment for acute ON for almost 30 years (Beck et al. 1992), even though the therapeutic efficacy remains controversial. Existing data indicated that high-dose steroids over 3-5 days led to a more rapid recovery from the symptoms of ON, but did not influence long-term functional outcomes (Beck and Cleary 1993; Beck and Gal 2008; Shams and Plant 2009; Bennett, Nickerson, et al. 2015; Petzold et al. 2020). Despite these disadvantages, the use of intravenous or oral steroids with or without oral taper is still the mainstay of therapy for ON (Jenkins and Toosy 2017).

Given these facts, there is a strong need for visual rehabilitation and neuroprotective therapies tailored specifically to the visual system. In the hopes of finding new and quickly available therapeutic options that specifically target long-term prevention of persistent visual disability, we performed an interdisciplinary literature search (chapter 5 of this thesis).

We found several preclinical studies in rodent models of optic neuropathies that showed a decreased number of atrophic RGCs in rats treated with low-current electrical stimulation of the retina and optic

nerve as opposed to non-treated animals (Morimoto et al. 2005; Tagami et al. 2009; Henrich-Noack, Lazik, et al. 2013). It has been suggested that neuroprotective- and restorative effects on RGCs such as upregulation of neurotrophic factors, improved chorioretinal blood circulation, and an inhibition of pro-inflammatory mechanisms are responsible for this increased survival of RGCs (Sato, Fujikado, Lee, et al. 2008; Sato, Fujikado, Morimoto, et al. 2008; Zhou et al. 2012; Morimoto et al. 2014; Fu et al. 2015; Yin et al. 2016).

In addition, basic research has shown that the myelination of RGC axons is dependent on endogenous electrical neuronal activity (Barres and Raff 1993; Demerens et al. 1996). Therefore, it is possible that the enhancement of neuronal activity via exogenous stimulation could improve remyelination of injured nerves (Stankoff et al. 2016; de Faria et al. 2019). Facilitation of the differentiation of oligodendrocyte progenitor cells (OPCs) into myelinating oligodendrocytes upon the presence of electrical activity has been proposed to explain the activity-dependence of the myelination process (Stevens et al. 2002; Gibson et al. 2014; Wake et al. 2015). In MS, the failure of differentiation of OPCs into oligodendrocytes has been suggested to be one of the main obstacles for successful remyelination attempts (Kuhlmann et al. 2008; Zawadzka et al. 2010). Experimental modification of neuronal activity has been shown to influence remyelination in injured neurons of the peripheral nervous system (Zhang et al. 2013; McLean et al. 2014), the spinal cord (Li and Li 2017), and the cerebellum (Gautier et al. 2015).

The role of non-invasive therapeutic electrical stimulation of the retina and optic nerve has also previously been investigated in human optic neuropathies of different origins, using a methodology called repetitive transorbital alternating current stimulation (rtACS). Using stimulation in the α - and β -frequency range with an intensity just above the individuals' phosphene perception threshold, these studies provided some evidence for a beneficial effect of rtACS on functional vision restoration (Fedorov et al. 2010; Gall et al. 2010; Fedorov et al. 2011; Gall et al. 2011; Sabel, Fedorov, et al. 2011; Schmidt et al. 2013; Bola et al. 2014; Gall et al. 2014; Gall et al. 2015; Gall et al. 2016). It has been proposed that the stimulation triggers neuronal entrainment of endogenous oscillations or a synchronous activation of RGCs, which induces the strengthening of synaptic transmission through long-term potentiation-like mechanisms, which then in turn enhances visual perception (Sabel, Thut, et al. 2020).

Clinical studies exclusively examining the effects of rtACS as an interventional approach in patients with acute autoimmune ON, however, are not yet available. Based on the previous research summarized above, we speculate that the hostile milieu that provokes the RGCs to undergo cell death in acute ON could be partially counteracted through effects of rtACS if applied within a critical time window after the onset of symptoms.

To test this hypothesis, we have designed the *ACSON* (alternating current stimulation in optic neuritis) trial, a phase I/IIa pilot study, which we deem appropriate to assess the safety, tolerability, and preliminary efficacy of rtACS as a treatment for patients with an episode of acute autoimmune ON (trial registration on ClinicalTrials.gov [NCT03862313](https://clinicaltrials.gov/ct2/show/study/NCT03862313) and kofam [SNCTP000003201](https://clinicaltrials.gov/ct2/show/study/SNCTP000003201)).

To fulfill eligibility criteria, patients must present with a first-ever episode of unilateral acute ON resulting in a HCVA of 0.63 or worse (Snellen decimal) in the affected eye. Moreover, patients must present in clinics within 14 days of symptom onset. Exclusion criteria will include, but are not limited to, the presence of retinal pathology other than that associated with ON and the existence of contraindications for the electric stimulation.

In addition to standard-of-care corticosteroid treatment, patients will receive 10-days of active- or sham- rtACS treatment, using a proprietary approach from Neuromodtronic GmbH, (previously named EBS Technologies GMBH, Germany), which is commercially available since 2014 (Antal et al. 2017).

In order to assess safety, the number of adverse events will be ascertained on a regular basis using a structured safety interview. LCVA will be used as the primary functional outcome measure to investigate if rtACS has a favourable impact on functional recovery following ON. To address if the extent of RGC damage can be attenuated by rtACS, the OCT-derived thickness-change of the macular GCIP will be used as the primary structural outcome measure. To gain more insight on possible effects of rtACS on the main pathological processes involved in ON-related persistent visual damage, a number of secondary outcome measures have been added to the study protocol. For instance, in order to address a potential effect on remyelination, the extent of the recovery of the VEP latency following ON will be analysed. Because the ultimate goal is the improvement of patients QoL, also patient-reported visual QoL will be obtained. Demonstrating safety and neuroprotective and -regenerative effects of a novel, non-pharmacological treatment in ON would be a major breakthrough.

6.5 Concluding remarks

Taken together, the AVP is involved frequently in MS and is functionally highly relevant for patients. The AVP in ON may serve as a model to translationally investigate the development of an individual inflammatory demyelinating MS lesion, its consequences on tissue integrity, and the effect of treatments on these processes. Despite previous efforts, it remains the case that no effective treatments for the prevention of permanent visual disability following an episode of ON exist, a clear unmet medical need.

References

- Abalo-Lojo, J. M., C. C. Limeres, M. A. Gomez, S. Baleato-Gonzalez, C. Cadarso-Suarez, C. Capeans-Tome, and F. Gonzalez. 2014. 'Retinal nerve fiber layer thickness, brain atrophy, and disability in multiple sclerosis patients', *J Neuroophthalmol*, 34: 23-8.
- Abalo-Lojo, J. M., A. Treus, M. Arias, F. Gomez-Ulla, and F. Gonzalez. 2017. 'Longitudinal study of retinal nerve fiber layer thickness changes in a multiple sclerosis patients cohort: A long term 5 year follow-up', *Mult Scler Relat Disord*, 19: 124-28.
- Abd Hamid, A. I., C. Gall, O. Speck, A. Antal, and B. A. Sabel. 2015. 'Effects of alternating current stimulation on the healthy and diseased brain', *Front Neurosci*, 9: 391.
- Aktas, O., P. Albrecht, and H. P. Hartung. 2016. 'Optic neuritis as a phase 2 paradigm for neuroprotection therapies of multiple sclerosis: update on current trials and perspectives', *Curr Opin Neurol*, 29: 199-204.
- Al-Louzi, O. A., P. Bhargava, S. D. Newsome, L. J. Balcer, E. M. Frohman, C. Crainiceanu, P. A. Calabresi, and S. Saidha. 2016. 'Outer retinal changes following acute optic neuritis', *Mult Scler*, 22: 362-72.
- Antal, A., and W. Paulus. 2013. 'Transcranial alternating current stimulation (tACS)', *Frontiers in Human Neuroscience*, 7: 317.
- Antal, A., and C. S. Herrmann. 2016. 'Transcranial Alternating Current and Random Noise Stimulation: Possible Mechanisms', *Neural Plast*, 2016: 3616807.
- Antal, A., I. Alekseichuk, M. Bikson, J. Brockmoller, A. R. Brunoni, R. Chen, L. G. Cohen, G. Dowthwaite, J. Ellrich, A. Floel, F. Fregni, M. S. George, R. Hamilton, J. Haueisen, C. S. Herrmann, F. C. Hummel, J. P. Lefaucheur, D. Liebetanz, C. K. Loo, C. D. McCaig, C. Miniussi, P. C. Miranda, V. Moliadze, M. A. Nitsche, R. Nowak, F. Padberg, A. Pascual-Leone, W. Poppendieck, A. Priori, S. Rossi, P. M. Rossini, J. Rothwell, M. A. Rueger, G. Ruffini, K. Schellhorn, H. R. Siebner, Y. Ugawa, A. Wexler, U. Ziemann, M. Hallett, and W. Paulus. 2017. 'Low intensity transcranial electric stimulation: Safety, ethical, legal regulatory and application guidelines', *Clin Neurophysiol*, 128: 1774-809.
- Ascherio, A., and K. L. Munger. 2007a. 'Environmental risk factors for multiple sclerosis. Part II: Noninfectious factors', *Ann Neurol*, 61: 504-13.
- . 2007b. 'Environmental risk factors for multiple sclerosis. Part I: the role of infection', *Ann Neurol*, 61: 288-99.
- . 2016. 'Epidemiology of Multiple Sclerosis: From Risk Factors to Prevention-An Update', *Semin Neurol*, 36: 103-14.
- Aung, W. Y., S. Mar, and T. L. Benzinger. 2013. 'Diffusion tensor MRI as a biomarker in axonal and myelin damage', *Imaging Med*, 5: 427-40.
- Ayache, S. S., and M. A. Chalah. 2016. 'Stem Cells Therapy in Multiple Sclerosis - A New Hope for Progressive Forms', *J Stem Cells Regen Med*, 12: 49-51.
- Backner, Y., J. Kuchling, S. Massarwa, T. Oberwahrenbrock, C. Finke, J. Bellmann-Strobl, K. Ruprecht, A. U. Brandt, H. Zimmermann, N. Raz, F. Paul, and N. Levin. 2018. 'Anatomical Wiring and Functional Networking Changes in the Visual System Following Optic Neuritis', *JAMA Neurol*.
- Backner, Y., I. Ben-Shalom, J. Kuchling, N. Siebert, M. Scheel, K. Ruprecht, A. Brandt, F. Paul, and N. Levin. 2020. 'Cortical topological network changes following optic neuritis', *Neurol Neuroimmunol Neuroinflamm*, 7.
- Balcer, L. J., M. L. Baier, A. M. Kunkle, R. A. Rudick, B. Weinstock-Guttman, N. Simonian, S. L. Galetta, G. R. Cutter, and M. G. Maguire. 2000. 'Self-reported visual dysfunction in multiple sclerosis: results from the 25-Item National Eye Institute Visual Function Questionnaire (VFQ-25)', *Mult Scler*, 6: 382-5.
- Balcer, L. J., D. H. Miller, S. C. Reingold, and J. A. Cohen. 2015. 'Vision and vision-related outcome measures in multiple sclerosis', *Brain*, 138: 11-27.
- Balcer, Laura J., Jenelle Raynowska, Rachel Nolan, Steven L. Galetta, Raju Kapoor, Ralph Benedict, Glenn Phillips, Nicholas LaRocca, Lynn Hudson, and Richard Rudick. 2017. 'Validity of low-contrast letter acuity as a visual performance outcome measure for multiple sclerosis', *Multiple Sclerosis Journal*: 1352458517690822.

References

- Balk, L. J., J. W. Twisk, M. D. Steenwijk, M. Daams, P. Tewarie, J. Killestein, B. M. Uitdehaag, C. H. Polman, and A. Petzold. 2014. 'A dam for retrograde axonal degeneration in multiple sclerosis?', *J Neurol Neurosurg Psychiatry*, 85: 782-9.
- Balk, L. J., A. Cruz-Herranz, P. Albrecht, S. Arnow, J. M. Gelfand, P. Tewarie, J. Killestein, B. M. Uitdehaag, A. Petzold, and A. J. Green. 2016. 'Timing of retinal neuronal and axonal loss in MS: a longitudinal OCT study', *J Neurol*, 263: 1323-31.
- Balk, L. J., D. Coric, B. Knier, H. G. Zimmermann, R. Behbehani, R. Alroughani, E. H. Martinez-Lapiscina, A. U. Brandt, B. Sanchez-Dalmau, A. Vidal-Jordana, P. Albrecht, V. Koska, J. Havla, M. Pisa, R. C. Nolan, L. Leocani, F. Paul, O. Aktas, X. Montalban, L. J. Balcer, P. Villoslada, O. Outteryck, T. Korn, and A. Petzold. 2019. 'Retinal inner nuclear layer volume reflects inflammatory disease activity in multiple sclerosis; a longitudinal OCT study', *Mult Scler J Exp Transl Clin*, 5: 2055217319871582.
- Barres, B. A., and M. C. Raff. 1993. 'Proliferation of oligodendrocyte precursor cells depends on electrical activity in axons', *Nature*, 361: 258-60.
- Barton, Joshua L., Justin Y. Garber, Alexander Klistorner, and Michael H. Barnett. 2019. 'The electrophysiological assessment of visual function in Multiple Sclerosis', *Clinical neurophysiology practice*, 4: 90-96.
- Battleday, Ruairidh M., Timothy Muller, Michael S. Clayton, and Roi Cohen Kadosh. 2014. 'Mapping the mechanisms of transcranial alternating current stimulation: a pathway from network effects to cognition', *Bacteriologia, Virusologia, Parazitologia, Epidemiologia (Bucur.)*, 5: 162-62.
- Beck, R. W., P. A. Cleary, M. M. Anderson, Jr., J. L. Keltner, W. T. Shults, D. I. Kaufman, E. G. Buckley, J. J. Corbett, M. J. Kupersmith, N. R. Miller, and et al. 1992. 'A randomized, controlled trial of corticosteroids in the treatment of acute optic neuritis. The Optic Neuritis Study Group.', *N Engl J Med*, 326: 581-8.
- Beck, R. W., and P. A. Cleary. 1993. 'Optic neuritis treatment trial. One-year follow-up results', *Arch Ophthalmol*, 111: 773-5.
- Beck, R. W., and R. L. Gal. 2008. 'Treatment of acute optic neuritis: A summary of findings from the optic neuritis treatment trial', *Archives of Ophthalmology*, 126: 994-95.
- Bennett, J. L., J. de Seze, M. Lana-Peixoto, J. Palace, A. Waldman, S. Schippling, S. Tenenbaum, B. Banwell, B. Greenberg, M. Levy, K. Fujihara, K. H. Chan, H. J. Kim, N. Asgari, D. K. Sato, A. Saiz, J. Wuerfel, H. Zimmermann, A. Green, P. Villoslada, and F. Paul. 2015. 'Neuromyelitis optica and multiple sclerosis: Seeing differences through optical coherence tomography', *Mult Scler*, 21: 678-88.
- Bennett, J. L., M. Nickerson, F. Costello, R. C. Sergott, J. C. Calkwood, S. L. Galetta, L. J. Balcer, C. E. Markowitz, T. Vartanian, M. Morrow, M. L. Moster, A. W. Taylor, T. W. Pace, T. Frohman, and E. M. Frohman. 2015. 'Re-evaluating the treatment of acute optic neuritis', *J Neurol Neurosurg Psychiatry*, 86: 799-808.
- Bermel, R. A., and P. Villoslada. 2014. 'Retrograde trans-synaptic degeneration in MS: a missing link?', *Neurology*, 82: 2152-3.
- Bikson, M., P. Grossman, C. Thomas, A. L. Zannou, J. Jiang, T. Adnan, A. P. Mourdoukoutas, G. Kronberg, D. Truong, P. Boggio, A. R. Brunoni, L. Charvet, F. Fregni, B. Fritsch, B. Gillick, R. H. Hamilton, B. M. Hampstead, R. Jankord, A. Kirton, H. Knotkova, D. Liebetanz, A. Liu, C. Loo, M. A. Nitsche, J. Reis, J. D. Richardson, A. Rotenberg, P. E. Turkeltaub, and A. J. Woods. 2016. 'Safety of Transcranial Direct Current Stimulation: Evidence Based Update 2016', *Brain Stimul*, 9: 641-61.
- Bikson, M., Z. Esmaeilpour, D. Adair, G. Kronberg, W. J. Tyler, A. Antal, A. Datta, B. A. Sabel, M. A. Nitsche, C. Loo, D. Edwards, H. Ekhtiari, H. Knotkova, A. J. Woods, B. M. Hampstead, B. W. Badran, and A. V. Peterchev. 2019. 'Transcranial electrical stimulation nomenclature', *Brain Stimul*, 12: 1349-66.
- Bittner, Stefan, Ali M. Afzali, Heinz Wiendl, and Sven G. Meuth. 2014. 'Myelin oligodendrocyte glycoprotein (MOG35-55) induced experimental autoimmune encephalomyelitis (EAE) in C57BL/6 mice', *J Vis Exp*: 51275.
- Bjartmar, C., J. R. Wujek, and B. D. Trapp. 2003. 'Axonal loss in the pathology of MS: consequences for understanding the progressive phase of the disease', *J Neurol Sci*, 206: 165-71.

References

- Bogosian, A., A. Hughes, S. Norton, E. Silber, and R. Moss-Morris. 2016. 'Potential treatment mechanisms in a mindfulness-based intervention for people with progressive multiple sclerosis', *Br J Health Psychol*.
- Bola, M., C. Gall, C. Moewes, A. Fedorov, H. Hinrichs, and B. A. Sabel. 2014. 'Brain functional connectivity network breakdown and restoration in blindness', *Neurology*, 83: 542-51.
- Bouwmeester, L., J. Heutink, and C. Lucas. 2007. 'The effect of visual training for patients with visual field defects due to brain damage: a systematic review', *J Neurol Neurosurg Psychiatry*, 78: 555-64.
- Brambilla, R. 2019. 'The contribution of astrocytes to the neuroinflammatory response in multiple sclerosis and experimental autoimmune encephalomyelitis', *Acta Neuropathol*, 137: 757-83.
- Brandt, Alexander U., Svenja Specovius, Timm Oberwahrenbrock, Hanna G. Zimmermann, Friedemann Paul, and Fiona Costello. 2018. 'Frequent retinal ganglion cell damage after acute optic neuritis', *Mult Scler Relat Disord*, 22: 141-47.
- Brooks, D. E., A. M. Komáromy, and M. E. Källberg. 1999. 'Comparative retinal ganglion cell and optic nerve morphology', *Veterinary Ophthalmology*, 2: 3-11.
- Brown, D. A., and P. E. Sawchenko. 2007. 'Time course and distribution of inflammatory and neurodegenerative events suggest structural bases for the pathogenesis of experimental autoimmune encephalomyelitis', *J Comp Neurol*, 502: 236-60.
- Bruce, C. C., C. Zhao, and R. J. Franklin. 2010. 'Remyelination - An effective means of neuroprotection', *Horm Behav*, 57: 56-62.
- Burman, J., R. Raininko, and J. Fagius. 2011. 'Bilateral and recurrent optic neuritis in multiple sclerosis', *Acta Neurol Scand*, 123: 207-10.
- Burrows, David John, Alexander McGown, Saurabh A Jain, Milena De Felice, Tennore M Ramesh, Basil Sharrack, and Arshad Majid. 2019. 'Animal models of multiple sclerosis: From rodents to zebrafish', *Multiple Sclerosis Journal*, 25: 306-24.
- Burton, J. M., M. Eliasziw, J. Trufyn, C. Tung, G. Carter, and F. Costello. 2017. 'A prospective cohort study of vitamin D in optic neuritis recovery', *Mult Scler*, 23: 82-93.
- Buzsaki, G., and B. O. Watson. 2012. 'Brain rhythms and neural syntax: implications for efficient coding of cognitive content and neuropsychiatric disease', *Dialogues in Clinical Neuroscience*, 14: 345-67.
- Calabrese, M., M. Atzori, V. Bernardi, A. Morra, C. Romualdi, L. Rinaldi, M. J. McAuliffe, L. Barachino, P. Perini, B. Fischl, L. Battistin, and P. Gallo. 2007. 'Cortical atrophy is relevant in multiple sclerosis at clinical onset', *J Neurol*, 254: 1212-20.
- Calabrese, M., R. Magliozzi, O. Ciccarelli, J. J. Geurts, R. Reynolds, and R. Martin. 2015. 'Exploring the origins of grey matter damage in multiple sclerosis', *Nat Rev Neurosci*, 16: 147-58.
- Calabresi, Peter A., Laura J. Balcer, and eds. Elliot M. Frohman. 2015. *Optical Coherence Tomography in Neurologic Diseases* (Cambridge University Press).
- Chalupa, Leo M., and Robert W. Williams (Eds.). 2008. *Eye, retina, and visual system of the mouse* (MIT Press: Cambridge, MA, US).
- Chiang, C. W., Y. Wang, P. Sun, T. H. Lin, K. Trinkaus, A. H. Cross, and S. K. Song. 2014. 'Quantifying white matter tract diffusion parameters in the presence of increased extra-fiber cellularity and vasogenic edema', *Neuroimage*, 101: 310-9.
- Constantinescu, Cris S., Nasr Farooqi, Kate O'Brien, and Bruno Gran. 2011. 'Experimental autoimmune encephalomyelitis (EAE) as a model for multiple sclerosis (MS)', *British Journal of Pharmacology*, 164: 1079-106.
- Coric, Danko, Lisanne J. Balk, Merike Verrijp, Anand Eijlers, Menno M. Schoonheim, Joep Killestein, Bernard M. J. Uitdehaag, and Axel Petzold. 2017. 'Cognitive impairment in patients with multiple sclerosis is associated with atrophy of the inner retinal layers', *Multiple Sclerosis Journal*: 1352458517694090.
- Costello, F., S. Coupland, W. Hodge, G. R. Lorello, J. Koroluk, Y. I. Pan, M. S. Freedman, D. H. Zackon, and R. H. Kardon. 2006. 'Quantifying axonal loss after optic neuritis with optical coherence tomography', *Ann Neurol*, 59: 963-9.
- Costello, F., W. Hodge, Y. I. Pan, J. M. Burton, M. S. Freedman, P. K. Stys, J. Trufyn, and R. Kardon. 2012. 'Sex-specific differences in retinal nerve fiber layer thinning after acute optic neuritis', *Neurology*, 79: 1866-72.
- Costello, F. 2013. 'The afferent visual pathway: designing a structural-functional paradigm of multiple sclerosis', *ISRN Neurol*, 2013: 134858.

References

- Costello, F., Y. I. Pan, E. A. Yeh, W. Hodge, J. M. Burton, and R. Kardon. 2015. 'The temporal evolution of structural and functional measures after acute optic neuritis', *J Neurol Neurosurg Psychiatry*, 86: 1369-73.
- Costello, F. 2016. 'Vision Disturbances in Multiple Sclerosis', *Semin Neurol*, 36: 185-95.
- Cruz-Herranz, A., L. J. Balk, T. Oberwahrenbrock, S. Saidha, E. H. Martinez-Lapiscina, W. A. Lagreze, J. S. Schuman, P. Villoslada, P. Calabresi, L. Balcer, A. Petzold, A. J. Green, F. Paul, A. U. Brandt, and P. Albrecht. 2016. 'The APOSTEL recommendations for reporting quantitative optical coherence tomography studies', *Neurology*, 86: 2303-9.
- Cunha-Vaz, J., R. Bernardes, and C. Lobo. 2011. 'Blood-retinal barrier', *Eur J Ophthalmol*, 21 Suppl 6: S3-9.
- de Faria, Omar, Jr., David G. Gonsalvez, Madeline Nicholson, and Junhua Xiao. 2019. 'Activity-dependent central nervous system myelination throughout life', *Journal of Neurochemistry*, 148: 447-61.
- Demerens, C., B. Stankoff, M. Logak, P. Anglade, B. Allinquant, F. Couraud, B. Zalc, and C. Lubetzki. 1996. 'Induction of myelination in the central nervous system by electrical activity', *Proceedings of the National Academy of Sciences of the United States of America*, 93: 9887-92.
- Devin D. MacKay, Steven L. Galetta, Sashank Prasad, Devin D. MacKay, Steven L. Galetta, and Sashank Prasad. 2015. *Anatomy of the anterior visual pathway Optical Coherence Tomography in Neurologic Diseases* (Cambridge University Press).
- Diem, R., A. Tschirne, and M. Bähr. 2003. 'Decreased amplitudes in multiple sclerosis patients with normal visual acuity: a VEP study', *Journal of Clinical Neuroscience*, 10: 67-70.
- Dietrich, M., O. Aktas, H. P. Hartung, and P. Albrecht. 2019. 'Assessing the anterior visual pathway in optic neuritis: recent experimental and clinical aspects', *Curr Opin Neurol*.
- Dobson, R., and G. Giovannoni. 2019. 'Multiple sclerosis - a review', *Eur J Neurol*, 26: 27-40.
- Dundon, N. M., C. Bertini, E. Ladavas, B. A. Sabel, and C. Gall. 2015. 'Visual rehabilitation: visual scanning, multisensory stimulation and vision restoration trainings', *Front Behav Neurosci*, 9: 192.
- Erskine, L., and E. Herrera. 2014. 'Connecting the retina to the brain', *ASN Neuro*, 6.
- Fawcett, James W., and Dennis D. M. O'Leary. 1985. 'The role of electrical activity in the formation of topographic maps in the nervous system', *Trends in Neurosciences*, 8: 201-06.
- Fedorov, A., Y. Chibisova, A. Szymaszek, M. Alexandrov, C. Gall, and B. A. Sabel. 2010. 'Non-invasive alternating current stimulation induces recovery from stroke', *Restor Neurol Neurosci*, 28: 825-33.
- Fedorov, A., S. Jobke, V. Bersnev, A. Chibisova, Y. Chibisova, C. Gall, and B. A. Sabel. 2011. 'Restoration of vision after optic nerve lesions with noninvasive transorbital alternating current stimulation: a clinical observational study', *Brain Stimul*, 4: 189-201.
- Ferris, F. L., 3rd, A. Kassoff, G. H. Bresnick, and I. Bailey. 1982. 'New visual acuity charts for clinical research', *American Journal of Ophthalmology*, 94: 91-6.
- Fertonani, A., C. Ferrari, and C. Miniussi. 2015. 'What do you feel if I apply transcranial electric stimulation? Safety, sensations and secondary induced effects', *Clin Neurophysiol*, 126: 2181-8.
- Fields, R. Douglas. 2015. 'A new mechanism of nervous system plasticity: activity-dependent myelination', *Nature reviews. Neuroscience*, 16: 756-67.
- Findling, O., M. Baltisberger, S. Jung, C. P. Kamm, H. P. Mattle, and J. Sellner. 2015. 'Variables related to working capability among Swiss patients with multiple sclerosis--a cohort study', *PLoS One*, 10: e0121856.
- Fischer, M. T., R. Sharma, J. L. Lim, L. Haider, J. M. Frischer, J. Drexhage, D. Mahad, M. Bradl, J. van Horssen, and H. Lassmann. 2012. 'NADPH oxidase expression in active multiple sclerosis lesions in relation to oxidative tissue damage and mitochondrial injury', *Brain*, 135: 886-99.
- Fischer, M. T., I. Wimmer, R. Hoftberger, S. Gerlach, L. Haider, T. Zrzavy, S. Hametner, D. Mahad, C. J. Binder, M. Krumbholz, J. Bauer, M. Bradl, and H. Lassmann. 2013. 'Disease-specific molecular events in cortical multiple sclerosis lesions', *Brain*, 136: 1799-815.
- Fisher, E., J. C. Lee, K. Nakamura, and R. A. Rudick. 2008. 'Gray matter atrophy in multiple sclerosis: a longitudinal study', *Ann Neurol*, 64: 255-65.

References

- Forooghian, F., C. Cukras, C. B. Meyerle, E. Y. Chew, and W. T. Wong. 2008. 'Evaluation of time domain and spectral domain optical coherence tomography in the measurement of diabetic macular edema', *Invest Ophthalmol Vis Sci*, 49: 4290-6.
- Franklin, R. J., and C. Ffrench-Constant. 2008. 'Remyelination in the CNS: from biology to therapy', *Nat Rev Neurosci*, 9: 839-55.
- Franklin, Robin J. M., Charles Ffrench-Constant, Julia M. Edgar, and Kenneth J. Smith. 2012. 'Neuroprotection and repair in multiple sclerosis', *Nature Reviews Neurology*, 8: 624-34.
- Friese, M. A., B. Schattling, and L. Fugger. 2014. 'Mechanisms of neurodegeneration and axonal dysfunction in multiple sclerosis', *Nat Rev Neurol*, 10: 225-38.
- Fröhlich, Flavio. 2015. 'Chapter 3 - Experiments and models of cortical oscillations as a target for noninvasive brain stimulation.' in Sven Bestmann (ed.), *Progress in Brain Research* (Elsevier).
- Frohman, E. M., J. G. Fujimoto, T. C. Frohman, P. A. Calabresi, G. Cutter, and L. J. Balcer. 2008. 'Optical coherence tomography: a window into the mechanisms of multiple sclerosis', *Nat Clin Pract Neurol*, 4: 664-75.
- Frohman, E. M., M. G. Dwyer, T. Frohman, J. L. Cox, A. Salter, B. M. Greenberg, S. Hussein, A. Conger, P. Calabresi, L. J. Balcer, and R. Zivadinov. 2009. 'Relationship of optic nerve and brain conventional and non-conventional MRI measures and retinal nerve fiber layer thickness, as assessed by OCT and GDx: a pilot study', *J Neurol Sci*, 282: 96-105.
- Fu, L., A. C. Lo, J. S. Lai, and K. C. Shih. 2015. 'The role of electrical stimulation therapy in ophthalmic diseases', *Graefes Arch Clin Exp Ophthalmol*, 253: 171-6.
- Fu, Peng, and Quan Hu. 2016. '3,4-Dihydroxyphenylethanol alleviates early brain injury by modulating oxidative stress and Akt and nuclear factor- κ B pathways in a rat model of subarachnoid hemorrhage', *Experimental and Therapeutic Medicine*, 11: 1999-2004.
- Gabilondo, I., E. H. Martinez-Lapiscina, E. Martinez-Heras, E. Fraga-Pumar, S. Llufriu, S. Ortiz, S. Bullich, M. Sepulveda, C. Falcon, J. Berenguer, A. Saiz, B. Sanchez-Dalmau, and P. Villoslada. 2014. 'Trans-synaptic axonal degeneration in the visual pathway in multiple sclerosis', *Ann Neurol*, 75: 98-107.
- Gabilondo, I., E. H. Martinez-Lapiscina, E. Fraga-Pumar, S. Ortiz-Perez, R. Torres-Torres, M. Andorra, S. Llufriu, I. Zubizarreta, A. Saiz, B. Sanchez-Dalmau, and P. Villoslada. 2015. 'Dynamics of retinal injury after acute optic neuritis', *Ann Neurol*, 77: 517-28.
- Gall, C., A. B. Fedorov, L. Ernst, A. Borrmann, and B. A. Sabel. 2010. 'Repetitive transorbital alternating current stimulation in optic neuropathy', *NeuroRehabilitation*, 27: 335-41.
- Gall, C., S. Sgorzaly, S. Schmidt, S. Brandt, A. Fedorov, and B. A. Sabel. 2011. 'Noninvasive transorbital alternating current stimulation improves subjective visual functioning and vision-related quality of life in optic neuropathy', *Brain Stimul*, 4: 175-88.
- Gall, C., P. M. Rossini, T. Tatlisumak, W. Waleszczyk, D. Broesel, and B. A. Sabel. 2014. 'O26: Non-invasive alternating current stimulation to improve visual impairment after post-chiasmatic lesions', *Clinical Neurophysiology*, 125: S36.
- Gall, C., K. Silvennoinen, G. Granata, F. de Rossi, F. Vecchio, D. Brosel, M. Bola, M. Sailer, W. J. Waleszczyk, P. M. Rossini, T. Tatlisumak, and B. A. Sabel. 2015. 'Non-invasive electric current stimulation for restoration of vision after unilateral occipital stroke', *Contemp Clin Trials*, 43: 231-6.
- Gall, C., S. Schmidt, M. P. Schittkowski, A. Antal, G. G. Ambrus, W. Paulus, M. Dannhauer, R. Michalik, A. Mante, M. Bola, A. Lux, S. Kropf, S. A. Brandt, and B. A. Sabel. 2016. 'Alternating Current Stimulation for Vision Restoration after Optic Nerve Damage: A Randomized Clinical Trial', *PLoS One*, 11: e0156134.
- Gallo, A., F. Esposito, R. Sacco, R. Docimo, A. Bisecco, M. Della Corte, A. D'Ambrosio, D. Corbo, N. Rosa, M. Lanza, S. Cirillo, S. Bonavita, and G. Tedeschi. 2012. 'Visual resting-state network in relapsing-remitting MS with and without previous optic neuritis', *Neurology*, 79: 1458-65.
- Garcia-Martin, E., D. Rodriguez-Mena, R. Herrero, C. Almarcegui, I. Dolz, J. Martin, J. R. Ara, J. M. Larrosa, V. Polo, J. Fernandez, and L. E. Pablo. 2013. 'Neuro-ophthalmologic evaluation, quality of life, and functional disability in patients with MS', *Neurology*, 81: 76-83.
- Gautier, H. O., K. A. Evans, K. Volbracht, R. James, S. Sitnikov, I. Lundgaard, F. James, C. Lao-Peregrin, R. Reynolds, R. J. Franklin, and R. T. Karadottir. 2015. 'Neuronal activity regulates remyelination via glutamate signalling to oligodendrocyte progenitors', *Nat Commun*, 6: 8518.

References

- Gelfand, J. M., R. Nolan, D. M. Schwartz, J. Graves, and A. J. Green. 2012. 'Microcystic macular oedema in multiple sclerosis is associated with disease severity', *Brain*, 135: 1786-93.
- Gelfand, J. M., B. A. Cree, R. Nolan, S. Arnow, and A. J. Green. 2013. 'Microcystic inner nuclear layer abnormalities and neuromyelitis optica', *JAMA Neurol*, 70: 629-33.
- Gibson, E. M., D. Purger, C. W. Mount, A. K. Goldstein, G. L. Lin, L. S. Wood, I. Inema, S. E. Miller, G. Bieri, J. B. Zuchero, B. A. Barres, P. J. Woo, H. Vogel, and M. Monje. 2014. 'Neuronal activity promotes oligodendrogenesis and adaptive myelination in the mammalian brain', *Science*, 344: 1252304.
- Gordon-Lipkin, E., B. Chodkowski, D. S. Reich, S. A. Smith, M. Pulicken, L. J. Balcer, E. M. Frohman, G. Cutter, and P. A. Calabresi. 2007. 'Retinal nerve fiber layer is associated with brain atrophy in multiple sclerosis', *Neurology*, 69: 1603-9.
- Goverman, Joan. 2009. 'Autoimmune T cell responses in the central nervous system', *Nature reviews. Immunology*, 9: 393-407.
- Green, A. J., S. McQuaid, S. L. Hauser, I. V. Allen, and R. Lyness. 2010. 'Ocular pathology in multiple sclerosis: retinal atrophy and inflammation irrespective of disease duration', *Brain*, 133: 1591-601.
- Haberbosch, L., S. Schmidt, A. Jooss, A. Kohn, L. Kozarzewski, M. Ronnefarth, M. Scholz, and S. A. Brandt. 2019. 'Rebound or Entrainment? The Influence of Alternating Current Stimulation on Individual Alpha', *Frontiers in Human Neuroscience*, 13: 43.
- Haberbosch, Linus, Abhishek Datta, Chris Thomas, Andreas Jooß, Arvid Köhn, Maria Rönnefarth, Michael Scholz, Stephan A. Brandt, and Sein Schmidt. 2019. 'Safety Aspects, Tolerability and Modeling of Retinofugal Alternating Current Stimulation', *Frontiers in Neuroscience*, 13.
- Hanif, A. M., M. K. Kim, J. G. Thomas, V. T. Ciavatta, M. Chrenek, J. R. Hetling, and M. T. Pardue. 2016. 'Whole-eye electrical stimulation therapy preserves visual function and structure in P23H-1 rats', *Exp Eye Res*, 149: 75-83.
- Hanson, J. V., S. C. Lukas, M. Pless, and S. Schippling. 2016. 'Optical Coherence Tomography in Multiple Sclerosis', *Semin Neurol*, 36: 177-84.
- Hanson, J. V. M., M. Hediger, P. Manogaran, K. Landau, N. Hagenbuch, S. Schippling, and C. Gerth-Kahlert. 2018. 'Outer Retinal Dysfunction in the Absence of Structural Abnormalities in Multiple Sclerosis', *Invest Ophthalmol Vis Sci*, 59: 549-60.
- Hanson, James V. M., Carla A. Wicki, Praveena Manogaran, Axel Petzold, and Sven Schippling. 2020. 'OCT and Multiple Sclerosis.' in Andrzej Grzybowski and Piero Barboni (eds.), *OCT and Imaging in Central Nervous System Diseases: The Eye as a Window to the Brain* (Springer International Publishing: Cham).
- Havla, J., T. Kumpf, R. Schinner, M. Spadaro, E. Schuh, E. Meinl, R. Hohlfeld, and O. Outteryck. 2017. 'Myelin-oligodendrocyte-glycoprotein (MOG) autoantibodies as potential markers of severe optic neuritis and subclinical retinal axonal degeneration', *J Neurol*, 264: 139-51.
- Hayreh, Sohan Singh. 2011. 'Blood-Optic Nerve Barrier.' in *Ischemic Optic Neuropathies* (Springer Berlin Heidelberg: Berlin, Heidelberg).
- Heesen, C., S. M. Gold, I. Huitinga, and J. M. Reul. 2007. 'Stress and hypothalamic-pituitary-adrenal axis function in experimental autoimmune encephalomyelitis and multiple sclerosis - a review', *Psychoneuroendocrinology*, 32: 604-18.
- Heesen, C., R. Haase, S. Melzig, J. Poettgen, M. Berghoff, F. Paul, U. Zettl, M. Marziniak, K. Angstwurm, R. Kern, T. Ziemssen, and J. P. Stellmann. 2018. 'Perceptions on the value of bodily functions in multiple sclerosis', *Acta Neurol Scand*, 137: 356-62.
- Heidari, Moones, Abigail B. Radcliff, Gillian J. McLellan, James N. Ver Hoeve, Kore Chan, Julie A. Kiland, Nicholas S. Keuler, Benjamin K. August, Dylan Sebo, Aaron S. Field, and Ian D. Duncan. 2019. 'Evoked potentials as a biomarker of remyelination', *Proceedings of the National Academy of Sciences*: 201906358.
- Helfrich, R. F., T. R. Schneider, S. Rach, S. A. Trautmann-Lengsfeld, A. K. Engel, and C. S. Herrmann. 2014. 'Entrainment of brain oscillations by transcranial alternating current stimulation', *Curr Biol*, 24: 333-9.
- Henderson, A. P., D. R. Altmann, A. S. Trip, C. Kallis, S. J. Jones, P. G. Schlottmann, D. F. Garway-Heath, G. T. Plant, and D. H. Miller. 2010. 'A serial study of retinal changes following optic neuritis with sample size estimates for acute neuroprotection trials', *Brain*, 133: 2592-602.

References

- Henrich-Noack, P., S. Lazik, E. Sergeeva, S. Wagner, N. Voigt, S. Prilloff, A. Fedorov, and B. A. Sabel. 2013. 'Transcorneal alternating current stimulation after severe axon damage in rats results in "long-term silent survivor" neurons', *Brain Res Bull*, 95: 7-14.
- Henrich-Noack, P., N. Voigt, S. Prilloff, A. Fedorov, and B. A. Sabel. 2013. 'Transcorneal electrical stimulation alters morphology and survival of retinal ganglion cells after optic nerve damage', *Neurosci Lett*, 543: 1-6.
- Henrich-Noack, P., E. G. Sergeeva, T. Eber, Q. You, N. Voigt, J. Kohler, S. Wagner, S. Lazik, C. Mawrin, G. Xu, S. Biswas, B. A. Sabel, and C. K. Leung. 2017. 'Electrical brain stimulation induces dendritic stripping but improves survival of silent neurons after optic nerve damage', *Sci Rep*, 7: 627.
- Henrich-Noack, P., E. G. Sergeeva, and B. A. Sabel. 2017. 'Non-invasive electrical brain stimulation: from acute to late-stage treatment of central nervous system damage', *Neural Regen Res*, 12: 1590-94.
- Henry, R. G., M. Shieh, D. T. Okuda, A. Evangelista, M. L. Gorno-Tempini, and D. Pelletier. 2008. 'Regional grey matter atrophy in clinically isolated syndromes at presentation', *J Neurol Neurosurg Psychiatry*, 79: 1236-44.
- Hickman, S. J., C. M. Dalton, D. H. Miller, and G. T. Plant. 2002. 'Management of acute optic neuritis', *The Lancet*, 360: 1953-62.
- Hickman, S. J., A. T. Toosy, K. A. Miszkiel, S. J. Jones, D. R. Altmann, D. G. MacManus, G. T. Plant, A. J. Thompson, and D. H. Miller. 2004. 'Visual recovery following acute optic neuritis--a clinical, electrophysiological and magnetic resonance imaging study', *J Neurol*, 251: 996-1005.
- Hirsch, J., and C. A. Curcio. 1989. 'The spatial resolution capacity of human foveal retina', *Vision Res*, 29: 1095-101.
- Hobom, M., M. K. Storch, R. Weissert, K. Maier, A. Radhakrishnan, B. Kramer, M. Bähr, and R. Diem. 2004. 'Mechanisms and time course of neuronal degeneration in experimental autoimmune encephalomyelitis', *Brain Pathology*, 14: 148-57.
- Hohlfeld, R., K. Dornmair, E. Meinl, and H. Wekerle. 2016. 'The search for the target antigens of multiple sclerosis, part 2: CD8+ T cells, B cells, and antibodies in the focus of reverse-translational research', *Lancet Neurol*, 15: 317-31.
- Horstmann, L., H. Schmid, A. P. Heinen, F. C. Kurschus, H. B. Dick, and S. C. Joachim. 2013. 'Inflammatory demyelination induces glia alterations and ganglion cell loss in the retina of an experimental autoimmune encephalomyelitis model', *J Neuroinflammation*, 10: 120.
- Huang, Y. Z., M. K. Lu, A. Antal, J. Classen, M. Nitsche, U. Ziemann, M. Ridding, M. Hamada, Y. Ugawa, S. Jaberzadeh, A. Suppa, W. Paulus, and J. Rothwell. 2017. 'Plasticity induced by non-invasive transcranial brain stimulation: A position paper', *Clin Neurophysiol*, 128: 2318-29.
- Hyvärinen, L., A. N. Raninen, and R. E. Näsänen. 2002. 'Vision rehabilitation in homonymous hemianopia', *Neuro-Ophthalmology*, 27: 97-102.
- Ibrahim, J. G., and G. Molenberghs. 2009. 'Missing data methods in longitudinal studies: a review', *Test (Madr)*, 18: 1-43.
- Ikuta, F., and H. M. Zimmerman. 1976. 'Distribution of plaques in seventy autopsy cases of multiple sclerosis in the United States', *Neurology*, 26: 26-8.
- Jarius, S., F. Paul, D. Franciotta, P. Waters, F. Zipp, R. Hohlfeld, A. Vincent, and B. Wildemann. 2008. 'Mechanisms of disease: aquaporin-4 antibodies in neuromyelitis optica', *Nat Clin Pract Neurol*, 4: 202-14.
- Jarius, S., K. Ruprecht, I. Kleiter, N. Borisow, N. Asgari, K. Pitarokoili, F. Pache, O. Stich, L. A. Beume, M. W. Hummert, M. Ringelstein, C. Trebst, A. Winkelmann, A. Schwarz, M. Buttman, H. Zimmermann, J. Kuchling, D. Franciotta, M. Capobianco, E. Siebert, C. Lukas, M. Korporal-Kuhnke, J. Haas, K. Fechner, A. U. Brandt, K. Schanda, O. Aktas, F. Paul, M. Reindl, and B. Wildemann. 2016. 'MOG-IgG in NMO and related disorders: a multicenter study of 50 patients. Part 2: Epidemiology, clinical presentation, radiological and laboratory features, treatment responses, and long-term outcome', *J Neuroinflammation*, 13: 280.
- Jelcic, I., J. V. M. Hanson, S. Lukas, K. P. Weber, K. Landau, M. Pless, M. Reindl, M. Weller, R. Martin, A. Lutterotti, and S. Schippling. 2019. 'Unfavorable Structural and Functional Outcomes in Myelin Oligodendrocyte Glycoprotein Antibody-Associated Optic Neuritis', *J Neuroophthalmol*, 39: 3-7.

References

- Jenkins, T. M., and A. T. Toosy. 2017. 'Optic neuritis: the eye as a window to the brain', *Curr Opin Neurol*, 30: 61-66.
- Kaczorowski, K., M. Mulak, D. Szumny, and M. Misiuk-Hojlo. 2015. 'Heidelberg Edge Perimeter: The New Method of Perimetry', *Adv Clin Exp Med*, 24: 1105-12.
- Kanai, R., L. Chaieb, A. Antal, V. Walsh, and W. Paulus. 2008. 'Frequency-dependent electrical stimulation of the visual cortex', *Curr Biol*, 18: 1839-43.
- Kasten, E., S. Wust, W. Behrens-Baumann, and B. A. Sabel. 1998. 'Computer-based training for the treatment of partial blindness', *Nat Med*, 4: 1083-7.
- Kasten, Florian H., James Dowsett, and Christoph S. Herrmann. 2016. 'Sustained Aftereffect of α -tACS Lasts Up to 70 min after Stimulation', *Frontiers in Human Neuroscience*, 10.
- Kilkenny, C., W. J. Browne, I. C. Cuthill, M. Emerson, and D. G. Altman. 2010. 'Improving bioscience research reporting: the ARRIVE guidelines for reporting animal research', *PLoS Biology*, 8: e1000412.
- Kim, J. S., H. Ishikawa, K. R. Sung, J. Xu, G. Wollstein, R. A. Bilonick, M. L. Gabriele, L. Kagemann, J. S. Duker, J. G. Fujimoto, and J. S. Schuman. 2009. 'Retinal nerve fibre layer thickness measurement reproducibility improved with spectral domain optical coherence tomography', *Br J Ophthalmol*, 93: 1057-63.
- Kingwell, E., J. J. Marriott, N. Jette, T. Pringsheim, N. Makhani, S. A. Morrow, J. D. Fisk, C. Evans, S. G. Beland, S. Kulaga, J. Dykeman, C. Wolfson, M. W. Koch, and R. A. Marrie. 2013. 'Incidence and prevalence of multiple sclerosis in Europe: a systematic review', *BMC Neurol*, 13: 128.
- Klimesch, W., P. Sauseng, and S. Hanslmayr. 2007. 'EEG alpha oscillations: the inhibition-timing hypothesis', *Brain Res Rev*, 53: 63-88.
- Klistorner, A., H. Arvind, T. Nguyen, R. Garrick, M. Paine, S. Graham, and C. Yiannikas. 2009. 'Fellow eye changes in optic neuritis correlate with the risk of multiple sclerosis', *Mult Scler*, 15: 928-32.
- Klistorner, A., H. Arvind, R. Garrick, C. Yiannikas, M. Paine, and S. L. Graham. 2010. 'Remyelination of optic nerve lesions: spatial and temporal factors', *Mult Scler*, 16: 786-95.
- Klistorner, A., P. Sriram, N. Vootakuru, C. Wang, M. H. Barnett, R. Garrick, J. Parratt, N. Levin, N. Raz, A. Van der Walt, L. Masters, S. L. Graham, and C. Yiannikas. 2014. 'Axonal loss of retinal neurons in multiple sclerosis associated with optic radiation lesions', *Neurology*, 82: 2165-72.
- Klistorner, A., Y. Chai, L. Leocani, P. Albrecht, O. Aktas, H. Butzkueven, T. Ziemssen, F. Ziemssen, J. Frederiksen, L. Xu, and D. Cadavid. 2018. 'Assessment of Opicinumab in Acute Optic Neuritis Using Multifocal Visual Evoked Potential', *CNS Drugs*, 32: 1159-71.
- Klistorner, A., C. Wang, C. Yiannikas, J. Parratt, M. Dwyer, J. Barton, S. L. Graham, Y. You, S. Liu, and M. H. Barnett. 2018. 'Evidence of progressive tissue loss in the core of chronic MS lesions: A longitudinal DTI study', *Neuroimage Clin*, 17: 1028-35.
- Knier, B., P. Schmidt, L. Aly, D. Buck, A. Berthele, M. Muhlau, C. Zimmer, B. Hemmer, and T. Korn. 2016. 'Retinal inner nuclear layer volume reflects response to immunotherapy in multiple sclerosis', *Brain*.
- Knier, B., G. Leppenhetier, C. Wetzlmair, L. Aly, M. M. Hoshi, V. Pernpeintner, V. Biberacher, A. Berthele, M. Muhlau, C. Zimmer, B. Hemmer, and T. Korn. 2017. 'Association of Retinal Architecture, Intrathecal Immunity, and Clinical Course in Multiple Sclerosis', *JAMA Neurol*.
- Koch, M., E. Kingwell, P. Rieckmann, and H. Tremlett. 2010. 'The natural history of secondary progressive multiple sclerosis', *J Neurol Neurosurg Psychiatry*, 81: 1039-43.
- Kolappan, M., A. P. Henderson, T. M. Jenkins, C. A. Wheeler-Kingshott, G. T. Plant, A. J. Thompson, and D. H. Miller. 2009. 'Assessing structure and function of the afferent visual pathway in multiple sclerosis and associated optic neuritis', *J Neurol*, 256: 305-19.
- Kolbe, S., C. Chapman, T. Nguyen, C. Bajraszewski, L. Johnston, M. Kean, P. Mitchell, M. Paine, H. Butzkueven, T. Kilpatrick, and G. Egan. 2009. 'Optic nerve diffusion changes and atrophy jointly predict visual dysfunction after optic neuritis', *Neuroimage*, 45: 679-86.
- Kollias, S. 2009. 'Parcelation of the White Matter Using DTI: Insights into the Functional Connectivity of the Brain', *The Neuroradiology Journal*, 22: 74-84.
- Kuchling, J., A. U. Brandt, F. Paul, and M. Scheel. 2017. 'Diffusion tensor imaging for multilevel assessment of the visual pathway: possibilities for personalized outcome prediction in autoimmune disorders of the central nervous system', *Epma j*, 8: 279-94.

References

- Kuhlmann, T., V. Miron, Q. Cui, C. Wegner, J. Antel, and W. Bruck. 2008. 'Differentiation block of oligodendroglial progenitor cells as a cause for remyelination failure in chronic multiple sclerosis', *Brain*, 131: 1749-58.
- Kupersmith, M. J., G. Mandel, S. Anderson, D. E. Meltzer, and R. Kardon. 2011. 'Baseline, one and three month changes in the peripapillary retinal nerve fiber layer in acute optic neuritis: relation to baseline vision and MRI', *J Neurol Sci*, 308: 117-23.
- Kupersmith, M. J., S. Anderson, and R. Kardon. 2013. 'Predictive value of 1 month retinal nerve fiber layer thinning for deficits at 6 months after acute optic neuritis', *Mult Scler*, 19: 1743-8.
- Kurimoto, T., S. Oono, H. Oku, Y. Tagami, R. Kashimoto, M. Takata, N. Okamoto, T. Ikeda, and O. Mimura. 2010. 'Transcorneal electrical stimulation increases chorioretinal blood flow in normal human subjects', *Clin Ophthalmol*, 4: 1441-6.
- Kurtzke, J. F. 1983. 'Rating neurologic impairment in multiple sclerosis: an expanded disability status scale (EDSS)', *Neurology*, 33: 1444-52.
- Lampert, E. J., M. Andorra, R. Torres-Torres, S. Ortiz-Perez, S. Llufrui, M. Sepulveda, N. Sola, A. Saiz, B. Sanchez-Dalmau, P. Villoslada, and E. H. Martinez-Lapiscina. 2015. 'Color vision impairment in multiple sclerosis points to retinal ganglion cell damage', *J Neurol*, 262: 2491-7.
- Lassmann, H., and J. van Horssen. 2016. 'Oxidative stress and its impact on neurons and glia in multiple sclerosis lesions', *Biochimica et Biophysica Acta*, 1862: 506-10.
- Li, Dan C., and Qun Li. 2017. 'Electrical stimulation of cortical neurons promotes oligodendrocyte development and remyelination in the injured spinal cord', *Neural Regeneration Research*, 12: 1613-15.
- Li, M., J. Li, H. He, Z. Wang, B. Lv, W. Li, N. Hailla, F. Yan, J. Xian, and L. Ai. 2011. 'Directional diffusivity changes in the optic nerve and optic radiation in optic neuritis', *The British journal of radiology*, 84: 304-14.
- London, A., I. Benhar, and M. Schwartz. 2013. 'The retina as a window to the brain-from eye research to CNS disorders', *Nat Rev Neurol*, 9: 44-53.
- Lubetzki, C., A. Williams, and B. Stankoff. 2005. 'Promoting repair in multiple sclerosis: problems and prospects', *Curr Opin Neurol*, 18: 237-44.
- Lubetzki, C., and B. Stankoff. 2014. 'Demyelination in multiple sclerosis', *Handb Clin Neurol*, 122: 89-99.
- Lubetzki, C., B. Zalc, A. Williams, C. Stadelmann, and B. Stankoff. 2020. 'Remyelination in multiple sclerosis: from basic science to clinical translation', *Lancet Neurol*, 19: 678-88.
- Lublin, F. D., S. C. Reingold, J. A. Cohen, G. R. Cutter, P. S. Sørensen, A. J. Thompson, J. S. Wolinsky, L. J. Balcer, B. Banwell, F. Barkhof, B. Bebo, P. A. Calabresi, M. Clanet, G. Comi, R. J. Fox, M. S. Freedman, A. D. Goodman, M. Inglese, L. Kappos, B. C. Kieseier, J. A. Lincoln, C. Lubetzki, A. E. Miller, X. Montalban, P. W. O'Connor, J. Petkau, C. Pozzilli, R. A. Rudick, M. P. Sormani, O. Stüve, E. Waubant, and C. H. Polman. 2014. 'Defining the clinical course of multiple sclerosis: The 2013 revisions', *Neurology*, 83: 278-86.
- Luessi, F., V. Siffrin, and F. Zipp. 2012. 'Neurodegeneration in multiple sclerosis: novel treatment strategies', *Expert Rev Neurother*, 12: 1061-76; quiz 77.
- Mahad, D. H., B. D. Trapp, and H. Lassmann. 2015. 'Pathological mechanisms in progressive multiple sclerosis', *Lancet Neurol*, 14: 183-93.
- Mahajan, Kedar R., and Daniel Ontaneda. 2017. 'The Role of Advanced Magnetic Resonance Imaging Techniques in Multiple Sclerosis Clinical Trials', *Neurotherapeutics*, 14: 905-23.
- Manogaran, P., C. Walker-Egger, M. Samardzija, C. Waschkies, C. Grimm, M. Rudin, and S. Schippling. 2018. 'Exploring experimental autoimmune optic neuritis using multimodal imaging', *Neuroimage*.
- Manogaran, Praveena, James Hanson, Elisabeth Olbert, Christine Egger, Carla Wicki, Christina Gerth-Kahlert, Klara Landau, and Sven Schippling. 2016. 'Optical Coherence Tomography and Magnetic Resonance Imaging in Multiple Sclerosis and Neuromyelitis Optica Spectrum Disorder', *International Journal of Molecular Sciences*, 17: 1894.
- Manogaran, Praveena, Marijana Samardzija, Anaïs Nura Schad, Carla Andrea Wicki, Christine Walker-Egger, Markus Rudin, Christian Grimm, and Sven Schippling. 2019. 'Retinal pathology in experimental optic neuritis is characterized by retrograde degeneration and gliosis', *Acta Neuropathologica Communications*, 7: 116.

References

- Martin, R., M. Sospedra, M. Rosito, and B. Engelhardt. 2016. 'Current multiple sclerosis treatments have improved our understanding of MS autoimmune pathogenesis', *European Journal of Immunology*, 46: 2078-90.
- Martinez-Lapiscina, E. H., B. Sanchez-Dalmau, E. Fraga-Pumar, S. Ortiz-Perez, A. I. Tercero-Urbe, R. Torres-Torres, and P. Villoslada. 2014. 'The visual pathway as a model to understand brain damage in multiple sclerosis', *Mult Scler*, 20: 1678-85.
- Martinez-Lapiscina, Elena H., Sam Arnow, James A. Wilson, Shiv Saidha, Jana Lizrova Preiningerova, Timm Oberwahrenbrock, Alexander U. Brandt, Luis E. Pablo, Simone Guerrieri, Ines Gonzalez, Olivier Outteryck, Ann-Kristin Mueller, Phillip Albrecht, Wesley Chan, Sebastian Lukas, Lisanne J. Balk, Clare Fraser, Jette L. Frederiksen, Jennifer Resto, Teresa Frohman, Christian Cordano, Irati Zubizarreta, Magi Andorra, Bernardo Sanchez-Dalmau, Albert Saiz, Robert Bermel, Alexander Klistorner, Axel Petzold, Sven Schippling, Fiona Costello, Orhan Aktas, Patrick Vermersch, Celia Oreja-Guevara, Giancarlo Comi, Letizia Leocani, Elena Garcia-Martin, Friedemann Paul, Eva Havrdova, Elliot Frohman, Laura J. Balcer, Ari J. Green, Peter A. Calabresi, and Pablo Villoslada. 2016. 'Retinal thickness measured with optical coherence tomography and risk of disability worsening in multiple sclerosis: a cohort study', *The Lancet Neurology*, 15: 574-84.
- May, C. A., and E. Lutjen-Drecoll. 2002. 'Morphology of the murine optic nerve', *Invest Ophthalmol Vis Sci*, 43: 2206-12.
- May, C. A. 2008. 'Comparative anatomy of the optic nerve head and inner retina in non-primate animal models used for glaucoma research', *Open Ophthalmol J*, 2: 94-101.
- McFarland, H. F., F. Barkhof, J. Antel, and D. H. Miller. 2002. 'The role of MRI as a surrogate outcome measure in multiple sclerosis', *Mult Scler*, 8: 40-51.
- McLean, N. A., B. F. Popescu, T. Gordon, D. W. Zochodne, and V. M. Verge. 2014. 'Delayed nerve stimulation promotes axon-protective neurofilament phosphorylation, accelerates immune cell clearance and enhances remyelination in vivo in focally demyelinated nerves', *PLoS One*, 9: e110174.
- Miller, D., F. Barkhof, X. Montalban, A. Thompson, and M. Filippi. 2005a. 'Clinically isolated syndromes suggestive of multiple sclerosis, part 2: non-conventional MRI, recovery processes, and management', *Lancet Neurol*, 4: 341-8.
- . 2005b. 'Clinically isolated syndromes suggestive of multiple sclerosis, part I: natural history, pathogenesis, diagnosis, and prognosis', *Lancet Neurol*, 4: 281-8.
- Miller, David H., Declan T. Chard, and Olga Ciccarelli. 2012. 'Clinically isolated syndromes', *The Lancet Neurology*, 11: 157-69.
- Miller, T. R., S. Mohan, A. F. Choudhri, D. Gandhi, and G. Jindal. 2014. 'Advances in multiple sclerosis and its variants: conventional and newer imaging techniques', *Radiol Clin North Am*, 52: 321-36.
- Miyake, Ken-ichiro, Miho Yoshida, Yoshitsugu Inoue, and Yoshio Hata. 2007. 'Neuroprotective Effect of Transcorneal Electrical Stimulation on the Acute Phase of Optic Nerve Injury', *Investigative Ophthalmology & Visual Science*, 48: 2356-61.
- Mori, S., and J. Zhang. 2006. 'Principles of diffusion tensor imaging and its applications to basic neuroscience research', *Neuron*, 51: 527-39.
- Morimoto, T., T. Miyoshi, T. Fujikado, Y. Tano, and Y. Fukuda. 2002. 'Electrical stimulation enhances the survival of axotomized retinal ganglion cells in vivo', *Neuroreport*, 13: 227-30.
- Morimoto, T., T. Miyoshi, S. Matsuda, Y. Tano, T. Fujikado, and Y. Fukuda. 2005. 'Transcorneal electrical stimulation rescues axotomized retinal ganglion cells by activating endogenous retinal IGF-1 system', *Invest Ophthalmol Vis Sci*, 46: 2147-55.
- Morimoto, T., T. Miyoshi, H. Sawai, and T. Fujikado. 2010. 'Optimal parameters of transcorneal electrical stimulation (TES) to be neuroprotective of axotomized RGCs in adult rats', *Exp Eye Res*, 90: 285-91.
- Morimoto, T., H. Kanda, T. Miyoshi, Y. Hirohara, T. Mihashi, Y. Kitaguchi, K. Nishida, and T. Fujikado. 2014. 'Characteristics of retinal reflectance changes induced by transcorneal electrical stimulation in cat eyes', *PLoS One*, 9: e92186.
- Moura, A. L., R. A. Teixeira, N. N. Oiwa, M. F. Costa, C. Feitosa-Santana, D. Callegaro, R. D. Hamer, and D. F. Ventura. 2008. 'Chromatic discrimination losses in multiple sclerosis patients with and without optic neuritis using the Cambridge Colour Test', *Visual Neuroscience*, 25: 463-8.

References

- Naismith, R. T., J. Xu, N. T. Tutlam, A. Snyder, T. Benzinger, J. Shimony, J. Shepherd, K. Trinkaus, A. H. Cross, and S. K. Song. 2009. 'Disability in optic neuritis correlates with diffusion tensor-derived directional diffusivities', *Neurology*, 72: 589-94.
- Naismith, R. T., J. Xu, N. T. Tutlam, P. T. Scully, K. Trinkaus, A. Z. Snyder, S. K. Song, and A. H. Cross. 2010. 'Increased diffusivity in acute multiple sclerosis lesions predicts risk of black hole', *Neurology*, 74: 1694-701.
- Naismith, R. T., J. Xu, N. T. Tutlam, K. Trinkaus, A. H. Cross, and S. K. Song. 2010. 'Radial diffusivity in remote optic neuritis discriminates visual outcomes', *Neurology*, 74: 1702-10.
- Neuling, T., S. Rach, and C. S. Herrmann. 2013. 'Orchestrating neuronal networks: sustained after-effects of transcranial alternating current stimulation depend upon brain states', *Frontiers in Human Neuroscience*, 7: 161.
- Newman, E., and A. Reichenbach. 1996. 'The Muller cell: a functional element of the retina', *Trends Neurosci*, 19: 307-12.
- Nishioka, C., H. F. Liang, C. F. Chung, and S. W. Sun. 2017. 'Disease stage-dependent relationship between diffusion tensor imaging and electrophysiology of the visual system in a murine model of multiple sclerosis', *Neuroradiology*, 59: 1241-50.
- Nishioka, Christopher, Hsiao-Fang Liang, Barsam Barsamian, and Shu-Wei Sun. 2018. 'Sequential phases of RGC axonal and somatic injury in EAE mice examined using DTI and OCT', *Mult Scler Relat Disord*.
- Oberwahrenbrock, T., S. Schippling, M. Ringelstein, F. Kaufhold, H. Zimmermann, N. Keser, K. L. Young, J. Harmel, H. P. Hartung, R. Martin, F. Paul, O. Aktas, and A. U. Brandt. 2012. 'Retinal damage in multiple sclerosis disease subtypes measured by high-resolution optical coherence tomography', *Mult Scler Int*, 2012: 530305.
- Oberwahrenbrock, T., M. Ringelstein, S. Jentschke, K. Deuschle, K. Klumbies, J. Bellmann-Strobl, J. Harmel, K. Ruprecht, S. Schippling, H. P. Hartung, O. Aktas, A. U. Brandt, and F. Paul. 2013. 'Retinal ganglion cell and inner plexiform layer thinning in clinically isolated syndrome', *Mult Scler*, 19: 1887-95.
- Oberwahrenbrock, T., M. Weinhold, J. Mikolajczak, H. Zimmermann, F. Paul, I. Beckers, and A. U. Brandt. 2015. 'Reliability of Intra-Retinal Layer Thickness Estimates', *PLoS One*, 10: e0137316.
- Oberwahrenbrock, Timm, Ghislaine L. Traber, Sebastian Lukas, Iñigo Gabilondo, Rachel Nolan, Christopher Songster, Lisanne Balk, Axel Petzold, Friedemann Paul, Pablo Villoslada, Alexander U. Brandt, Ari J. Green, and Sven Schippling. 2018. 'Multicenter reliability of semiautomatic retinal layer segmentation using OCT', *Neurology - Neuroimmunology Neuroinflammation*, 5.
- Odom, J. V., M. Bach, M. Brigell, G. E. Holder, D. L. McCulloch, A. Mizota, and A. P. Tormene. 2016. 'ISCEV standard for clinical visual evoked potentials: (2016 update)', *Doc Ophthalmol*, 133: 1-9.
- Okazaki, Y., T. Morimoto, and H. Sawai. 2008. 'Parameters of optic nerve electrical stimulation affecting neuroprotection of axotomized retinal ganglion cells in adult rats', *Neuroscience Research*, 61: 129-35.
- Ontaneda, D., K. Sakaie, J. Lin, X. F. Wang, M. J. Lowe, M. D. Phillips, and R. J. Fox. 2017. 'Measuring Brain Tissue Integrity during 4 Years Using Diffusion Tensor Imaging', *AJNR Am J Neuroradiol*, 38: 31-38.
- Ortiz-Perez, S., M. Andorra, B. Sanchez-Dalmau, R. Torres-Torres, D. Calbet, E. J. Lampert, S. Alba-Arbalat, A. M. Guerrero-Zamora, I. Zubizarreta, N. Sola-Valls, S. Llufrui, M. Sepulveda, A. Saiz, P. Villoslada, and E. H. Martinez-Lapiscina. 2016. 'Visual field impairment captures disease burden in multiple sclerosis', *J Neurol*, 263: 695-702.
- Pache, F., H. Zimmermann, J. Mikolajczak, S. Schumacher, A. Lacheta, F. C. Oertel, J. Bellmann-Strobl, S. Jarius, B. Wildemann, M. Reindl, A. Waldman, K. Soelberg, N. Asgari, M. Ringelstein, O. Aktas, N. Gross, M. Buttman, T. Ach, K. Ruprecht, F. Paul, and A. U. Brandt. 2016. 'MOG-IgG in NMO and related disorders: a multicenter study of 50 patients. Part 4: Afferent visual system damage after optic neuritis in MOG-IgG-seropositive versus AQP4-IgG-seropositive patients', *J Neuroinflammation*, 13: 282.
- Papadopoulos, M. C., and A. S. Verkman. 2012. 'Aquaporin 4 and neuromyelitis optica', *Lancet Neurol*, 11: 535-44.

References

- Paulus, W. 2011. 'Transcranial electrical stimulation (tES - tDCS; tRNS, tACS) methods', *Neuropsychol Rehabil*, 21: 602-17.
- Paulus, W., A. V. Peterchev, and M. Ridding. 2013. 'Transcranial electric and magnetic stimulation: technique and paradigms', *Handb Clin Neurol*, 116: 329-42.
- Pawlitzki, Marc, Marc Horbrügger, Kristian Loewe, Jörn Kaufmann, Roland Opfer, Markus Wagner, Khaldoon Al-Nosairy, Sven Meuth, Michael Hoffmann, and Sven Schippling. 2020. 'MS optic neuritis-induced long-term structural changes within the visual pathway', *Neurology - Neuroimmunology Neuroinflammation*, 7: e665.
- Pernet, Vincent, and Martin E. Schwab. 2014. 'Lost in the jungle: new hurdles for optic nerve axon regeneration', *Trends in Neurosciences*, 37: 381-87.
- Peter A. Calabresi, Laura J. Balcer, Elliot M. Frohman, Peter A. Calabresi, Laura J. Balcer, and Elliot M. Frohman. 2015. *Introduction to optical coherence tomography in neurological diseases* (Cambridge University Press).
- Peterchev, A. V., T. A. Wagner, P. C. Miranda, M. A. Nitsche, W. Paulus, S. H. Lisanby, A. Pascual-Leone, and M. Bikson. 2012. 'Fundamentals of transcranial electric and magnetic stimulation dose: definition, selection, and reporting practices', *Brain Stimul*, 5: 435-53.
- Petzold, A., J. F. de Boer, S. Schippling, P. Vermersch, R. Kardon, A. Green, P. A. Calabresi, and C. Polman. 2010. 'Optical coherence tomography in multiple sclerosis: a systematic review and meta-analysis', *Lancet Neurol*, 9: 921-32.
- Petzold, A., M. P. Wattjes, F. Costello, J. Flores-Rivera, C. L. Fraser, K. Fujihara, J. Leavitt, R. Marignier, F. Paul, S. Schippling, C. Sindic, P. Villoslada, B. Weinschenker, and G. T. Plant. 2014. 'The investigation of acute optic neuritis: a review and proposed protocol', *Nat Rev Neurol*, 10: 447-58.
- Petzold, A. 2017. 'Neuroprotection and visual function after optic neuritis', *Curr Opin Neurol*, 30: 67-73.
- Petzold, A., L. J. Balcer, P. A. Calabresi, F. Costello, T. C. Frohman, E. M. Frohman, E. H. Martinez-Lapiscina, A. J. Green, R. Kardon, O. Outteryck, F. Paul, S. Schippling, P. Vermersch, P. Villoslada, and L. J. Balk. 2017. 'Retinal layer segmentation in multiple sclerosis: a systematic review and meta-analysis', *Lancet Neurol*, 16: 797-812.
- Petzold, A., T. Braithwaite, B. W. van Oosten, L. Balk, E. H. Martinez-Lapiscina, R. Wheeler, N. Wiegerinck, C. Waters, and G. T. Plant. 2020. 'Case for a new corticosteroid treatment trial in optic neuritis: review of updated evidence', *J Neurol Neurosurg Psychiatry*, 91: 9-14.
- Pfueller, C. F., A. U. Brandt, F. Schubert, M. Bock, B. Walaszek, H. Waiczies, T. Schwentek, J. Dorr, J. Bellmann-Strobl, C. Mohr, N. Weinges-Evers, B. Ittermann, J. T. Wuerfel, and F. Paul. 2011. 'Metabolic changes in the visual cortex are linked to retinal nerve fiber layer thinning in multiple sclerosis', *PLoS One*, 6: e18019.
- 'Photocoagulation for diabetic macular edema. Early Treatment Diabetic Retinopathy Study report number 1. Early Treatment Diabetic Retinopathy Study research group'. 1985. *Arch Ophthalmol*, 103: 1796-806.
- Polman, C. H., S. C. Reingold, B. Banwell, M. Clanet, J. A. Cohen, M. Filippi, K. Fujihara, E. Havrdova, M. Hutchinson, L. Kappos, F. D. Lublin, X. Montalban, P. O'Connor, M. Sandberg-Wollheim, A. J. Thompson, E. Waubant, B. Weinschenker, and J. S. Wolinsky. 2011. 'Diagnostic criteria for multiple sclerosis: 2010 revisions to the McDonald criteria', *Ann Neurol*, 69: 292-302.
- Potsaid, B., I. Gorczynska, V. J. Srinivasan, Y. Chen, J. Jiang, A. Cable, and J. G. Fujimoto. 2008. 'Ultrahigh speed spectral / Fourier domain OCT ophthalmic imaging at 70,000 to 312,500 axial scans per second', *Opt Express*, 16: 15149-69.
- Prasad, S., and S. L. Galetta. 2011. 'Anatomy and physiology of the afferent visual system', *Handb Clin Neurol*, 102: 3-19.
- Prilloff, S., P. Henrich-Noack, S. Kropf, and B. A. Sabel. 2010. 'Experience-dependent plasticity and vision restoration in rats after optic nerve crush', *J Neurotrauma*, 27: 2295-307.
- Prineas, John W., Eunice E. Kwon, Eun-Sook Cho, Leroy R. Sharer, Michael H. Barnett, Emilia L. Oleszak, Brad Hoffman, and Bryan P. Morgan. 2001. 'Immunopathology of secondary-progressive multiple sclerosis', *Annals of Neurology*, 50: 646-57.
- Raphael, Brian A., Kristin M. Galetta, Dina A. Jacobs, Clyde E. Markowitz, Grant T. Liu, M. Ligia Nano-Schiavi, Steven L. Galetta, Maureen G. Maguire, Carol M. Mangione, Denise R. Globe,

References

- and Laura J. Balcer. 2006. 'Validation and Test Characteristics of a 10-Item Neuro-Ophthalmic Supplement to the NEI-VFQ-25', *American Journal of Ophthalmology*, 142: 1026-35.e2.
- Raz, N., S. Chokron, T. Ben-Hur, and N. Levin. 2013. 'Temporal reorganization to overcome monocular demyelination', *Neurology*, 81: 702-9.
- Reato, D., A. Rahman, M. Bikson, and L. C. Parra. 2013. 'Effects of weak transcranial alternating current stimulation on brain activity-a review of known mechanisms from animal studies', *Frontiers in Human Neuroscience*, 7: 687.
- Reed, Thomas, and Roi Cohen Kadosh. 2018. 'Transcranial electrical stimulation (tES) mechanisms and its effects on cortical excitability and connectivity', *Journal of Inherited Metabolic Disease*, 41: 1123-30.
- Rocca, M. A., P. Preziosa, S. Mesaros, E. Pagani, J. Dackovic, T. Stosic-Opincal, J. Drulovic, and M. Filippi. 2016. 'Clinically Isolated Syndrome Suggestive of Multiple Sclerosis: Dynamic Patterns of Gray and White Matter Changes-A 2-year MR Imaging Study', *Radiology*, 278: 841-53.
- Roed, H., J. Frederiksen, A. Langkilde, T. L. Sorensen, M. Lauritzen, and F. Sellebjerg. 2005. 'Systemic T-cell activation in acute clinically isolated optic neuritis', *J Neuroimmunol*, 162: 165-72.
- Runkle, E. A., and D. A. Antonetti. 2011. 'The blood-retinal barrier: structure and functional significance', *Methods Mol Biol*, 686: 133-48.
- Sabel, B. A., and E. Kastner. 2000. 'Restoration of vision by training of residual functions', *Curr Opin Ophthalmol*, 11: 430-6.
- Sabel, B. A., S. Kenkel, and E. Kastner. 2004. 'Vision restoration therapy (VRT) efficacy as assessed by comparative perimetric analysis and subjective questionnaires', *Restor Neurol Neurosci*, 22: 399-420.
- Sabel, B. A., and S. Trauzettel-Klosinski. 2005. 'Improving vision in a patient with homonymous hemianopia', *J Neuroophthalmol*, 25: 143-9.
- Sabel, B. A., A. B. Fedorov, N. Naue, A. Borrmann, C. Herrmann, and C. Gall. 2011. 'Non-invasive alternating current stimulation improves vision in optic neuropathy', *Restor Neurol Neurosci*, 29: 493-505.
- Sabel, B. A., P. Henrich-Noack, A. Fedorov, and C. Gall. 2011. 'Vision restoration after brain and retina damage: the "residual vision activation theory"', *Prog Brain Res*, 192: 199-262.
- Sabel, B. A., J. Flammer, and L. B. Merabet. 2018. 'Residual vision activation and the brain-eye-vascular triad: Dysregulation, plasticity and restoration in low vision and blindness - a review', *Restor Neurol Neurosci*, 36: 767-91.
- Sabel, B. A., G. Thut, J. Haueisen, P. Henrich-Noack, C. S. Herrmann, A. Hunold, T. Kammer, B. Matteo, E. G. Sergeeva, W. Waleszczyk, and A. Antal. 2020. 'Vision modulation, plasticity and restoration using non-invasive brain stimulation - An IFCN-sponsored review', *Clin Neurophysiol*, 131: 887-911.
- Sabel, B. A., J. Wang, S. Fähse, L. Cárdenas-Morales, and A. Antal. 2020. 'Personality and stress influence vision restoration and recovery in glaucoma and optic neuropathy following alternating current stimulation: implications for personalized neuromodulation and rehabilitation', *EPMA Journal*.
- Sahraie, A., C. T. Trevethan, M. J. MacLeod, A. D. Murray, J. A. Olson, and L. Weiskrantz. 2006. 'Increased sensitivity after repeated stimulation of residual spatial channels in blindsight', *Proc Natl Acad Sci U S A*, 103: 14971-6.
- Saidha, S., S. B. Syc, M. K. Durbin, C. Eckstein, J. D. Oakley, S. A. Meyer, A. Conger, T. C. Frohman, S. Newsome, J. N. Ratchford, E. M. Frohman, and P. A. Calabresi. 2011. 'Visual dysfunction in multiple sclerosis correlates better with optical coherence tomography derived estimates of macular ganglion cell layer thickness than peripapillary retinal nerve fiber layer thickness', *Mult Scler*, 17: 1449-63.
- Saidha, S., S. B. Syc, M. A. Ibrahim, C. Eckstein, C. V. Warner, S. K. Farrell, J. D. Oakley, M. K. Durbin, S. A. Meyer, L. J. Balcer, E. M. Frohman, J. M. Rosenzweig, S. D. Newsome, J. N. Ratchford, Q. D. Nguyen, and P. A. Calabresi. 2011. 'Primary retinal pathology in multiple sclerosis as detected by optical coherence tomography', *Brain*, 134: 518-33.
- Saidha, S., E. S. Sotirchos, M. A. Ibrahim, C. M. Crainiceanu, J. M. Gelfand, Y. J. Sepah, J. N. Ratchford, J. Oh, M. A. Seigo, S. D. Newsome, L. J. Balcer, E. M. Frohman, A. J. Green, Q.

References

- D. Nguyen, and P. A. Calabresi. 2012. 'Microcystic macular oedema, thickness of the inner nuclear layer of the retina, and disease characteristics in multiple sclerosis: a retrospective study', *Lancet Neurol*, 11: 963-72.
- Saidha, S., O. Al-Louzi, J. N. Ratchford, P. Bhargava, J. Oh, S. D. Newsome, J. L. Prince, D. Pham, S. Roy, P. van Zijl, L. J. Balcer, E. M. Frohman, D. S. Reich, C. Crainiceanu, and P. A. Calabresi. 2015. 'Optical coherence tomography reflects brain atrophy in multiple sclerosis: A four-year study', *Ann Neurol*, 78: 801-13.
- Sanchez-Dalmau, B., E. H. Martinez-Lapiscina, R. Torres-Torres, S. Ortiz-Perez, I. Zubizarreta, I. V. Pulido-Valdeolivas, S. Alba-Arbalat, A. Guerrero-Zamora, D. Calbet, and P. Villoslada. 2017. 'Early retinal atrophy predicts long-term visual impairment after acute optic neuritis', *Mult Scler*: 1352458517718628.
- Sato, T., T. Fujikado, T. S. Lee, and Y. Tano. 2008. 'Direct effect of electrical stimulation on induction of brain-derived neurotrophic factor from cultured retinal Muller cells', *Invest Ophthalmol Vis Sci*, 49: 4641-6.
- Sato, T., T. Fujikado, T. Morimoto, K. Matsushita, T. Harada, and Y. Tano. 2008. 'Effect of electrical stimulation on IGF-1 transcription by L-type calcium channels in cultured retinal Muller cells', *Jpn J Ophthalmol*, 52: 217-23.
- Savini, G., M. Zanini, V. Carelli, A. A. Sadun, F. N. Ross-Cisneros, and P. Barboni. 2005. 'Correlation between retinal nerve fibre layer thickness and optic nerve head size: an optical coherence tomography study', *Br J Ophthalmol*, 89: 489-92.
- Schatz, A., T. Rock, L. Naycheva, G. Willmann, B. Wilhelm, T. Peters, K. U. Bartz-Schmidt, E. Zrenner, A. Messias, and F. Gekeler. 2011. 'Transcorneal electrical stimulation for patients with retinitis pigmentosa: a prospective, randomized, sham-controlled exploratory study', *Invest Ophthalmol Vis Sci*, 52: 4485-96.
- Schatz, A., J. Pach, M. Gosheva, L. Naycheva, G. Willmann, B. Wilhelm, T. Peters, K. U. Bartz-Schmidt, E. Zrenner, A. Messias, and F. Gekeler. 2017. 'Transcorneal Electrical Stimulation for Patients With Retinitis Pigmentosa: A Prospective, Randomized, Sham-Controlled Follow-up Study Over 1 Year', *Invest Ophthalmol Vis Sci*, 58: 257-69.
- Schippling, S., L. J. Balk, F. Costello, P. Albrecht, L. Balcer, P. A. Calabresi, J. L. Frederiksen, E. Frohman, A. J. Green, A. Klistorner, O. Outteryck, F. Paul, G. T. Plant, G. Traber, P. Vermersch, P. Villoslada, S. Wolf, and A. Petzold. 2015. 'Quality control for retinal OCT in multiple sclerosis: validation of the OSCAR-IB criteria', *Mult Scler*, 21: 163-70.
- Schippling, S. 2017. 'MRI for multiple sclerosis diagnosis and prognosis', *Neurodegener Dis Manag*, 7: 27-29.
- Schippling., Sven. 2015. *Basic principles of optical coherence tomography - Optical Coherence Tomography in Neurologic Diseases* (Cambridge University Press).
- Schmidt, S., A. Mante, M. Ronnefarth, R. Fleischmann, C. Gall, and S. A. Brandt. 2013. 'Progressive enhancement of alpha activity and visual function in patients with optic neuropathy: a two-week repeated session alternating current stimulation study', *Brain Stimul*, 6: 87-93.
- Schnurman, Z. S., T. C. Frohman, S. C. Beh, D. Conger, A. Conger, S. Saidha, S. Galetta, P. A. Calabresi, A. J. Green, L. J. Balcer, and E. M. Frohman. 2014. 'Retinal architecture and mfERG: Optic nerve head component response characteristics in MS', *Neurology*, 82: 1888-96.
- Schuman, Joel S., Tamar Pedut-Kloizman, Ellen Hertzmark, Michael R. Hee, Jason R. Wilkins, Jeffery G. Coker, Carmen A. Puliafito, James G. Fujimoto, and Eric A. Swanson. 1996. 'Reproducibility of Nerve Fiber Layer Thickness Measurements Using Optical Coherence Tomography', *Ophthalmology*, 103: 1889-98.
- Schürmann, M., and E. Basar. 2001. 'Functional aspects of alpha oscillations in the EEG', *International Journal of Psychophysiology*, 39: 151-8.
- Sekirnjak, Chris, Pawel Hottowy, Alexander Sher, Wladyslaw Dabrowski, A. M. Litke, and E. J. Chichilnisky. 2008. 'High-resolution electrical stimulation of primate retina for epiretinal implant design', *J Neurosci*, 28: 4446-56.
- Selhorst, J. B., and Y. Chen. 2009. 'The optic nerve', *Semin Neurol*, 29: 29-35.
- Sergeeva, E. G., A. B. Fedorov, P. Henrich-Noack, and B. A. Sabel. 2012. 'Transcorneal alternating current stimulation induces EEG "aftereffects" only in rats with an intact visual system but not after severe optic nerve damage', *J Neurophysiol*, 108: 2494-500.
- Shams, P. N., and G. T. Plant. 2009. 'Optic neuritis: a review', *Int MS J*, 16: 82-9.

References

- Shindler, K. S., E. Ventura, M. Dutt, and A. Rostami. 2008. 'Inflammatory demyelination induces axonal injury and retinal ganglion cell apoptosis in experimental optic neuritis', *Exp Eye Res*, 87: 208-13.
- Siffrin, V., J. Vogt, H. Radbruch, R. Nitsch, and F. Zipp. 2010. 'Multiple sclerosis - candidate mechanisms underlying CNS atrophy', *Trends Neurosci*, 33: 202-10.
- Smith, A. J., R. E. Clutton, E. Lilley, K. E. A. Hansen, and T. Brattelid. 2018. 'PREPARE: guidelines for planning animal research and testing', *Laboratory Animals*, 52: 135-41.
- Song, S. K., S. W. Sun, W. K. Ju, S. J. Lin, A. H. Cross, and A. H. Neufeld. 2003. 'Diffusion tensor imaging detects and differentiates axon and myelin degeneration in mouse optic nerve after retinal ischemia', *Neuroimage*, 20: 1714-22.
- Song, S. K., J. Yoshino, T. Q. Le, S. J. Lin, S. W. Sun, A. H. Cross, and R. C. Armstrong. 2005. 'Demyelination increases radial diffusivity in corpus callosum of mouse brain', *Neuroimage*, 26: 132-40.
- Soni, M. G., G. A. Burdock, M. S. Christian, C. M. Bitler, and R. Crea. 2006. 'Safety assessment of aqueous olive pulp extract as an antioxidant or antimicrobial agent in foods', *Food and Chemical Toxicology*, 44: 903-15.
- Sormani, M. P., and M. Pardini. 2017. 'Assessing Repair in Multiple Sclerosis: Outcomes for Phase II Clinical Trials', *Neurotherapeutics*.
- Sospedra, M., and R. Martin. 2005. 'Immunology of multiple sclerosis', *Annu Rev Immunol*, 23: 683-747.
- . 2016. 'Immunology of Multiple Sclerosis', *Semin Neurol*, 36: 115-27.
- Sotirchos, E. S., A. Filippatou, K. C. Fitzgerald, S. Salama, S. Pardo, J. Wang, E. Ogbuokiri, N. J. Cowley, N. Pellegrini, O. C. Murphy, M. A. Mealy, J. L. Prince, M. Levy, P. A. Calabresi, and S. Saidha. 2019. 'Aquaporin-4 IgG seropositivity is associated with worse visual outcomes after optic neuritis than MOG-IgG seropositivity and multiple sclerosis, independent of macular ganglion cell layer thinning', *Mult Scler*: 1352458519864928.
- Srinivasan, V. J., B. K. Monson, M. Wojtkowski, R. A. Bilonick, I. Gorczynska, R. Chen, J. S. Duker, J. S. Schuman, and J. G. Fujimoto. 2008. 'Characterization of outer retinal morphology with high-speed, ultrahigh-resolution optical coherence tomography', *Invest Ophthalmol Vis Sci*, 49: 1571-9.
- Sriram, P., C. Wang, C. Yiannikas, R. Garrick, M. Barnett, J. Parratt, S. L. Graham, H. Arvind, and A. Klistorner. 2014. 'Relationship between optical coherence tomography and electrophysiology of the visual pathway in non-optic neuritis eyes of multiple sclerosis patients', *PLoS One*, 9: e102546.
- Stagg, C. J., and M. A. Nitsche. 2011. 'Physiological basis of transcranial direct current stimulation', *Neuroscientist*, 17: 37-53.
- Stangel, Martin, Tanja Kuhlmann, Paul M. Matthews, and Trevor J. Kilpatrick. 2017. 'Achievements and obstacles of remyelinating therapies in multiple sclerosis', *Nature Reviews Neurology*, 13: 742-54.
- Stankoff, B., J. J. Jadasz, H. P. Hartung, P. Kury, B. Zalc, and C. Lubetzki. 2016. 'Repair strategies for multiple sclerosis: challenges, achievements and perspectives', *Curr Opin Neurol*, 29: 286-92.
- Steinman, L. 2001. 'Multiple sclerosis: a two-stage disease', *Nat Immunol*, 2: 762-4.
- Stevens, B., S. Porta, L. L. Haak, V. Gallo, and R. D. Fields. 2002. 'Adenosine: a neuron-glial transmitter promoting myelination in the CNS in response to action potentials', *Neuron*, 36: 855-68.
- Stiebel-Kalish, H., M. A. Hellmann, M. Mimouni, F. Paul, O. Bialer, M. Bach, and I. Lotan. 2019. 'Does time equal vision in the acute treatment of a cohort of AQP4 and MOG optic neuritis?', *Neurol Neuroimmunol Neuroinflamm*, 6: e572.
- Sun, S. W., H. F. Liang, T. Q. Le, R. C. Armstrong, A. H. Cross, and S. K. Song. 2006. 'Differential sensitivity of in vivo and ex vivo diffusion tensor imaging to evolving optic nerve injury in mice with retinal ischemia', *Neuroimage*, 32: 1195-204.
- Sun, S. W., H. F. Liang, K. Trinkaus, A. H. Cross, R. C. Armstrong, and S. K. Song. 2006. 'Noninvasive detection of cuprizone induced axonal damage and demyelination in the mouse corpus callosum', *Magn Reson Med*, 55: 302-8.

References

- Sun, S. W., H. F. Liang, R. E. Schmidt, A. H. Cross, and S. K. Song. 2007. 'Selective vulnerability of cerebral white matter in a murine model of multiple sclerosis detected using diffusion tensor imaging', *Neurobiol Dis*, 28: 30-8.
- Sun, S. W., C. Nishioka, C. F. Chung, J. Park, and H. F. Liang. 2017. 'Anterograde-propagation of axonal degeneration in the visual system of wild mice characterized by diffusion tensor imaging', *Journal of Magnetic Resonance Imaging*, 45: 482-91.
- Syc, S. B., S. Saidha, S. D. Newsome, J. N. Ratchford, M. Levy, E. Ford, C. M. Crainiceanu, M. K. Durbin, J. D. Oakley, S. A. Meyer, E. M. Frohman, and P. A. Calabresi. 2012. 'Optical coherence tomography segmentation reveals ganglion cell layer pathology after optic neuritis', *Brain*, 135: 521-33.
- Tagami, Y., T. Kurimoto, T. Miyoshi, T. Morimoto, H. Sawai, and O. Mimura. 2009. 'Axonal regeneration induced by repetitive electrical stimulation of crushed optic nerve in adult rats', *Jpn J Ophthalmol*, 53: 257-66.
- Tallantyre, E. C., L. Bo, O. Al-Rawashdeh, T. Owens, C. H. Polman, J. S. Lowe, and N. Evangelou. 2010. 'Clinico-pathological evidence that axonal loss underlies disability in progressive multiple sclerosis', *Mult Scler*, 16: 406-11.
- Tewarie, P., L. Balk, F. Costello, A. Green, R. Martin, S. Schippling, and A. Petzold. 2012. 'The OSCAR-IB consensus criteria for retinal OCT quality assessment', *PLoS One*, 7: e34823.
- Thompson, A. J., B. L. Banwell, F. Barkhof, W. M. Carroll, T. Coetzee, G. Comi, J. Correale, F. Fazekas, M. Filippi, M. S. Freedman, K. Fujihara, S. L. Galetta, H. P. Hartung, L. Kappos, F. D. Lublin, R. A. Marrie, A. E. Miller, D. H. Miller, X. Montalban, E. M. Mowry, P. S. Sorensen, M. Tintore, A. L. Traboulsee, M. Trojano, B. M. J. Uitdehaag, S. Vukusic, E. Waubant, B. G. Weinschenker, S. C. Reingold, and J. A. Cohen. 2018. 'Diagnosis of multiple sclerosis: 2017 revisions of the McDonald criteria', *Lancet Neurol*, 17: 162-73.
- Toosy, A. T., S. J. Hickman, K. A. Miszkiel, S. J. Jones, G. T. Plant, D. R. Altmann, G. J. Barker, D. H. Miller, and A. J. Thompson. 2005. 'Adaptive cortical plasticity in higher visual areas after acute optic neuritis', *Ann Neurol*, 57: 622-33.
- Toosy, Ahmed T., Deborah F. Mason, and David H. Miller. 2014. 'Optic neuritis', *The Lancet Neurology*, 13: 83-99.
- Trapp, B. D., and K. A. Nave. 2008. 'Multiple sclerosis: an immune or neurodegenerative disorder?', *Annu Rev Neurosci*, 31: 247-69.
- Tremoleda, J. L., S. Macholl, and J. K. Sosabowski. 2018. 'Anesthesia and Monitoring of Animals During MRI Studies', *Methods Mol Biol*, 1718: 423-39.
- Trip, S. A., C. Wheeler-Kingshott, S. J. Jones, W. Y. Li, G. J. Barker, A. J. Thompson, G. T. Plant, and D. H. Miller. 2006. 'Optic nerve diffusion tensor imaging in optic neuritis', *Neuroimage*, 30: 498-505.
- Tur, C., O. Goodkin, D. R. Altmann, T. M. Jenkins, K. Miszkiel, A. Mirigliani, C. Fini, C. A. Gandini Wheeler-Kingshott, A. J. Thompson, O. Ciccarelli, and A. T. Toosy. 2016. 'Longitudinal evidence for anterograde trans-synaptic degeneration after optic neuritis', *Brain*, 139: 816-28.
- van der Walt, A., S. C. Kolbe, Y. E. Wang, A. Klistorner, N. Shuey, G. Ahmadi, M. Paine, M. Marriott, P. Mitchell, G. F. Egan, H. Butzkueven, and T. J. Kilpatrick. 2013. 'Optic nerve diffusion tensor imaging after acute optic neuritis predicts axonal and visual outcomes', *PLoS One*, 8: e83825.
- Vanni, S., L. Henriksson, L. Hyvarinen, R. Nasanen, and A. Raninen. 2010. 'Vision restoration through extrastriate stimulation in patients with visual field defects: a double-blind and randomized experimental study', *Neurorehabil Neural Repair*, 24: 204; author reply 05-6.
- Veleri, S., C. H. Lazar, B. Chang, P. A. Sieving, E. Banin, and A. Swaroop. 2015. 'Biology and therapy of inherited retinal degenerative disease: insights from mouse models', *Dis Model Mech*, 8: 109-29.
- Villoslada, P., and E. H. Martinez-Lapiscina. 2017. 'Time is vision: The importance of the early discovery and diagnosis of optic neuritis', *Mult Scler*, 23: 1806-07.
- Villoslada, Pablo. 2016. 'Neuroprotective therapies for multiple sclerosis and other demyelinating diseases', *Multiple Sclerosis and Demyelinating Disorders*, 1: 1.
- Villoslada, Pablo, and Elena H. Martinez-Lapiscina. 2019. 'Remyelination: a good neuroprotective strategy for preventing axonal degeneration?', *Brain*, 142: 233-36.

References

- Vossen, A., J. Gross, and G. Thut. 2015. 'Alpha Power Increase After Transcranial Alternating Current Stimulation at Alpha Frequency (alpha-tACS) Reflects Plastic Changes Rather Than Entrainment', *Brain Stimul*, 8: 499-508.
- Wake, H., F. C. Ortiz, D. H. Woo, P. R. Lee, M. C. Angulo, and R. D. Fields. 2015. 'Nonsynaptic junctions on myelinating glia promote preferential myelination of electrically active axons', *Nat Commun*, 6: 7844.
- Walter, S. D., H. Ishikawa, K. M. Galetta, R. E. Sakai, D. J. Feller, S. B. Henderson, J. A. Wilson, M. G. Maguire, S. L. Galetta, E. Frohman, P. A. Calabresi, J. S. Schuman, and L. J. Balcer. 2012a. 'Ganglion cell loss in relation to visual disability in multiple sclerosis', *Ophthalmology*, 119: 1250-7.
- Walter, Scott D., Hiroshi Ishikawa, Kristin M. Galetta, Reiko E. Sakai, Daniel J. Feller, Sam B. Henderson, James A. Wilson, Maureen G. Maguire, Steven L. Galetta, Elliot Frohman, Peter A. Calabresi, Joel S. Schuman, and Laura J. Balcer. 2012b. 'Ganglion Cell Loss in Relation to Visual Disability in Multiple Sclerosis', *Ophthalmology*, 119: 1250-57.
- Watanabe, A., Y. Hashimoto, E. Ochiai, A. Sato, and K. Kamei. 2009. 'A simple method for confirming correct endotracheal intubation in mice', *Laboratory Animals*, 43: 399-401.
- Wicki, C. A., J. V. M. Hanson, and S. Schippling. 2018. 'Optical coherence tomography as a means to characterize visual pathway involvement in multiple sclerosis', *Curr Opin Neurol*.
- Wicki, C. A., P. Manogaran, T. Simic, J. V. M. Hanson, and S. Schippling. 2020. 'Bilateral retinal pathology following a first-ever clinical episode of autoimmune optic neuritis', *Neurol Neuroimmunol Neuroinflamm*, 7.
- Wingerchuk, D. M., B. Banwell, J. L. Bennett, P. Cabre, W. Carroll, T. Chitnis, J. de Seze, K. Fujihara, B. Greenberg, A. Jacob, S. Jarius, M. Lana-Peixoto, M. Levy, J. H. Simon, S. Tenenbaum, A. L. Traboulsee, P. Waters, K. E. Wellik, and B. G. Weinschenker. 2015. 'International consensus diagnostic criteria for neuromyelitis optica spectrum disorders', *Neurology*, 85: 177-89.
- Winklewski, P. J., A. Sabisz, P. Naumczyk, K. Jodzio, E. Szurowska, and A. Szarmach. 2018. 'Understanding the Physiopathology Behind Axial and Radial Diffusivity Changes-What Do We Know?', *Front Neurol*, 9: 92.
- Wischnewski, M., M. Engelhardt, M. A. Salehinejad, D. J. L. G. Schutter, M. F. Kuo, and M. A. Nitsche. 2018. 'NMDA Receptor-Mediated Motor Cortex Plasticity After 20 Hz Transcranial Alternating Current Stimulation', *Cerebral Cortex*, 29: 2924-31.
- Woods, A. J., A. Antal, M. Bikson, P. S. Boggio, A. R. Brunoni, P. Celnik, L. G. Cohen, F. Fregni, C. S. Herrmann, E. S. Kappenman, H. Knotkova, D. Liebetanz, C. Miniussi, P. C. Miranda, W. Paulus, A. Priori, D. Reato, C. Stagg, N. Wenderoth, and M. A. Nitsche. 2016. 'A technical guide to tDCS, and related non-invasive brain stimulation tools', *Clin Neurophysiol*, 127: 1031-48.
- Wu, G. F., M. R. Brier, C. A. Parks, B. M. Ances, and G. P. Van Stavern. 2015. 'An Eye on Brain Integrity: Acute Optic Neuritis Affects Resting State Functional Connectivity', *Invest Ophthalmol Vis Sci*, 56: 2541-6.
- Xie, H., C. H. Shek, Y. Wang, and L. L. H. Chan. 2019. 'Effect of interphase gap duration and stimulus rate on threshold of visual cortical neurons in the rat', *Conf Proc IEEE Eng Med Biol Soc*, 2019: 1817-20.
- Xu, Junqian, Shu-Wei Sun, Robert T. Naismith, Abraham Z. Snyder, Anne H. Cross, and Sheng-Kwei Song. 2008. 'Assessing optic nerve pathology with diffusion MRI: from mouse to human', *NMR in Biomedicine*, 21: 928-40.
- Yin, H., H. Yin, W. Zhang, Q. Miao, Z. Qin, S. Guo, Q. Fu, J. Ma, F. Wu, J. Yin, Y. Yang, and X. Fang. 2016. 'Transcorneal electrical stimulation promotes survival of retinal ganglion cells after optic nerve transection in rats accompanied by reduced microglial activation and TNF-alpha expression', *Brain Res*, 1650: 10-20.
- You, Y., E. C. Graham, T. Shen, C. Yiannikas, J. Parratt, V. Gupta, J. Barton, M. Dwyer, M. H. Barnett, C. L. Fraser, S. L. Graham, and A. Klistorner. 2018. 'Progressive inner nuclear layer dysfunction in non-optic neuritis eyes in MS', *Neurol Neuroimmunol Neuroinflamm*, 5: e427.
- You, Y., M. H. Barnett, C. Yiannikas, J. Parratt, J. Matthews, S. L. Graham, and A. Klistorner. 2020. 'Chronic demyelination exacerbates neuroaxonal loss in patients with MS with unilateral optic neuritis', *Neurol Neuroimmunol Neuroinflamm*, 7.

References

- You, Yuyi, Chitra Joseph, Chenyu Wang, Vivek Gupta, Sidong Liu, Con Yiannikas, Brian E. Chua, Nitin Chitranshi, Ting Shen, Yogita Dheer, Alessandro Invernizzi, Robert Borotkanics, Michael Barnett, Stuart L. Graham, and Alexander Klistorner. 2019. 'Demyelination precedes axonal loss in the transneuronal spread of human neurodegenerative disease', *Brain*: awy338-awy38.
- Zaehle, T., S. Rach, and C. S. Herrmann. 2010. 'Transcranial alternating current stimulation enhances individual alpha activity in human EEG', *PLoS One*, 5: e13766.
- Zawadzka, M., L. E. Rivers, S. P. Fancy, C. Zhao, R. Tripathi, F. Jamen, K. Young, A. Goncharevich, H. Pohl, M. Rizzi, D. H. Rowitch, N. Kessaris, U. Suter, W. D. Richardson, and R. J. Franklin. 2010. 'CNS-resident glial progenitor/stem cells produce Schwann cells as well as oligodendrocytes during repair of CNS demyelination', *Cell Stem Cell*, 6: 578-90.
- Zhang, X., N. Xin, L. Tong, and X. J. Tong. 2013. 'Electrical stimulation enhances peripheral nerve regeneration after crush injury in rats', *Mol Med Rep*, 7: 1523-7.
- Zhou, W. T., Y. Q. Ni, Z. B. Jin, M. Zhang, J. H. Wu, Y. Zhu, G. Z. Xu, and D. K. Gan. 2012. 'Electrical stimulation ameliorates light-induced photoreceptor degeneration in vitro via suppressing the proinflammatory effect of microglia and enhancing the neurotrophic potential of Muller cells', *Exp Neurol*, 238: 192-208.